Air pollution in La Paz and El Alto, two high-altitude Bolivian cities

Valeria Paola Mardonez Balderrama

THÈSE

Pour obtenir le grade de

DOCTEUR DE L'UNIVERSITÉ GRENOBLE ALPES

École doctorale : STEP - Sciences de la Terre de l'Environnement et des Planètes
Spécialité : Sciences de la Terre et de l'Environnement
Unité de recherche : Institut des Géosciences de l'Environnement

La pollution atmosphérique dans des villes de haute altitude : La Paz et El Alto

Air pollution in La Paz and El Alto, two high-altitude Bolivian cities

Présentée par :

Valeria Paola MARDONEZ BALDERRAMA

Direction de thèse :

Paolo LAJ PHYSICIEN, Université Grenoble Alpes	Directeur de thèse
Gaëlle UZU DIRECTRICE DE RECHERCHE, Université Grenoble Alpes	Co-directrice de thèse

Rapporteurs :

Nikolaos MIHALOPOULOS
PROFESSEUR, University of Crete
Stéphane SAUVAGE
PROFESSEUR DES UNIVERSITES, IMT Nord Europe

Thèse soutenue publiquement le **27 avril 2023**, devant le jury composé de :

Paolo LAJ PHYSICIEN, Université Grenoble Alpes	Directeur de thèse
Nikolaos MIHALOPOULOS PROFESSEUR, University of Crete	Rapporteur
Stéphane SAUVAGE PROFESSEUR DES UNIVERSITES, IMT Nord Europe	Rapporteur
Gaëlle UZU DIRECTRICE DE RECHERCHE, IRD délégation régionale Sud Est	Co-directrice de thèse
Aurélien DOMMERGUE PROFESSEUR DES UNIVERSITES, Université Grenoble Alpes	Président
Evelyn FRENEY CHARGE DE RECHERCHE, CNRS délégation Rhône Auvergne	Examinatrice
Céline MARI DIRECTRICE DE RECHERCHE, CNRS délégation Occitanie Ouest	Examinatrice

ABSTRACT

Air pollution has been ranked by the World Health Organization (WHO) as the worldwide second-highest risk factor for noncommunicable diseases, responsible for almost 7 million premature deaths around the world every year. The majority of premature deaths attributed to ambient air pollution take place in low- and middle-income countries. Latin American countries, in addition, have experienced in the last decades a fast growth in population, urbanization and industry, with the majority of its population living in urban centers. Only few studies have documented the state of the air quality in these countries, especially in high altitude conditions. Hence, this work intended to contribute to the documentation and characterization of the sources of particulate matter (PM) affecting air quality in the metropolitan region of La Paz and El Alto (Bolivia), and to assess the impact of exposure to air pollution on the health of the inhabitants in the conurbation.

For this purpose, a long-term urban background monitoring station was installed in each city between 2016 and 2018. Filter samples of PM were collected at each site, from which the concentrations of a wide range of chemical species (e.g. OC, EC, water-soluble ions, sugar anhydrides, sugar alcohols, trace metals, PAHs, hopanes and alkanes), and the oxidative potential (OP) of the ensemble of the collected particles was analyzed. In addition, equivalent Black Carbon (eBC) was monitored during the same period at a high temporal resolution. Through the use of several statistical tools and source apportionment methods, including the US-EPA Positive Matrix Factorization tool (PMF), a two-source apportionment model and multilinear regression models, it was possible to identify the main sources contributing to the observed concentrations of PM, eBC and the observed activity of OP.

While dust and vehicular emissions represent the primary sources in terms of mass contributions, the sources responsible for the most part of the observed OP activity contributed very little to the total mass of PM_{10} (e.g. open waste burning). In the case of eBC, vehicular emissions and biomass burning stood out as the main sources of absorbing aerosols. The three studied air quality parameters (PM, OP, eBC) were then associated to two respiratory health outcomes (acute respiratory infections and cases of pneumonias) to assess air quality's impact on health.

This study showed that concentrations of PM in La Paz and El Alto region are mostly impacted by a limited number of local sources and the extreme conditions of hypoxia. The obtained results can serve as a basis for effective air quality policies and pave the way for future studies on the potential health effects of air pollution in both cities and the rest of the country. The scientific contribution of this work will also provide a better understanding of the role that the city plays in terms of regional pollution.

RESUMÉ

La pollution atmosphérique a été classée par l'Organisation mondiale de la santé (OMS) comme le deuxième facteur de risque de maladies non transmissibles dans le monde, responsable de près de 7 millions de décès prématurés dans le monde chaque année. La majorité des décès prématurés attribués à la pollution de l'air ambiant ont lieu dans les pays à revenu faible ou intermédiaire. Les pays d'Amérique latine, en outre, ont connu au cours des dernières décennies une croissance rapide de leur population, de leur urbanisation et de leur industrie, la majorité de leur population vivant dans des centres urbains. Peu d'études ont documenté l'état de la qualité de l'air dans ces pays, en particulier dans des conditions de haute altitude. Ce travail a donc pour but de contribuer à la documentation et à la caractérisation des sources de particules (PM) affectant la qualité de l'air dans la région métropolitaine de La Paz et El Alto (Bolivie), et d'évaluer l'impact de l'exposition à la pollution atmosphérique sur la santé des habitants de l'agglomération.

À cette fin, une station de surveillance de fond urbaine à long terme a été installée dans chaque ville entre 2016 et 2018. Des échantillons filtrants de PM ont été collectés sur chaque site, à partir desquels ont été analysées les concentrations d'un large éventail d'espèces chimiques (par exemple OC, EC, ions hydrosolubles, anhydrides de sucre, alcools de sucre, métaux traces, HAP, hopanes et alcanes), ainsi que le potentiel oxydant (PO) de l'ensemble des particules collectées. En outre, le carbone suie équivalent (eBC) a été surveillé pendant la même période à une haute résolution temporelle. Grâce à l'utilisation de plusieurs outils statistiques et de méthodes de répartition des sources, notamment l'outil de factorisation matricielle positive (PMF) de l'US-EPA, la "méthode Aethalometer" et des modèles de régression, il a été possible d'identifier les principales sources contribuant aux concentrations observées de PM, d'eBC et à l'activité observée du PO.

Alors que les émissions de poussières et de véhicules représentent les principales sources en termes de contributions massiques, les sources responsables de la plus grande partie de l'activité observée des PO ont contribué très peu à la masse totale de PM_{10} (par exemple, la combustion de déchets à l'air libre). Dans le cas de l'eBC, les émissions des véhicules et la combustion de la biomasse se sont distinguées comme les principales sources d'aérosols absorbants. Les trois paramètres de qualité de l'air étudiés (PM, OP, eBC) ont ensuite été associés à deux pathologies respiratoires signalées (infections respiratoires aiguës et cas de pneumonies) afin d'évaluer l'impact de la qualité de l'air sur les résultats sanitaires observés.

Cette étude a montré que les concentrations de PM dans la région de La Paz et El Alto sont principalement influencées par un nombre limité de sources locales. Les résultats obtenus peuvent servir de base à des politiques efficaces en matière de qualité de l'air et ouvrir la voie à de futures études sur les effets potentiels de la pollution atmosphérique sur la santé dans les deux villes et dans le reste du pays. L'apport scientifique de ce travail permettra de mieux comprendre le rôle que joue la ville en termes de pollution régionale.

AKNOWLEDGEMENTS

It feels so surreal to be writing this section, that represents the end of the PhD, and with it, a very special chapter in my professional and personal life. I would like to take this opportunity to thank all the people who have contributed directly and indirectly to this achievement, which is indubitably not only mine.

First of all, I would like to thank my supervisors, Paolo, Gaëlle and Marcos, for having bet on me and for having offered me your trust, support, time and knowledge. It has been a privilege to work under your guidance, and to learn from your qualities that go beyond the merely scientific.

I would like to thank in a special manner the mentoring and supervision of Dr. Marcos Andrade, who was the Bolivian counterpart in the supervision of my thesis, and who for bureaucratic reasons is not listed among the supervisors on the cover page. The knowledge, support and resources he gave me individually and as head of the Laboratory for Atmospheric Physics (LFA) were crucial for the successful completion of my thesis.

I would like to equally thank the Institut de Recherche pour le Developpement (IRD) who financed my doctoral scholarship through the program ARTS, and that provided me the administrative support necessary to overcome the challenges encountered throughout my doctoral studies.

I would also like to thank the wonderful scientific community that has surrounded me for many years, but especially during these past three years. To all my co-authors (in submitted and soon to be submitted papers), it has been a privilege to have been able to learn from each of you and to discover how amazing it is to work in collaboration. I especially want to thank the CHIANTI team, who have received me so warmly and imparted me with knowledge in kindness. I cannot leave out my beloved LFA, that has trusted me, trained me, supported me, cheered me and given me the opportunity to get here.

I want to thank my family for supporting my dream and for sustaining me in the good days and in the not so good days. For being my safe place and my source of unconditional love. I could not have made it this far had it not been for you: Mami, Papi, Veli, Vicky, I love you.

I am particularly grateful to the group of women scientists I admire greatly and who have supported me, advised me, accompanied me, sometimes nurtured me, and celebrated with me every little accomplishment. This experience would not have been so much fun without you by my side. Ana, Romane, Anouk, Lucille, it has been a great pleasure to share this little piece of life with you.

To the group of Latinos who have been like family abroad, I would not have the space to mention all of you, but I will carry you forever in my heart.

Finally, I want to thank the source of life and all good things for granting me this adventure.

TABLE OF CONTENTS

INTRODUCTION

1 Air pollution in Latin-American cities.

Air pollution, as defined by Seinfeld & Pandis (2016), is the situation in which substances resulting from anthropogenic activities are present in concentrations sufficiently high above normal ambient values that they produce negative effects on humans, wildlife, vegetation or certain materials. Such substances are called air pollutants. Air pollution has been recognized as the second highest risk factor for noncommunicable diseases (WHO, 2019). It was estimated that in 2019 outdoor ambient air pollution was responsible for 4.2 million premature deaths worldwide, a figure that increases to 6.7 million when indoor air pollution is considered (WHO, 2021a).

In order to assist the policies needed to improve air quality, the World Health Organization (WHO) has proposed a list of pollutants that have proven to be hazardous to health, along with levels above which significant public health risks can be expected (Table 1). The same organization has estimated that about 99% of the world's population lives in conditions that do not meet the proposed air quality guidelines. Moreover, although air pollution is mostly a local matter, people are often exposed to emissions that took place elsewhere due to regional airmass transport. Furthermore, exposure is not the same at all socio-economic levels. The WHO estimated that about 89% of the worldwide premature deaths caused by outdoor air pollution took place in low-and middle-income countries, which makes of air pollution a social injustice issue (WHO, 2021a).

Table 1. Recommended Air Quality Guidelines (AQG) levels and interim targets by the WHO (Table extracted from WHO, 2021b)

Pollutant	Averaging time	Interim target				AQG level
		1	2	3	4	
$PM_{2.5}$, μg/m³	Annual	35	25	15	10	5
	24-hour[a]	75	50	37.5	25	15
PM_{10}, μg/m³	Annual	70	50	30	20	15
	24-hour[a]	150	100	75	50	45
O_3, μg/m³	Peak season[b]	100	70	–	–	60
	8-hour[a]	160	120	–	–	100
NO_2, μg/m³	Annual	40	30	20	–	10
	24-hour[a]	120	50	–	–	25
SO_2, μg/m³	24-hour[a]	125	50	–	–	40
CO, mg/m³	24-hour[a]	7	–	–	–	4

[a] 99th percentile (i.e. 3–4 exceedance days per year).
[b] Average of daily maximum 8-hour mean O_3 concentration in the six consecutive months with the highest six-month running-average O_3 concentration.

Most countries in Latin America (LA) are classified as middle-income countries, whose air quality is increasingly degraded due to their fast growth in population, urbanization and industry, and the lack of rigorous

environmental protection policies. Even though population density is relatively low in this region, almost 80% of the population in LA lives in urban centers around which industry is often concentrated (Bravo & Torres, 2000; Husaini et al., 2022; UNEP & CCAC, 2016, 2018). In fact, 5 of the 21 largest metropolitan areas in the world are found in the LA region: Mexico City (Mexico), Sao Paulo (Brazil), Buenos Aires (Argentina), Rio de Janeiro (Brazil) and Bogotá (Colombia).

Biomass burning is one of the biggest Climate and air quality problem faced by the LA region. This can be driven by the change in land use or the clearing of agricultural soils, but also by accidental forest fires that are increasingly frequent and that are reinforced by climate change (Barlow et al., 2020; Mataveli et al., 2021). Although there are not many large-scale studies in the region, some studies estimate that 48% of $PM_{2.5}$ emissions from biomass burning in South America originated in the Amazonia, where an average of 16,686 km^2 $year^{-1}$ are burned (Mataveli et al., 2021). The reach of these emissions can even extend to a regional scale. These emissions not only have enormous impacts on climate and the local ecosystems, but also have a direct impact on health (Alves et al., 2017; Marlier et al., 2020; Nawaz & Henze, 2020).

Despite the large superficial extension of the LA region, there is a reduced number of air quality studies compared to North America or Europe. With not enough studies to entirely describe this region, estimating the real impact of air pollution becomes a difficult task. Nonetheless, the existing studies show that vehicular emissions represent the main source of direct and indirect pollution. Although on a smaller scale, this is also the reality faced by medium-sized cities in LA.

1.1 Air pollution in high altitude Latin-American cities

Several large cities in LA were built at high altitude (>2000 m a.s.l.), which represents an added challenge in terms of air quality. Since atmospheric pressure decreases exponentially with altitude, in high altitude regions the availability of oxygen decreases accordingly with altitude. Thus, altitude can have direct impacts on both emissions and exposure to air pollutants.

Studies have shown that the efficiency of vehicle combustion of fossil fuels reduces with altitude, due to low atmospheric pressure and low oxygen concentration, resulting in an increase in fuel consumption and particulate matter (PM) emissions. Likewise, high-altitude cities experience higher doses of solar radiation than other regions at the same latitude, favoring the photochemical processes that take place in the atmosphere (Chaffin & Ullman, 1994; Giraldo & Huertas, 2019; Graboski & McCormick, 1996; He et al., 2011; Nagpure et al., 2011; Pan et al., 2011; Wang et al., 2013a, b).

Moreover, people living in high-altitude need to compensate for the reduced availability of oxygen per volume of air. The first physiological response when exposed to low oxygen concentrations in high-altitude conditions is an increase in the basal metabolic rate (BMR, the amount of energy needed to maintain the body functioning), which induces an increase of the ventilation rate among other mechanisms. BMR is normally increased by approximately 17 to 27% for the first few weeks after exposure to hypoxia conditions and

gradually returns toward sea-level baseline (Beall, 2007). However, people living in the highlands have developed different physiological mechanisms that allow them to overcome the lack of oxygen (e.g. Andeans and Tibetans, two of the most ancient high-altitude cultures). It has been observed that some of the people living in very high-altitude regions share certain traits that result from the conditions in which they live; among them are: a shorter average height, enlarged thoracic cage, narrower alveolar to arterial O_2 gradients, increased lung capacities, greater uterine artery blood flow during pregnancy, and increased cardiac O_2 utilization, which overall suggests greater efficiency of O_2 transfer and utilization (Akunov et al., 2018; Beall, 2007; Fierce et al., 2016; Frisancho, 1977; Frisancho, 2013; Frisancho et al., 1999; Jansen & Basnyat, 2011; Julian & Moore, 2019; Li et al., 2018; Pérez-Padilla, 2022).

Tibetans, for instance, have shown to have a higher resting ventilation (15.0 L/min) compared to people living at sea level (11 L/min) as a way of coping with hypoxia (Beall, 2007). In contrast, Andeans have been shown to have similar resting ventilation than people living at sea level, but higher hemoglobin concentrations and higher erythropoietin levels. Oxygen saturation and hemoglobin concentration determine arterial oxygen content; hence, Andean highlanders appear to overcompensate for environmental hypoxia, showing higher arterial oxygen content. In contrast, Tibetans appear to be profoundly hypoxic compared to people living at sea level. In addition, pregnant high-altitude Andean natives have shown to increase the oxygen delivery to the uterus and placenta by increasing their ventilation and oxygen saturation (Beall, 2007; Julian & Moore, 2019). Therefore, although the magnitude and mechanisms through which altitude impacts exposure to air pollution remain under study, extreme conditions of hypoxia (leading to increased ventilation) increase the risks associated to air pollution exposure.

Among the largest high-altitude cities in LA ($\gtrsim$ 2 million inhabitants) we can mention: Mexico City (2850 m a.s.l., Mexico), Bogotá (2620 m a.s.l., Colombia), Quito (2240 m a.s.l., Ecuador), La Paz (3200-3600 m a.s.l.) and El Alto (4050 m a.s.l.). The limited number of existing air quality studies show that the most populated cities such as Mexico and Bogota, as well as the smaller city of Quito, experience a deteriorated air quality. The concentrations of PM_{10} and $PM_{2.5}$ recorded in these cities are summarized in Table 2 and 3. It is possible to observe that all studies show that the average concentrations exceed by far the maximum daily and annual average levels recommended by the WHO for both PM_{10} and $PM_{2.5}$.

Air quality studies conducted in these cities report two major common sources of PM, traffic and dust (Ramírez, et al., 2018a; Raysoni et al., 2017; Vega et al., 2012), often having an important anthropogenic element in dust resuspension. However, the implementation of emission control strategies such as the reduction of sulfur content in fuel, restriction of vehicular traffic and technological upgrades of industry are beginning to show results in the cities of Mexico and Bogota. For example, in Bogota, despite the fact that mobile sources have increased by 100% in the last decade, PM_{10} concentrations showed a consistent downward drift, and $PM_{2.5}$ concentrations did not appear to have worsened according to Mura (2020). On the other hand, in Mexico City, although the PM_{10} concentrations had not shown a significant improvement, Morton-Bermea et al. (2021)

reported that Pb, Co, Hg, Mn, As and Cd concentrations display a decreasing trend. This evidences the encouraging beneficial impact that actions propelled by air quality policies can have on PM emissions and the air quality in a city.

Table 2. Reported average concentrations of PM_{10} in high-altitude LA cities

	Average PM_{10} (Min-Max) [µg m^{-3}]	**Period**	**Study**
Mexico City, Mexico	(51-132)	March, 2006	(Mugica et al., 2009)
	(19-174)	Jul-Dec, 2000	(Gutiérrez-Castillo et al., 2005)
	66.1	Oct-Jan 2004-2014	(Morton-Bermea et al., 2021)
Quito, Ecuador	24.9-26.2	Jan-Oct, 2017	(Zalakeviciute, et al., 2020)
Bogotá, Colombia	55.64	1998-2018	(Mura et al., 2020)
	37.5	Jun 2015-May 2016	(Ramírez, et al., 2018a)

Table 3. Reported average concentrations of $PM_{2.5}$ in high-altitude LA cities

	Average $PM_{2.5}$ (Min-Max) [µg m^{-3}]	**Period**	**Study**
Mexico City, Mexico	35.05	2000-2002	(Vega et al., 2012)
	(32-70)	March, 2006	(Mugica et al., 2009)
	13.23-20.63	2015-2016	(Peralta et al., 2019)
Quito, Ecuador	10.87-13.45	2010	(Raysoni et al., 2017)
Bogota, Colombia	20.5	Feb, 2019- Mar 2019	(Mura et al., 2020)

2 Objectives of the present study

La Paz and El Alto form the second largest metropolitan region in Bolivia, and are considered among the highest metropolitan regions in the world (3000-4000 m a.s.l.). This conurbation is currently home to almost 2 million people (INE, 2020c). In the last decade, efforts have been made by the government, municipalities and the scientific community to assess air quality in this region. Regulations regarding the age of imported cars, implementation of alternative means of public transport, establishment of air quality monitoring networks, vehicle restrictions in city centers are some examples of these efforts. However, to our knowledge, no long-term air quality studies have been carried out to investigate the mass and chemical composition of particulate matter in this region with extreme and challenging conditions for its inhabitants.

In this context, this thesis seeks to identify and characterize the sources of particulate matter affecting air quality in the metropolitan region of La Paz and El Alto, as well as to investigate the dynamics and transport of pollutants from/towards/between both cities. It is also intended to assess the impact of exposure to air

pollution on the health of the inhabitants in the conurbation and to provide a baseline for air quality in this area onto which policy making and air quality regulations can be advised.

This work will be based on the air quality, meteorological and health parameters data collected between 2016 and 2019 at both cities. To achieve these objectives, it is intended to:

- Combine simultaneous online and offline measurements of physical and chemical properties of aerosol particles measured in La Paz and El Alto.
- Apply different source apportionment methods.
- Include existing emission inventories
- Combine air quality data with epidemiological responses to assess the possible existence and magnitude of the association between them.

These objectives will be developed through the following chapters:

Chapter II will be dedicated to the overall description of the sampling site, and the sampling and analysis techniques that were necessary to obtained the complete dataset.

Chapter III will describe the mathematical and statistical analysis performed on the datasets that enabled us to arrive to the results describe in chapters IV-VI.

Chapter IV will analyze the chemical composition of particulate matter in the PM_{10} fraction collected during the first year of the campaign in the cities of La Paz and El Alto. We will also assess the main sources of particulate matter by applying the PMF receptor model, in order to investigate the chemical profile, contribution and temporal variability of such sources.

Chapter V will proceed to characterize the concentrations of equivalent black carbon (eBC) measured between 2016 and 2018 at both cities. Both intensive and extensive properties of these absorbing particles will be described and different methods of black carbon source apportionment will be compared to quantify the contribution of local and regional combustion sources to the measured eBC mass concentrations.

Finally, Chapter VI will use the results of Chapters IV and V to identify the main sources of toxic particulate matter that contribute to the oxidative potential activity measured in both cities. Also, epidemiological records of the number of medical consultations due to acute respiratory infections (ARI) and pneumonias recorded in both cities will be combined with the air quality parameters developed in the previous two chapters in order to address the possible associations of these medical conditions to air pollution.

It is hoped that the scientific contribution of this work will not only allow a better understanding of the role that the city plays in terms of regional pollution, but also serve as a basis for effectively improving air quality policies, both in this region and in the rest of the country. It is also hoped that it can help to inform and raise awareness among the population about their own role in terms of emissions and exposure.

State of the Art

1. Air pollution and human health

The AQG proposed by the WHO include both, gaseous and particulate pollutants, which have been found closely linked to different health outcomes. Amongst the gaseous compounds included on the list are ozone (O_3), nitrogen dioxide (NO_2), sulfur dioxide (SO_2) and carbon monoxide (CO). Amongst the particulate pollutants are the mass concentrations of particulate matter (PM) and Lead (Pb), with PM as the most commonly parameter monitored by environmental institutions around the world (WHO, 2021b).

Ozone is a gas naturally found and balanced in the atmosphere with increased concentrations between 15 and 30 km a.s.l. (Ozone layer). However, tropospheric (ground-level) ozone concentrations can be increased due to the perturbation of its natural production cycle, mainly by the photochemical reactions of primary vehicular and industrial emissions of gaseous pollutants such as volatile organic compounds (VOC), carbon monoxide and nitrogen oxides (NO_2). Exposure to high concentrations of ozone have been associated to breathing problems, asthma triggering, reduced lung function and can lead to lung diseases (WHO, 2021b).

Nitrate oxides (including NO_2) result from high temperature combustion processes (e.g. vehicular and industrial emissions), and apart from being a precursor for tropospheric O_3, they can irritate the airways and aggravate respiratory diseases. CO is a byproduct of incomplete combustion of carbonaceous fuels, predominantly from vehicular emissions, that impairs the cells capability to bind to O_2 molecules. SO_2 is mainly emitted by sulfur containing fossil fuels used for transportation, industry, power generation or heating. The latter has been associated to hospital admissions for asthma (WHO, 2021b).

1.1. Effect of exposure to PM on human health

Mass concentrations of PM are commonly reported in two fractions: PM_{10} and $PM_{2.5}$, defined as the mass concentrations of aerosol particles having an aerodynamic diameter <10 µm and <2.5 µm, respectively. Due to their small size, $PM_{2.5}$ are more likely to deposit deep into the lung and reach the bloodstream. On the other hand, the PM_{10} fraction also includes the larger particles (coarse) which reach mainly the upper respiratory tract. PM_{10} concentrations are one of the most widely used air quality metrics worldwide in terms of particulate matter.

The impact that particles can have on health depends not only on their concentrations and their reach in the respiratory tract (i.e. their size), but also on their morphology and chemical composition. Epidemiological and toxicological studies have shown that exposure to compounds such as heavy metals (As, Cd, Co, Cu, Cr, Mn, Ni, Pb, V, Zn) can be toxic, carcinogenic, or mutagenic (Kong et al., 2012; Tchounwou et al., 2012; U.S. EPA, 2007). On the other hand, a statistically significant association between Cd, Zn, Pb, and acute changes in the cardiovascular and respiratory physiology was evidenced by studies like Cakmak et al. (2014). Other studies have demonstrated a statistically significant association between ED visits for asthma and fine particulate Zn,

as well as significant alterations in cardiac autonomic function as a result of exposure to Pb and V (Claiborn et al., 2002; Magari et al., 2002).

Although significant associations between PM_{10} and $PM_{2.5}$ concentrations have been widely found, this metric is not able to provide an insight into the elements that make up particulate matter. Moreover, the mass concentrations of PM are strongly influenced by the mass of particles in the coarse mode, while fine particles have shown to be the bigger health threat. Thus, there is a need to develop a metric that is more closely related to the health effects of air pollution, which would allow for more efficient emission reduction policies.

1.2. New metric for evaluating the effect of PM on human health – Oxidative potential (OP)

Oxidative stress is considered as one of the main mechanisms by which particulate aerosol particles induce biologic effects, and is defined as the imbalance between oxidant and antioxidant responses in the organism (Alfaro-Moreno et al., 2010). Therefore, excess oxidants will induce an increase in the production of reactive oxidant species in the cell (ROS). Oxidative potential (OP) is then defined as the ability of PM to generate ROS and is considered one of the most relevant indicators of PM toxicity (Gupta et al., 2020). This is why the Directive of the European Parliament and of the Council on Ambient air quality and Cleaner air for Europe has included OP as one of the air quality parameters to be monitored to understand the effects of air pollution on health and the environment (EU COMMISSION, 2022).

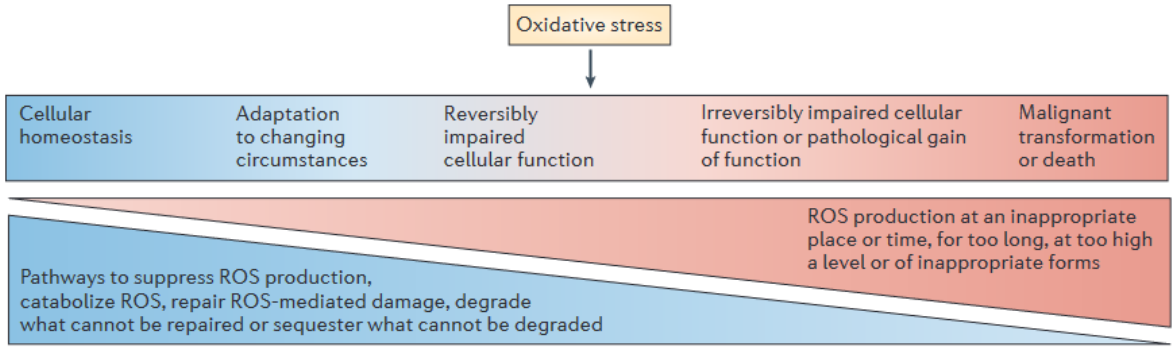

Figure 1. The broad spectrum of the ROS presence in the organism and the associated biological responses (Image extracted from Nathan & Cunningham-bussel, 2013)

The biological effects observed in the organism can be produced directly by certain PM components that stimulate ROS production within the cell, or indirectly by ROS produced by inflammatory mediators released by PM-stimulated macrophages. Chronic exposure to PM could severely affect cellular homeostasis by causing damage to lung, myocardial or neuronal cells, or could induce a state of general systemic inflammation and oxidative stress. Among the components identified as ROS generators of PM are As, Cd, Cr, Pb, Cu, Mn; ferrous ions and PAHs (Alfaro-Moreno et al., 2010).

Although progress on the standardization of OP measurements is being made, there is not an assay capable of completely mimicking the mechanisms of ROS production in the organism. Each of the different assays has a different sensitivity to different compounds. The use of one assay or another is limited by the availability and

accessibility of the assays. Thus, it is not possible to speak of one assay being superior to the others, but they are rather complementary and allow a more complete picture of oxidative stress.

Several methods have been developed over the last decades to measure OP of PM which can be classified into two main groups: cellular and acellular assays. Cellular assays measure the biological and molecular mechanisms associated with PM cell toxicity. In contrast, acellular assays provide a faster, more practical, less controlled and less expensive reading of PM toxicity (Gupta et al., 2020; Hedayat et al., 2015). These assays usually measure the consumption of a cellular reductant surrogate (e.g. dithiothreitol, DTT), the consumption of antioxidants (e.g. ascorbic acid, AA), the formation of OH radicals, or the ROS concentration (H_2O_2) by chemiluminescence or fluorescence (dichlorofluorescin, DCFH) (Gupta et al., 2020). In the following, three of the most extensively used assays, which were used in the framework of this thesis, will be described:

- OP_{DTT}: DTT is considered a chemical surrogate to cellular reductant agents (e.g. nicotinamide adenine dinucleotide phosphate oxidase, NADPH; nicotinamide adenine dinucleotide, NADH) used to mimic in vivo interactions of PM and biological oxidants (Bates et al., 2019; Borlaza et al., 2021b; Kumagai et al., 2002). The DTT assay is based on the ability of the redox-active compounds in PM to transfer electrons from DTT to oxygen, hence producing ROS (Cho et al., 2005). OP_{DTT} is typically sensitive to organic species (e.g. polycyclic aromatic hydrocarbons (PAHs) and quinones, and high concentrations of transition metal ions (Charrier & Anastasio, 2012).
- OP_{AA}: AA is one form of vitamin C and is one of the physiological antioxidants that inhibits the oxidation of lung cells (Hedayat et al., 2015; Valko et al., 2005). The in-vitro measured AA depletion due to PM represents the in-vivo degree of antioxidants oxidation. OP_{AA} have shown to be most sensitive to transition metals and organic biomass tracers (Charrier & Anastasio, 2012; Daellenbach et al., 2020).
- OP DCFH: DCFH is a non-fluorescent reagent that becomes fluorescent when oxidized. In the presence of reactive oxygen species and horseradish peroxidase, DCFH could be rapidly oxidized to a fluorescent compound (DCF). This technique is commonly used to measure the ROS present within and/or or attached to PM (Bates et al., 2019). It has been extensively used for investigating atmospheric ROS, and ROS derived from cigarette smoke and diesel (Hedayat et al., 2015).

2. Atmospheric aerosol particles

Defined as the solid or liquid particulate material suspended in the air (excluding water vapor), aerosol particles can have its origin in natural (e.g. mineral dust, pollen, sea salt) and anthropogenic (e.g. heavy metals, soot) emissions. Depending on the atmospheric region in which they are found, a distinction can be made between tropospheric and stratospheric particulate aerosols. They are considered primary if they are emitted by sources directly into the atmosphere, and secondary when they arise from the transformation of primary precursor components by atmospheric chemical processes (e.g. ammonium nitrate (NH_4NO_3), ammonium sulfate ($(NH_4)_2SO_4$)) (Ahrens, 2012; Seinfeld & Pandis, 2016).

2.1. Physical properties of atmospheric aerosol particles

2.1.1. Size and morphology of aerosol particles

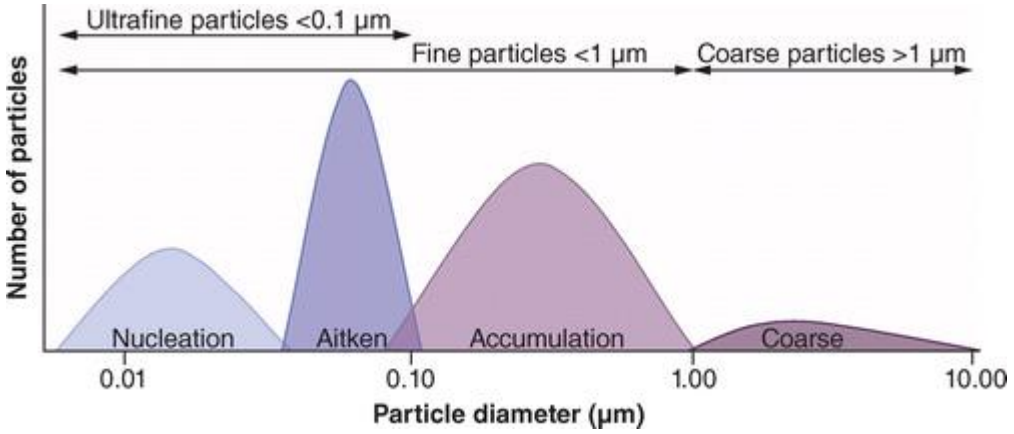

Figure 2. Graphical representation of the different particle size modes (Extracted from Sánchez de la Campa et al., 2013).

Particle size is a fundamental parameter for particle description. Due to their small size, particles become a threat for human health since, when inhaled, they can reach deep into the lungs. The size range of atmospheric aerosol particles comprises 5 orders of magnitude (~1-10^5 nm), and it is divided into 3 main groups according to their size: coarse, fine and ultrafine (Figure 2). Moreover, ultrafine particles are divided into two sub-modes: the nucleation and the Aitken mode. Each group has different chemical, optical and aerodynamic properties that will determine their interaction with the environment and its effect on human health. Larger particles (coarse) have a shorter lifetime in the atmosphere and generally result from natural or mechanical processes and mostly affect the upper tract of the respiratory system. Smaller particles, on the other hand, result from the formation of stable clusters of primary gaseous components that are found in the atmosphere. This process takes place naturally in the atmosphere, but can also be induced by anthropogenic emissions (Baron & Willeke, 2005; Seinfeld & Pandis, 2016). Moreover, ultrafine particles can potentially reach the bloodstream, which allows them to be distributed to the rest of the body.

During their stay in the atmosphere, aerosol particles undergo aging processes that modify their physical and chemical properties. This happens due to three main physical processes: Adhesive forces, coagulation and condensation (Baron & Willeke, 2005).

The growth of ultrafine particles happens in a matter of hours, yet becomes less efficient as the particles grow. In the atmosphere the dominant mode in terms of particle numbers concentrations is the accumulation mode since the aging and removal processes in this fraction of the size spectrum are less efficient. Typical particle number concentrations (PNC) within this mode are around the tens of thousands of particles per cubic meter (cm^{-3}), whereas in the coarse mode, ambient concentrations can even be lower than one. In contrast, particle mass concentrations (PM) are dominated by the coarse mode. (Seinfeld & Pandis, 2016).

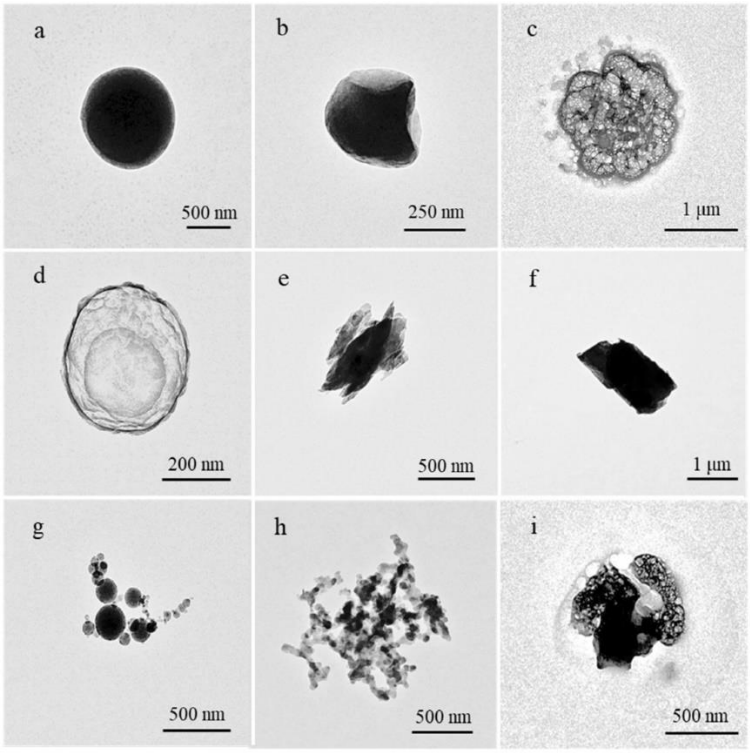

Figure 3. TEM images of different aerosol particles types. (a) Spherical organic particle. (b) Irregularly shaped organic particle. (c) Non-volatile sulfate. (d) Foamed sulfate. (e) Mineral: Si + Al. (f) Mineral: Ca. (g) Fly ash particles. (h) Soot particles. (i) K-rich particle (Image extracted from Liu et al., 2022).

Atmospheric aerosol particles can often present irregular shapes. Figure 3 is an example of images taken with a transmission electron microscope that shows the different size and shapes ambient aerosol particles can have. Thus, the shape factor χ is defined as the ratio between the drag force felt by a non-spherical particle and the drag force experienced by a spherical particle of equivalent volume. This parameter allows to quantify the degree of particle irregularity, i.e. the effect that the shape of a non-spherical particle has on the drag force it experiences when being transported in a flow. χ takes the value of 1 if the particle is spherical, and greater than one if the particle is irregular. The larger this parameter is, the more the shape of the particle will differ from that of a sphere, thus decreasing its mechanical mobility. Shape is an important factor to consider when studying the aerodynamic properties of aerosol (Seinfeld & Pandis, 2016). Morphology of particles is equally important in terms of health, since the exposure to fiber-shaped aerosols (e.g. asbestos) has proven to be highly detrimental to health, increasing the risk of developing lung diseases such as cancer (Bernstein, 2022; U.S. EPA, 2022).

2.1.2. Optical properties of aerosol particles.

Similar to molecules, aerosol particles have the ability to interact with electromagnetic radiation in different ways (Figure 4). When a beam of light reaches a particle, depending on its size, its physical structure and its chemical composition, the incoming radiation can be:

- absorbed: when the incident radiation is transformed into thermal radiation (Seinfeld & Pandis, 2016).
- elastically scattered: redirected without loss of energy (reflection, refraction, diffraction; $\lambda_0=\lambda_1$) (Seinfeld & Pandis, 2016).
- momentarily absorbed (exciting the electrons in the particle) and re-emitted with a lower energy proportional to the energy difference between two electron levels (i.e. fluorescence, $\lambda_0<\lambda_1$) (Seinfeld & Pandis, 2016).
- Inelastically scattered: redirected with a loss of energy (Raman scattering: less frequent process; $\lambda_0<\lambda_1$) (Seinfeld & Pandis, 2016).

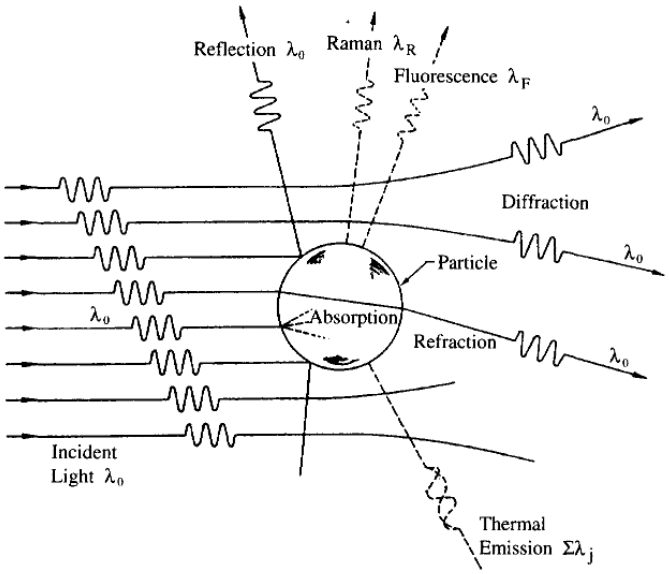

Figure 4. Schematic illustration of the interactions of electromagnetic radiation and aerosol particles (Image extracted from Seinfeld & Pandis, 2002, page 692)

2.2. Chemical properties of atmospheric aerosol particles

The chemical composition of atmospheric aerosol particles depends both on the emission sources and on the biological, physical and chemical processes that take place in the atmosphere. It is also strongly linked to meteorological conditions that change throughout the seasons. Among the major components of PM, we can broadly distinguish between organic and inorganic compounds, which can come from both natural and anthropogenic sources.

2.2.1. Organic compounds

Organic compounds or organic matter (OM) are chemical compounds whose structure contains carbon atoms that form covalent bonds with atoms such as hydrogen, oxygen and nitrogen (Seinfeld & Pandis, 2016). Organic compounds make up a significant fraction of the mass of PM. In turn, between 50% and 60% of the mass of organic matter is made up of organic carbon (OC) (Kchih et al., 2015; Ni et al., 2013; Terzi et al., 2010; Turpin et al., 2010). OC is defined as the fraction of carbonaceous aerosol particles that volatilizes at

temperatures below 550°C (Bond & Bergstrom, 2006). It can be emitted from both natural and anthropogenic sources, such as vehicular traffic, biomass burning, or by the condensation of low-volatility products of the photooxidation of hydrocarbons (Seinfeld & Pandis, 2002).

Examples of particulate organic compounds emitted naturally into the atmosphere include sugar alcohols and methanesulphonic acid (MSA). These compounds are emitted by primary and secondary aerosol sources, respectively. While sugar alcohols, also known as polyols (arabitol, sorbitol, mannosan) are emitted by bacteria and fungi between late spring and early fall, MSA comes from the oxidation of dimethyl sulfide (DMS), a precursor naturally emitted by living organisms such as phytoplankton in oceans and lakes, the forest biota and other terrestrial biogenic sources (Samaké, et al., 2019a, b; Seinfeld & Pandis, 2002).

Anthropogenic organic compounds include monosaccharide anhydrides (levoglucosan, mannosan, galactosan), polyaromatic aromatic aerosol particles (PAH), alkanes and hopanes. All these compounds result from combustion. In the case of monosaccharide anhydrides, these are the product of the degradation of cellulose contained in vegetation when subjected to temperatures above 300°C and are considered unequivocal tracers of biomass burning. On the other hand, PAHs, alkanes and hopanes are emitted by the burning of fossil fuels and lubricating oils (Fraser 2000; Zielinska et al., 2004a, b).

2.2.2. Inorganic compounds

This second group comprises the rest of the components found in PM, including elemental carbon (EC). They can also be natural or anthropogenic in origin. Inorganic compounds naturally emitted into the atmosphere include compounds that form part of sea salts (Na^+, Cl^-,SO_4^{2-}, Ca, K) (Lewis et al., 2004), crustal material (Al, Fe, Ti, Ca, K, Mg, Mn, P, Si) (Alastuey et al., 2016; Pérez et al., 2008), or those that arise from the disaggregation of magma in volcanic eruptions (e.g. Ti, Fe, Al, Mn, F, Li) (Henley & Berger, 2013). Sea salts, on one hand, are released from sea-spray droplets produced at the air-sea interface due to the dynamic effect of the wind on the sea surface (Lewis et al., 2004). Similarly, mineral dust is naturally resuspended by the dynamic effect of wind on the land surface, or anthropogenically resuspended by the friction of vehicle tires with the road, or near construction sites. Mineral dust represents an important fraction of PM mass concentrations, especially in arid and desertic areas (Alastuey et al., 2016; Goudie & Middleton, 2001; Pérez et al., 2008).

Inorganic compounds related to anthropogenic activities include EC, compounds related to vehicular emissions (Fe, Cu, Sn, Sb, Ba, S, Pb, Mn, Zn), biomass burning (K^+, Rb), and mining (Ni, V, Pb, Ag, Cs, Rb) (Bond & Bergstrom, 2006; Charron et al., 2019; Godoy et al., 2005; Jordan et al., 2006; Nava et al., 2015). In urban areas, vehicular emissions represent an important fraction of the PM mass (Querol et al., 2004). Not far behind is biomass burning as an energy source or for agricultural purposes, affecting air quality globally (Nava et al., 2015). On their side, industrial emissions are important sources of heavy metal emissions in industrial regions (Querol et al., 2002).

The group of inorganic compounds that are formed from chemical reactions that take place in the atmosphere are called secondary inorganic aerosol particles (SIA). Amongst the gaseous precursors of such aerosol particles are sulfur dioxide (SO_2), nitrogen oxides (NO_x) and ammonium (NH_4). SO_2 can be emitted by both natural sources (volcanic emissions) and anthropogenic sources (fossil fuel burning, industrial processes). On the other hand, NO_x is mainly emitted by vehicular sources, and NH_4 comes from the volatilization of fertilizers used in agriculture (Seinfeld & Pandis, 2016).

2.3. Light absorbing aerosol particles

Despite their scarce presence in the atmosphere, absorbing aerosol particles have become the object of major concern. They have proven to be a major absorbing component in the atmosphere, and the main absorber in the visible spectrum. The first step in understanding this sub-group of aerosol particles lies in understanding the terminology used to describe them.

2.3.1. Terminology

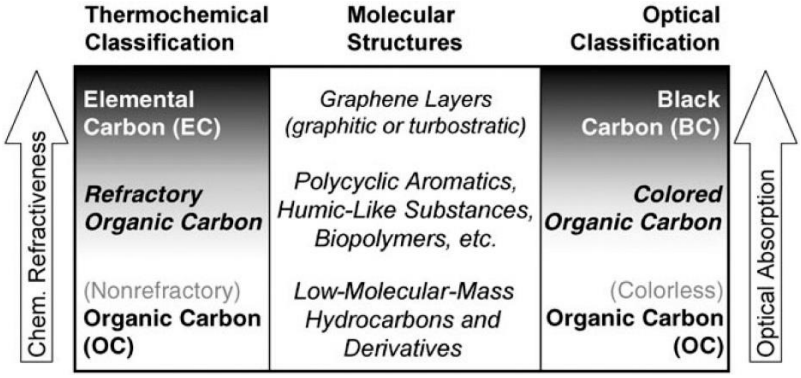

Figure 5. Optical and thermochemical classification of atmospheric carbonaceous particulate matter (Image extracted from Laskin et al., 2015)

In the literature there are several different terms to refer to aerosol particles capable of absorbing radiation in the visible spectrum. These terms are strongly related to the technique used for their detection. Among them, the following terms stand out:

- *Soot:* This refers broadly to any type of atmospheric aerosol generated in combustion that has a dark appearance and contains carbon (Bond & Bergstrom, 2006).
- *Elemental Carbon (EC):* This term refers to the stability of carbonaceous compounds with respect to elevated temperatures, i.e. carbonaceous compounds that are non-volatile below 550°C (Bond & Bergstrom, 2006).
- *Black carbon (BC):* This term is used to refer to black-appearing particles that absorb efficiently across the entire visible radiation spectrum, whose absorption has a weak dependence on wavelength (λ), that have a vaporization temperature above 4000 K and which are also insoluble in water or other organic solvents. This term is strongly linked to optical absorption measurement techniques, especially filter-based techniques (Bond & Bergstrom, 2006; Lack et al., 2014).

- *Refractory carbon (rBC):* Refractory materials are inorganic, non-metallic, porous and heterogeneous materials that have a thermally stable structure. For vehicular emissions using diesel fuel, a strong correlation between EC and rBC was found. This correlation, however, does not necessarily hold for all forms of carbon (Bond & Bergstrom, 2006).
- *Brown carbon (BrC):* Although organic carbon was initially considered to be a non-absorbing compound, in recent decades it has been observed that a fraction of organic carbon is capable of absorbing radiation in the visible spectrum, and that its absorption efficiency increases as the wavelength decreases, thus giving it a brown appearance (Bond & Bergstrom, 2006; Laskin et al., 2015).

2.3.2. Intensive and extensive properties of absorbing aerosol particles.

The term extensive refers to the group of properties that help describe the material but are dependent on the abundance of it, e.g. mass concentration. In contrast, the intensive properties are intrinsic to the material, regardless the abundance. Among the most important physical properties used to describe the absorbing aerosol particles can be found:

- Absorption coefficient $b_{abs}(\lambda)$: This extensive property quantifies the amount of visible light lost by absorption due to the presence of absorbing aerosol particles in the optical path and its units are [Mm^{-1}]. The more abundant absorbing particles are in the optical path, the larger the magnitude of the absorption coefficient. Typical urban background absorption coefficients vary between cero and a few hundred Mm^{-1} (Bond & Bergstrom, 2006; Seinfeld & Pandis, 2016).
- Absorption Ångström exponent (AAE): This dimensionless intensive parameter describes the wavelength dependency of the particle's absorption coefficients within the visible spectrum of electromagnetic radiation (Seinfeld & Pandis, 2016).

$$b_{abs}(\lambda) \sim \lambda^{-AAE} \quad [1]$$

Typical values of strongly absorbing aerosol are in the order of 1. The AAE reported in the literature for BrC, in contrast, ranges between 0.9 and 2.5 depending on the conditions in which it is produced. Dust particles have also shown to be less efficient absorbing agents with very high AAE, typically > 2 (Bond et al., 2013; Bond & Bergstrom, 2006; Caponi et al., 2017; Kirchstetter et al., 2004; Sandradewi et al., 2008).

- Mass absorption cross section (MAC): This intensive parameter quantifies the probability of photons being absorbed by the presence of an absorbing aerosol particle, and is normalized by the mass of given particle. At the same time, this parameter represents the link between the mass concentration of absorbing aerosol particles and their impact on climate, as follows:
  - $m_{BC} \cdot MAC(\lambda) = b_{abs}(\lambda)$ [2]

The units in which it is described are [$m^2\ g^{-1}$]. Several MAC values have been reported in the literature for different types of aerosol particles ranging from 5 to 13.6 check [$m^2\ g^{-1}$], the lowest being the MAC

expected for fresh BC. At the higher end of the range are found the MAC values obtained for BrC or aged aerosol particles.

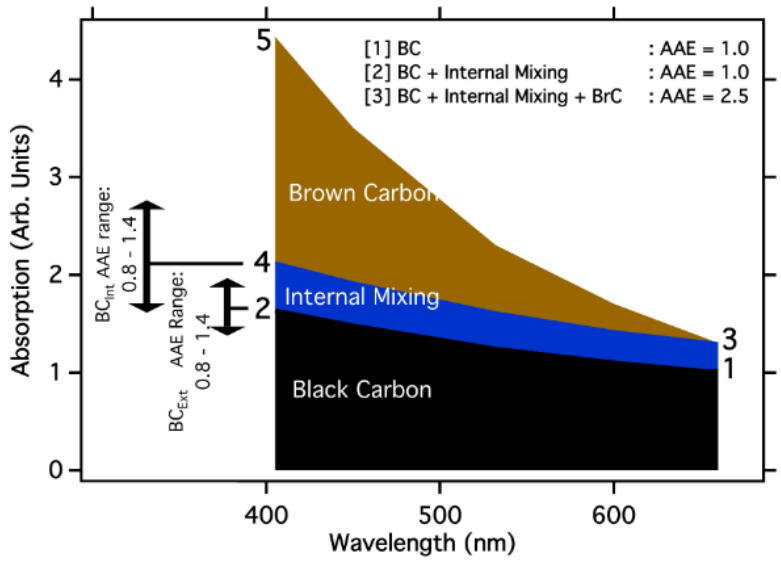

Figure 6. Illustration of the wavelength dependency of absorption throughout the visible spectrum of BC and BrC (Image extracted from Lack & Langridge, 2013).

2.3.3. Mixing state and aerosol absorption enhancement.

The interaction between radiation in the visible spectrum and absorbing particles does not only depends on the optical properties of individual aerosol particles but can be modified by the type of mixing that exists in the aerosol population. Aerosol mixing can occur on very short time scales for polluted urban air (within hours), where black carbon (BC) particles are rapidly coated with additional materials (Jacobson, 2001; Moteki et al., 2007; Riemer et al., 2004; Shiraiwa et al., 2007). Among the most studied mixing states of absorbing aerosol particles with other non/slightly absorbing particles, the following three can be highlighted (Figure 7):

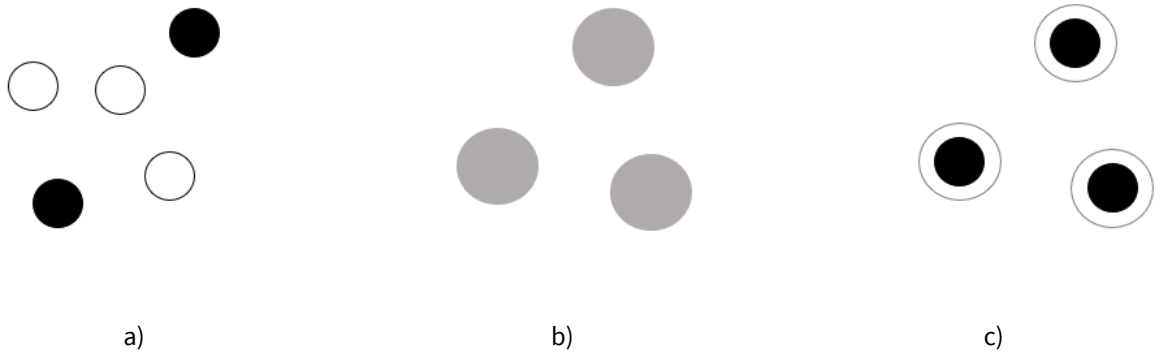

a) b) c)

Figure 7. Illustrative diagram of the types of aerosol mixture: a) External mixture, b) Homogeneous internal mixture and c) Heterogeneous internal mixture (core-shell).

- External mixing: This type of mixing occurs when different types of aerosol particles coexist independently of each other (Figure 7.a). This type of mixing usually occurs close to the emission source.
- Homogeneous internal mixing: In this type of mixing the aerosol species are completely mixed, to the point of being practically indistinguishable (Figure 7.b). In the atmosphere, this type of mixing is very unlikely to occur.
- Heterogeneous internal mixture: This is the most studied type of mixture in the literature; more precisely, the case in which absorbing particles are encapsulated by an envelope of non-absorbing material. This system is often called core-shell. (Figure 7.c) (Bond & Bergstrom, 2006; Bond et al., 2006; Gangl et al., 2008; Jacobson, 2001).

When non-absorbing substances coat the absorbing nuclei, they can focus the incident light towards the center of the particle, thus increasing their absorption efficiency. This effect is called the "lens effect" (Chan et al., 2011; Fuller et al., 1999; Lack & Cappa, 2010). Thus, the absorption efficiency of absorbing particles increases when some type mixing exists, i.e., the MAC of the resulting aged particle increases. Theoretical studies that have addressed this issue from a theoretical point of view suggest absorption amplification factors ranging from 1.3 to 4.0 for atmospheric aerosol particles (Bond et al., 2011; Bond & Bergstrom, 2006; Bond et al., 2006; Chung et al., 2012; Fuller et al., 1999; Sato et al., 2003). On the other hand, laboratory experiments using absorbing and non-absorbing aerosol surrogates with optical properties similar to those of atmospheric aerosol particles report amplification factors ranging from 1.2 to 3.5 (Khalizov et al., 2009; Mikhailov et al., 2006; Saathoff et al., 2003; Schnaiter et al., 2005; Shiraiwa et al., 2010; Xue et al., 2009; R. Zhang et al., 2008). Experimental studies under ambient conditions that quantified this effect reported enhancement factors between 1.06 and 10, which depend on the location of the experiment, the meteorological characteristics of the experiment and the experimental design (Cappa et al., 2012; Cheng et al., 2009; Moffet & Prather, 2009; Nakayama et al., 2014; Schwarz et al., 2008; Shiraiwa et al., 2008; Wang et al., 2014).

2.3.4. Detection techniques for absorbing aerosol particles

Although there is no reference instrument for absorption measurements, there are four commonly used methods for measuring absorption. Depending on the application and availability of resources, certain techniques may be more appropriate than others. Each method has certain advantages over the others, but also certain limitations, which will be briefly discussed below:

- The **extinction minus scattering** method: Independent measurements of extinction and scattering coefficients are taken, and the absorption coefficients are calculated as the difference of the previous two magnitudes. However, for low concentrations or predominantly dispersed aerosol particles, the uncertainties of the absorption coefficients derived from this method can be very large. (Horvath, 1993, 1997; Arnott et al., 1999; Bond et al., 1999; Weingartner et al., 2003; Sheridan et al., 2005; Virkkula et al., 2005; Bond & Bergstrom, 2006; Moosmüller et al., 2009).

- In the **photo-acoustic** method, the absorption coefficient is retrieved from the sound wave produced by the heat transfer resulting from the modulated exposure of the aerosol sample to intense visible radiation (laser) at a certain frequency. Although this method is much more accurate, there is an uncertainty related to the energy lost by the vaporization of volatile compounds inside the chamber (which can be counted as absorbed energy), and to the reduction of the photo-acoustic signal associated with the relaxation time (which depends on the particle diameter). These instruments are often used as calibration references. (Arnott et al., 2003; Raspet et al., 2003; Bond & Bergstrom, 2006; Moosmüller et al., 2009).
- The **incandescence** method consists of exposing the sampled atmospheric particles (still suspended in the collected air sample inside a chamber) to a very intense laser. These suspended particles interact by scattering and absorbing the laser light elastically. Thus, the absorbing particles are heated to their vaporization temperature, producing a laser-induced incandescence (LII) pulse. This LII signal is a function of the mass of BC (Gao et al., 2007; Moteki & Kondo, 2007).
- **Filter-based** measurements, in which aerosol particles are deposited on a filter tape, are commonly performed in field campaigns due to their simplicity and relative low cost. They are widely used by environmental monitoring networks. In this method, the absorption coefficients are deduced from the change in attenuation of a light source, when passing through the filter, caused by the presence of absorbing particles deposited onto it. One of the disadvantages of filter-based instruments is that in situ measurements are not possible, leading to artifacts related to multiple scattering by the filter media and media loading effects. However, many studies have focused on the necessary corrections for possible alterations of aerosol properties using this method. (Bond et al., 1999; Moosmüller et al., 2009; Virkkula et al., 2005; Ogren, 2010, Nakayama, 2010). Some examples of filter-based absorption photometers are the Multi-angle Absorption Photometer (MAAP; Thermo Scientific, Waltham, USA; described in Petzold et al. (2005)) and the Aethalometers (Magee Scientific, Berkley, USA.; described in Arnott et al., 2005; Drinovec et al., 2015; Weingartner et al., 2003). In addition to allowing the calculation of the absorption coefficients of the particles collected on the filter, these instruments often report the equivalent concentrations of BC mass deposited on the filter (eBC), i.e., the equivalent mass of BC required to produce the measured absorption. This is achieved by using a MAC factor determined by the instrument supplier (equation [2] presented in the previous section). It is important to make this distinction between BC and eBC since filter-based instruments have proven to be also sensitive to the absorption of organic compounds such as BrC (Bond et al., 2013).

2.4. The role of aerosol particles in the environment and their impact on Climate

Since both, air pollution and climate change, are driven by anthropogenic activities, they come about as two intertwined issues that cannot be isolated from each other. Regulating emissions to improve air quality will indisputably have repercussions on climate change. However, the timescales for the observables improvements resulting from reducing emissions are very different. Whilst almost immediate air quality

improvements can be expected following a decrease in pollutant emissions, improvements in terms of climate change can only be expected after several decades due to the long lifetime of climate change main drivers.

Specifically, due to their ability to interact with radiation and their small size, aerosol particles have both direct and indirect impacts on climate. Among the immediate and most noticeable effects of aerosol particles is the decreased visibility. Moreover, the International Panel for Climate Change (IPCC) has included aerosol particles as an important component in the radiative forcing calculations. The overall effect of atmospheric aerosol particles results in negative forcing (-1.1 [-1.7 to -0.4] Wm^{-2} (medium confidence) i.e. cooling effect), mitigating the effect of greenhouse gases (GHG) (Forster et al., 2021). At the same time, aerosol particles inhomogeneous distribution and its indirect effects on Climate make of aerosol particles one of the important sources of uncertainties in the radiative forcing (RF) calculations (Arias et al., 2021). Hence, a general decrease in particle concentrations in the interest of public health would actually reduce the mitigative radiative effect of aerosol particles, thus contributing to climate change.

Furthermore, BC is considered the most absorbing component in the visible spectrum. This compound reemits the absorbed radiation in the form of thermal energy and has the capability of heating adjacent air molecules, thus potentially changing the thermal profile of the surrounding atmosphere. Moreover, BC has the ability to change the albedo of the surfaces onto which it is deposited, e.g. ice and snow, which causes more energy to be absorbed by those surfaces, accelerating the melting process (Arias et al., 2021).

In addition, an increase in anthropogenic aerosol emissions can have important secondary effects on the climate. Since aerosol particles are excellent condensation nuclei, an increase in aerosol particles concentrations leads to an increased number of droplets in clouds with a smaller size. This prolongs in return the cloud's lifetime, changes its optical properties and can potentially modify the precipitation patterns. According to the IPCC report, the overall effect of anthropogenic aerosol particles is to reduce global precipitation through surface radiative cooling effects (high confidence) (Arias et al., 2021).

Sampling Methodology and Data Acquisition

1. Study site

The long-term "campaign", had its origin on the influence the metropolitan region of La Paz-El Alto had on the measurements taken at the Chacaltaya Global Atmospheric Monitoring Station (CHC-GAW), located approximately 20 km away from the metropolitan area. This gave rise to the joint effort of installing two complete air quality monitoring stations working simultaneously in each city in order to characterize the urban emissions[1].

On one hand, El Alto (4050 m a.s.l.) is a fast growing and relatively new city. El Alto city initially began as an extension of the city of La Paz and was only established as an independent city less than fifty years ago. However, El Alto has become the second largest city in Bolivia in terms of population, with over 1.109 million inhabitants estimated by 2022 (INE, 2020c). It is situated on the plateau formed between the two branches of the Andes passing through Bolivia, which is a region characterized for being very high, flat, dry (hence dusty) and open. Due to the recentness of their constitution as a city and its fast growth, the number of streets that are not yet paved is large and there are still plenty unoccupied areas. Hosting the largest international airport in the country, El Alto constitutes one of the most important connections of the Bolivian seat of government (La Paz) to other regions within and outside the country. The airport and two of the biggest interprovincial highways that traverse El Alto converge at the most congested part of the city, at the cliff that delimits the city of La Paz from the city of El Alto. At this point also converge the main uphill highway connecting both cities, which is why in the recent years vehicular restrictions were implemented around this area to reduce traffic congestions. Moreover, the little Industry found in the metropolitan area is mostly located in the city of El Alto.

In contrast, La Paz (3200-3600 m a.s.l.) spreads along the mountain valley formed between the Altiplano plateau and the Oriental Andes mountain range. Characterized by its hilly topography and steep streets, La Paz hosts approximately over 956 thousand inhabitants (INE, 2020c). In La Paz, scarce space for urban growth is left, and most streets and avenues are paved. During rush hours, traffic congestion is experienced all throughout the city for which vehicular restrictions were implemented in the city center.

---

[1] Former Laboratoire de Glaciologie et Géophysique de l'environnement (LGGE), current Institut des Géosciences de l'Environnement (IGE)
Leibniz Institute for Tropospheric Research (TROPOS)
Institute of Environmental Assessment and Water Research (IDAEA-CSIC)
Laboratoire Environnements, Dynamiques et Territoires de Montagne (EDYTEM)
Department of Environmental Science & Bolin Centre for Climate Research, Stockholm University
Institut de Recherche pour le Développement (IRD)
Institute for Atmospheric and Earth System Research, Helsinki University
Aerosol d.o.o. (Magee Scientific)
Institute of Atmospheric Sciences and Climat (ISAC)
Paul Scherrer Institute (PSI)

2. Sampling sites.

In order to assess the properties of the urban background pollution, an urban background sampling site was installed in each city, where several ambient and meteorological parameters were measured simultaneously. The sampling sites were located 7 km apart, with an altitude difference of more than 400 m, and distancing approximately 20 km from the Chacaltaya Global Atmosphere Watch (CHC-GAW) monitoring station (Figure 1).

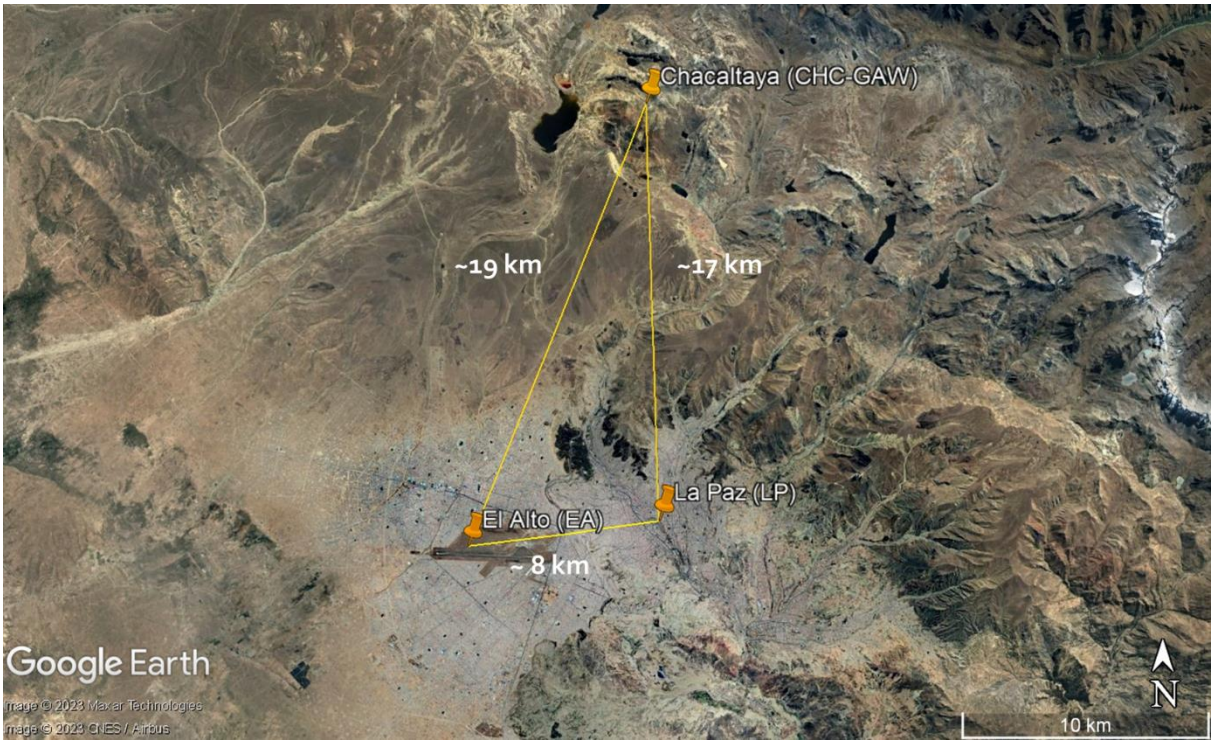

Figure 1. Google Earth® satellite images of the sampling sites of the campaign (EA and LP), with respect to the Global GAW monitoring station (CHC-GAW).

The El Alto (EA) measurement site was installed within the El Alto International Airport, in the facilities of the meteorological observatory (16.5100° S, 68.1987° W, 4025 m a.s.l.). The observatory was at a distance of approximately 300 m from the airport runway and 500 m from the nearest major road. The airport traffic is generally low, especially during the day and no significant spikes in the measured parameters (CO_2, PM) was observed during takeoff or landing of aircrafts. Road traffic within the airport perimeter is almost non-existent. The area around the sampling site is unpaved, hence dusty, and there are no other buildings in the proximity of the observatory (Figure 2).

La Paz measurement site (LP) was placed on the rooftop of the city's Museum Pipiripi (Espacio Interactivo Memoria y Futuro Pipiripi: 16.5013°S, 68.1259°W, 3600 m a.s.l.). This municipal building is located on a small hilltop downtown La Paz. Unlike the EA site, within a 1 km radius, the LP site is surrounded by many busy roads and dense residential areas, with a horizontal and vertical minimum distance to the nearest road of approximately 70 and 45 m, respectively. Otherwise, the site's immediate surroundings (~100 m radius) are

covered by green areas and a municipality buses parking lot at the base of the hill. Since the sampling site is located within downtown, the transit of heavy vehicles (apart from public buses) is limited (Figure 3).

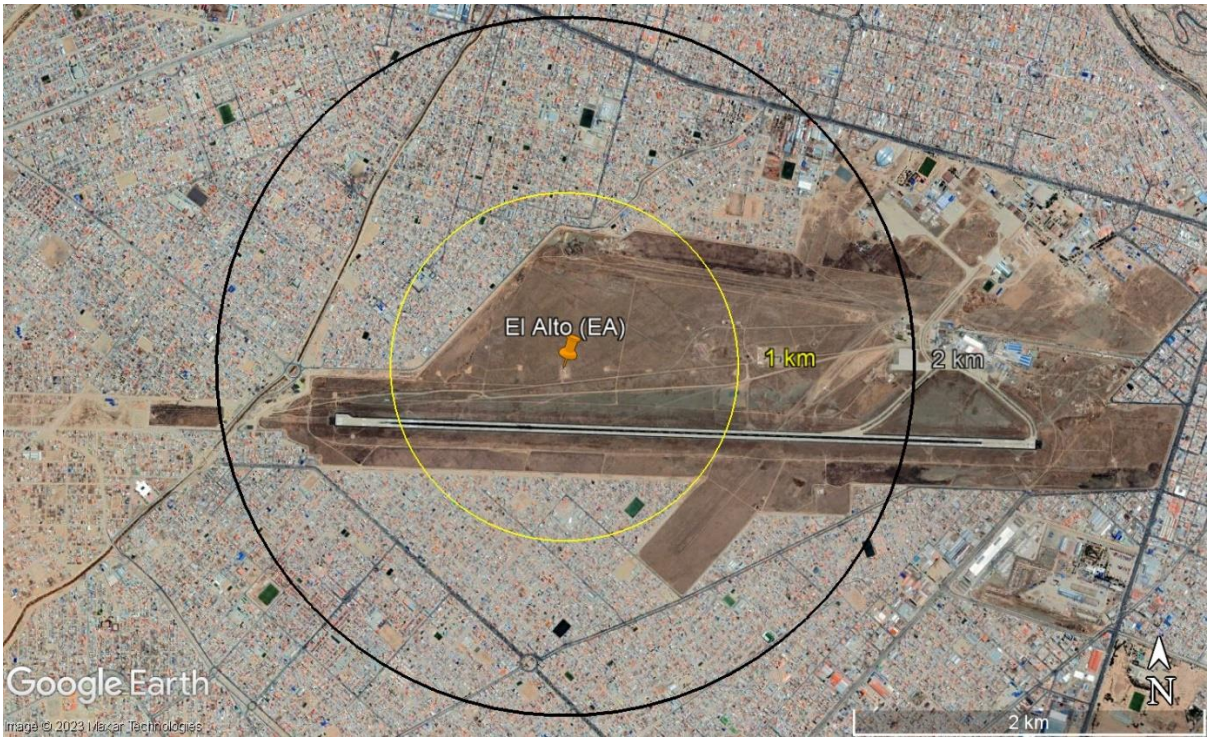

Figure 2. Google Earth® satellite images, closer look on EA sampling site.

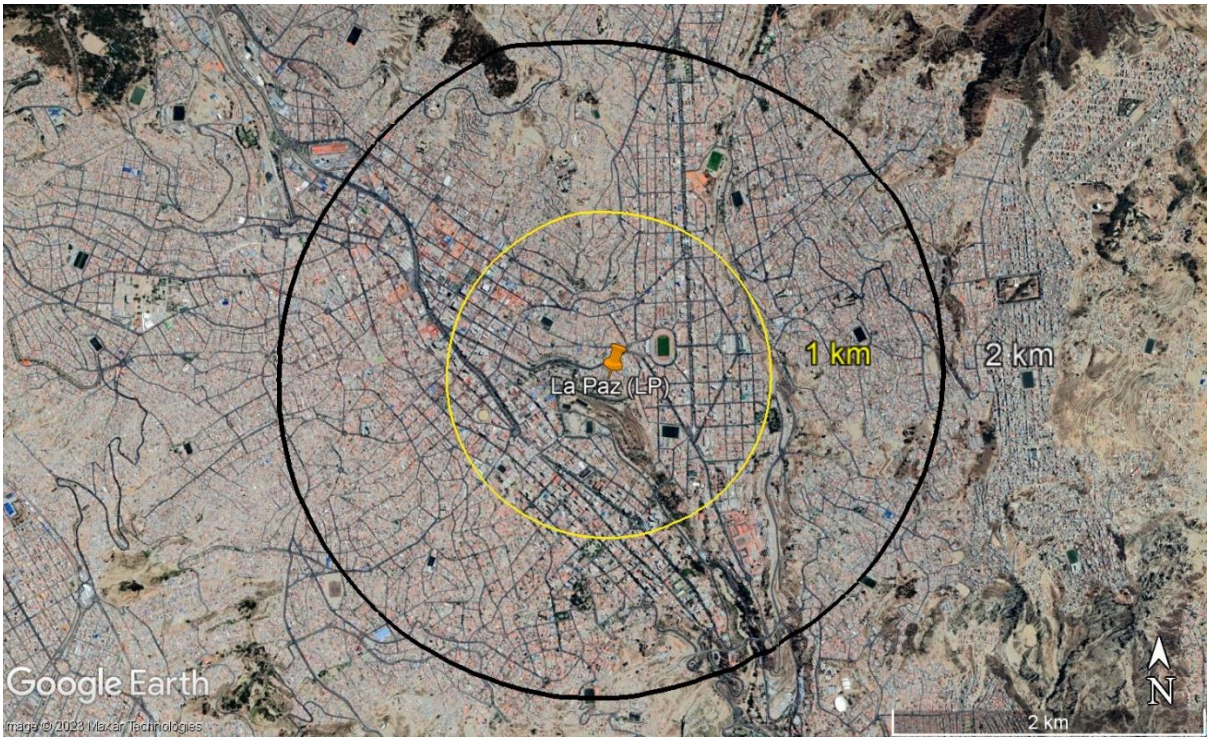

Figure 3. Google Earth® satellite images, closer look on LP sampling site.

The sampling campaign of particulate matter was carried between April 2016 and November 2018, with an extension of PM sampling in La Paz until March 2019. In addition, O_3 online monitoring started in 2021. The campaign combined online and offline techniques for the chemical and physical characterization of the atmospheric aerosol particles. To better understand the different sampling periods of each of the instruments and samplers employed, Figure 4 displays the availability of data throughout the years 2016 to 2019 on a weekly basis. Having a clear idea of the data availability will facilitate the discussion on the advantages and limitations on the dataset in the following sections.

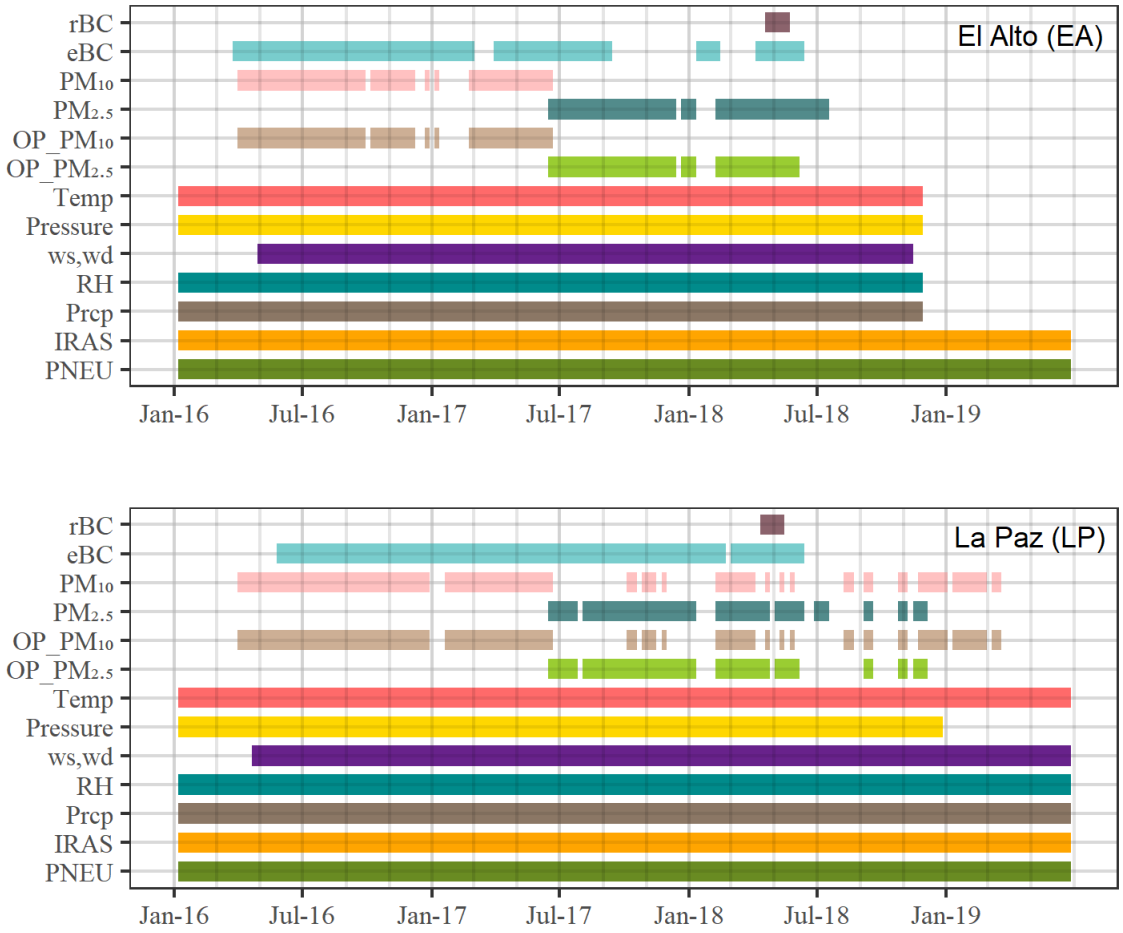

Figure 4. Graphical description of the available data of all the atmospheric, meteorological and epidemiological parameters measured throughout the campaign at each site.

3. Offline sampling

3.1. Filter sampling

High-volume samplers (MCV CAV-A/mb with an MCV PM1025UNE (PM_{10}) cut-off inlet) were used to collect 24-h filter samples of PM every third day at both sites between April 2016 and June 2017. For simplicity, the high-volume sampler installed in El Alto will be referred as HVS1 and the one in La Paz as HVS2. Between June 2017 and July 2018, the cut-off inlets of the samplers HVS1 and HVS2 were changed to an MCV PM1025UNE ($PM_{2.5}$)

at both sites, and a parallel homemade high-volume sampler with a DIGITEL PM_{10} cut-off inlet was added at LP site (hereafter called HVS3). Due to technical problems with sampler HVS3 (mainly flow control and possible cupper contamination), filter collection of PM_{10} during this period was intermittent. After July 2018, PM sampling was stopped at EA and the sampler HVS1 was moved to the LP station to replace HVS3 and continue the PM_{10} sampling. Finally, filter collection of $PM_{2.5}$ was stopped at LP in December 2018 and PM_{10} collection continued until March 2019. The samplers were placed on the edge of the rooftop of the buildings in order to avoid interference of near-ground particle resuspension (> 3m above ground level).

The aerosol particles were collected onto 150 mm-diameter quartz fiber filters (Pallflex 2500QAT-UP) that were previously heated (during 8 hours at 500°C) and pre-weighted, prior transportation to the field. Filter sampling, regardless the size cut, started at 9:00 a.m. with a 30 $m^3 h^{-1}$ flow. A total of 97 and 85, PM_{10} and $PM_{2.5}$ filters were collected at EA, respectively. At LP, 150 and 90 samples of PM_{10} and $PM_{2.5}$ were collected. After sampling, the filters were folded and wrapped in aluminum foil, sealed in impermeable plastic bags, and stored in a cool environment before being transported back to Europe for analysis.

3.2. Analysis of filter samples

Mass concentrations were first measured gravimetrically as the difference of the pre-sampling and the post-sampling filter weighs, divided by the total sampled volume. The mass concentrations of PM and other species measured at both sampling sites are hereafter reported in ambient conditions (EA: $\overline{T}$=280.8 K, $\overline{P}$=628.2 hPa, LP: $\overline{T}$=286.0 K, $\overline{P}$=664.7 hPa), unless stated otherwise (e.g. when compared to literature reported concentrations). In order to convert to standard conditions of temperature and pressure ($\overline{T}$=273 K, $\overline{P}$=1013.5 hPa) the concentrations must be multiplied by a factor of 1.66 and 1.60 in El Alto and La Paz, respectively. Since the difference in ambient concentrations between the sites due to a difference in mean temperature and pressure is of approximately 4%, ambient concentrations are directly compared between the sites throughout the manuscript.

After being weighed, the samples were divided to be chemically analyzed in three collaborating European laboratories. The analyses were performed on the different filter fractions by the laboratory platforms: EGAR (IDAEA-CSIC), Zone Critique (EDYTEM) and AirOsol (IGE), and will be shortly described in the following sections. Laboratory blank filters were handled in the same manner as field filters (prior deployment to the field) for quality assurance.

3.2.1. Chemical speciation of particulate matter

a. Analysis of the carbonaceous fraction

The analysis of the carbonaceous material was performed on a 1- 1.5 cm^2 portion of the filter at the Institut des Géosciences de l'Environnement (IGE) by a thermal-optical technique using the Sunset Lab EC/OC analyzer (Birch & Cary, 1996). Briefly, this instrument separates the organic from the elemental fraction of carbon contained in a sample by the step-wise volatilization of the organic fraction in a helium (He) environment. After

the organic fraction is removed at about 650°C, the environment is diluted with O_2 resulting in 98% He and 2% O_2. Then, the temperature in the chamber is further increased to volatilize EC. After volatilization, the resulting vapors are oxidized to CO_2, and subsequently reduced to methane (CH_4). Finally, the quantity of methane produced is monitored by a flame ionization detector (FID), which is proportional to the collected mass of OC (when the temperature of the oven is low, <650°C), and to EC mass (when the oven temperatures are higher, >650°C). A more detailed description of the followed EUSAAR-2 protocol can be found in Cavalli et al. (2010).

b. Analysis of water-soluble ions (IC)

The ion fraction of PM that was soluble in water was extracted and analyzed at IGE using an ion chromatographer (IC, Dionex ICS 3000). The separation between ions in the IC is made based on their interactions with the resin and the eluent used. Different columns and eluents are used for the detection of anions (negatively charged ions) and cations (positively charged ions). Hence, the extracted ions are introduced in the eluent and the solution is passed through the resin column. The separation will be then based on the affinity of ions to the used resin. Ions with weaker affinity will pass through the column faster and be eluted first than ions with stronger affinities, which are slowed down in their passage due to the electrical interaction with the column. Finally, upon exiting the column, a conductivity detector measures the passage of the exiting ions. The conductivity peaks vs time, together with the height of the peaks are used to determine the concentrations and nature of the measured ions.

A Dionex AS11HC column (constituted of a positively charged resin) was used in the IC to measure anions, using pure water as eluant. For cations, a CS16 column was used, with methyl sulfonic acid as eluent. The analyzed ions included SO_4^{2-}, NO_3^-, Cl^-, MSA^-, NH_4^+, Na^+, K^+, Mg^{2+}, Ca^{2+} and oxalate. More detailed information on the followed procedure can be found at Jaffrezo et al. (2005).

c. Analysis of the anhydrosugars, primary saccharides and polyols (HPLC-PAD).

The analysis of these species was performed at IGE, where particles from filter punches (3.46 cm^2) were firstly extracted into ultrapure water. Non-soluble particles are then filtered out and the remaining solution is introduced into a high-performance liquid chromatographer (HPLC) with pulsed amperometric detection (PAD) (model Thermo 5000+), with Metrostep columns (Carb 2 – Guard/4.0, Carb 2 – 150). The operational principle is the same as the one described in the previous section, with the difference that the separation is based on the polarity of the species instead of their charge. The followed procedure is further described in Piot et al. (2012).

d. Analysis of metals (ICP-MS, ICP-AES)

The analysis of metals was performed by the Institute of Environmental Assessment and Water Research (IDAEA-CSIC) using an inductively coupled plasma mass spectrometer (ICP-MS). In this technique the portion of the filter is firstly digested in acid (e.g. HF, HNO_3, $HClO_4$), which solubilizes both polar and non-polar

compounds. Then the sample is introduced into the instrument and it is fractioned into charged ions through the collision with electrons and charged ions arising from a plasma gas. Finally, the detection of the different species is based on their mass-to-charge ratio using a magnetic quadrupole.

Metals as Al, K, Ca, Na, Mg, Fe were measured using an ICP-AES. The difference between both techniques is found on the detection principle. The latter detects optically the amount and the wavelength of the light released by the atoms and ions when transitioning between an excited state and their ground state. The nature of the elements is thus associated to the specific wavelength of the emitted light and the amount to the concentrations of given element.

e. Analysis of polycyclic aromatic hydrocarbons (HPLC-FLD)

The polycyclic aromatic hydrocarbons (PAH) were measured at the Laboratoire Environnements, Dynamiques et Territoires de Montagne (EDYTEM) using an HPLC coupled with a fluorescence detector (FLD). In this case, a C18 (NUCLEOSIL 100-5 C_{18} PAH, 25 cm x 4,6 cm) resin column is used and a mix of methanol and water as eluant. With this technique, the concentrations of a total of 16 PAH (containing 2-5 rings) were analyzed, including: Phe, Ant, Fla, Pyr, Tri, Ret, B(a)A, Chr, B(e)P, B(b)F, B(k)F, B(a)P, B(ghi)P, IP, Cor (Besombes et al., 2001).

f. Analysis of polar and non-polar organic tracers (GC-MS)

The polar (methoxyphenols, sterols and methyl-nitrocatechols) and non-polar (alkanes, thiophens, hopanes and methyl-PAHs) organic tracers as were measured at EDYTEM using a gaseous coupled mass spectrometer (GC-MS). The separation of compounds in this technique is made by the passage of the sample through a capillary chromatographic column Optima 5 MS Accent (30 m x 0,25 mm x 0,25 µm) (Macherey-Nagel) with helium as the mobile phase. In the case of polar compounds, the analysis is preceded by a derivatization of the sample to replace active hydrogens in the sample (Golly, 2014). Finally, the sample is introduced into a magnetic quadrupole mass spectrometer, and the detection principle is the same as for the previously mentioned mass spectrometers.

g. Detection limit and quantification limit

The detection limit (DL) is defined as the minimum concentration at which an instrument can detect the presence of a given compound. This is determined by the repeated dilution of a standard solution. In contrast, the quantification limit (QL) is defined as the minimum concentration at which an exact quantification of the presence of a given compound can be performed. It is normally determined from the field or laboratory blanks and it is calculated as the mean concentrations measured from the blanks plus two times the standard deviation. If the concentrations are undetectable, the QL is considered equal to the DL. The present data were corrected with laboratory blanks. A complete list of the analyzed species and the average associated QL can be found in the Annex I.

3.2.2. Measurements of oxidative potential (OP)

The measurements of OP through three acellular assays (DTT, AA, DCFH) were performed at IGE on fraction of the filter samples by plate spectrophotometry. For the performed acellular analysis, a lung-fluid surrogate solution (Gamble) was used to extract the particles from the filter samples. The measurements were done using the two Infinite® M200 Pro and M1000 PRO, TECAN, plate readers through fluorescence (230-850 nm) luminescence and absorbance (230-1000 nm). Triplicates of the different extractions were used for all the assays in order to quantify the uncertainty of the measurement. A positive control containing is used 1,4-naphtoquinone, and laboratory blanks are subtracted from the samples.

a. Dithiothreitol assay (OP-DTT)

In this assay, the production of superoxide (O2•-) anions in vivo, as the result of the exposure to particulate matter, is simulated. This is done by monitoring the consumption of DTT (a substitute of the pulmonary antioxidants) due to the presence or generation of reactive oxygen species (ROS) in the Gamble. The assessment of the remaining DTT in the sample is done in regular intervals of time by its reaction with acide5-5'-dithiobis-2-nitrobenzoïque (DTNB). This reaction will return as product thionitrobenzoate (TNB), a yellowish compound that can be quantified by its absorbance of light at 465 nm (Cho et al., 2005).

b. Ascorbic acid (OP-AA)

This assay uses ascorbic acid (vitamin C) as antioxidant introduced to the Gamble. The absorbance of AA incubated with PM extracts is measured at 265 nm wavelength every 4 minutes (starting at minute 2 after injection), for 30 minutes. The depletion rate of ascorbic acid is then calculated by the linear regression of absorbance against time (nmol min^{-1}).

c. Dichlorofluorescin (OP-DCFH)

This assay measures the oxidation of DCFH, forming a fluorescent product 2',7'-dichlorofluorescein (DCF). Prior to analysis, the DCFH was mixed in sodium phosphate buffer (pH = 7.2) with horseradish peroxidase (HRP). The DCF is then measured by fluorescence at the excitation and emission wavelengths of 485 and 530 nm. This experiment has to be performed under dark conditions to prevent DCFH photooxidation and reduce the variability of H_2O_2. The measured fluorescence intensities are then converted into equivalent concentrations of H_2O_2 based on a calibration curve of H_2O_2 (Rao et al., 2020).

3.2.3. Volume normalized vs mass normalized oxidative potential (OP_v vs OP_m)

Since the measured OP activity corresponds to the toxicity of the particles present in the filter sample, their significance is inevitably linked to the amount and the nature of the particles existing in every individual sample. A way to express this dependency is normalizing the OP activity [nmol min^{-1}] by the mass of PM (OP_m,

intrinsic OP, [nmol min^{-1} μg^{-1}]), or by the sampled volume in which given mass of PM was contained (OP_v, extrinsic OP, [nmol min^{-1} m^{-3}]).

4. Online sampling

4.1. Equivalent black carbon (eBC)

A 7-wavelenght (370, 470, 520, 590, 660, 880 et 950 nm) aethalometer was installed at each sampling site to measure the attenuation due to absorbing particles and the concentrations of eBC. These measurements are inferred from the change in attenuation of light passing through a filter matrix onto which aerosol particles are deposited. Hence, attenuation coefficients are calculated as:

$$b_{ATN}(\lambda) = \frac{A}{Q \cdot 100} \cdot \frac{ATN_t(\lambda) - ATN_{t-\Delta t}(\lambda)}{\Delta t} \qquad [3]$$

where ATN_t is the attenuation of light passing through the filter at a given time t, Δt the interval between measurements, A the surface of the filter onto which particles are deposited and Q the flow. The mass of equivalent carbon is then calculated as the ratio between the attenuation coefficient and the product of the cross sensitivity to scattering (C_f) [2] and the mass absorption cross section for each wavelength[3]. The last two parameters are wavelength dependent and provided by the company. Typically, the eBC mass concentration calculated at 880 nm is the one used to compare to other techniques measuring the mass of BC.

The Aethalometer, model AE33 (Magee Scientific, Drinovec et al., 2015), was placed at EA station measuring with the minimum 1-minute time resolution provided by the instrument (Apr 2016 – Sep 2017). Due to technical problems, the instrument had to be replaced by a previous model Aethalometer AE31 (Magee Scientific, Arnott et al., 2005) for the end of the campaign (Jan – Jun 2018). A PM_{10} inlet was used at the end of the sampling line throughout the campaign (6 m above the instrument level). During the period between April 2017 to September 2017 a larger size cut is expected since the sampling flow required for a PM_{10} cut at the inlet was not met.

Between May and September 2016 an aethalometer AE31 (the one that later replaced AE33 at EA) was placed at LP measuring whole air (TSP, total suspended particles). The same model, AE31, was operated in parallel in La Paz from mid-June 2016 until the end of the campaign, at its minimum 5-minute time resolution. The PM_{10} inlet was placed at the end of the line (2 m above instrument level). As in El Alto, a larger size cut was expected at the inlet head since the sampling flow required for a PM_{10} cut at the inlet was not met until December 2017.

An average flow of 2.9 lpm registered by the instrument was maintained for the aethalometer AE33, whereas, average flows of 3.9 and 4.9 lpm were maintained for the aethalometers AE31 in La Paz and El Alto,

[2] $C_{f,AE31}$= 2.14; $C_{f,AE33}$= 1.57

[3] MAC_{370nm}= 18.47 [m^2g^{-1}]; MAC_{470nm}= 14.54 [m^2g^{-1}]; MAC_{520nm}= 13.14 [m^2g^{-1}]; MAC_{590nm}= 11.58 [m^2g^{-1}]; MAC_{660nm}= 10.35 [m^2g^{-1}]; MAC_{880nm}= 7.77 [m^2g^{-1}]; MAC_{950nm}= 7.19 [m^2g^{-1}]

respectively. At both sites, the instruments were set to report eBC concentrations at standard conditions of temperature and pressure (STP: $\overline{T}$=273 K, $\overline{P}$=1013.5 hPa).

At the CHC-GAW station, measurements of eBC are permanently taken using an aethalometer AE31 since 2011, at a 5 min resolution. The instrument is connected to a whole air inlet equipped with a PM_{10} head and an automatic dryer.

4.2. Single Particle Soot Photometer (SP2)

A Single-Particle Soot Photometer (SP2, Droplet Measurement Technologies; Baumgardner et al., 2004) was installed between April and May 2018 at the three stations (CHC-GAW, LP, EA), as part of the SALTENA campaign (Bianchi et al., 2022). At the stations of La Paz and El Alto SP2-XR (Droplet Measurement Technology, DMT, Longmont, CO, USA) were installed, from which hourly refractory black carbon mass concentrations (rBC) were retrieved. This instrument is based on the incandescence produced by BC particles when vaporized as a result of them being exposed to a laser beam. Since the measurements are made one particle at the time, the instrument can then provide the mass size distribution of BC particles. This instrument is typically sensitive to absorbing particles with a diameter above 80 nm.

4.3. Ozone analyzers

Two new O_3 analyzers (Model 49i, Thermo Fischer Scientific) were installed at the stations of LP and EA in May 2021 up to present. The instruments were installed after testing the fabric calibration by intercomparing them for a week with a recently calibrated O_3 analyzer that permanently measures O_3 at CHC-GAW. The Teflon sampling line was kept under 3 m in longitude and 1.5 meters away from the roof in the case of LP. At EA, the shortest sampling line was installed through room window where the instrument was installed, and the inlet was placed 1.5 m away from the wall. Measurements are saved every minute and “zero” tests are performed with a carbon capsule (PALL) every two weeks to monitor the drift of the zero.

Although the main analysis of the thesis was focused on the characterization of airborne particulate matter, a short description of the concentrations of O_3 and their variability will be presented in Annex II.

4.4. Meteorological observations

Meteorological parameters were also monitored throughout the sampling period. Windspeeds and wind direction were measured with a 15-minute time resolution using an anemometer placed next to the measurements building in EA, and on top of the instruments shed in the case of La Paz,. Temperature, pressure and relative humidity were measured by the airport’s meteorological service on an hourly basis at EA. In La Paz, a weather station was not available during the campaign, hence, daily averages of temperature, pressure and relative humidity were retrieved from the official webpage of the National Service for Meteorology and Hydrology (SENAMI, Servicio Nacional de Meteorología e Hidrología) (*SENAMHI*, n.d.).

5. Fuel samples

In order to further investigate the differences between the two main types of fuel used in LP-EA, three samples of gasoline and three samples of diesel fuel were taken at 3 randomly chosen gas-stations located in different parts of the cities. The samples were analyzed for main metal composition using an ICP-MS. Firstly, 1 ml of sample (gasoline, diesel) was transferred into a Teflon microwave vessel (Anton Paar microwave laboratory unit). Then, 10 ml of HNO3 (double distilled, suprapure level) were added and the solution was decomposed by increasing temperature and pressure (175°C and 10 bar). In the microwave, the EPA 3051A method was run twice to assure that the solutions were indeed decomposed (USEPA, 2007). After cooling down the vessels, the solutions were diluted by a factor of 10 and directly introduced to the ICP-MS. A complete descriptive table of the analyzed species can be found in Annex I.

6. Epidemiological data

In order to assess the association between air pollution and observed health outcomes, and thanks to the collaboration of the Bolivian Health Ministry, a database on the number of acute respiratory infections (ARI) and pneumonias registered at a city level were obtained. This dataset consists on the weekly addition of the number of visits made to any hospital or health care facility in each city for any of these conditions.

Amongst ARI are considered any kind of respiratory infection that difficult the normal breathing. It can affect, both, the upper and the lower part of the respiratory system. It ranges from a simple cold, cough or a sore throat, to laryngitis, bronchitis, otitis, bronchiolitis and pneumonia. Other known respiratory infections include diphtheria, measles and pertussis. Pneumonia is considered separately from other ARI because, if not diagnosed and treated properly, it can lead to death in 10% to 20% of the cases. The criteria to diagnose an IRA as pneumonia include the following symptoms, but not necessarily all of them at the same time: persistent inflammation of airways, fever, chest indrawing (in children), auscultation of lung crackles, reduced oxygen saturation, difficulty breathing, lung consolidation observed on X-ray scans (Moreno et al., 2006; WHO, 1990, 2020).

The dataset obtained includes weekly ARI and pneumonias at each city split by gender and age group (0-6 months, 6-12 months, 1-5 years old, 5-9 years old, 10-14 years old, 15-19 years old, 20-39 years old, 40-49 years old, 50-59 years old, over 60 years old), between 2016 and 2019. However, no information on the residence, exposure or economic conditions of the patients is known.

Mathematical and statistical methodology

In this chapter are compiled and explained in more detailed the mathematical and statistical tools that were used in the main analysis of the thesis. It will be divided into three sections corresponding to each of the results chapters that follow the present chapter.

1 Source Apportionment of Airborne Particulate Matter in the Bolivian Cities of La Paz and El Alto

1.1 Source apportionments of particulate matter (PM)

An important step in implementing policies to improve air quality is the identification and targeting of major pollution sources. For this purpose, several methods have been developed that use the different physical and chemical properties, and the temporal variation of aerosols to discriminate between major pollution sources and their contribution to observed pollution levels (Belis et al., 2019).

Following the classification of Viana et al. (2008) review on source apportionment methods, they can be grouped into three main categories:

- Methods based on the evaluation of monitoring data: Basically, they seek for simple mathematical relationships of PM and its components to other complementary variables, like gaseous compounds or meteorological parameters (Viana et al., 2008).
- Methods based on emission inventories and/or dispersion models: These methods rely on existing emission inventories and the knowledge of local atmospheric dynamics to simulate aerosol emissions, formation, transport and deposition rates as well as their spatial distribution (Belis C, et al., 2019; Viana et al., 2008).
- Methods based on statistical evaluation of PM chemical data acquired at receptor sites: These methods look at the task inversely. They try to discriminate between the possible sources that are responsible for the observed PM at a specific site. Mass and species conservation between the emission source and the study site is the basic assumption. The main equation that these models seek to solve is the mass balance equation:

$$x_{ij} = \sum_{k=1}^{p} g_{ik} f_{kj} + e_{ij} \qquad [1]$$

where x_{ij} represents the concentrations of specie j to sample i, g_{ik} are the contribution of the source k, f_{kj} are the concentrations of specie j in source k, and e_{ij} are the residual term.

Two widely used examples of receptor models are the chemical mass balance (CMB) and factor analysis (principal components analysis, PCA; positive matrix factorization, PMF). These two types of models stand at the two extremes of the prior-required-knowledge of the pollution sources. For the CMB model, prior information of the composition and the emission patterns of the main sources is

required. On the other hand, for factor analyses such as PMF little to no information is pre-required to run the model. This have made the PMF gain considerable traction in the recent decades. The geochemical knowledge is, thus, required for the interpretation and evaluation of the analysis results (Belis et al., 2019; Viana et al., 2008).

1.2 Positive matrix factorization (PMF)

The PMF receptor model differs from other factor analyses in that it allows the possibility of weighting the concentrations of the various species to be included in the analysis, based on their uncertainties. In addition, the term "positive" comes from the fact that the computational process does not allow for negative contributions. The performance of the source apportionment using this model is highly dependent on the inclusion of specific source tracers (often organic compounds) and the availability of a significant number of samples compared to the number of species included. This methodology has been applied to on-line and off-line measurements of PM constituents in the size ranges of PM_{10}, $PM_{2.5}$, and PM_1. One of the main software programs used to run PMF factor analysis, and the one used for the present work, is the US EPA PMF v.5.0 program (Belis, et al., 2019).

In PMF analysis, the number of factors and the geochemical interpretation of the obtained factors are ultimately operator-dependent, with the help of quantitative indicators that must necessarily be met to consider a solution as valid. The first of these is the Q value. PMF analysis tries to find the optimal solution by minimizing the Q-value, which is basically a goodness-of-fit parameter mathematically defined as:

$$Q = \sum_{i,j} \frac{e_{ik}^2}{\sigma_{ik}^2} \qquad [2]$$

where σ_{ik}^2 are the uncertainties associated to specie j in sample i. It is then possible to distinguish between 2 calculated Q values: Q(true) which includes all datapoints, and Q(robust), which is calculated excluding outliers. Consistent solutions are expected to have a ratio Q(true)/Q(robust) < 1.5.

The validity of a solution is also assessed by analyzing the scaled residuals, which should be normally distributed around 0, in the interval (-3,3). The reconstruction of the input variables is then controlled and the rotational ambiguity of the obtained solution is evaluated by bootstrap analysis (BS>75%). Such ambiguity can be controlled by the existing external information that constrains the solution. Finally, the uncertainty of the individual variables in the source profile matrix (F) can be estimated by shifting each variable from its original value in the solution to analyze the upper and lower bounds that a variable can take without altering the original solution (Belis, et al., 2019; Paatero & Tapper, 1994).

This methodology was used in our study to apportion the sources of PM measured from the PM_{10} filter samples collected during the first 15 months of the campaign.

1.2.1 Sample and chemical species selection

A key step when running the PMF is selecting the input variables for the model. As described in the previous chapter, 178 species were analyzed from each filter sample but not all of them were suitable for the PMF analysis. Moreover, a healthy balance between the number of observations (samples) and explanatory variables (species) should be maintained. As many species as observations is minimally required. Ideally, the number of observations should be at least two to three times the number of species. Hence, species with irregularities in their time series were excluded from the analysis, together with the ones that had over 25% of the data below the quantification limit (<QL, defined as the mean field-blank concentrations measured per specie, plus two times the standard deviation), remaining 86 potentially useful species for the analysis. Then, from the species that were measured through both Ion Chromatography (IC) and Inductive Coupled Plasma-Mass Spectrometry (ICP-MS), only the ICP-MS metals were included in order to avoid double counting, except for K^+, for which the IC measurements were used, as water soluble K^+ is a known tracer for biomass Burning (BB) (Li et al., 2021). Galactosan and sorbitol were considered unnecessary tracers for biomass burning and primary biogenic aerosols, respectively, given the presence of other specific tracers as levoglucosan, mannosan, mannitol and arabitol. Thus, they were excluded from the analysis. Finally, other non-specific-tracer metal species were excluded after several attempts of including them in the PMF input data, since they proved to only add instability to the solution.

Based on the results of Samaké et al. 2019b, arabitol and mannitol were added as one Polyol-representative specie, given that they are emitted by the same source and have a Pearson correlation of r>0.7, for both sites. The same was done for PAHs that presented a r>0.9 (PAH_1: [BghiP]+[IP]+[BbF]; PAH_2: [Fla]+[Pyr]). Lastly, OC was replaced in the PMF analysis by OC*, which is defined as the subtraction of the carbon mass concentration of all the included organic compounds from the measured OC mass concentrations, to avoid double counting, as was done by Weber et al. (2019). Thus:

$$OC^* = OC - \left(\begin{array}{c} 0.12 \cdot [MSA] + 0.40 \cdot [Polyols] + 0.44 \cdot ([Levoglucosan] + [Mannosan]) + \\ 0.95 \cdot ([BghiP] + [IP] + [BbF] + [Fla] + [Pyr] + [BaA] + [Chr] + [Tri] + [BaP] + [Cor]) + \\ 0.85 \cdot ([C21] + [C22] + [C23] + [C24] + [C25] + [C26]) + \\ 0.87 \cdot ([HP3] + [HP4]) \end{array} \right) \quad [3]$$

1.2.2 Uncertainty calculation and specie weight-assignment

A crucial step in PMF analysis is the attribution of uncertainties to the measured input variables. In general, it is sought that these uncertainties are proportional to the measurements, and that they increase for values close to the detection limit (DL). This allows more weight to be given to higher concentrations than to those that are relatively close to or below the detection limit (DL). There are several methodologies in the literature for such attribution, among which we can mention the formulas of Gianini et al. (2012) and Polissar et al. (1998). In both cases, the values ≤ DL don replaced by $\frac{DL}{2}$ and uncertainties are calculated as follows:

- Gianini et al. (2012): $$u_{ij} = \sqrt{\left(DL_j\right)^2 + \left(CV_j \cdot x_{ij}\right)^2 + (a \cdot x_{ij})^2} \quad [4]$$

where CV is the variation coefficient of specie j, defined as 2 times the standard deviation of the field blank filters, and a is the variation coefficient of PM measurements.

- Polissar et al. (1998):

$$u_{ij} = \begin{cases} x_{ij} + \frac{2}{3}DL & ; x_{ij} \leq DL \\ 0.2 \cdot x_{ij} + \frac{2}{3}DL & ; DL < x_{ij} \leq 3 \cdot DL \\ 0.1 \cdot x_{ij} + \frac{2}{3}DL & ; x_{ij} > 3 \cdot DL \end{cases} \quad [5]$$

In the case of the present study, a constant 10% uncertainty was assigned to PM mass measurements since the measured PM concentrations were at least two orders of magnitude above the detection limit. Moreover, PM was set in the software as the total variable, which automatically set the variable as a weak variable. The uncertainties of a weak variable are automatically triplicated by the software, downweighing its influence in the analysis.

The uncertainty calculation for polyols, monosaccharide anhydrides, and ions was performed using the formula proposed by Gianini et al. 2012, using the variation coefficients (CV) and the additional coefficients of variation (a) proposed and used by Weber et al. (2019), with the average QL associated to each specie instead of DL. The uncertainties associated to EC, OC, and metals, were calculated following the method proposed by Amato et al. (2009) and Escrig et al. (2009). Finally, the uncertainties assigned to the molecular organic species were calculated using the formulas proposed by Polissar et al. (1998) and Reff et al. (2007), replacing the DL values by QL.

Values under the QL in the concentration matrix were replaced by the average of their corresponding QL divided by 2, and their uncertainties were set to $\frac{5}{6}$ QL (Norris & Duvall, 2014). The outliers encountered in the time series of some species (a total of 4 values) were set as missing values, which were then replaced in the software by the median value of the corresponding specie and their associated uncertainties were automatically set to four times the species-specific median values.

The weight of the species in the factor analysis was determined based on their signal to noise ratio (S/N). Species with a S/N>2 were defined as strong. Species with a signal to noise ratio: $0.2 \leq S/N \leq 2$ were defined as weak. Species with a S/N<0.2 were not included in the analysis. After several tests, some variables were also set as weak (i.e. K^+, V), because setting them as strong would result in a separate specific factor without any relevant meaning. The PAH, alkanes and hopanes were set as weak species, to prevent them from driving the solution.

1.2.3 Solution evaluation criteria

Solutions ranging from 8 to 13 factors were explored, in order to select the appropriate number of factors contributing to each site. A series of statistical and geochemical control parameters were then evaluated in order to choose the final solution (Belis. et al. 2019):

- $Q_{true}/Q_{robust} < 1.5$.
- Residuals per specie centered and symmetrically distributed around 0, and within -3 and 3 (with the exception of a few outliers).
- Bootstrap (BS) evaluation of the statistical robustness of the selected base run having a correlation coefficient for every factor > 0.8 after 100 iterations, before and after constraints.
- Displacements (DISP) analysis evaluating the rotational ambiguity and tolerance of the solution to small perturbations (No observed rotation was observed for dQmax = 4, 8).
- Geochemical consistency of the obtained factor chemical profiles based on literature and knowledge of the study site.

1.2.4 Multisite PMF

Single-site PMF analysis were initially run in parallel, showing indeed similar main sources contributing to particulate matter. Increasing the number of factors showed a promising possibility of splitting the traffic profile but at the cost of altering the statistical stability of the solution. These results were a motivation to run a multisite PMF. Such approach has proven to reduce the rotational ambiguity in factor analyses (Dai et al., 2020; Hernández-Pellón & Fernández-Olmo, 2019; Hopke, 2021; Pandolfi et al., 2020), increasing the statistical robustness while increasing the number of samples. For this purpose, in order to combine both datasets as one (EA-LP) the dates of the La Paz dataset were shifted in time by two years and then appended to El Alto's dataset. In this manner, repeated dates were avoided resulting in a single input matrix for PMF that respected the natural seasonal variability of the original datasets. The multisite approach stands on the hypothesis that the major sources contributing to PM_{10} in both sites are similar and display similar chemical profiles, which has been verified within the single site solutions.

1.2.5 Set of Constraints

Once the optimum number of factors was selected in the multisite base solution, a set of "soft" constraints (Table 1) was applied to the selected solution based on previous studies (Borlaza et al., 2021a; Samaké, et al., 2019a; Weber et al., 2019):

Table 1. Set of constraints applied to final solution

Factor	Specie	Constraint	Value
Biomass Burning	Levoglucosan	Pull up maximally	%dQ 0.50
Biomass Burning	Mannosan	Pull up maximally	%dQ 0.50
Primary Biogenic Aerosol	Polyols	Pull up maximally	%dQ 0.50
MSA-Rich	MSA	Pull up maximally	%dQ 0.50

2. Combustion Sources Affecting the Air Quality in the Metropolitan Area of La Paz and El Alto

The results presented in chapter V revolves around the description of the optical absorbing properties of aerosol particles measured using filter-based absorption photometers (i.e. aethalometers).

2.1. Data preparation

As for all filter-based instruments, instrumental artifacts need to be accounted for in the post processing data analysis. The first one accounts for the so called "loading effect". As the filter gets loaded, particles deposited on the filter may interact with the incoming light beam, increasingly reducing the amount of light reaching the detector. This constitutes the main difference between models AE31 and model AE33. The aethalometer AE33 performs this correction online, thanks to its dual spot design. In contrast, measurements taken with the aethalometer AE31 need to be corrected as part of the post processing of the data (Drinovec et al., 2015b; A Virkkula et al., 2015). However, an overcompensation of the loading effect was spotted in the measurements of AE33, for which the correction made by the instrument was overlooked. Thus, the following correction scheme proposed by Virkkula et al. (2015) was used for both models in the present study:

$$eBC(\boldsymbol{\lambda}) = \frac{BC_0(\boldsymbol{\lambda})}{(1+k(\boldsymbol{\lambda})\cdot ATN_t(\boldsymbol{\lambda}))} = \frac{1}{(1+k(\boldsymbol{\lambda})\cdot ATN_t(\boldsymbol{\lambda}))} \cdot \left(\frac{1}{C_{f0}} \cdot \frac{1}{MAC(\boldsymbol{\lambda})} \cdot \frac{A}{Q\cdot 100} \cdot \frac{ATN_t(\boldsymbol{\lambda}) - ATN_{t-\Delta t}(\boldsymbol{\lambda})}{\Delta t}\right) \quad [6]$$

where ATN corresponds to the ratio of the light intensity reaching the detector after passing through the loaded filter, compared to the attenuation of the light passing through a clean portion of the filter; k is the loading correcting factor introduced by Virkkula et al. (2015); BC_0 are the original black carbon concentrations reported by the instrument; C_{f0} are the constant cross-sensitivity to scattering factor that corresponds to the model of aethalometer and the filter tape used[4]; MAC are the mass absorption cross-sections established by the manufacturer for each of the wavelengths of the aethalometer[5]; A is the area of the filter onto which particles are collected[6], Q is the flow rate of the air sample passing through the instrument. Monthly k values were calculated as the ratio of the slope over the intercept of the linear fit of the eBC concentrations with respect to ATN. They were then used to correct the data on a monthly basis.

The noise in the concentrations reported by the AE33 at the minimum time resolution was high. Hence, the noise reduction method presented by Backman et al. (2017) was applied to the dataset, Briefly, Backman et al. (2017) proposed to increase the original averaging period Δt from the original sampling time resolution to a higher interval of time in equation [1], when calculating eBC concentrations. Therefore, eBC concentrations

[4] $C_{f0,\,AE31}$= 2.14; $C_{f0,\,AE33}$= 1.57

[5] MAC_{370nm}= 18.47 [m^2g^{-1}]; MAC_{470nm}= 14.54 [m^2g^{-1}]; MAC_{520nm}= 13.14 [m^2g^{-1}]; MAC_{590nm}= 11.58 [m^2g^{-1}]; MAC_{660nm}= 10.35 [m^2g^{-1}]; MAC_{880nm}= 7.77 [m^2g^{-1}]; MAC_{950nm}= 7.19 [m^2g^{-1}]

[6] A_{AE31}= 0.5 cm^2; A_{AE33}= 0.785 cm^2

were recalculated using a Δt=30 min to efficiently reduce the noise of the data set. This procedure was only applied to eBC concentrations measured from the same filter-spot, hence, the Δt of the first 30 minutes of every new filter-spot were defined as $\Delta t = t - t_0$.

2.2. Intrinsic properties of BC.

2.2.1. Absorption Angstrom Exponent (AAE)

The absorption efficiency of particulate matter varies throughout the visible spectrum of radiation and is determined by the chemical and physical properties of the aerosol particles. This wavelength dependency can be described by the Absorption Ångström Exponent (AAE) (Seinfeld & Pandis, 2016). An orthogonal non-linear least squares regression was used to describe the power-law dependency of absorption with wavelength:

$$b_{abs}(\lambda) = a \cdot \lambda^{-AAE} \qquad [7]$$

Only wavelengths 2 470 – 950 nm were used in the regression as recommended by Zotter et al. (2017). The obtained time series of AAE showed to be equally noisy as the untreated BC concentrations, therefore only AAE corresponding to absorption coefficients $b_{abs,880}$>2 [Mm^{-1}] were considered in the rest of the analysis.

2.2.2. Mass Absorption Cross-section (MAC)

The mass absorption cross-section at a given wavelength (MAC) is an intrinsic property of absorbing aerosol particles that also depends on wavelength, aerosol type and ageing. MAC values of a specific sample of absorbing aerosol particles, are thus calculated as follows:

$$MAC_{BC}(\lambda)\ [m^2 g^{-1}] = \frac{b_{abs}(\lambda)\ [Mm^{-1}]}{m_{BC}\ [\mu g\ m^{-3}]} = \frac{b_{ATN}\ (\lambda)[Mm^{-1}]}{C_f \cdot m_{BC}\ [\mu g\ m^{-3}]} \qquad [8]$$

where b_{abs} are the absorption coefficients at wavelength λ, b_{ATN} are the attenuation coefficients at λ, and m_{BC} are the mass concentrations of BC. To compare with other studies, the obtained MAC values were interpolated to other wavelengths typically found in the literature (550, 637 and 880 nm).

2.3. Source apportionment of Black Carbon

2.3.1. Aethalometer method

Based on the differences in the source-specific AAE, a bilinear regression model was proposed by Sandradewi et al. (2008) that allows to determine the contribution of each source to total absorption. Generally, this technique is used to apportion the contributions of vehicular emissions and biomass burning emissions or dust (Harrison et al., 2012; Lanz et al., 2008; Sandradewi et al., 2008; Zotter et al., 2017). This method is also known in the literature as the “Aethalometer method”.

Considering that:

$$b_{abs}(\lambda_i) = b_{abs,TR}(\lambda_i) + b_{abs,BB}(\lambda_i) \qquad [9]$$

where the subscripts TR and BB represent absorption due to traffic and biomass burning, respectively, and the power law dependence of b_{abs} with wavelength described in equation [7]:

$$\frac{b_{abs,TR}(\lambda_1)}{b_{abs,TR}(\lambda_2)} = \left(\frac{\lambda_1}{\lambda_2}\right)^{-AAE_{TR}} \quad [10]$$

$$\frac{b_{abs,BB}(\lambda_1)}{b_{abs,BB}(\lambda_2)} = \left(\frac{\lambda_1}{\lambda_2}\right)^{-AAE_{BB}} \quad [11]$$

this transforms the equations system [9] in:

$$\left.\begin{aligned} b_{abs,total}(\lambda_1) &= \left(\frac{\lambda_1}{\lambda_2}\right)^{-AAE_{TR}} \cdot b_{abs,TR}(\lambda_2) + b_{abs,BB}(\lambda_1) \\ b_{abs,total}(\lambda_2) &= b_{abs,TR}(\lambda_2) + \left(\frac{\lambda_1}{\lambda_2}\right)^{+AAE_{BB}} \cdot b_{abs,BB}(\lambda_1) \end{aligned}\right\} \quad [10]$$

The equation system [10] possess 4 unknowns. However, if the AAE values of the evaluated sources are known or assumed, the equation system can be resolved, and the contributions of each source to total b_{abs} can be determined. The pair of wavelengths chosen to apply this method were 470 and 950 nm. The representative source-specific AAE were chosen as the 5th and 99th percentiles of the frequency distribution of the hourly averages of AAE (AAE_{TR}= 0.9, AAE_{BB}=1.5).

2.3.2. Multilinear Linear Regression method (MLR)

One of the limitations of the Aethalometer method bilinear method for source apportioning is that it only supports two sources of absorbing aerosol particles with different absorption wavelength dependencies. In addition, this method is very sensitive to the selection of the selected representative AAE, which sometimes can be somewhat arbitrary. The extrapolation of literature values can significantly influence the eBC partitioning as well. Therefore, an alternative method was explored to identify other possible sources of absorbing aerosol particles and calculate their source-specific AAEs.

Following the methodology described in Weber et al. (2021), the observed absorption coefficients (b_{abs}) in La Paz and El Alto, at the 7 aethalometer wavelengths, were calculated based on the PMF-resolved PM_{10} sources. The source deconvolution was performed applying an ordinary multi-linear regression (OLS) of the form:

$$b_{abs}(\lambda)_{m,1} = \left(G_{m,n} \times \beta(\lambda)_{n,1}\right) + \varepsilon(\lambda)_{m,1} \quad [11]$$

where b_{abs} are the daily averaged absorption coefficients in Mm^{-1} (starting at 9 a.m. to match the filter sampling time), $G_{m,n}$ are the STP mass contributions of the n sources for each of the m filters in $\mu g\ m^{-3}$, β are the regression coefficients representing the mass absorption cross-section of each of the sources in $m^2 g^{-1}$, and ε are the residuals that account for the difference between the observed and the modelled b_{abs}. Thus, the wavelength-dependent contribution to b_{abs} of the individual sources can be calculated. The uncertainties of β were estimated by a bootstrapping method (*n*=500) using random selection of samples to account for outliers and

seasonal variation in each source-specific MAC (λ). Finally, the average source-specific AAE can be calculated through the non-linear regression of the multiwavelength $b_{abs}(\lambda)$ (eq. [7])

3. Air Pollution and its Association to Health Outcomes

3.1. Source apportionment of oxidative potential (OP)

As mentioned in the previous chapter, the mass concentrations of PM, its chemical components, and the toxicity of the collected particles, expressed in terms of oxidative potential (OP), were measured from the filter samples. As in the previous section, following the methodology described in Weber et al. (2021), the sources of each of the OP assays (DTT, AA, DCFH) were then apportioned by using a weighted multi-linear least squares regression (WLS) of the form:

$$OP_{obs} = (G \times \beta) + \varepsilon \qquad [12]$$

where OP_{obs} are the observed OP_v measured either assay (nmol min^{-1} m^{-3}), G are the source contributions (μg m^{-3}) obtained from the PMF model described in section 1 of the present chapter, β are the regression coefficients representing the mass-normalized ("intrinsic") source-specific OP (OP_m) (nmol min^{-1} μg^{-1}) ε are the model residuals, and the weight apply was defined as $1/SD^2$ associated to each measurement of OP. The uncertainties of β were estimated by a bootstrapping method (*n*=500) using random selection of samples to account for outliers and seasonal variation in each source-specific OP_m. Finally, the source-specific OP contribution was calculated by multiplying the median obtained β of each source by the mass contribution of the source. Only the OP measurements > 2*SD were included in the model. Since the measured OP_{AA} were generally low (close to the detection limit), and the reconstruction of OP was poor, it was decided to remove OP_{AA} from the rest of the analysis.

3.2. Epidemiological associations of OP with ARI and Pneu

We then proceeded to investigate the short-term association between exposures: PM, OP_{DTT}, OP_{DCFH} and BC vs. the weekly reported respiratory outcomes: pneumonia and acute respiratory infections (ARI). This is a time series regression analysis in which the results are presented as counts. The usual regression method for analyzing count data is Poisson regression, since counts never admit negative values. The model was constructed as follows:

$$\ln(outcome) = \frac{exposure}{IQR} + s1(time, df1) + s2(T, df2) + s3(RH, df3) + s4(ws, df4) \quad [13]$$

Where, s1-s4 represent the spline functions of time, mean temperature, relative humidity and wind speed, that adjust the associations for possible confounding. In order to increase the statistical power of the analyses we followed a multisite approach as for the previous sections, combining the datasets from La Paz and El Alto. The adjustment factors considered in the models were chosen based on the literature, and a random effect representing the possible city-specific variability. We modelled time as a natural spline with 6 degrees of

freedom per year, representing time-varying unmeasured confounders having a period of two months or more. We modelled each meteorological variable as a natural spline with three degrees of freedom to capture potentially non-linear associations with health outcomes. In the main model (eq. [13]) each studied exposure was normalized by its interquartile range (IQR) for comparability purposes. Due to high overdispersion, a quasi-Poisson regression model was used in the single-exposure models, which were ran for each size fraction (PM_{10} and $PM_{2.5}$), and each health outcome. We fit a separate model for each lag of 0, 1, and 2 weeks where lag 0 is the week of the medical visit count and lag 1 is the previous week. This approach was driven by the possibility that there may be a time lag between exposure, the manifestation of biological effects, and an individual seeking medical care.

A similar analysis was also applied to the sources of PM resolved by the PMF, with the difference that for this model a multi-pollutant approach was followed i.e. the linearly independent normalized contributions of each source to PM_{10} were simultaneously included as additive terms in the model.

As preliminary and exploratory analysis, unadjusted associations were also estimated for each exposure using univariate regression models (i.e. excluding the confounding terms), and stratified analyses were also performed for three age groups (adults age ≥20 years, children-teenagers age 1 to 19 years old, and infants age < 1 year) and gender. Only the results obtained for the total number of counts for each outcome will be discussed in Chapter VI. The adjusted analyses used the glmmPQL function from the MASS package (Venables & Ripley, 2002).

Source Apportionment of Airborne Particulate Matter in the Bolivian Cities of La Paz and El Alto

Although air quality regulations make part of the Bolivian legislation, the reference levels are not as strict as the ones proposed by the WHO (a summary table of the reference levels for the pollutants regulated by the Bolivian law can be found in Annex I). In terms of particulate matter, the maximum mass concentrations of PM_{10} allowed by the Bolivian law triplicate the values proposed by the WHO, and $PM_{2.5}$ concentrations are not yet regulated by law.

Air quality monitoring in Bolivia officially started in 2001, with the implementation of air quality monitoring networks (Redes de Monitoreo de la Calidad del Aire, Red MoniCA) in many of the biggest urban centers throughout the following decades. The establishment of the monitoring networks was executed by the NGO Swisscontact together with universities and the municipal governments through the project “Aire Limpio” (Clean Air) of the Swiss Confederation in Bolivia. These networks surveil the air quality parameters regulated by the Bolivian legislation in the different departments in Bolivia, with the recent addition of $PM_{2.5}$ in the last years. The implementation of monitoring networks constitutes a very important first step necessary to the characterization and comprehension of the state of air quality in Bolivia. However, one of the limitations of the data produced by the monitoring stations that integrate the networks is that the majority of them rely on passive detection methods which provide low time-resolution data with high associated uncertainties. Moreover, ensuring the collection of continuous quality data is crucial, yet, finding the economic and human resources necessary for regularly maintaining the monitoring instruments and for training employees becomes a challenge that limits the optimal functioning of these networks. Nevertheless, the available measurements from the monitoring networks already enabled them to pick out mobile sources as a major source of pollution (Red MoniCA, 2021).

Transportation represents one of the most important economic activities in La Paz-El Alto (DAPRO, 2020a; INE, 2020d). The second largest registered vehicle fleet of Bolivia is found in this conurbation, accounting for 20% of the national vehicle fleet, which mainly uses gasoline as fuel (>80%), followed by diesel and natural gas (INE, 2016, 2020a; Red MoniCA, 2021). Although Industry in Bolivia is not largely developed, the department of La Paz is the second main industrial center in Bolivia, contributing with 22% of the national manufacturing industry production (DAPRO, 2020b). Most of its industries are located in the city of El Alto (>85%, Evia, 2009). Industry in LP-EA is mainly dedicated to the production of textiles and clothing, followed by the manufacturing of food and beverages, furniture, metalwork, non-metallic mineral products, leather and footwear (DAPRO, 2022). Mining is an important economic activity that develops in the vicinity of the metropolitan area of La Paz and El Alto. The main extracted minerals by this sector are Zn, Sn, Cu, Pb, W, Sb, Au and Ag, in order of produced tons in 2019, with Zn being the dominant extracted mineral (DAPRO, 2021). Finally, construction is a very important activity in the city of El Alto, given the vast room for potential expansion it possesses. This activity

follows Industry in terms of its contribution to the credit portfolio of El Alto (DAPRO, 2020a, 2022) and is, hence, associated to the industry of construction materials, one of them being the artisanal production of bricks.

Even though great progress had been made in air quality monitoring and the inference of the potential sources of pollution, a measurements-based quantitative and qualitative description of the emitting sources of PM sources was still pending. Understanding the role played by each of these sources is the cornerstone for establishing effective air quality policies that protect the population.

In this chapter is presented the first source apportionment analysis performed in the metropolitan area of La Paz-El Alto. This analysis is based on the chemical speciation obtained from the PM_{10} filter samples collected at both sites during the first 15 months of the measurements campaign and the use of the US EPA PMF tool. The methodology employed and the results obtained were submitted in the form of a scientific article to the journal Atmospheric Chemistry and Physics (ACP) and has been accepted for publication. The preprint version as well as the discussions thread can be found at: https://acp.copernicus.org/preprints/acp-2022-780/.

Source apportionment study on particulate air pollution in two high-altitude Bolivian cities: La Paz and El Alto

Valeria Mardoñez[1,2], Marco Pandolfi[3], Lucille Joanna S. Borlaza[1], Jean-Luc Jaffrezo[1], Andrés Alastuey[3], Jean-Luc Besombes[4], Isabel Moreno R.[2], Noemi Perez[3], Griša Močnik[5,6,7], Diego Aliaga[8], Federico Bianchi[8], Claudia Mohr[9], Patrick Ginot[1], Radovan Krejci[9], Vladislav Chrastny[10], Alfred Wiedensohler[11], Paolo Laj[1,8], Marcos Andrade[2], Gaëlle Uzu[1].

[1] Institute des Géosciences de l'Environnement, Université Grenoble Alpes, CNRS, IRD, Grenoble INP, Grenoble, France.

[2] Laboratorio de Física de la Atmósfera, Instituto de Investigaciones Físicas, Universidad Mayor de San Andrés, La Paz, Bolivia.

[3] Institute of Environmental Assessment and Water Research (IDAEA-CSIC), Barcelona, 08034, Spain

[4] Université Savoie Mont Blanc, CNRS, EDYTEM (UMR 5204), Chambéry 73000 France

[5] Center for Atmospheric Research, University of Nova Gorica, 5270 Ajdovščina, Slovenia

[6] Haze Instruments d.o.o., 1000 Ljubljana, Slovenia

[7] Department of Condensed Matter Physics, Jozef Stefan Institute, 1000 Ljubljana, Slovenia

[8] Institute for Atmospheric and Earth System Research (INAR), University of Helsinki, 00014 Helsinki, Finland

[9] Department of Environmental Science & Bolin Centre for Climate Research, Stockholm University, 10691 Stockholm, Sweden

[10] Department of Environmental Geosciences, Faculty of Environmental Sciences, Czech University of Life Sciences Prague, Kamýcká 129, 165 00, Prague-Suchdol, Czech Republic

[11]Leibniz Institute for Tropospheric Research (TROPOS), 04318 Leipzig, Germany

Abstract

La Paz and El Alto are two fast-growing high-altitude Bolivian cities forming the second-largest metropolitan area in the country. Located between 3200 and 4050 m a.s.l., these cities are home to a burgeoning population of approximately 1.8 million residents. The air quality in this conurbation is heavily influenced by urbanization; however, there are no comprehensive studies evaluating the sources of air pollution and their health impacts. Despite their proximity, the substantial variation in altitude, topography, and socio-economic activities between La Paz and El Alto result in distinct sources, dynamics, and transport of particulate matter (PM). In this investigation, PM_{10} samples were collected at two urban background stations located in La Paz and El Alto between April 2016 and June 2017. The samples were later analyzed for a wide range of chemical species including numerous source tracers (OC, EC, water-soluble ions, sugar anhydrides, sugar alcohols, trace metals, and molecular organic species). The US-EPA Positive Matrix Factorization (PMF v.5.0) receptor model was employed for the source apportionment of PM_{10}. This is one of the first source apportionment studies in South America incorporating an extensive suite of organic markers, including levoglucosan, polycyclic aromatic hydrocarbons (PAHs), hopanes, and alkanes, alongside inorganic species. The multisite PMF resolved 11 main

sources of PM. The largest annual contribution to PM_{10} came from two major sources: the ensemble of the four vehicular emissions sources (exhaust and non-exhaust), accountable for 35% and 25% of the measured PM in La Paz and El Alto, respectively, and dust, which contributed 20% and 32% to the total PM mass. Secondary aerosols accounted for 22% (24%) in La Paz (El Alto). Agricultural smoke resulting from biomass burning in the Bolivian lowlands and neighboring countries contributed to 9% (8%) of the total PM_{10} mass annually, increasing to 17% (13%) between August-October. Primary biogenic emissions were responsible for 13% (7%) of the measured PM_{10} mass. Additionally, a profile associated with open waste burning occurring from May to August was identified. Although this source contributed only to 2% (5%) of the total PM_{10} mass, it constitutes the second largest source of PAHs, compounds potentially hazardous to health. Our analysis additionally resolved two different traffic-related factors, as well as a lubricant source (not frequently identified) and a non-exhaust emissions source. Overall, this study demonstrates that PM_{10} concentrations in La Paz and El Alto region are predominantly influenced by a limited number of local sources. In conclusion, to improve air quality in both cities, efforts should primarily focus on addressing dust, traffic emissions, open waste burning, and biomass burning.

1. Introduction

Outdoor air pollution has undeniably proven to be an important threat for public health, being responsible for about 4.2 million yearly premature deaths around the world every year (WHO, 2021a). The exposure to air pollution becomes more complex at higher altitudes due to the decrease in oxygen per volume of air, as people have developed a higher lung capacity in order to fulfill the body oxygen demand (Frisancho, 1977; Frisancho, 2013; Frisancho et al., 1999; Madueño et al., 2020; U.S. EPA, 2011).

Many of the high-altitude large cities in the world (> 2000 m a.s.l., ≳2 million inhabitants) are located in Latin American low and middle-income countries, among which are Mexico City, Bogotá and Quito. These cities are also subject of a developing industry and a growing vehicular fleet that results in a constantly increasing energy consumption, heavily dependent on non-renewable energy sources (Castro Verdezoto et al., 2019; Molina et al., 2019; Pardo Martínez, 2015). Most of the cities in this region, for which data is available, face a deteriorated air quality, with particulate matter (PM) concentrations that exceed the World Health Organization (WHO) guidelines (Gutiérrez-Castillo et al., 2005; Mugica et al., 2009; Ramírez, et al., 2018a; Zalakeviciute, et al., 2020; WHO, 2021b).

High-altitude cities exhibit distinct characteristics due to complex topography and associated meteorology, influencing the transport, accumulation and dispersion of air pollution. Moreover, high altitude is linked to strong solar radiation that favors photochemical activity and high daily temperature variations. Compared to other regions at similar latitudes, high altitude cities in South America experience lower temperature, lower atmospheric pressure and saturation vapor pressures, as well as complex wind patterns and reduced precipitation (Vega et al., 2010; Zalakeviciute et al., 2018). Previous studies have shown that these specific high-altitude atmospheric and thermodynamic conditions can strongly favor new aerosol particle formation

(NPF)) (Boulon et al., 2010; Brines et al., 2015; Hallar et al., 2011; Sellegri et al., 2019; Singla et al., 2018; Sorribas et al., 2015). Additionally, it has been observed that low oxygen environments alter the performance and reduce the efficiency of combustion engines (Martínez et al., 2022; Wang et al., 2013a), thus, changing the vehicular emissions of gaseous and particulate pollutants (Bishop et al., 2001; Giraldo & Huertas, 2019; He et al., 2011; Nagpure et al., 2011; Wang et al., 2013b) .

Listed amongst the highest metropolitan areas in the world, La Paz (between 3200-3600 m a.s.l.) and El Alto (4050 m a.s.l.) are two Bolivian cities constituting a conurbation with a population of approximately 1.8 million people. Despite their close proximity, significant topographical, meteorological and socio-economic differences exist between them. While Bolivian legislation regulates concentrations of certain pollutants (CO, SO_2, NO_2, O_3, TSP, PM_{10}, Pb; Table S1), very few air quality studies which include long term measurements at moderate time resolution have been performed in the country or in the region. The few previous existing studies have reported PM_{10} mass concentrations ranging from 10 and 100 µg m^{-3} measured at urban and urban-background stations in La Paz and El Alto (Red MoniCA, 2016, 2017, 2018; Wiedensohler et al., 2018). However, no particle chemical speciation has been conducted to identify the major sources contributing to the high PM concentrations. Furthermore, measurements taken at the nearby Chacaltaya GAW station (CHC-GAW: 16.350500°S, 68.131389°W, 5240 m a.s.l.) show that the emissions of the city not only impact the local environment but also act as a point source influencing regional atmospheric composition (Aliaga et al., 2021).

While little is known about the sources of PM in the country, since industry is not largely developed, vehicular emissions potentially represent an important contributor to air pollution, particularly considering the absence of restrictions on the age of the vehicle fleet. Statistics indicate that 43% of the circulating vehicles are less than 10 years old, 15% are 10-20 years old and another 24% are 20-30 years old (INE, 2020a, 2020b). At a regional scale, agricultural biomass burning in the Bolivian and Brazilian valleys and rain-forests constitutes an important seasonal source of particulate pollutants (Mataveli et al., 2021). The latter has a significant impact on the air quality of the cities close to where the fires take place (Nawaz & Henze, 2020) and can be transported over large distances. Studies have shown that air masses coming from the Amazon can traverse the Andes, carrying pollutants and ultimately reaching the Bolivian Altiplano Altiplano (Bourgeois et al., 2015; Chauvigne et al., 2019; Magalhães et al., 2019; Segura et al., 2020). Additionally, previous studies based on emission inventories adapted to the data availability in LP-EA pointed out road dust, food industry, cooking and vehicle emissions as the major sources of PM_{10}, whereas for Cochabamba (the third largest urban area in Bolivia) estimations showed mobile sources to be responsible for almost 90% of PM_{10} emissions emissions (Herbst, 2007; Pareja et al., 2011). Although there are some indications of the most outstanding sources of particulate matter in La Paz and El Alto, currently there is not comprehensive study on the composition and sources of particulate matter air pollution. Therefore, the aim of this study is to apportion and characterize the sources of PM that affect air quality in the metropolis of La Paz-El Alto, which can be used as a baseline for future policy making.

To achieve this goal, the EPA-Positive Matrix Factorization (PMF v.5.0) receptor model was applied on the PM_{10} chemical speciation obtained from 24-h filter samples collected simultaneously in La Paz and El Alto over a 15-months campaign. This study represents one of the few conducting PM characterization in Bolivia over an extended period. Given the limited number of studies in this region, identifying the sources and chemical profiles of PM in the study sites proved to be more challenging. The analysis included a comprehensive chemical speciation, encompassing ionic species, monosaccharide anhydrides, polyols, metals, PAHs, alkanes, and hopanes. To the best of our knowledge, this is the first study on source apportionment at high-altitude cities that incorporates such a large set of organic and inorganic species.

2. Method

2.1. Sampling sites

Significant topographical differences exist between the two study sites, La Paz (LP) and El Alto (EA), in addition to the notable disparity in altitude and pressure. While the city of El Alto lies on the open and flat Altiplano plateau, the city of La Paz sprawls along the mountain valleys formed below the Altiplano in a closed area with steep and complex topography. The meteorological conditions throughout the year are governed by the seasonal transition between a dry and a wet season, typical of tropical regions. Temperature and wind patterns vary substantially between the two cities due to the differences in altitude and local topography.

Moreover, the city of El Alto originally developed as a peri-urban zone of the city of La Paz, welcoming migrants from nearby towns and communities who settled on the outskirts of the city of La Paz (Fernández, 2021). This gave rise to significant economic and social disparities between the cities that, to some extent, persist and are evident among the general population (Foster & Irusta, 2003). Such differences could have an impact on air pollutant emissions, due to the different practices in each of the cities, in addition to the daily commute of a significant part of the population of El Alto towards the city of La Paz.

The few existing industries are mostly located within or in the surroundings of El Alto, and the vehicular fleet observed in both cities is not homogeneous. The density of heavy vehicle traffic – trucks and buses, is more prevalent in El Alto, since it is the main regional and international connection from and to the metropolis. These factors uphold the need for having independent representative sampling sites for each city rather than relying on a single site, despite both being part of the same conurbation.

The sampling campaign was carried between April 2016 and June 2017. Several ambient and meteorological parameters were measured simultaneously at two urban background sites, one in each city. The sampling sites were located 7 km apart, with an altitude difference of over 400 m, and located at approximately 20 km from the Chacaltaya Global Atmosphere Watch (CHC-GAW) monitoring station (Fig. 1).

The El Alto measurement site was installed within the El Alto International Airport, in the facilities of the meteorological observatory (16.5100° S, 68.1987° W, 4025 m a.s.l.). The observatory is situated at a distance of approximately 250 m from the airport runway and 500 m from the nearest major road and has been described

elsewhere (Wiedensohler et al., 2018). Pre-campaign measurements were conducted to assess whether the takeoff and landing of airplanes had any significant influence on the measurements, revealing no substantial impact on CO_2, PM_1 and $PM_{2.5}$ during each airplane arrival and departure. Road traffic within the airport was minimal. The area around the sampling site is unpaved, hence dusty, and there are no other buildings in the proximity of the observatory. In March 2016, just prior the beginning of the sampling, the airport administration cleared the ground within the perimeter fence of the meteorological observatory, leaving the site dustier than the rest of the airport.

La Paz measurement site (LP) was placed on the rooftop of the city's Museum Pipiripi (Espacio Interactivo Memoria y Futuro Pipiripi: 16.5013°S, 68.1259°W, 3600 m a.s.l.). This municipal building is located atop a small hill in downtown La Paz. Unlike the EA site, within a 1 km radius, the LP site is surrounded by many busy roads and dense residential areas, with a horizontal and vertical minimum distance to the nearest road of approximately 70 and 45 m respectively. Otherwise, the site's immediate surroundings (~100 m radius) are covered by green areas and a municipality buses parking lot at the base of the hill.

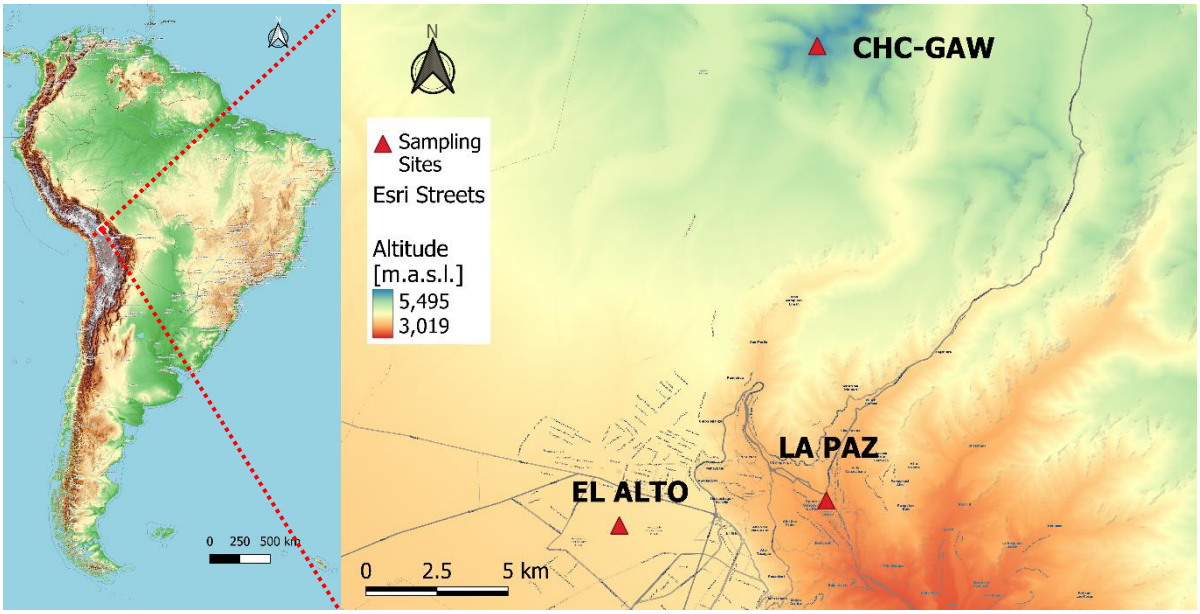

Figure 1. Geographical location of the sampling sites (left panel) La Paz (LP) and El Alto (EA) zoomed in (right panel) and positioned with respect to the regional Chacaltaya-GAW monitoring station (CHC-GAW). Color scale represents the altitude above sea level.

2.2. Sampling methods

High-volume samplers (MCV CAV-A/mb with an MCV PM1025UNE (PM_{10}) head) were employed to collect 24-h filter samples of PM every third day at both sites. Sampling started at 9:00 a.m. and the flow was automatically maintained at 30 $m^3\ h^{-1}$. To avoid interference of near-ground particle resuspension, the samplers were placed on the rooftop of the buildings. Throughout the analyzed period of the present study, an impactor with a 50% collection efficiency for aerosol particles with an aerodynamic equivalent diameter of 10 µm was installed at the inlet of the samplers at both sites to establish an upper size-cut.

The mass concentrations measured at both sampling sites are hereafter reported in ambient conditions (EA: $\overline{T} = 280.8$ K , $\overline{P} = 628.2$ hPa, LP: $\overline{T} = 286.0$ K , $\overline{P} = 664.7$ hPa), unless stated otherwise (e.g. when compared to literature reported concentrations). To convert to standard conditions of temperature and pressure ($\overline{T} = 273$ K , $\overline{P} = 1013.5$ hPa) the concentrations must be multiplied by a factor of 1.66 and 1.60 in El Alto and La Paz, respectively. Since the difference in ambient concentrations between the sites resulting from a difference in mean temperature and pressure is of approximately 4%, ambient concentrations are directly compared between the sites in the subsequent sections.

The aerosol particles were collected onto pre-heated (8 hours at 500°C) and pre-weighted 150 mm-diameter quartz fiber filters (Pallflex 2500QAT-UP). After sampling, the filters were folded and wrapped in aluminum foil, sealed in impermeable plastic bags, and stored in a cool environment prior to transportation for analysis. Mass concentrations were initially determined gravimetrically, and then the samples were divided for chemical analysis among three European laboratories. The resulting chemical speciation comprised elemental carbon (EC), organic carbon (OC), sugar anhydrides (Levoglucosan, mannosan), sugar alcohols (arabitol, mannitol), water soluble ions (SO_4^{2-}, NO_3^-, Cl^-, MSA^-, NH_4^+, Na^+, K^+, Mg^{2+}, Ca^{2+}) measured at IGE, Grenoble, France; metals (Al, Ca, K, Na , Mg, Fe, Ti, V, Mn, Cu, Zn, Rb, Sn, Sb, Pb) measured at IDAEA, CSIC, Barcelona, Spain; Polycyclic aromatic hydrocarbons (PAHs: Fla, Pyr, Tri, BaA, Chr, BaP, BghiP, IP, BbF, Cor), alkanes (C21-C26), methyl PAHs, thiophens, hopanes (HP3-HP4) alkane methoxyphenols, and methylnitricatechols measured at EDYTEM, Chambéry, France (Table S2). A total of 92 and 103 filter-samples were collected in the cities of El Alto and La Paz, respectively, excluding samples having sampling flow issues or influenced by specific events (c.a. San Juan local festivity, Christmas, New Year's Eve). In addition, laboratory blank filters were used to calculate the limits of quantification (QL). The average concentrations measured from the laboratory-blanks were then subtracted from the atmospheric concentrations measured from the filter samples.

2.3. Source apportionment (PMF)

The Positive Matrix Factor PMF 5.0 tool (Norris & Duvall, 2014; Paatero & Tapper, 1994), developed by the U.S. Environmental Protection Agency (EPA), was used to apportion the sources that contribute to the observed particulate material in the collected samples at both sites. This non-negative multivariate factor analysis seeks to solve the chemical mass balance equation [1], applying a weighted least-squares fit algorithm, x_{ij} representing each of the elements of the concentration matrix (having n number of samples and m number of chemical species measured), g_{ik} are the contributions of each k factor to the ith sample, f_{kj} are the chemical profile of the factors, and e_{ij} are the residuals (i.e. the difference between the calculated and the measured concentration).

$$x_{ij} = \sum_{k=1}^{p} g_{ik} f_{kj} + e_{ij} \quad [1]$$

The optimal solution is then achieved by minimizing the function Q defined as:

$$Q = \sum_{i=1}^{n}\sum_{j=1}^{m}\left[\frac{x_{ij} - \sum_{k=1}^{p} g_{ik} f_{kj}}{u_{ij}}\right]^2 \quad [2]$$

where u_{ij} are the uncertainties associated to each measurement.

2.3.1. Sample and chemical species selection

Out of the 197 PM_{10} samples initially included, 12 of them were later excluded from the analysis for having over 6 species with missing values (EA: 19 Sep 2016, 11 Jan 2017; LP: 14 May 2016, 07 Jun 2016, 12 Dec 2016, 02 May 2017) or because they presented unusual concentrations of PM or multiple species (LP: 04 Apr 2016, 22 May 2017, 30 May 2017, 11 Jun 2017, 15 May 2017, 19 Jun 2017). A total of 178 chemical species were measured for each filter. Species displaying irregularities in their time series were excluded from the analysis, as were those with over 25% of the data falling below the quantification limit (<QL, defined as the mean field-blank concentrations measured per specie, plus two times the standard deviation). From the remaining 86 species, the ones that were measured through both Ion Chromatography (IC) and Inductive Coupled Plasma-Mass Spectrometry (ICP-MS), only the ICP-MS metals were included in order to avoid duplicative counting, except for K^+, for which the IC measurements were used since water soluble K^+ is a known tracer for biomass burning (BB), soil resuspension, and fertilizers (Li et al., 2021; Urban et al., 2012). Galactosan and sorbitol were deemed unnecessary tracers for biomass burning and primary biogenic aerosols, respectively, as other specific tracers such as levoglucosan, mannosan, mannitol and arabitol were present. Consequently, they were excluded from the analysis. Additionally, other non-specific-tracer metal species were excluded after several attempts to including them in the PMF input data, as they introduced instability to the solution. Following the findings of Samaké et al., (2019a), arabitol and mannitol were added as one representative polyol specie, given that they are emitted by the same source and have a Pearson correlation of r>0.7, at both sites. The same was done for PAHs that presented a r>0.9 (PAH_1: [BghiP]+[IP]+[BbF]; PAH_2: [Fla]+[Pyr]). Finally, in the PMF analysis, OC was substituted with OC*, which represents the difference between the measured OC concentrations and the carbon mass concentration of all the included organic compounds, to avoid double counting (e.g. Weber et al., 2019):

$$OC^* = OC - \left(\begin{array}{c} 0.12\cdot[MSA] + 0.40\cdot[Polyols] + 0.44\cdot([Levoglucosan] + [Mannosan]) + \\ 0.95\cdot([BghiP] + [IP] + [BbF] + [Fla] + [Pyr] + [BaA] + [Chr] + [Tri] + [BaP] + [Cor]) + \\ 0.85\cdot([C21] + [C22] + [C23] + [C24] + [C25] + [C26]) + \\ 0.87\cdot([HP3] + [HP4]) \end{array}\right) \quad [3]$$

2.3.2. Uncertainty calculation and specie weight-assignment

In the uncertainty matrix, a 10% uncertainty was assigned to PM mass concentrations. The uncertainty calculation for polyols, monosaccharide anhydrides, and ions was followed the formula proposed by Gianini et al. (2012), employing the variation coefficients (CV) and the additional coefficients of variation (a) proposed and used by Weber et al. (2019), with the average QL associated to each species instead of DL. The

uncertainties associated to EC, OC, and metals, were calculated following the method proposed Amato et al. (2009) and Escrig et al. (2009). Finally, the uncertainties assigned to the molecular organic species were calculated using the formulas proposed by Polissar et al. (1998) and Reff et al. (2007), replacing the DL values by QL.

Values below the QL in the concentration matrix were replaced by the average of QL divided by 2 for each specie. The corresponding uncertainties were then set to $\frac{5}{6}$ QL (Norris et al., 2014). The outliers encountered in the time series of some species (a total of 4 values) were replaced by NA. Subsequently, the missing values in the input file were set to be replaced in the software by the median value of the corresponding species and their associated uncertainty was automatically set to four times the species-specific median.

The weight of the species in the factor analysis was determined based on their signal to noise ratio (S/N). Species with a S/N>2 were set as strong. Species with a signal to noise ratio: $0.2 \leq S/N \leq 2$ were defined as weak, resulting in a down-weighing of their influence in the analysis by triplicating their uncertainties. Species with a S/N<0.2 were not included in the analysis. Finally, PM was set as total variable, thus setting it as a weak variable. After conducting several tests, certain variables were also set as weak (K^+, V), for setting them as strong variables resulted in the creation of artificial factors, without any geochemical meaning. The PAHs, alkanes and hopanes were set as weak species to prevent them from driving the solution.

2.3.3. Solution evaluation criteria

A range of solutions, spanning from 8 to 13 factors, was examined to determine the suitable number of factors contributing to each site. Subsequently, a final solution was chosen based on the evaluation of various statistical and geochemical control parameters, as described by Belis et al. (2019):

- $Q_{true}/Q_{robust} < 1.5$.
- Residuals per species were centered and exhibited a symmetrical distribution around 0, falling within the range of -3 and 3, with a few exceptions for outliers.
- Bootstrap (BS) evaluation of the statistical robustness of the selected base run having a correlation coefficient for every factor > 0.8 after 100 iterations, before and after constraints.
- Displacements (DISP) analysis was performed to evaluate the rotational ambiguity and the solution's tolerance to minor perturbations (No rotations were observed for dQmax = 4, 8).
- Geochemical consistency of the obtained factor chemical profiles based on literature and knowledge of the study site.

2.3.4. Multisite PMF.

Initial parallel runs of single-site PMF analysis revealed similar main sources contributing to particulate matter. Increasing the number of factors showed potential for separating the traffic profile, albeit with a compromise on the statistical stability of the solution. Motivated by these findings, a multisite PMF analysis

was conducted. Such approach has proven its ability to reduce the rotational ambiguity in factor analyses (Dai et al., 2020; Hernández-Pellón & Fernández-Olmo, 2019; Hopke, 2021; Pandolfi et al., 2020), increasing the statistical robustness through an increased number of samples.

To combine both datasets into a single dataset (EA-LP) the dates in the La Paz dataset were shifted in time by two years and then appended to El Alto's dataset. Thus, duplicated dates were avoided and while composing a single input matrix for PMF that respected the natural seasonal variability of the original datasets. The dimensions of the resulting matrix were 185 rows (samples) x 40 columns (species). The multisite approach stands on the hypothesis that the major sources contributing to PM_{10} in both sites are similar and exhibit similar chemical profiles, which has been verified within the single site solutions.

2.3.5. Set of Constraints

Once the optimum number of factors was selected in the multisite base solution, a set of "soft" constraints (Table) was applied to the selected solution based on previous studies (Borlaza et al., 2021a; Samaké, et al., 2019b; Weber et al., 2019):

Table 1. Set of constraints applied to final solution

Factor	Specie	Constraint	Value
Biomass Burning	Levoglucosan	Pull up maximally	%dQ 0.50
Biomass Burning	Mannosan	Pull up maximally	%dQ 0.50
Primary Biogenic Aerosol	Polyols	Pull up maximally	%dQ 0.50
MSA-Rich	MSA	Pull up maximally	%dQ 0.50

2.3.6. Additional analysis of one local specific source: fuel chemical fingerprint.

To further investigate the differences between the two main types of fuel used in LP-EA, 3 samples of both gasoline and diesel were taken at 3 randomly chosen gas-stations located in different areas of the city. The main metal composition of these samples was subsequently analyzed using the following procedure: 1 ml of sample (gasoline, diesel) was transferred into a Teflon microwave vessel (Anton Paar microwave laboratory unit). Then, 10 ml of HNO_3 (double distilled, suprapure level) were added and the solution was decomposed by increasing temperature and pressure (175°C and 10 bar). In the microwave, the EPA 3051A method was run twice to assure that the solutions were indeed decomposed (US EPA, 2007). After cooling down the vessels, the solutions were diluted by a factor of 10 and directly measured using inductively coupled plasma mass spectrometer (ICP-MS). A complete descriptive table of the analyzed species can be found in the SI (Table S3).

3. Results and Discussions

3.1. Seasonal variations of chemical components of PM_{10}

A yearly alternation between the dry and the wet season as presented in Fig. 2, shows an annual maximum of PM_{10} concentrations coinciding with the middle of the dry season (Southern hemisphere winter). During this season, negligible wet deposition occurs and favorable conditions for particle resuspension are prevalent. Maximum daily ambient PM_{10} concentrations of 37.2 ± 10.5 µg m^{-3} and 33.2 ± 7.5 µg m^{-3} were measured during this period (May-August) in El Alto and La Paz, respectively. Conversely, the wet season (Southern hemisphere summer, December-March) exhibits frequent precipitation events and the highest daily minimum temperatures.

Similar PM_{10} variability and concentrations were observed at the International Airport of El Alto, using the C^{14} beta-attenuation technique, between 2011 and 2015 (ranging between ca. 10-50 µg m^{-3} throughout the year, Red MoniCA, 2016b). In the case of La Paz, the variability observed while also using the C^{14} beta-attenuation technique was similar to the one observed in the present study. However, the reported PM_{10} concentrations were higher (Red MoniCA, 2016a, 2017, 2018). The discrepancy in the measured concentrations in the case of La Paz can likely be attributed the different measurement site locations, as the sampling site in La Paz described in the Red MoniCA (2016a, 2017, 2018) reports was located in the downtown area, next to a busy avenue.

Among all the samples collected during the measurements campaign, 5 and 12% of the daily samples collected in La Paz and El Alto exceeded, respectively, the 24-hour PM_{10} concentration of 45 µg m^{-3} not to be exceeded more than 3-4 days per year, according to the short-term PM_{10} Air Quality Guideline (AQG) level recommended by the World Health Organization (WHO, 2021b). Moreover, the annual PM_{10} concentrations in both cities are at least 1.2 times higher than the PM_{10} levels of 15 µg m^{-3} recommended as annual AQG by the same organization (WHO, 2021b). Average measured PM_{10} concentrations were found to be 29.9 ± 12.0 µg m^{-3} (STP: 49.6 ± 19.9 µg m^{-3}) in El Alto and 27.2 ± 8.9 µg m^{-3} in La Paz (STP: 43.5 ± 14.2 µg m^{-3}). However, the annual average values can be relatively lower due to the under sampling during the wet season.

The observed concentrations are lower compared to those reported for Mexico City, a high-altitude (2850 m a.s.l) Latin-American megacity (Table 2), but higher than those observed in the cities of Bogotá and Quito. The average concentrations found in La Paz-El Alto are nearly double the reported average concentrations for most suburban and urban background sites in Europe, and similar to those measured in Turkey, certain regions in Poland (Rybnik: 44.1 µg m^{-3}), Bulgaria (Vidin: 41.3 µg m^{-3}), North Macedonia (Skopje: 48.7 µg m^{-3}) and Italy (Napoli: 46.9 µg m^{-3}) in 2019 (EEA, 2020; EEA, 2022).

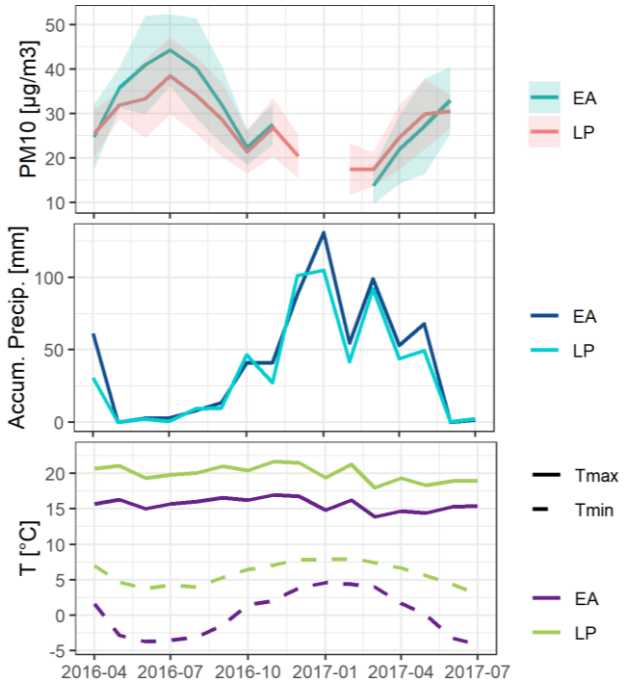

Figure 2. Monthly PM_{10} mean concentrations (µg m^{-3}), monthly accumulated precipitation (Accum. Precip., mm), and monthly mean maximum/minimum temperature (°C).

Table 2. Air quality studies at high-altitude Latin American cities.

	Average PM_{10} (Min-Max) [µg m^{-3}]	Period	Study	Population[i]	Altitude [m a.s.l.]
Mexico City, Mexico	(45.38-80.10) [ii]	2015-2016	(Cárdenas-Moreno et al., 2021)	18,457,000	2,850
Quito, Ecuador	24.9-26.2[iii,iv]	Jan 2017-Dec 2018	(Zalakeviciute, Rybarczyk, et al., 2020)	1,793,000	2,240
Bogota, Colombia	37.5 (9.89-160) [iii, iv]	Jun, 2015-May 2016	(Ramírez, et al., 2018a)	9,989,000	2,620
El Alto, Bolivia	29.9 (6.6-59.0) [iii,v]	April 2016-June 2017	Present study		4050
La Paz, Bolivia	27.2 (11.6-50.9) [iii, v]	April 2016-June 2017	Present study		3200-3600

[i] https://populationstat.com/
[ii] Range of spatial variation
[iii] Range of seasonal variation
[iv] Concentrations reported in standard conditions of temperature and pressure
[v] Campaign average PM_{10} concentrations that could slightly over estimate annual mean values due to a low number of samples collected during the wet season, where the minimum mass concentrations expected.

The reconstruction of the measured PM_{10} mass resulted from the mass closure procedure described for organic matter in Favez et al. (2010), Putaud et al., (2004), Seinfeld & Pandis (1998), Cesari et al. (2016;) and Pérez et al. (2008):

$$\mathrm{PM(recons)} = \{(1.8[\mathrm{OC}])\} + \{[\mathrm{EC}]\} + \{([\mathrm{SO_4^{2-}}] - 0.252[\mathrm{Na^+}]) + [\mathrm{NO_3^-}] + [NH_4^-]]\} + \{2.54[Na^+]\} + \{1.15 \cdot ((1.89[\mathrm{Al}]) + (2.14 \cdot (2.65[\mathrm{Al}])) + 1.67[\mathrm{Ti}] + (1.4 \cdot ([\mathrm{Ca}] - [\mathrm{Ca^{2+}}])) + (1.2 \cdot ([\mathrm{K}] - [\mathrm{K^+}])) + 1.36[\mathrm{Fe}]) + (1.5[\mathrm{Ca^{2+}}] + 2.5[\mathrm{Mg^{2+}}])\} \quad [4]$$

where the first curly bracket accounts for the organic matter, the third one accounts for the sum of the mass of secondary inorganic aerosol particles (non-sea-salt sulfate, nitrate, and ammonium), the fourth accounts for sea salt, and the fifth curly bracket accounts for the mass of the main components of crustal material: Al_2O_3, SiO_2, TiO_2, CaO, K_2O, FeO and Fe_2O_3 (multiplied by 1.15 to take into account sodium and magnesium oxides), and the mass of unmeasured carbonates.

Average PM_{10} (recons.) / PM_{10} (meas.) ratios of 0.91 in El Alto and 0.82 in La Paz were found. The remaining unidentified mass fraction may be attributed to the loss of volatile organic matter and secondary aerosols post-weighing, during the transport of the filter fractions to be analyzed. The difference can also be associated to the presence of non-measured species (i.e. carbonates) or to the adsorption of water in the aerosol particles or the filter (Pio et al., 2013). Moreover a 10% uncertainty associated with the gravimetry measurements could also have a role in the observed difference.

The average percentage contribution of the chemical species that significantly contribute to the measured PM_{10} concentrations in El Alto was: 22±5% OM (i.e. 1.8·OC), 5±2% EC, 9±5% secondary inorganic aerosols ($\mathrm{NH_4^+}$, $\mathrm{NO_3^-}$, and $\mathrm{SO_4^{2-}}$), and 12±3% of crustal material (Al, Fe, Ti, Ca, K, Mg, Mn, P). In La Paz, 25±5% OM, 6±2% EC, 8±5% secondary inorganic aerosols, and 10±2% of crustal material. Moreover, Fig. S3 in the SI shows the monthly behavior of the principal species contributing to PM, along with certain specific source tracers.

Mean OC/EC mass ratios of 2.6±1.1 and 2.8±1.6 were found for El Alto and La Paz, respectively, during the measurements period. This average OC/EC ratio results from the combination of various sources including vehicle emissions and other primary and secondary local and regional sources of carbonaceous particles (such as biomass burning, primary biogenic emissions and secondary organic aerosols). The highest OC/EC ratios, with the largest standard deviation, were observed between August and October, peaking in September. The mean OC/EC ratios during this period is of 3.5±1.3 for El Alto and 3.8±1.6, indicating to the long-range influence of biomass burning emissions at the end of the agricultural year, as well as the influence of primary organic emissions (Brines et al. 2019; Hays et al. 2002; Robert et al. 2007a, b; Samaké, et al. 2019a, b; Waked et al. 2014). It was observed that biomass burning tracers peak in August, while polyols display an increase in concentrations peaking in September. In contrast, minimum OC/EC ratios that display a smaller dispersion around the mean were observed between March and April: 1.9±0.6 and 2.0±0.6 in El Alto and in La Paz, respectively.

3.2. Source apportionment

After approaching the analysis individually for each site and observing that both sites shared similar sources, as well as considering the proximity of both cities, the multisite approach allowed to overcome the challenge posed by the relatively low number of samples compared to the number of species included in the single site analysis. This approach immediately provided a solution with greater stability, maintaining the previously observed profiles and making it possible to achieve a stable 11-factor solution. Figure 3 displays the percentage contribution attributed by the PMF analysis to each of the resolved sources after applying the constraints described in the previous section.

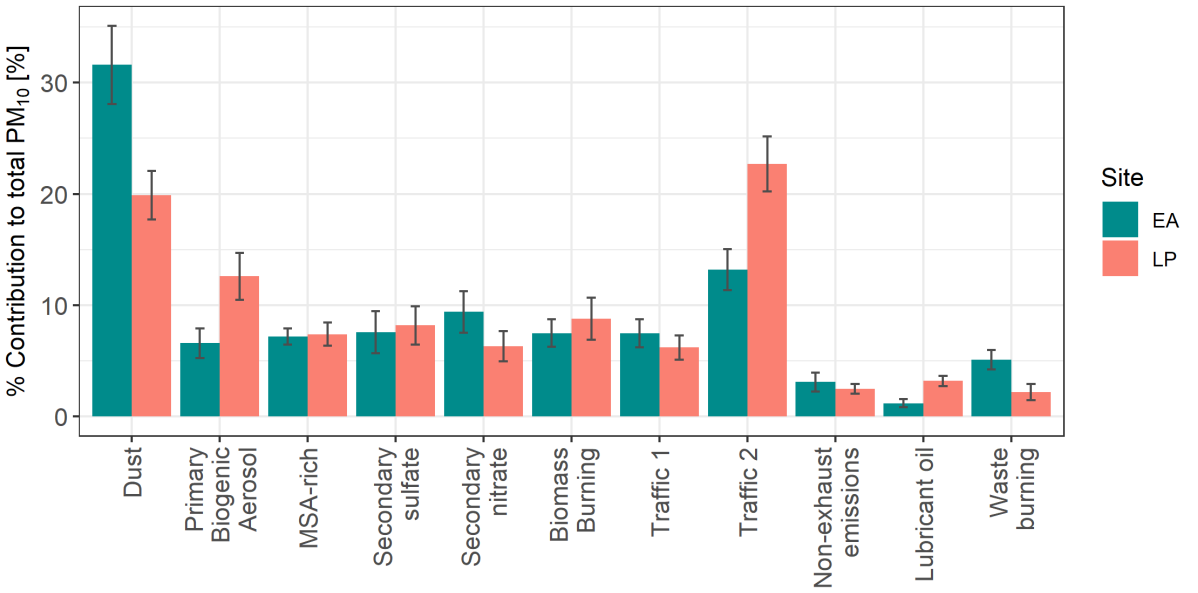

Figure 3. Average factor contributions to total PM_{10} at each site, resulting from the multisite PMF. The bars represent the 95% confidence interval of the mean values.

The measured PM_{10} concentrations versus the modeled PM_{10} concentrations through the multisite approach exhibited a linear relationship with a slope of 1.01 and an R^2=0.95, indicating that the factor analysis adequately reproduced the measured concentrations. The 11 resolved sources include dust, secondary sulfate, secondary nitrate, primary biogenic aerosols (PBA), MSA-rich, biomass burning (BB), traffic 1 (TR2), traffic 2 (TR2), lubricant, non-exhaust emissions, and waste burning (Fig. 3). Most of the resolved sources are consistent with the emission sources observed in previous studies performed in other sites sites (Chevrier, 2016; Waked et al., 2014; Weber et al., 2019; Yang et al., 2016). A comparison of the chemical profile of the sources resolved in the present study, and the chemical profile of the sources resolved by Borlaza et al. (2021a) and Weber et al. (2019)using the PD-SID method described in Belis (2015) and Pernigotti & Belis (2018) can be found in the SI. Furthermore, a separation of the traffic exhaust emissions (TR1, TR2) linked to the type of fuel used will also be presented in the following sections.

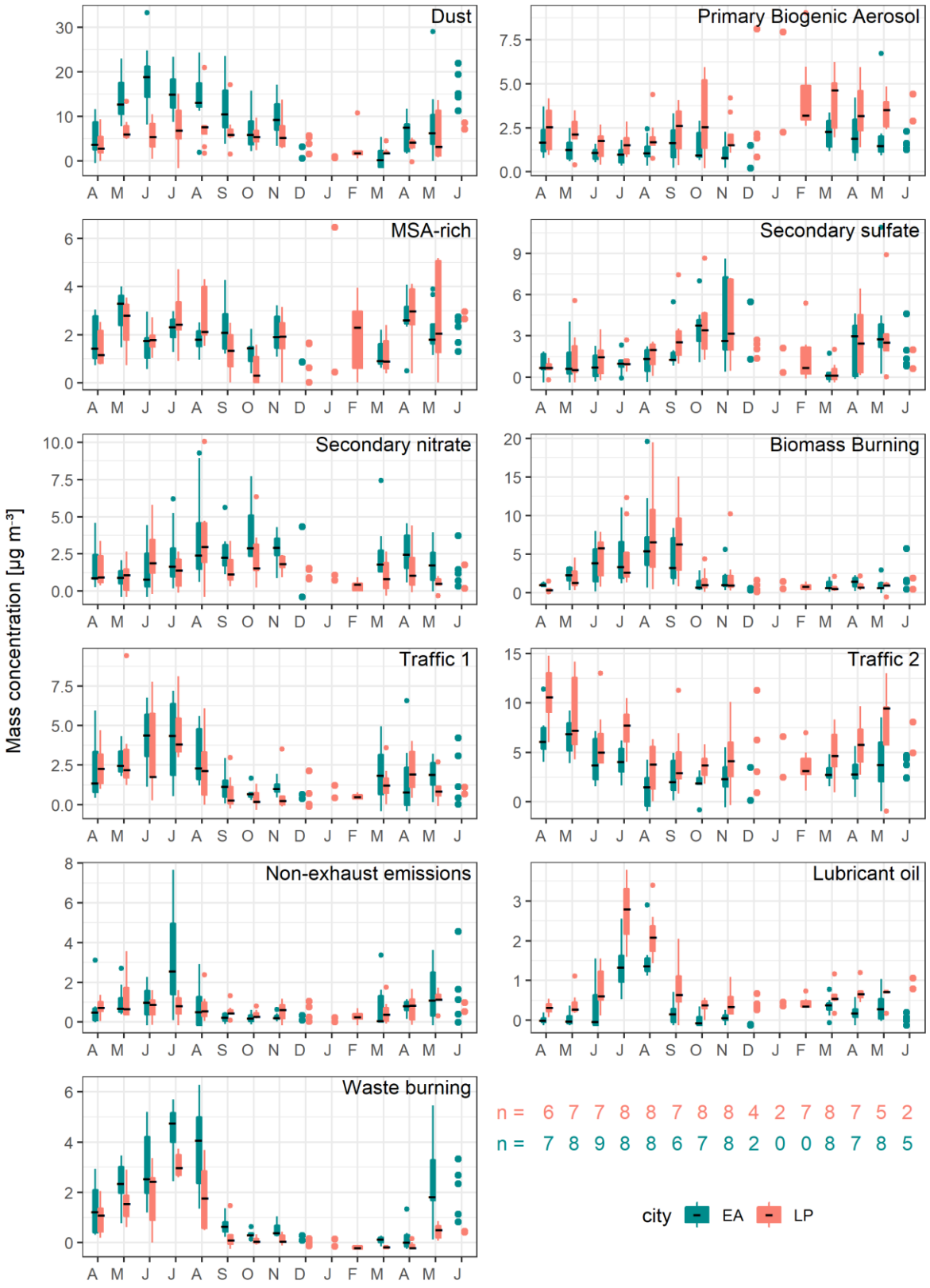

Figure 4. Source mass-contribution monthly variations (n = number of modeled data points included in the average) between April 2016 and July 2017.

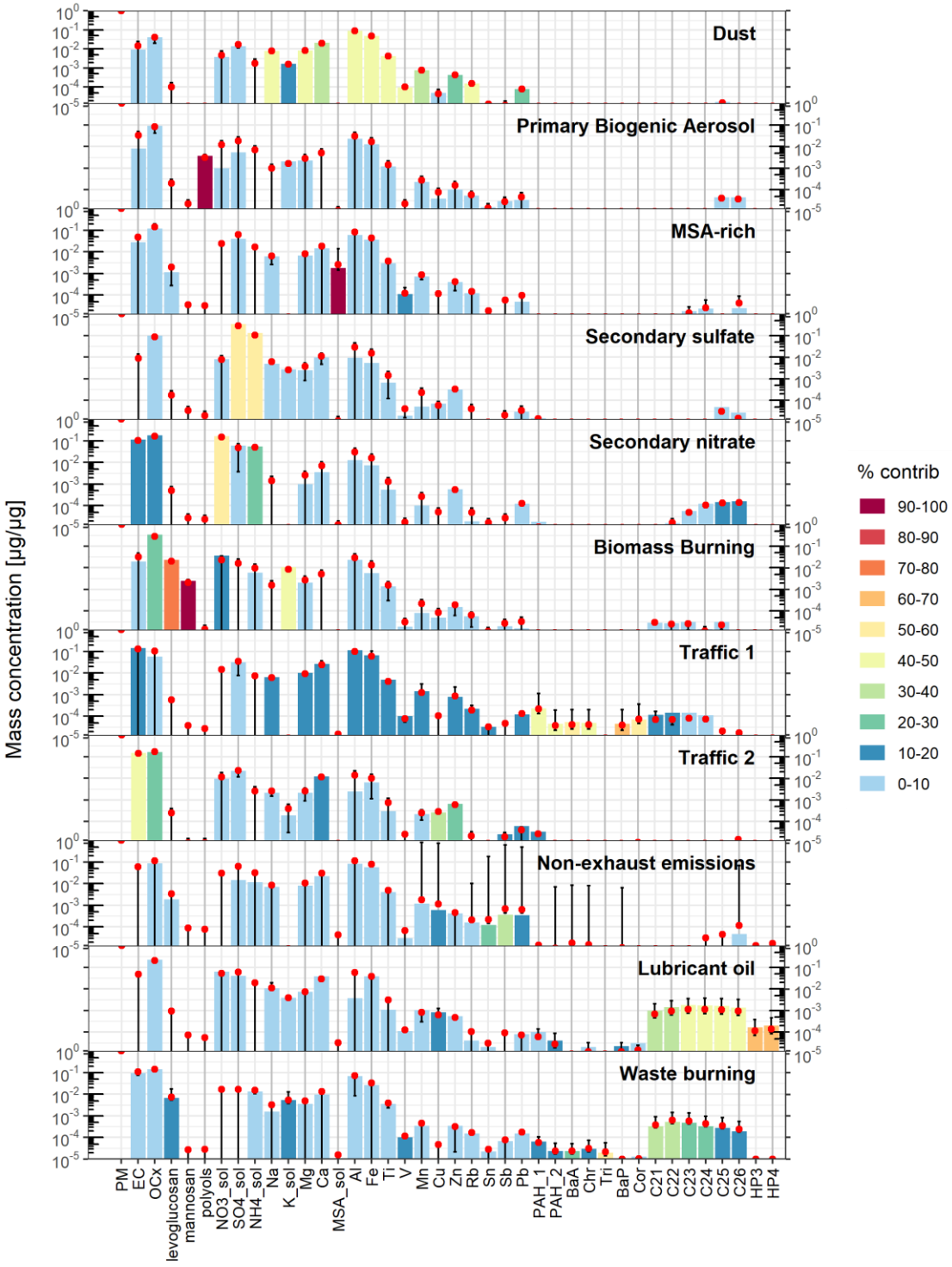

Figure 5. Source chemical profiles (bars representing median bootstrap mass contributions of each specie per µg of PM mass attributed to each source in y-axis, red dots represent mean DISP values, error bars represent DISP confidence intervals, color scale represent the contribution in percentage). The name of each source is further described and developed in the individual factor descriptions[8].

[8] PAH_1: [BghiP]+[IP]+[BbF]; PAH_2: [Fla]+[Pyr]).

Dust and the ensemble of vehicular contributions (i.e. Traffic 1, Traffic 2, Lubricant, Non-exhaust emissions) together account for 55% and 57% of the measured PM_{10} mass concentrations in La Paz and El Alto, respectively. The dust factor exhibits outstanding contributions of 32% in the city of El Alto, making it the dominant source in this city. Although the volume sampler was placed on the roof of the observatory building, it cannot be excluded that the samples were influenced by the local dust**.** In La Paz, the vehicular emissions take the lead in terms of percentage contributions (35%). The factors associated with secondary aerosol particles (secondary sulfate, secondary nitrate, MSA-rich) were responsible for nearly 22% and 24% of total PM (La Paz and El Alto respectively), only a slight difference can be observed between the cities except for the nitrate rich profile. Finally, the biomass burning factor was responsible for an average of 9 and 8% of the total measured PM_{10} (in LP and EA, respectively). The chemical profiles and seasonality of each factor are displayed in Fig. 4 and Fig. 5, respectively, and One of the advantages of performing a multisite PMF in the present study is the possibility to differentiate between two traffic profiles that could hardly be observed in the individual solutions. Similarly, some factor profiles that remained mixed in the single-site-solution for one site were polished as a result of combining both datasets. That was the case for the dust, MSA-rich, traffic 2, and non-exhaust profiles (Single site solutions can be found in the SI for comparison with the multisite solution.

3.2.1. Dust

This factor is the major contributor to the observed PM_{10} mass at both sites and is traced by crustal elements, such as Al, Fe, Ti, Mg, Mn, Ca, Na, K, V, Rb. The confidence interval for these species is narrow around the average displacement value, indicating that these species are mainly the ones that define this source profile. The presence of other elements, including sulfate, OC, Zn and Pb (with tight confidence interval), along with EC and Cu (with confidence intervals that allow negligible concentrations), supports the influence of road traffic in this source, through road dust resuspension. This factor has an average contribution of 32% (Ambient: 10.6±7.6 μg m^{-3}, STP: 15.7±11.2 μg m^{-3}) to the total PM_{10} mass observed in El Alto during the measurements period, and 20% (Ambient: 5.5±4.1 μg m^{-3}, STP: 8.0±5.7 μg m^{-3}) in the city of La Paz. This factor significantly contributes to the difference in PM mass concentrations observed between La Paz and El Alto. The factor contribution can rise up to 46% of the mass in El Alto during winter time (specifically in June), whereas its percentage contribution in La Paz reached their maximum during the transition month of October (27%).

The difference in contribution between these two sites can be attributed to difference in La Paz and El Alto characteristics. Particularly, El Alto is a fast-growing city located on the edge of the Altiplano region, a dry and arid area with mostly unpaved streets and active construction works. On the other hand, the city of La Paz shows to be less influenced by this factor, likely due to a higher fraction of paved roads compared to El Alto. Additionally, La Paz is situated at a lower elevation, surrounded by mountains and hillsides, which reduces the impact of strong winds from the Altiplano. Although both stations were considered to represent urban background, the terrain surrounding the two stations is very different. The El Alto station is located in the middle of the airport facilities, in a rather dusty area, while the La Paz station is located on the rooftop of a

building located in the middle of the city. Nevertheless, combining the time series obtained from the PMF analysis for this factor and the meteorological information from both sites, it was observed that the highest contributions from this factor were associated with higher wind speeds coming from the North West (NW). The seasonality observed in this factor is also consistent with the variation in precipitation favoring the main removal mechanism of dust in air (i.e., wet deposition). Similar contributions of dust to PM_{10} (with comparable or lower mass concentrations) have been reported by other studies in South America, like Sao Paulo: 25.7% (11.3 µg m^{-3}, Pereira et al. 2017a), Bogotá: 28% (10.5 µg m^{-3} (STP), Ramírez, et al 2018a), and Quito: 19.11-20.79.% (4.8-5.3 µg m^{-3}, Zalakeviciute et al. 2020) (Absolute mass concentrations of dust [µg m^{-3}] were calculated based on the percentage contributions reported on the studies mentioned and the reported average PM mass concentrations).

3.2.2. Primary biogenic aerosol (PBA)

The Primary biogenic aerosol (PBA) factor is associated with the highest fraction of polyols, which serve as tracers of soil and fungi activity, as well as plant debris (Elbert et al., 2007; Samaké et al., 2019a,b). The following most important contributors to this factor, with narrow confidence intervals are OC, K^+ and heavier alkanes, species that have been observed accompanying this source in other similar studies (Borlaza, et al., 2021a; Chevrier, 2016). On average, PBA contributes 7 and 13% (1.5±1.0 µg m^{-3} and 2.8±1.8 µg m^{-3}) to the annual PM_{10} mass observed in El Alto and La Paz, respectively. However, its contribution increased up to 11 and 17% (2.1±1.1 µg m^{-3} and 3.4±1.7 µg m^{-3}) of the mass concentrations during early autumn (March-April). Minimum concentrations were observed during winter. Similar results were found in France by Chevrier (2016) and Samaké et al. (2019a) where maximum concentrations of primary biogenic tracers were observed between late spring and early autumn. Highest contribution of this factor was observed in late summer (February) in La Paz 4.4±2.4 µg m^{-3}, becoming the second largest source in terms of mass during this month (28%). However, it should be noted that fewer number of samples collected in the rest of the summer months. Higher contributions of this factor were consistently observed in LP compared to EA, most likely due to its closer proximity to vegetation (both, local and in the valleys to the East).

3.2.3. MSA rich

This factor is predominantly identified by MSA, accounting for 100% of the MSA present in the samples. A small fraction of OC, V, Mn, Zn, and certain heavy alkanes is also present in this factor, suggesting a potential minor contribution from anthropogenic sources. It contributes to 7% (2.0±0.9 µg m^{-3} and 2.0±1.4 µg m^{-3}) to the observed PM_{10} mass in El Alto and La Paz. MSA is known to result from the oxidation of the primary emissions of dimethylsulfide (DMS) typically produced by marine phytoplankton, however studies have shown other possible sources of DMS as terrestrial biogenic sources, forest biota or lacustrine phytoplankton (Du et al., 2017; Ganor et al., 2000; Jardine et al., 2015; Saltzman et al., 1983). No clear seasonality was observed, except for the slight decrease in concentrations in the months of March and October.

Neither back trajectory analysis nor association with local wind direction were useful to elucidate on the specific origin of this factor. However, Aliaga et al. (2021) showed that air masses passing by the Titicaca Lake formed part of the third main air mass pathway arriving to the nearest GAW station (CHC-GAW) between December 2017 and May 2018. Moreover, Scholz et al. (2022) showed that the observed DMS in CHC-GAW during the same period was mostly linked to long-range transport of marine air masses, with a smaller contribution from the Titicaca Lake. Considering that air masses originating from the coast do not represent an important source of PM in the conurbation, terrestrial or lacustrine sources could be more likely to be the origin of this factor. The Titicaca Lake, the largest freshwater lake in South America, is located about 50 kilometers outside the metropolitan area (about 50 km) and long-range transport of air masses from the Amazon can also be observed at the sampling sites.

3.2.4. Secondary sulfate

This factor contributes to 8% of the total observed mass concentrations at both sites (1.9±2.1 µg m^{-3} and 2.0±2.1 µg m^{-3} in El Alto and La Paz, respectively) and is characterized by the presence of sulfate and ammonium. This factor is generally associated to long range transport of air masses in preceding European studies (Amato et al., 2016; Borlaza et al., 2021a; Waked et al., 2014) due to the time scales and conditions necessary to form ammonium sulfate from its gaseous precursors: sulfuric acid (H_2SO_4) and ammonia (NH_3) (Viana et al., 2008). Additionally, a small fraction of other inorganic elements such as Na, K, Mg, Ca are also found with tight confidence intervals in this factor. These elements have been observed to be associated with sulfate rich factors in previous European studies, occasionally linked to long-range transport factors (aged sea salt) (Borlaza, et al., 2021a; Dai et al., 2020; Veld et al., 2021; Weber et al., 2019).. Nevertheless, the small contribution of Zn and some heavy alkanes in the factor shows there could also be an influence of local sources to this factor. This could be attributed to the relaxed regulations of sulfur concentrations in imported fuels (<5000 ppm for diesel and <500 ppm for gasoline, Decree 1499/2013 of the Bolivian government), which represents 41 to 46% of the national fuel consumption (Correo del Sur, 2022). Furthermore, this factor also includes a small fraction of OC, that could originate either from anthropogenic emissions or from biogenic SOA formation (Borlaza et al., 2021).

The highest contributions from this factor were observed during October and November (local spring) where favorable conditions for ammonium sulfate formation are met, including strong solar radiation, moderate temperature and relative humidity (Karamchandani & Seigneur, 1999; Korhonen et al., 1999). A similar temporal variability was observed in the city of Arequipa (Peru) (Olson et al., 2021), the closest urban high-altitude large agglomeration (ca. 2300 m a.s.l., ~1 million inhabitants) located 300 km to the west of LP-EA. The aforementioned study found urban combustion emissions to be the main sources of sulfate aerosols in the city (50%), followed by dust (20%), despite its proximity to the coast and to the Central Andes volcanic region. However, it is important to highlight that an increase in sulfur concentrations associated to an increase in the regional volcanism activity occurred during the same period (Manrique et al., 2018; Masías et al., 2016), which

could contribute to the observed seasonality. Nonetheless, the fact that the average contributions of this factor to total PM_{10} are nearly identical in both cities indicates an even distribution of this factor throughout the metropolitan region. Although the overall contribution of this factor to total PM is relatively low compared to other factors, it accounts for 14-15% of the observed mass in both sites during spring, while comprising only 3-4% of the total mass during winter.

3.2.5. Secondary nitrate

This factor is responsible of 53% of the nitrate found in the samples and represents the second largest source for the ammonium found at both sites (23%). This factor also exhibits a secondary contribution with a narrow confidence interval for EC, OC, Zn, Pb, and heavy alkanes, tracers of traffic emissions. This evidences that the main source of the nitrates observed in La Paz and El Alto is linked to the combustion of fossil fuels, and is mostly locally produced from the oxidation of NO_x emitted from traffic. Previous studies of emission inventories in the country have also estimated that mobile (transportation-related) sources to be the main source of NO_x (Herbst, 2007; Pareja et al., 2011)

The contribution of this factor to total PM_{10} was of 9 and 6% (2.3±2.0 µg m^{-3} and 1.6±1.6 µg m^{-3}) in El Alto and La Paz, respectively. Higher concentrations are observed in El Alto compared to La Paz. Since NO_x concentrations were not monitored at either of the stations, we can only speculate that the difference between La Paz and El Alto is partly attributed to the difference in ambient temperature between both cities, as colder temperatures favor the partitioning of nitrate in particulate phase.

3.2.6. Biomass combustion

The main source of for biomass burning pollution in the tropical South America is agricultural practices and land use change (Mataveli et al., 2021). Although it is not a common practice in the Andean region, long-range transport of air masses coming from the Bolivian lowlands and neighboring countries contributes to PM at both sites. The main species represented in this factor are OC, levoglucosan, mannosan, and K^+, which are typical tracers of biomass burning burning (Li et al., 2021; Simoneit, 2002; Simoneit & Elias, 2000).. While 100% of mannosan is explained by this factor, only 76% of the levoglucosan present in the samples can be explained by this source (despite the applied constraint). Low contributions of EC to this factor produce a median OC/EC ratio of 17.8. This factor exhibits similar annual contributions of 9% and 8% to PM_{10} concentrations in La Paz and El Alto, with maximum average contributions of 17% and 13% (6.4±5.4 µg m^{-3} and 5.4±4.7 µg m^{-3}) in the middle of the dry season (July-September), peaking in August. In contrast, concentrations during autumn are much lower (1.0±1.0 µg m^{-3} and 1.3±0.9 µg m^{-3}). The median levoglucosan to mannosan ratios (Lev/Man=9.1) of this profile were found to be close to ratios previously reported for sugarcane burning (one of the main plantations in the Brazilian Amazon region) in laboratory and field studies (Hall et al. 2012: 10; Pereira et al. 2017a: 11; Pereira et al. 2017b: 12; Zhang et al., 2015). The difference between cities in the observed

concentrations assigned to this factor during the biomass burning season might be explained by the fact that EA, located higher up on Altiplano, is potentially less influenced by long range transport from the low lands.

Although agricultural biomass burning practiced in the Andean valleys and the Amazon region of Bolivia and neighboring countries has a relatively low annual contribution, it is important during the dry season. On days when PM_{10} concentrations exceeded the short-term exposure AQG recommended by the WHO (45 µg m^{-3} in 24-hr), the biomass burning factor accounted for 13% of the total mass in EA (7.0±5.9 µg m^{-3}) and 23% in LP (11.9±7.4 µg m^{-3}, making biomass burning the second most important source of PM after dust during those episodes.

3.2.7. Non-exhaust vehicular emissions

This factor is identified by the presence of metals such as Cu, Sn, Sb, and Pb, along with a significant contribution of Fe in terms of mass. These species have been previously identified as tracers for break and tire wears (Amato et al., 2011; Charron et al., 2019; Fukuzaki et al., 1986), generated by vehicles through mechanical abrasion. However, some studies have also found these tracers to be associated with industrial emissions (La Colla et al., 2021), for which we could not entirely neglect the possibility of having an influence of industrial emissions masked within this factor. This factor appeared at an early stage in the single site PMF in El Alto but it was not observable in La Paz. The multisite PMF allowed to clearly identify this factor in La Paz, splitting it from another traffic related source. This factor contributes to 3% of the total PM_{10} mass at both sites, with slightly higher contributions during the dry season, following a similar seasonality pattern as the dust factor. However, this factor frequently presents high concentration spikes in El Alto that are not observed in La Paz.

3.2.8. Open waste burning

With the inclusion of PAHs and alkanes into the PMF analysis, a specific factor tentatively associated to waste burning was identified. This factor is characterized by the presence of levoglucosan, K^+, EC, OC, metal species such as Al, Ti, V, Rb, Pb, PAHs and alkanes. It accounts for 57% of the Triphenylene observed in the samples. This factor also contributes in median to 10-20% of the observed concentrations of PAH_1, PAH_2, BaA and Chr, and 15 to 35% of the measured alkanes. It represents the second major source of the observed alkanes. Although Cl^- was not included in the final PMF solution due to the instability it added to all the explored solutions, preliminary runs indicated a significant fraction of total Cl^- associated with this factor. A Spearman correlation >0.67 was found between the concentrations of Cl^- and the PM concentrations attributed to this factor (Table S6). These elements are typical byproducts of the combustion of plastic mixed with vegetation or wood (Cash et al., 2021; Christian et al., 2010; Guttikunda et al., 2013, 2019; Kumar et al., 2018; Lanz et al., 2008; Rivellini et al., 2017; Simoneit, 2002; Singh et al., 2008). Similar factors have been observed in prior studies Pereira et al., 2017; Rai et al., 2020; Zíková et al., 2016), although only few of these studies were able to distinguish it as a separate factor from biomass burning or traffic, given the ubiquity of some of the tracers.

On an annual average, the total mass of PM_{10} attributed to this factor amounts to only 5% and 2% (1.8±1.8 µg m^{-3} and 0.8±1.2 µg m^{-3}) in El Alto and La Paz, respectively. However, during winter, its contribution can increase to 9 and 6% (3.4±1.6 µg m^{-3} and 2.1±1.2 µg m^{-3}). The seasonality of this factor is evident, with higher contributions in May and decreasing contributions in August. Although the exact source of this factor remains unidentified, the higher contributions in El Alto compared to La Paz suggest the presence of local sources within the El Alto area. Analysis of wind characteristics shows that higher concentrations of this factor are linked to low wind speeds blowing from the North in the case of El Alto, and from the northwest and with higher wind speeds in the case of La Paz (Fig. S7). The local emissions could originate from punctual-sources of waste burning, or the emissions of industrial and open commercial areas in El Alto, later transported to the city of La Paz. Similar behavior was observed when associating Cl- to wind speed and wind direction (not presented here).

3.2.9. Traffic sources 1 and 2 (gasoline/diesel)

The first resolved traffic factor (TR1) is annually responsible for 6 and 8% of the observed PM mass in La Paz and El Alto, respectively (1.9±2.0 µg m^{-3} and 2.3±2.0 µg m^{-3}). The main tracers of this factor are a small fraction of EC and OC, the presence of metals such as Na, Ca, Mg, Al, Fe, Ti, V, Mn, Zn, Rb, Pb, and over 40% of most PAH concentrations, consistent with previously observed vehicular emission factor profiles (Amato et al., 2011; Waked et al., 2014; Charron et al., 2019). Some traces of sulfate, and lighter alkanes can also be observed in the chemical profile of this factor.

The second traffic factor (TR2) contributed with an average of 23% and 13% to total PM_{10} in La Paz and El Alto, respectively (5.7±3.5 µg m^{-3} and 3.6±2.5 µg m^{-3}). The chemical species identified in this factor are similar to those found in TR1, including: EC, OC, Zn, PAH_1 and Cor, with small contributions of sulfate, Na, Ca, Mg and Mn. It is noteworthy that no alkanes and almost no hopanes are found in TR2, even if these compounds are in principle emitted by road traffic.

The median OC/EC ratios obtained from the traffic chemical profiles of TR1 and TR2 are 0.4 and 1.1, respectively The low OC/EC ratios observed in high-altitude conditions are not surprising, as combustion processes are less efficient under low O_2 availability (Wang et al., 2013a)However, because of the very different conditions for combustion, literature values of the ratio OC/EC (> 1 for gasoline, and < 1 for diesel, (Brito et al., 2013; Cheng et al., 2010; Cheng et al., 2021; Wong et al., 2020; Yuan et al., 2019) were not useful to identify which of the traffic factors can be associated to gasoline- or diesel-powered vehicles, being both OC/EC ratios in the present study close to 1.

A key distinction between the two traffic factors is the Mn/Zn ratio, with TR1 exhibiting a ratio greater than 1 and TR2 showing the opposite trend. The fuel analysis (pre-combustion) revealed that the largest difference in the chemical composition between local gasoline and diesel fuels was the relative abundance of Mn compared to Zn. Whilst the measured prior-combustion ratios of Mn/Zn are not preserved, the Mn/Zn ratio

remains a characteristic feature of each profile. Additionally, TR1 have higher PAH concentrations, whereas TR2 shows much lower contributions of PAHs. Previous studies have demonstrated that gasoline-powered vehicles indeed emit more long-chain PAHs than diesel fuel (IFP, 2021; Leoz-Garziandia et al., 1999, Zielinska et al. 2004a) fuel. While gasoline-powered vehicles represent over 80% of the vehicle fleet in Bolivia, literature has shown that diesel-powered vehicles can emit 10 to 30 times more particles than gasoline-powered vehicles (Zielinska et al., 2004b).

In terms of contribution, TR2 has a greater overall influence than TR1 in La Paz and is almost twice as influential as TR2 in El Alto. This difference could be related to the difference in the topography, as previous studies have shown that steep slopes can significantly increase the vehicle fuel consumption consumption (Carrese et al., 2013; Wang & Boggio-Marzet, 2018). Additionally, the proximity of the LP sampling site to the nearest main avenue (~100 m) and to the parking lot of the municipality buses (~100 m, horizontal distance; ~45 m vertical distance), which are diesel powered vehicles, may play an important role in the respective influences of TR1 and TR2 in LP.

The PD-SID comparison of both traffic factors with the road traffic profiles of several urban/urban-background French sites presented in Borlaza et al. (2021) and Weber et al. (2019) (SI) revealed there is a significant similarity between TR2 and the French road-traffic factors (where diesel is the dominant fuel used). However, TR1 exhibits PD values outside the similarity thresholds established by Pernigotti & Belis (2018).

Based on the previous description of factors TR1 and TR2, we consider likely that TR1 is related to the emissions from gasoline-powered vehicles, whereas TR2 is most likely associated to diesel-powered vehicles. However, the number of registered cars reported by the Municipal Tax Administration in 2011 showed that the number of gasoline-powered vehicles in the city of La Paz (~90% of the registered vehicle fleet in La Paz) was 2.4 times larger than the ones registered in El Alto (~80% of the registered vehicle fleet in El Alto). In contrast, similar number of diesel-powered vehicles were registered at both sites. If these numbers were directly related to the flow of vehicles in the metropolitan area, they could imply the opposite of what can be concluded from the chemical profiles, i.e. TR1 associated to diesel powered-vehicles and TR2 associated to gasoline-powered vehicles. However, it should be noted that vehicle registration does not necessarily imply those are operating vehicles. This could be especially the case for trucks and buses that move between La Paz and El Alto. In addition, it is known that large contributions of emissions could come from a small number of vehicles (Ježek et al., 2015; La Colla et al., 2021; Brito et al., 2013). These factors make it challenging to estimate the contribution of the different types of vehicles circulating in the metropolitan area to the measurements obtained from the filters.

Together, TR1 and TR2 constitute the major source of particulate matter in La Paz, and the second largest source of PM_{10} particles in El Alto. TR1 displays a slight seasonality with higher concentrations during the dry season of 2016. On the other hand, TR2 does not display significant seasonality, except for higher concentrations observed between April-May 2016 and May-June 2017. Although, one might similar variability

for traffic-related profiles, this is not the first study to observe a difference in the yearly variability of gasoline and diesel emissions (Squizzato et al., 2018 for a study in New York State).

3.2.10. Lubricant oil

The inclusion of molecular organic species (PAH, alkanes, and hopanes) enabled the identification of a factor associated with lubricant combustion, likely originating from vehicle emissions. This factor is marked by the presence of hopanes and alkanes in the chemical profile, which serve as unequivocal tracers of oil combustion (Charron et al., 2019; El Haddad et al., 2009). It contributes to 36-47% of the total mass of alkanes present in the samples, and constitutes the major source of hopanes, accounting for 65% of their total mass. Additionally, this factor presents smaller percentage contributions of OC, K+, Na, Ca, V, Mn, Cu, Zn, and certain PAHs, elements commonly present in fuel combustion emissions. The contribution of this source to annual PM_{10} mass is of 3 and 1% (0.9±0.8 µg m-3 and 0.4±0.6 µg m^{-3}) in La Paz and El Alto, respectively. A clear increase in contributions during the coldest months of the year can be observed in the variability of this factor. A similar evolution of the hopanes with maximum concentrations during winter was observed in Marnaz (France) by Chevrier (2016). Likewise, a study in three cities of the United States of America (USA) observed an increase of concentrations of hopanes and alkanes during the coldest months of the year (Kioumourtzoglou et al., 2013). This seasonality could be associated to the cold start of vehicle engines in the early morning and late-night hours, in the period when minimum temperatures decrease.

Overall, the contribution of this factor is greater in the city of La Paz compared to El Alto. This discrepancy can be attributed to the additional strain experienced by vehicle engines while navigating the steep streets of La Paz, a challenge that is less pronounced in El Alto due to its flat topography. Although the contributions of this factor to total PM_{10} mass are relatively low, its significance in terms of air quality should not be underestimated, as it represents one of the major sources of alkanes and hopanes. The latter compound is considered hazardous for human health since it has proven to be associated to systemic inflammation biomarkers (Delfino et al., 2010).

3.3. Methodology discussions

The sampling strategy, the complete chemical characterization, and the multisite PMF, coupled with the specific geographical patterns, enabled this quite unique study to offer an extensive characterization of PM sources in high-altitude cities. The present investigation provides important information that can help policy-making towards better air quality in the region, however, we are aware of some limitations.

- PMF limitations

Having enough samples in the multisite approach and a fairly large chemical speciation including organic tracers allowed the identification of 11 factors in the PMF analysis. It is noteworthy that only a few studies have been able to resolve similar number of sources with good statistical indicators (Chevrier, 2016; Pandolfi et al., 2020; Waked et al., 2014; Weber et al., 2019; Borlaza et al., 2021a). Nevertheless, attempting a larger number

of factors generated instability in the otherwise geochemically stable profiles. Several factors may contribute to this limitation, including:

- Collinearity between sources, resulting in mixed factors. The presence of OC in both secondary sulfate and primary biogenic emissions could speak of a possible mixing of these factors with biogenic secondary organic aerosols (BSOA). A detachment of BSOA was not possible due to the lack of the specific tracers of this source (3-MBTCA, or cellulose, or methyltetrols).
- Although the industrial sector is not highly developed, there are factories within and the vecinity of the Metropolitan area that were not resolved by the PMF (e.g. cement plants, brickyards, PVC manufactory plants). This could be due to the lack of specific tracers for these sources in the analysis, a similarity of the chemical profile and temporal variability of the emissions compared to the resolved sources, or simply because they represent a very small fraction of PM_{10}
- The removal of chloride from the analysis for bringing instability to the solution. This instability was likely associated to the large variability of this volatile compound.

- Multisite approach limitations

While the multisite approach has added enhanced the findings compared to a single-site approach, it is important to note that *a priori* this method cannot be directly applied to sites that differ greatly from each other. It was important to verify the similarity of the single-site solutions. However, one drawback of the multisite approach is that it enforces the similarity of the common factors found between the two sites, smoothing out the specificity of them. Examples of this forced similarity are as follows:

- The multisite approach successfully separated EC (a traffic tracer) from the dust profile. However, considering that the Altiplano is a major source of dust and that the only path that the air masses take when transporting dust from the Altiplano to La Paz is traversing both cities, it is not surprising that the dust factor in the city of La Paz (single-site solution) is highly influenced by traffic tracers. For the multisite solution the indirect information of the mixing of sources during transport is lost.
- The average molar ratio of sulfate and ammonia concentrations differs between the two cities (2.05 and 1.63 in El Alto and La Paz, respectively), indicating a lower availability of ammonium to neutralize sulfate and nitrate ions in the city of La Paz. However, this distinction is no longer evident in the multisite analysis, which yields a median molar ratio of 1.96 representative of both cities.
- The MSA-rich profile in El Alto exhibits strong mixing with metallic species, among them crustal material, which hinted its path through the Altiplano towards the city of El Alto. This mixing pattern is no longer evident in the multisite analysis.

Considering the advantages of a more specific characterization of sources provided by the multisite approach outweigh the associated drawbacks, we believe it was the most appropriate technique to apply in the metropolitan region of La Paz and El Alto with such database in hand.

4. Conclusions

This study presents innovative information and a unique analysis of air pollution sources in the high-altitude urban environment of the fast-growing cities of La Paz and El Alto in Bolivia. It also provides a detailed description of the chemical profiles of 11 identified source types, resolved by the multisite PMF method, along with their temporal and spatial variability. The extensive and comprehensive dataset, combined with the inclusion of inorganic and organic species in the analysis, enabled an advanced source apportionment beyond classical solutions, allowing for the identification of several biogenic and combustion-related factors that would have remained unresolved otherwise. Notably, waste burning was separated from biomass burning, and traffic exhaust emissions were separated into two independent profiles.

On average, vehicular emissions represent 35 and 25% of the PM_{10} concentrations measured in La Paz and El Alto, respectively. Then, dust emerges as one of the two main sources contributing to 20 and 32%. Factors associated with secondary inorganic aerosols account for 22 and 24% and the primary biogenic emissions account for 7 and 13% annually. Although one of the smallest factors in terms of contribution to the total mass, the non-regulated burning of waste, predominantly occurring in El Alto between May and August, is the second most significant factor responsible for observed PAH concentration levels.

The observations in this study were made at urban background sites, representing wider regional pollution levels in La Paz and El Alto. Locally, especially near roads or landfills, the mass concentrations are expected to be higher. While most of the resolved sources are associated with local activities (dust resuspension, primary and secondary vehicular emissions, and waste burning), there is a significant contribution of regional natural and anthropogenic sources of PM (Primary and secondary biogenic emissions, and biomass burning).

Based on our findings, we can outline relevant actions towards the improvement of air quality in La Paz and El Alto:

1) Regulation of vehicular emissions have to improved. As the Metropolitan area continues to grow, more efficient means of transportation and stricter policies and control on combustion practices are needed to ensure that air quality is not further degraded.

2) Waste burning should be prohibited. It is a major source of PAHs and other pollutants with high human health risk factor.

3) Agricultural biomass burning is a seasonal source, a decrease in their emissions would result in a significant improvement in the air quality during the most polluted season, not only for the metropolis but also for the rest of the country.

4) Dust is an important source in terms of mass that has an anthropogenic component (e.g. vehicle resuspension, construction activities, mining) and should be addressed.

5) Updated policies of pollutant emissions are essential to regulate also the growing industry sector.

In order to have a comprehensive understanding of the pollution sources in the metropolitan area of La Paz and El Alto, information on the gaseous components is of utmost importance. A longer sampling time period together with an updated emissions inventory of the resolved sources would be beneficial for a better understanding of the resolved sources and their evolution in time. Furthermore, analyzing the potential impact on health of the resolved sources is crucial for efficiently targeting the most hazardous sources of PM.

Code availability

The software code is available upon request.

Data availability

The chemical and PMF datasets are available upon request.

Authors contribution

GU, MA, PL, JLJ, AA, JLB, RK, IM, NP and AW participated in the conceptualization of the experimental set up and design. IM participated in the data curation. VM, MP and LJB participated in the formal analysis and the development of the methodology. GU, MA, PL, JLJ, AA, JLB, RK, PG were involved in the funding and resource acquisition. JLB, IM, NP and VC contributed to the investigation by organizing the samples collection and performing the experiments. GU, MA, PL, MP, LJB, GM and JLJ helped with mentoring, supervision and validation of the methodology, techniques and results. VM was responsible for the data processing and the writing of the original draft. GU, PL and JLB revised the original draft. All the authors reviewed and edited the manuscript.

Competing interests

G. Močnik is employed by Haze Instruments d.o.o., the manufacturer of the aerosol instrumentation.

Acknowledgements

Authors wish to thank all the many people from the different laboratories (LFA, Idaea-CSIC, IGE, Air O Sol analytical platform, EDYTEM) who actively contributed over the years in filter sampling and/or analysis. Specifically, thanks to Samuel Weber, Federico Bianchi, Claudia Mohr and Diego Aliaga for the active participation in the discussions of the obtained results; J.C. Franconny and M. Pin who carried out the organic compounds analysis by GC-MS on the PTAL analytical platform of EDYTEM; the engineers F. Masson, F. Donaz, C. Vérin, A Vella, R El Azzouzi and many technicians who performed ECOC, ionic chromatography and HPLC-PAD on the Air-O Sol plateform; S. Rios and E. Miranda of GAMLP (Gobierno Autónomo Municipal de La Paz) who provided access and facilitated tasks at Pipiripi; IIF personnel that helped in logistics during the campaign; Undergrad students who collected samples: Y. Laura, G. Salvatierra, M. Roca, D. Calasich, E. Huanca, Z. Tuco, S. Herrera, M. Vicente, M. Zapata, R. Copa.

Financial support

This research has been supported by the Institute de Recherche pour le Développement (IRD) France and IRD delegation in Bolivia, Javna Agencija za Raziskovalno Dejavnost RS (grant nos. P1-0385), Grant Agency of the Czech Republic 19-15405S. The Labex OSUG@2020 (ANR10 LABX56) provided some financial support for instruments on the Air O Sol analytical platform, EU H2020 MSCA-RISE project PAPILA (Grant #: 777544).

Combustion Sources Affecting the Air Quality in the Metropolitan Area of La Paz and El Alto.

The major insight provided by the chemical speciation described in the previous chapter enabled the identification of the main sources of PM_{10} in the conurbation, as well as the description of the seasonal variability of each of them. As it was evidenced, the main sources affecting air quality in La Paz-El Alto are rather local. However, this approach does not allow studying the variability of the sources on short time scales.

In this chapter will be presented the long-term observations of black carbon (BC), a byproduct of combustion that is often used as a tracer for combustion-related anthropogenic activities. This will allow us to refine the analysis of the sources presented in the previous chapter, as well as to investigate in more depth the short-scale variability of these sources, among which vehicular traffic is one of the most important.

The Department of La Paz has experienced a rapid growth in population, surpassed by the growth of its vehicular fleet which duplicated within the last decade (INE, 2020a). To the moment, there is no restriction on the age of the circulating vehicle fleet in Bolivia, although imports are being restricted to vehicles that comply with the EURO II Atmospheric Emission Standard (*Ley 821,* 2016). This allows vehicles over four decades old to continue in circulation. Hence, vehicles ensembled within the last decade (2011-2020) make only 43% of the registered vehicle fleet (INE, 2020a).

In the city of La Paz are registered roughly 70% of the total vehicle fleet of the conurbation (over 400 thousand vehicles in 2018) (INE, 2020a; Red MoniCA, 2021). Public transportation represents the main mean of transportation in La Paz and El Alto, and is dominated by minibuses, old buses and small four-door sedans, organized by private syndicates. In the last decade, alternative massive means of transportation were provided by the government and the local municipalities. These include the municipality buses implemented in the city of La Paz (powered by diesel fuel) and the cable car system that takes advantage of the topography of the two cities. The latter efficiently connects the hillsides of the city of La Paz and constitutes a very important connection between La Paz and El Alto. Daily, over 400 thousand people commute between both cities, predominantly descending from the city of El Alto towards La Paz city for work, educational or administrative purposes (Garsous et al., 2017)

Given the significant impact BC particles have on human health and climate, its monitoring is fundamental. In this chapter are presented the analysis of the optical properties of BC and its variability in each city, as well as two approaches for apportioning its sources. This chapter is also presented in the form of a scientific article since it is currently being prepared to be submitted to the scientific journal: Atmospheric Chemistry and Physics (ACP). The manuscript is currently under the review of the coauthors.

Atmospheric Black Carbon in the metropolitan area of La Paz and El Alto, Bolivia: concentration levels and emission sources

Valeria Mardoñez[1,2], Griša Močnik[3,4,5], Marco Pandolfi[6], Robin Modini[7], Fernando Velarde[2], Laura Renzi[7,8], Angela Marinoni[8], Andres Alatuey[6], Isabel Moreno[2], Diego Aliaga[9], Federico Bianchi[9], Claudia Mohr[7,9], Martin Gysel-Beer[7], Radovan Krejci[9], Alfred Widensohler[10], Gaëlle Uzu[1], Marcos Andrade[2,12], Paolo Laj[1,9]

[1]Institut des Géosciences de l'Environnement, Université Grenoble Alpes, CNRS, INRE, IRD, Grenoble INP, 38000 Grenoble, France.

[2] Laboratorio de Física de la Atmósfera, Instituto de Investigaciones Físicas, Universidad Mayor de San Andrés, La Paz, Bolivia.

[3] Center for Atmospheric Research, University of Nova Gorica, 5270 Ajdovščina, Slovenia

[4] Haze Instruments d.o.o., 1000 Ljubljana, Slovenia

[5] Department of Condensed Matter Physics, Jozef Stefan Institute, 1000 Ljubljana, Slovenia

[6] Institute of Environmental Assessment and Water Research (IDAEA-CSIC), Barcelona, 08034, Spain

[7] Laboratory of Atmospheric Chemistry, Paul Scherrer Institute, 5232 Villigen PSI, Switzerland

[8] Istituto si Scienze dell'Atmosfera e del Clima – Consiglio Nazionale delle Ricerche (ISAC-CNR)

[9] Institute for Atmospheric and Earth System Research (INAR), and Department of Physics, University of Helsinki, 00014 Helsinki, Finland

[9] Department of Environmental Science & Bolin Centre for Climate Research, Stockholm University, 10691 Stockholm, Sweden

[10]Leibniz Institute for Tropospheric Research (TROPOS), 04318 Leipzig, Germany

[12] Department of Atmospheric and Oceanic Sciences, University of Maryland, College Park, MD, USA

Correspondence to: Valeria Mardoñez (valeria.mardonez@univ-grenoble-alpes.fr)

Abstract

Black carbon (BC), a byproduct of incomplete combustion, represents an important fraction of the sub-micron particles that can penetrate deep into the lung upon inhalation. In addition, its strong light absorbing properties make BC an important contributor to climate change. The lower efficiency of combustion that occurs in high-altitude environments, affecting BC emissions, is a phenomenon that is under documented while highly relevant in Latin America, with many cities built at high altitude. The aim of this study is to document the concentration levels, to identify the emission sources and to characterize the physical properties of BC in the high-altitude Bolivian cities of La Paz and El Alto (LP-EA). The study is based on simultaneous measurements of equivalent black carbon (BC), elemental carbon (EC), and refractory black carbon (rBC) at two urban background sites located at 3600 m and 4100 m a.s.l. (LP and EA, respectively) and their comparison to similar measurements at the regional Global Atmosphere Watch-Chacaltaya station (CHC-GAW). On a yearly basis, average BC concentrations are maximum during the dry season (May to Aug) and

minimum during the wet season (Dec-Mar) (EA: 1.0±0.8 [µg m^{-3}] - 1.9±2.0 [µg m^{-3}]; LP: 0.9±1.0 [µg m^{-3}] - 1.6±1.7 [µg m^{-3}]), and represent less than 5% of the mass concentrations of PM_{10} and $PM_{2.5}$. The influence of the urban centers can be observed in CHC-GAW, with average BC concentrations that range between 0.1±0.2 [µg m^{-3}] and 0.2±0.3 [µg m^{-3}]. On a daily basis, variability is driven by both intensity of emission sources and the height of the planetary boundary layer (PBL). A delayed and less intense diurnal cycle can also be observed in CHC-GAW, peaking between 10:00 and 16:00 as the urban PBL develops. BC displayed average absorption Ångström exponents (AAE) (1.1±0.2) and mass absorption cross sections (MAC) at 637 nm that are typical for urban background sites (7.8-8.5 [$m^2 g^{-1}$]). Two source apportionment techniques, a bilinear model and a multilinear regression (MLR on PMF results), were used independently to investigate the main sources of BC. Traffic, waste burning, biomass burning and secondary nitrates (associated to gaseous precursors emitted by traffic) were the sources showing the highest absorption efficiency (MAC). This revealed that besides vehicular emissions and biomass burning, open waste burning contributed in average to nearly 20% of the measured absorption at 880 nm in El Alto. Furthermore, the apportionment of the multiwavelength absorption coefficients allowed the estimation of source-specific AAEs, which are found within the range of the expected literature values.

1. Introduction

Black carbon (BC), a particulate byproduct of fuel combustion, is not only considered one of the most important pollutants contributing to climate change (Bond et al., 2013), but also a latent threat to air quality and human health. Named as BC due to its dark appearance, it possesses a great capability of absorbing radiation over a wide spectral range. This makes BC a very important short-lived climate forcing agent (Bond et al., 2013). Typically introduced into the atmosphere by vehicular emissions, industrial emissions and biomass burning (whether for residential heating, agricultural purposes, or from wildfires), BC is often used as a good tracer for continental emissions when monitoring air quality (Bockhorn, 2013; J. Seinfeld & Pandis, 2016; Subramanian et al., 2006).

Due to their size, these fine and ultrafine particles can be breathed deep into the lungs, reaching the blood stream and oxidizing the cardiopulmonary tissue on the way. (Janssen, et al., 2012; Janssen et al., 2014). This in return can decrease the lung function (Suglia et al., 2008), worsen preexisting cardiovascular conditions (Nichols et al., 2013) and increase the risk for chronic obstructive pulmonary disease hospitalizations and mortality (Gan et al., 2013). Moreover, due to its agglomerate structure, BC can carry potential carcinogen and mutagen organic species (Moosmüller et al., 2009; NTP, 2011). In consequence, BC has become a pollutant of big concern in terms of air quality.

The inhalation of BC has been associated with different respiratory and cardiovascular diseases such as asthma, lung cancer and cardiac arrest (US EPA, 2011), and high altitude can increase the risk of exposure to atmospheric pollutants. People in the Andean highlands have developed different physiological mechanisms to cope with hypoxia, amongst which are an increased lung capacity and increased hemoglobin

concentrations in their blood. Although, their resting ventilation has shown to remain the same as for people living at sea level, conditions that require a higher ventilation rate (e.g. physical activities, pregnancy) put highlanders at greater risk (Beall, 2007; Julian & Moore, 2019; U.S. EPA, 2011).

The formation of BC particles during combustion depends not only on the amount and type of fuel burned but also on the amount of oxygen available in the bonding process of carbon and oxygen atoms when forming CO and CO_2 molecules. Hence, the reduced oxygen available for combustion in high-altitude cities is expected to increase the production rate of carbonaceous particles (J. Seinfeld & Pandis, 2016). Furthermore, simulated and experimental studies have shown that the amount of PM particles produced by a diesel-fueled engines can increase from 1.2 to 4 times the production of particles at sea level when increasing altitude up to 1800 m.a.s.l. (Chaffin & Ullman, 1994; Graboski & McCormick, 1996; He et al., 2011; Human et al., 1990; Yu et al., 2014).

Fast growing cities are often subject to a degrading air quality resulting from a proportionally growing vehicular fleet, especially in low and middle-income countries. Air quality studies in high-altitude Latin-American cities have shown that Elemental Carbon (EC, closely related to BC) and Organic Aerosol particles (OA) account for about 60% of the PM_{10} mass concentrations in Bogota (2550 -2620 m a.s.l.) (Ramírez et al., 2018b), with average EC concentrations of $3.25 \pm 1.59\ \mu g\ m^{-3}$. In Quito (2850 m a.s.l.), traffic emissions have shown to be responsible for almost 46% of the annual PM emissions (Raysoni et al., 2017). In the case of Mexico City (2280 m a.s.l.), Peralta et al., 2019 reported annual BC levels of $2.95\ \mu g\ m^{-3}$ contributing to 16-20% of total $PM_{2.5}$ concentrations.

La Paz (between 3200-3600 m a.s.l.) and El Alto (4050 m a.s.l.) are two high-altitude Bolivian cities located in the Bolivian Andean region that form the second largest metropolitan region in the country. In addition to the extreme conditions of altitude (hence, lower oxygen concentrations), the rugged topography of the site can make the combustion processes even more complex. As recently showned by Mardoñez et al. (2022) and Wiedensohler et al. (2018), the air quality in these cities is predominantly influenced by local emission, with vehicular emissions (>80% powered by gasoline) as the main source of absorbing aerosol particles, and responsible for 20-30% of the measured PM_{10} concentrations in both cities. However, the cities are also subject to regional sources of pollution, being agricultural biomass burning one of the most important, and which is transported across the Andes from the valleys and low lands (Chauvigne et al., 2019; Mardoñez et al., 2022).

Improving air quality in La Paz and El Alto is not trivial and the effectiveness of any air quality action plan must be backed by sound scientific understanding of the lifecycle of the main pollutants in a high altitude, a high solar radiation environment. Knowledge of BC emission sources and of its characteristics in the urban environment is key to assessing the impact of air quality on health for the specific case of these high-altitude cities. Thus, the aims of this study are to contribute to documenting the atmospheric concentration, the variability and physical properties of BC in the unique La Paz-El Alto conurbation (LP-EA), as well as to determine the contribution of local and regional sources of BC. To do so, it is sought to make use of two-year

records of BC and other pollutants measured at two urban background sites. It is also intended to provide a spatial description of the BC concentrations, and to explore the effect of a half-kilometer altitude difference and the different topographical characteristics between the cities, thus paving the way for future studies on the potential health effects of air pollution in both cities.

2. Method

2.1. Site description.

Having started as an extension of La Paz city, El Alto has rapidly become the second largest city in Bolivia in terms of population, hosting over 1.1 million inhabitants (INE, 2020c). It is situated on the plateau formed between the two branches of the Andes, a very high, open, flat, and dry (hence dusty) area, with plenty of space for urban expansion. Hosting the largest international airport in the country, El Alto constitutes one of the most important connections of the Bolivian seat of government (La Paz) to other regions within and outside the country. In contrast, La Paz is located in a river valley formed between the Altiplano plateau and the Oriental branch of the Andes. Characterized by its hilly topography, it hosts approximately over 950 thousand inhabitants (INE, 2020c), with limited space for urban growth.

Seasons in La Paz and El Alto shift between a dry (May to August, austral winter) and a wet season (December to March, austral summer), with relatively low temperatures throughout the year. However, the difference in altitude and topography gives them very different local meteorological conditions. The mean annual temperature in El Alto is 8°C, whereas in La Paz it is 13°C. During the austral summer, mean temperature only increase by one-degree, with mean temperature amplitudes of 10 and 12 degrees along the day in El Alto and La Paz, respectively. In contrast, during the austral winter mean temperatures decrease by two degrees in both cities, and the diurnal temperature amplitudes increase to 17 and 15 degrees. The average annual rainfall between 2016 and 2018 was of 470 and 600 mm/year in El Alto and La Paz, respectively. Although not very often, precipitation in the form of snow is possible in El Alto during the transition periods. Moreover, wind patterns in La Paz are constrained by the North-South topographic features of the river valley. Average atmospheric pressure at La Paz and El Alto are near 664hPa and 630 hPa, respectively.

2.2. Sampling sites.

Urban background samplings sites were chosen in each city to obtain representative measurements of the base state of the air quality. This was not the first campaign that addressed BC concentrations in La Paz and El Alto. In 2012, a shorter campaign provided the first characterization of BC in this high-altitude conurbation and its transport towards the Global Atmosphere Watch station in mount Chacaltaya (CHC-GAW) (Wiedensohler et al., 2018). The results of the short campaign provided insights for the present long-term campaign, for which the same urban background sampling site was maintained in El Alto. The former traffic site in La Paz was transferred to a more secluded site, distanced from direct vehicular emissions. The distance

between the sampling sites is approximately 8 km, and they are located 17-19 km from the CHC-GAW global monitoring station (Figure 1) as described in Bianchi et al. (2022).

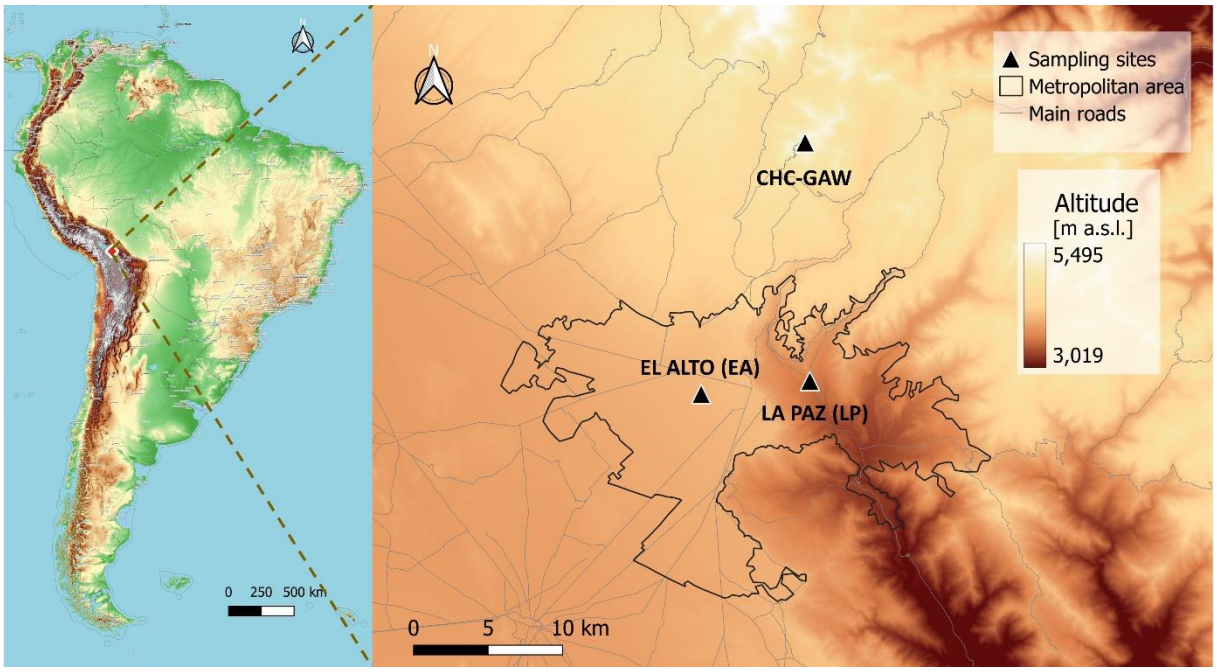

Figure 1. Location of the sampling sites. Left panel: Topographic map of South America. Right panel: Zoom-in to the study site with the color scale representing the altitude above sea level from digital elevation model (DEM) ©OpenTopoMap (CC-BY-SA).

The La Paz measurement site in the present study (LP) was installed on the rooftop of the four-story building of the city's Museum Pipiripi (Espacio Interactivo Memoria y Futuro Pipiripi: 16.5013°S, 68.1259°W, 3600 m a.s.l.). This municipal building is located on a small hilltop in downtown La Paz and distances approximately 70 m and 45 m from the nearest road (horizontal and vertical distance, respectively). Within a 1 km radius around the station, the LP site is surrounded by many busy roads and dense residential areas. However, the immediate surroundings (~100 m radius) are covered by green areas, with a parking lot for municipality buses at the base of the hill.

The El Alto station (EA) was placed at the ground level of the El Alto International Airport's. meteorological observatory (16.5100° S, 68.1987° W, 4025 m a.s.l.). The building of the meteorological station is located in an area restricted to general public, 250 m away from the airport runway. The shortest distance to a major road is 500 m as was described elsewhere (Mardoñez et al., 2022; Wiedensohler et al., 2018). The station is surrounded by approximately 3.5 km^2 of an empty, dry and arid field.

All stations were equipped with basic meteorological stations, measuring wind speed and direction at a 15-min time resolution using anemometers placed on the rooftops of the buildings where the rest of the instruments were installed. Other meteorological variables were measured and provided by the Airport's air navigation administration (Administración de Aeropuertos y Servicios Auxiliares a la Navegación Aérea,

AASANA) with a 1-hour time resolution, for El Alto, and from the National Meteorology and Hydrology Service (Servicio Nacional de Meteorología e Hidrología, SENAMHI) (SENAMHI, n.d.) for La Paz at a daily time-resolution.

2.3. Sampling methods.

The measurement campaigns took place between April 2016 and June 2018 with similar instrumentation at the two urban background sites (LP and EA). Several simultaneous online and offline measurements of chemical and physical aerosol particle properties were continuously performed at both sites during this period. In addition, continuous measurements of atmospheric parameters are taken at the nearest CHC-GAW station since 2012.

2.3.1. Aethalometers

Aethalometers are filter based absorption photometers that measure light attenuation by atmospheric aerosol particles at 7 wavelengths in the visible/near-visible spectrum (370, 470, 520, 590, 660, 880, 950 nm), which can be used to calculate equivalent BC mass concentrations (eBC). This term is reserved for optical measurements of BC that are inferred from the change in attenuation of light passing through a filter matrix onto which aerosol particles are deposited. For simplicity, the term BC will be used throughout the manuscript to refer to eBC.

The Aethalometer, model AE33 (Magee Scientific, Drinovec et al., 2015, Tape: Pallflex TFE-coated glass fiber T60A20 /M8020), was used at EA station at the minimum 1-minute time resolution provided by the instrument (Apr 2016 – Sep 2017). Due to technical problems, the instrument had to be replaced by an Aethalometer AE31 (Magee Scientific, Arnott et al., 2005, Tape: Pallflex Quartz fiber Q250F) for the end of the campaign (Jan – Jun 2018). The same model, AE31, operated in La Paz during the entire campaign at its minimum 5-minute time resolution (June 2016- June 2018). PM_{10} inlets were used at the front of the sampling lines at both sites throughout the campaign, except for the period from April 2017 to September 2017 where whole air was sampled at El Alto station. The PM_{10} heads were installed at 2 m and 6 m above the instrument level for La Paz and El Alto, respectively. The instruments were set to report BC concentrations at standard conditions of temperature and pressure (STP) at both urban sites. The data recorded by an aethalometer AE31 at CHC-GAW, between April 2016 and July 2018 was downloaded from the EBAS database (http://ebas.nilu.no/).

As for all filter-based instruments, instrumental artifacts need to be accounted for in the post processing of the data. The first one accounts for the so called “loading effect”. As the filter gets loaded, particles deposited on the filter may interact with the incoming light beam, increasingly reducing the amount of light reaching the detector. This constitutes the main difference between models AE31 and model AE33. The aethalometer AE33 performs this correction online, thanks to its dual spot design (Drinovec et al., 2015b). In contrast, measurements taken with the aethalometer AE31 need to be corrected afterwards (A Virkkula et al., 2015). However, an overcompensation of the loading effect was spotted in the AE33 measurements, for which the

correction made by the instrument was overlooked. Thus, the following correction scheme proposed by Virkkula et al. (2015) was used for both models:

$$eBC(\lambda) = \frac{BC_0(\lambda)}{(1+k(\lambda)\cdot ATN_t(\lambda))} = \frac{1}{(1+k(\lambda)\cdot ATN_t(\lambda))} \cdot \left(\frac{1}{C_{f0}} \cdot \frac{1}{MAC(\lambda)} \cdot \frac{A}{Q\cdot 100} \cdot \frac{ATN_t(\lambda) - ATN_{t-\Delta t}(\lambda)}{\Delta t}\right) \quad [1]$$

where ATN corresponds to the ratio of the light intensity reaching the detector after passing through the loaded filter, compared to the attenuation of the light passing through a clean portion of the filter; k is the loading correcting factor introduced by Virkkula et al., 2015; BC_0 are the original black carbon concentrations reported by the instrument; C_{f0} are the constant cross-sensitivity to scattering factor that corresponds to the model of aethalometer and the filter tape used[9]; MAC are the mass absorption cross-sections established by the manufacturer for each of the wavelengths of the aethalometer[10]; A is the area of the filter onto which particles are collected[11], Q is the flow rate of the air sample passing through the instrument. Monthly k values were calculated as the ratio of the slope over the intercept of the linear fit of the BC concentrations with respect to ATN. They were then used to correct the data on a monthly basis.

The noise in the concentrations reported by the AE33 at the minimum time resolution was high. Hence, the noise reduction method presented by Backman et al. (2017) was applied to the dataset, and a significant reduction in noise was achieved while preserving the original time resolution. Briefly, Backman et al (2017). proposed to increase the original averaging period Δt from the original sampling time resolution to a higher interval of time in equation [1] when calculating BC concentrations. Therefore, BC concentrations were recalculated using a Δt=30 min to efficiently reduce the noise of the data set. This procedure was only applied to BC concentrations measured from the same filter-spot, hence, the Δt of the first 30 minutes of every new filter-spot were defined as $\Delta t = t - t_0$.

In addition, systematic higher concentrations were observed at EA compared to LP when different models of aethalometers were employed. However, the difference between the sites was negligible when at both stations BC was measured using AE31 aethalometers. Moreover, no significant differences in the average concentrations of EC were found among the sites. This indicated that the observed difference was rather associated to differences between models AE33 and AE31. Given that several studies have shown that the manufacturer C_f factors accounting for the cross sensitivity to scattering are underestimated for both models in ambient concentrations, the measurements were re-scaled using more appropriate C_f values.

A local C_f=2.9 value was calculated for AE31, based on the comparison of the hourly attenuation coefficients measured by an AE31 at CHC-GAW station and the absorption coefficients measured simultaneously by a Multi

[9] $C_{f0,\,AE31}$= 2.14; $C_{f0,\,AE33}$= 1.57

[10] MAC_{370nm}= 18.47 [m^2g^{-1}]; MAC_{470nm}= 14.54 [m^2g^{-1}]; MAC_{520nm}= 13.14 [m^2g^{-1}]; MAC_{590nm}= 11.58 [m^2g^{-1}]; MAC_{660nm}= 10.35 [m^2g^{-1}]; MAC_{880nm}= 7.77 [m^2g^{-1}]; MAC_{950nm}= 7.19 [m^2g^{-1}]

[11] A_{AE31}= 0.5 cm^2; A_{AE33}= 0.785 cm^2

Angle Absorption Photometer (MAAP), which is often considered a reference instrument for light absorption measurements (eq. [2]) (Valentini et al., 2020; Yus-Díez et al., 2021). Only the measurements taken between 10:00 and 16:00 were included in the calculation of C_f, period in which the CHC-GAW station has shown to be under the influence of the urban area (Andrade et al., 2015), assuming the properties of the urban aerosol do not change drastically on their transport to CHC-GAW. The added 1.05 factor included in eq. [2] accounts for the difference between the measuring wavelength reported by the MAAP manufacturer (670 nm) and the actual wavelength (637 nm) measured by Müller et al. (2011):

$$b_{ATN,AE31,CHC}(637\ nm) = C_{f,31} \cdot (1.05 \cdot b_{abs,MAAP,CHC}(637\ nm)) + a \quad [2]$$

The attenuation coefficients measured by the AE31 at CHC-GAW were interpolated to the wavelength of MAAP using the calculated AAE corresponding to each data point (mean $AAE_{CHC\text{-}GAW}$ = 1.0±0.5).

Since the MAAP instrument was not available to assess the cross sensitivity to scattering of AE33, a C_f=2.78 was selected, which brought the measurements of both models of aethalometer closer together. This value was obtained by Bernardoni et al. (2021) for an urban background station in Milan during winter in 2018 using the same type of filter tape (T60A20). Re-scaling the BC concentrations using the new C_f factors decrease the instrumental difference to roughly 24%.

2.3.2. High volume Samplers

High-Volume Samplers (MCV CAV-A/mb) were used at both sites to collect aerosol particles on quartz fiber-filters to be later chemically analyzed. 24-hour filter samples were taken every 3 to 4 days at a flow rate of 30 m^2h^{-1} using PM_{10} heads (MCV PM1025UNE) during the first year of sampling for both sites. For the second year, the head was replaced with a $PM_{2.5}$ head (MCV PM1025UNE). Additionally, a second HV sampler was added in LP for the second year of measurements in order to collect simultaneous samples of particles with aerodynamic diameters smaller than 10 and 2.5 µm. Sampling always started at 9 a.m. at both sites. During the campaign, a total of 422 filters were collected between both sites, which were later weighed and chemically analyzed for over 180 different chemical species, including EC, OC and several organic and inorganic source tracers. A more detailed description of the methodology and protocols can be found at Mardoñez et al. (2022). The ambient concentrations obtained from the collected filters were then multiplied by a factor of 1.66 and 1.60 in El Alto and La Paz, respectively, in order to convert them to STP conditions (T=273 K, P=1013.5 hPa).

2.3.3. Single Particle Soot Photometer

The measurement period ended with a one-month measurements campaign where refractory black carbon concentrations (rBC) were measured with a Single-Particle Soot Photometer-Extended Range (SP2-XR, Droplet Measurement Technologies). The SP2-XR is a new, more compact version of the original SP2 instrument (Baumgardner et al., 2004; Schwarz et al., 2006). The SP2-XR provides real-time measurements of single-particle optical size and rBC mass, based on its elastic scattering and laser-induced incandescence signals,

respectively. Each station was equipped with one SP2-XR between April and May 2018, from which hourly rBC mass concentrations were retrieved. A more detailed description of the instruments and the analysis of the measurements can be found in Modini et al (2023, in preparation).

Table 1. Summary of the instrumentation placed at each of the urban stations, their operation period and time resolution

	El Alto	*La Paz*
Aethalometer AE33	Apr 2016 - Sep 2017 (1-min)	X
Aethalometer AE31	Jan 2018 - Jun 2018 (5-min)	Apr 2016 - Jun 2018 (5-min)
PM_{10} samples	Apr 2016 - Jun 2017 (24-h every 3rd day)	Apr 2016 - Jun 2018 (24-h every 3rd day)[12]
$PM_{2.5}$ samples	Jun 2017 - Jun 2018 (24-h every 3rd day)	Jun 2017 - Jun 2018 (24-h every 3rd day)
SP2-XR	Apr 2018 - May 2018 (1-min)	Apr 2018 - May 2018 (1-min)
Meteorology	Apr 2016 - Jun 2018 (1-hour)	Apr 2016 - Jun 2018 (1-day)

2.4. Intrinsic properties of BC.

2.4.1. Mass Absorption Cross-section (MAC)

Aethalometers, in principal, measure the attenuation coefficients of the particles collected on a filter-tape. By assuming a constant value of cross sensitivity to scattering (C_f) and an average mass absorption cross-section at a given wavelength (MAC), one can infer BC mass concentrations. However, C_f values depend on the aerosol type deposited on the filter as well as on the filter matrix characteristics (Yus-Díez et al., 2021). Moreover, the MAC is an intrinsic property of absorbing aerosol particles that also depends on wavelength, aerosol type and ageing. MAC values of absorbing aerosol particles are hence calculated as follows:

$$MAC_{BC}(\lambda)\ [m^2 g^{-1}] = \frac{b_{abs}(\lambda)\ [Mm^{-1}]}{m_{BC}\ [\mu g\ m^{-3}]} = \frac{b_{ATN}\ (\lambda)[Mm^{-1}]}{C_f \cdot m_{BC}\ [\mu g\ m^{-3}]} \quad [3]$$

where b_{abs} are the absorption coefficients at wavelength λ, b_{ATN} are the attenuation coefficients at λ, and m_{BC} are the mass concentrations of BC. For the complete extent of the campaign, daily averaged b_{abs} and EC mass concentrations were used to calculate the MAC values at both sites following eq. [3]. For the period where the higher-time resolution rBC data is available, MAC values were calculated similarly using hourly averages of b_{abs}.

[12] After June 2017, only 25 PM_{10} filter samples were intermittently collected due to technical problems.

To compare with other studies, the obtained MAC values were interpolated to other wavelengths typically found in the literature (550, 637 and 880 nm).

2.4.2. Absorption Angstrom Exponent (AAE)

The absorption efficiency of particulate matter varies throughout the visible spectrum of radiation and is determined by the chemical and physical properties of the aerosol particles. This wavelength dependency can be described by the Absorption Ångström Exponent (AAE) (J. Seinfeld & Pandis, 2016). BC particles coming from vehicular emissions are characterized by AAE values of ~1 (Bond et al., 2013). In contrast, Brown Carbon (BrC) is a combustion product that includes organic material and it has a stronger absorbance in the shorter wavelengths of the visible spectrum, leading to a wider range of AAE values ~0.9 to 2.2 depending on the type of solid fuel burned as well as on the combustion conditions (Helin et al., 2021; Kirchstetter et al., 2004; Sandradewi et al., 2008). Dust particles are also capable of absorbing visible radiation, more efficiently at shorter wavelengths, with AAE values usually > 2 (Bergstrom et al., 2007; Caponi et al., 2017). An orthogonal non-linear least squares regression was used to describe the power-law dependency of absorption with wavelength:

$$b_{abs}(\lambda) = a \cdot \lambda^{-AAE} \qquad [4]$$

Only wavelengths 2 to 7 (470 – 950 nm) were used in the regression as recommended by Zotter et al. (2017). The obtained time series of AAE displayed the same noisy pattern observed in the BC time series prior to noise reduction, therefore only AAE corresponding to absorption coefficients $b_{abs,880}$>2 [Mm^{-1}] were considered in the rest of the analysis.

2.5. Description of methods for performing Black Carbon source apportionment

2.5.1. Aethalometer method

Based on the differences in the source-specific AAE, a bilinear regression model was proposed by Sandradewi et al., 2008 in order to determine the contribution of each source to total absorption. Generally, this technique is used to apportion the contributions of vehicular emissions and biomass burning emissions or dust (Harrison et al., 2012; Lanz et al., 2008; Sandradewi et al., 2008; Zotter et al., 2017). This method is also known in the literature as the “Aethalometer method”.

Considering that:

$$b_{abs}(\lambda_i) = b_{abs,TR}(\lambda_i) + b_{abs,BB}(\lambda_i) \qquad [5]$$

where the subscripts TR and BB represent absorption due to traffic and biomass burning, respectively, and the power law dependence of b_{abs} with wavelength described in equation [4]:

$$\frac{b_{abs,TR}(\lambda_1)}{b_{abs,TR}(\lambda_2)} = \left(\frac{\lambda_1}{\lambda_2}\right)^{-AAE_{TR}} \qquad [6]$$

$$\frac{b_{abs,BB}(\lambda_1)}{b_{abs,BB}(\lambda_2)} = \left(\frac{\lambda_1}{\lambda_2}\right)^{-AAE_{BB}} \quad [7]$$

Eq. [6] and [7] result in a 2-equation system with 4 unknowns. However, if the AAE values of the evaluated sources are known or assumed, the equation system can be resolved, and the contributions of each source to total b_{abs} can be determined. The pair of wavelengths chosen to apply this method were 470 and 950 nm. The representative source-specific AAE were chosen as the 5th and 99th percentiles of the frequency distribution of AAE calculated from the hourly averaged multiwavelength b_{abs} (AAE_{TR}= 0.9, AAE_{BB}=1.5).

2.5.2. Multilinear Linear Regression method (MLR)

One of the limitations of the Aethalometer method for source apportioning is that it only admits two sources of absorbing aerosol particles. Given that the contribution to PM_{10} of dust and BB increases during the dry season in both cities (Mardoñez et al., 2022), the aethalometer method is not suitable to estimate the influence of multiple sources from the influence of traffic. Moreover, the results of the source apportionment through the Aethalometer method are highly sensitive to the selection of the source representative AAEs. Source specific AAEs can be highly dependent on the conditions under which combustion takes place and on the chemical properties of aerosol particles, and the selection of AAEs in the aethalometer method can be somewhat arbitrary. Thus, an alternative method was explored to calculate source-specific AAEs, identify other possible sources of absorbing aerosol particles and verify the results obtained with the two-source aethalometer method.

Mardoñez et al. (2022) used of the Positive Matrix Factorization tool (PMF v.5.0) to apportion the major sources of particulate matter, based on the chemical speciation of the PM_{10} filter samples collected during the first 15 months of the campaign at both sites (Section 2.2.2). The complete description of the factor analysis can be found in the mentioned article. Briefly, the temporal evolution of 40 chemical species including PM, EC, OC, water soluble ions, metals and source-specific organic tracers and their associated uncertainties were used as input in the PMF receptor model, following a multisite approach. A statistically stable solution was found at 11 factors assessed by the bootstraps and displacement methods, following the European source apportionment recommendations described in (Belis et al., 2019).

Out of the 11 resolved sources, dust and the ensemble of vehicular emissions (Traffic 1, Traffic 2, Lubricant oil, Non-exhaust emissions) were found to be responsible for almost 50% of the measured concentrations of PM_{10}. The overall contribution of BB was ~8% with maximum contributions between June and September. Two other factors associated to secondary aerosol formation (secondary sulfate and secondary nitrate) were responsible for roughly 15% on a yearly basis, and showed to be influenced by traffic, likely due to the fact that latter constitutes a source of gaseous precursors. A small factor in terms of percentage mass contribution was found to be associated to open waste burning taking place in El Alto between May and August. Finally, the natural sources of aerosol particles accounted for the remaining ~17% of PM_{10} (Mardoñez et al., 2022).

In the present study, a multilinear ordinary least-square regression (MLR) was performed to attribute the observed absorption coefficients (b_{abs}) to the PMF-resolved sources of PM_{10}. Using the calculated b_{abs} at each of the 7-wavelengths as dependent variables and the PMF-resolved source contributions as explanatory variables in eq. [8]:

$$b_{abs}(\lambda)_{m,1} = \left(G_{m,n} \times \beta(\lambda)_{n,1}\right) + \varepsilon(\lambda)_{m,1} \quad [8]$$

where b_{abs} are the daily averaged absorption coefficients in Mm^{-1} (starting at 9 a.m. to match the filter sampling time), $G_{m,n}$ are the STP mass contributions of the n sources for each of the m filters in $\mu g\ m^{-3}$, β are the regression coefficients representing the mass absorption cross-section of each of the sources in m^2g^{-1}, and ε are the residuals that account for the difference between the observed and the modelled b_{abs}. Out of the 11 resolved sources from the PMF analysis, only the sources that presented a p-value<0.05 were included in eq. [8] for the analysis (i.e. biomass burning (BB), secondary-nitrate, secondary sulfate, traffic 1 (TR1), traffic 2 (TR2), waste burning). The uncertainties of the coefficients β obtained by the MLR were estimated by bootstrapping the solutions 500 times, randomly selecting 70% of the datapoints each time to account for possible influence of extreme events. The median values of the estimated β coefficients were then considered as the source-specific MAC values for each wavelength and used to calculate the wavelength-dependent contribution to b_{abs} of the individual sources. Finally, the source-specific AAE was calculated as well through a power-law non-linear regression of the obtained source-specific MAC(λ).

Since the PMF analysis performed in Mardoñez et al. (2022) was done following a multisite approach, we chose to perform a multisite MLR in order to increase the number of data points included in the deconvolution. Nevertheless, the specific source contribution to the measured b_{abs} will be presented separately per site.

3. Results

3.1. Observed eBC concentration levels and variability

In Table 2 are displayed the mean STP concentrations of BC and EC measured in La Paz (LP), El Alto (EA) and Chacaltaya mountain station (CHC_GAW). EC concentrations showed to be similar at both urban sites (EC_{PM10} -LP: 2.1±1.2 $\mu g\ m^{-3}$, EC_{PM10} -EA: 2.4±1.1 $\mu g\ m^{-3}$; $EC_{PM2.5}$ -LP: 1.5±0.9 $\mu g\ m^{-3}$, $EC_{PM2.5}$ -EA: 1.6±0.8 $\mu g\ m^{-3}$). BC concentrations were consistently lower than EC in La Paz and El Alto (BC-LP: 1.2±1.3 $\mu g\ m^{-3}$, BC-EA: 1.6±1.7 $\mu g\ m^{-3}$). Although the urban background BC concentrations do not stand out as alarming, these concentrations can rapidly increase closer to the main roads as observed by Madueño et al (2020).

The CHC-GAW station is often influenced by the urban emissions, as previously reported by Andrade et al (2015) and Wiedensohler et al (2018). These emissions get rapidly diluted on their way to CHC and arrive to the station with a lag of nearly three hours as a result of the evolution of the boundary layer of the metropolitan area. The average concentrations of BC measured at CHC-GAW are c.a. 15% of what is measured in the cities.

However, during the hours CHC-GAW is influenced by the mixing layer of the metropolitan area (10 - 16h), the concentrations in the mountain station are roughly 35% of what is measured in the city

Table 2. Annual and seasonal average concentrations of eBC and EC in La Paz, El Alto and Mount Chacaltaya.

	mean ± sd [µg m-3]						
	eBC			EC (PM_{10})		EC ($PM_{2.5}$)	
	CHC-GAW	El Alto	La Paz	El Alto	La Paz	El Alto	La Paz
annual	0.2±0.2	1.6±1.7	1.2±1.2	2.4±1.1	2.1±1.2	1.6±0.8	1.5±0.9
wet season (December-March)	0.1±0.2	1.0±0.8	0.9±1.0	1.6±0.8	1.5±0.7	1.4±0.7	1.2±0.6
wet-to-dry transition (April)	0.1±0.2	1.5±1.5	0.9±1.1	2.6±1.1	2.5±1.3	1.2±0.2	1.0±0.3
dry season (May-August)	0.2±0.3	1.9±2.0	1.6±1.7	2.9±0.8	3.0±1.2	2.1±0.8	2.2±1.1
dry-to-wet transition (September-November)	0.2±0.3	1.3±1.3	1.0±0.9	1.7±0.5	1.6±0.8	1.2±0.7	1.2±0.6

In comparison with the other two high-altitude Latin-American cities that reported urban background concentrations of absorbing aerosol particles, EC_{STP} concentrations measured in La Paz and El Alto (PM_{10}) are nearly two thirds of what was reported in Bogota (Ramírez et al., 2018b). Compared to Mexico City, the BC concentrations in LP-EA are close to 43% and 57% of the concentrations reported by Peralta et al. (2019) for 2016. Since the conditions of temperature and pressure at which the concentrations were collected were not reported in the latter study, these percentages could decrease to roughly 30% and 40% if BC concentrations were reported in ambient conditions. Moreover, vehicle emissions have been highlighted as the main source of EC and BC in the three metropolitan areas, with >90% vehicle fleets dominated by gasoline fueled vehicles. Thus, the observed BC and EC concentrations in La Paz and El Alto seem rather high when compared to the values reported in the megacities of Bogota and Mexico City, whose populations are more than 4 times larger than the population in conurbation La Paz-El Alto. This phenomenon could be due to different factors such as the differences in the population density, the vehicle fleet density, the combustion efficiencies, or the pollutant dispersion efficiencies, however their description goes beyond the scope of the present study.

Black carbon mass concentrations (BC) in La Paz and El Alto are strongly influenced by the local meteorology. Maximum concentrations are found during the dry season and the minimum concentrations take place during the wet season (Figure 2.a). A significant decrease in concentrations can also be noted during the weekends compared to working days (Figure 2.b), giving evidence of the presence of anthropogenic sources of BC.

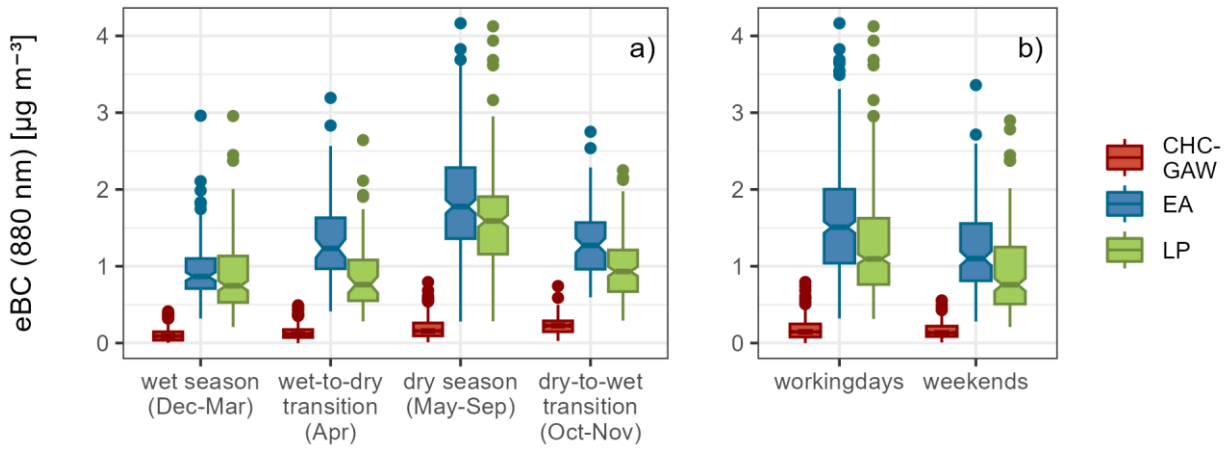

Figure 2. Boxplots describing a) the seasonal variation, and b) the difference between working days and weekends of the daily average concentrations of BC in La Paz an El Alto. The horizontal bar in the box represents the median value. The length of the box and bar represents the percentiles [25,75], and the points outside the boxes represent the outlier values.

In terms of diurnal variation, a clear bimodal pattern is observed throughout the seasons, which is characteristic of sites influenced by vehicular emissions (Figure 3.a). This pattern had already been described by Wiedensohler et al. (2018) in a shorter temporal scale at EA station (during the transition period to the wet season in 2012). A less pronounced bimodal behavior was observed by the same study in the road site station in La Paz installed during the 2012 short campaign.

Maximum concentrations were observed during the morning rush-hour peak around 8:00 at both sites, followed by a rapid decrease towards the minimum diurnal concentrations. This rapid decrease in concentrations result from the efficient ventilation and dilution caused by thermal convection, advection and growth of the boundary layer. During the midday minimum, lower concentrations are achieved at EA compared to LP, which could be related to a better ventilation in El Alto due to the openness of the site compared to the sheer sided canyon where the city of La Paz lies. At CHC-GAW, concentrations only start to increase at 9 a.m, when the urban boundary layer has expanded enough to submerge the station in it, reaching the maximum peak between 11 a.m. and 12 p.m. After mid-day, concentrations slowly decrease towards minimum concentrations during the evening.

While the maximum diurnal concentrations of BC are fairly similar at both sites, the magnitude of evening peak is much lower compared to the morning peak, and it constitutes the largest difference in the diurnal variation of BC between the sites. This second mode is associated to the evening rush-hour vehicular emissions coupling with the re-stratification of the atmosphere when the sun sets and temperature decreases. At EA, the evening peak reaches almost 60% of the morning peak's magnitude, whereas at LP the evening peak represents only 40% of the morning peak's concentrations. Furthermore, the second mode in La Paz starts to steadily increase around 16:00 whereas in El Alto it increases more abruptly around 18:00. This delay in the start of the evening mode is likely linked to a combination of the earlier setting time of the sun in the city of La Paz compared to El

Alto, and the delay in El Alto's evening traffic rush-hour due to the time it takes to commute back to El Alto from the city of La Paz.

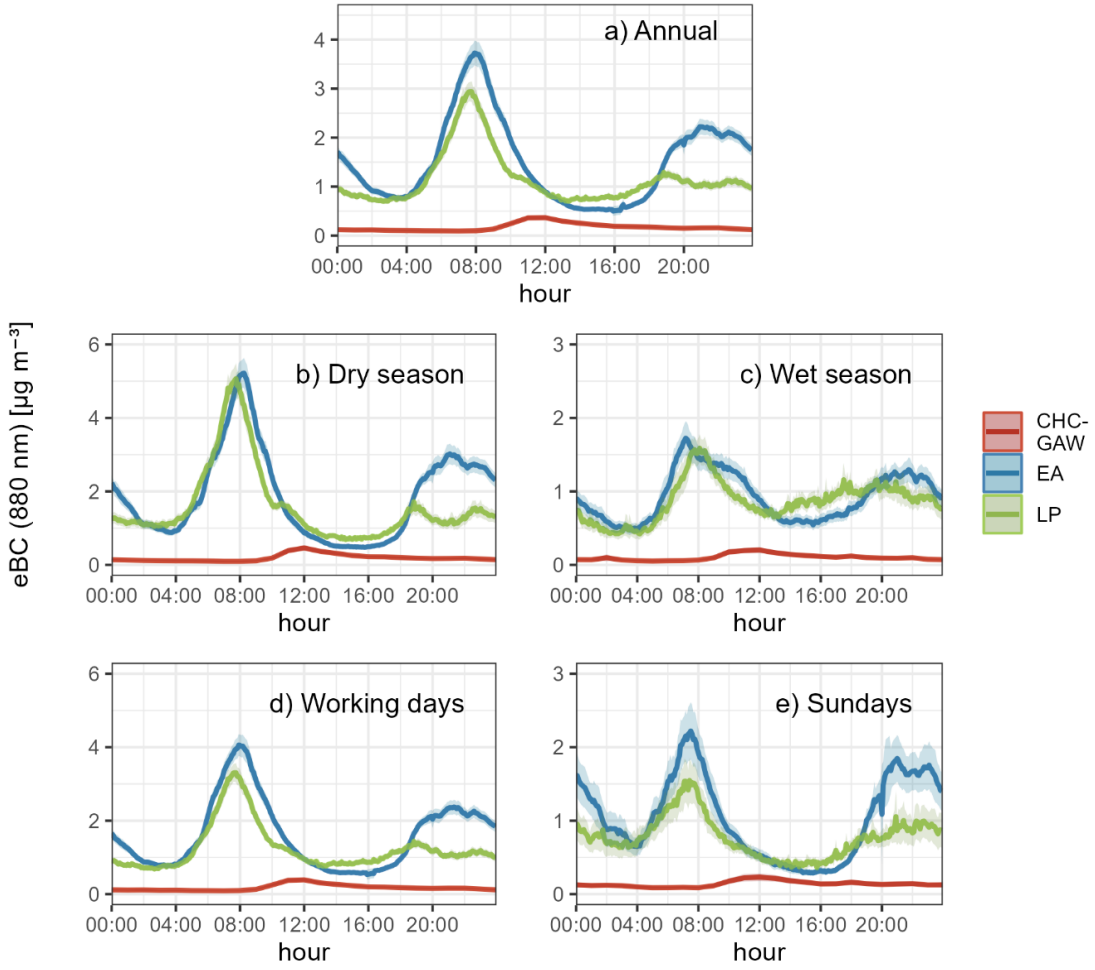

Figure 3. Average diurnal variation of BC concentration at the three sites during a) the complete sampling campaign, b) the dry season, c) the wet season, d) working days, and e) Sundays. The shaded areas around the mean values represent the 95% confidence interval.

Moreover, the evening mode in La Paz seems to be composed by two smaller peaks: one around 19:00 and one around 23:00. This becomes more evident during the dry season (austral winter) and is not observed in El Alto (Figure 3.b, 3.d). The first peak of the second mode of BC average diurnal concentrations in La Paz seems to correspond to the evening rush hour, hence, it is not observed on Sundays (Figure 3.e). Instead, evening concentrations on Sundays steadily increase until 23:00 in La Paz. In contrast, during the wet season (austral summer), the second evening peak is no longer observable, likely due to the increase in night-time temperatures during this period.

A reduction in vehicular traffic (as it can be expected during weekends) as well as meteorology (higher temperatures together with wet deposition) are both capable of reducing the average concentrations by a factor two at both urban sites. In addition, the difference in magnitude between the morning and the evening

peak is simultaneously modulated by the emitting sources and the meteorology. When the number of emitting sources is reduced, the difference between the morning and the evening peak is also reduced by 20% (Figure 3.c & 3.e). Finally, the combinations of precipitation and higher temperatures make the evening peak concentrations similar at both sites, but also makes the morning peak in El Alto less symmetrical. A slight lump with maximum concentrations between 6:00 and 8:00 can be noted during the wet season in the average diurnal pattern. This pattern was also observed in Wiedensohler et al. (2018) both for BC mass concentrations and particle number concentrations (PNC).

Wiedensohler et al. (2018) also reported BC concentrations at the road-site in La Paz being in average nearly 3 to over 10 times higher than at the EA station throughout the day, with a less smooth diurnal pattern than the one observed in the background station. In the present study, the average concentrations at LP are not significantly different than at EA, except for the difference in the evening peak. This suggest that the difference in distance from the sampling site to the nearest road (La Paz road site < 10 m, LP background site ~ 70 m horizontally and 40 m vertically) is enough to significantly dilute traffic emissions and make the observations at LP background station comparable to the observations at EA. Several studies as Alas et al. (2022) and Peters et al. (2014) have previously described rapid decreases in BC concentrations between road and urban-background sites, as well as between traffic hotspots and less crowded routes within a couple of hundred meters.

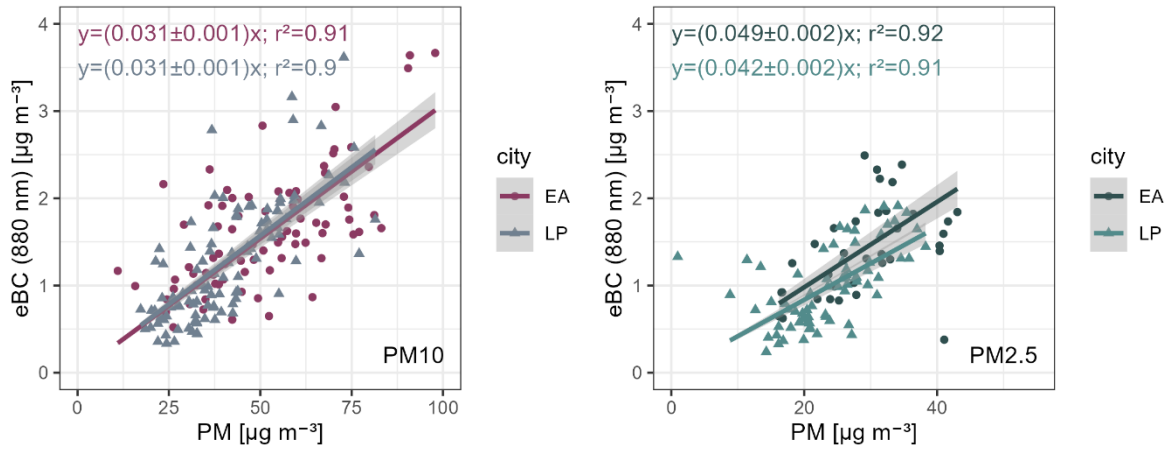

Figure 4. Scatter plot of daily average BC concentrations vs a) PM_{10} and b) $PM_{2.5}$ concentrations at both sites (Two outliers were excluded from the ordinary least square regression displayed in the right panel).

When compared to PM concentrations measured from daily samples collected during the same period of measurements, BC displays a similar trend as PM, with high dispersion around the linear fit (Figure 4). At both sites and for both PM_{10} and $PM_{2.5}$, BC represents less than 5% of the total measured PM. Similar trends are also observed when comparing EC and PM, where EC contributes with roughly 5 and 6% to total PM_{10} and $PM_{2.5}$, respectively. Comparing the fraction of PM that corresponds to BC and EC in other high-altitude cities we observe that both, the contribution of EC to PM_{10} in Bogotá is almost 1.3 times higher (8.2%-9%) than in La Paz-

El Alto (Ramírez, Sánchez de la Campa, Amato, et al., 2018). In contrast in Mexico City BC contributions to $PM_{2.5}$ were reported to be almost 5 times higher than the ones observed in LP-EA (16%, calculated from average concentrations of BC and $PM_{2.5}$ reported by Peralta et al., 2019).

3.2. Intrinsic properties of BC: Mass Absorption Coefficients and Absorption Ångström Exponents.

The Mass Absorption Coefficient (MAC) and the absorption Ångström exponent (AAE) are important parameters of BC used for characterizing both source origin and ageing processes. Here, we computed the variability of both parameters for the two cities, according to equation (3) and (4).

The comparison of the daily averaged BC concentrations to the measured EC concentrations obtained from the filter samples yielded good correlations for both cities ($r^2 \geq 0.5$), especially in La Paz ($r^2 \geq 0.8$). The slope obtained from given comparison is very similar for both sites and for both size cuts with slopes between 0.50-0.54 and offsets between 0.2 and 0.4 µg m^{-3}). It should be noted that, as shown in eq. [3], the MAC values calculated from Aethalometers depend directly on the C_f values chosen to convert the attenuation coefficients to absorption coefficients. Different correction schemes could potentially reduce MAC values by roughly a factor two compared to traditional correction schemes as shown by Li & May (2022). Thus, caution must be taken when comparing MAC values between sites, and the selection of C_f should always be considered in the comparison.

Table 3. Average MAC_{EC} and MAC_{rBC} calculated following eq. [3] using EC and rBC mass concentrations measured at the three sampling sites. The MAC values were extrapolated to other commonly reported wavelengths using the corresponding daily mean AAEs.

BC mass		λ	EA	LP
EC-PM_{10}	**MAC_{EC}**	550 nm	9.0±2.2	7.9 ±2.9
	±	637 nm	7.8±1.9	7.0±2.5
	SD **[m^2 g^{-1}]**	880 nm	5.4±1.3	4.7±1.8
EC-$PM_{2.5}$	**MAC_{EC}**	550 nm	9.5±3.6	9.2±1.9
	±	637 nm	8.4±3.0	8.1±1.8
	SD **[m^2 g^{-1}]**	880 nm	5.9±2.2	5.4±1.2
SP2-XR	**MAC_{rBC}**	550 nm	9.3±2.3	*15.1±14.2* [i]
	±	637 nm	8.5±2.0	*13.4±12.7* [i]
(SP2-XX in CHC)	**SD** **[m^2 g^{-1}]**	880 nm	5.9±1.2	*9.3±1.2* [i]

[i] average MAC values calculated for the few cases where the mass size distribution peaked within the SP2-XR detection limit

The average ratio of the calculated absorption coefficients b_{abs} and EC (using a C_f=2.78 for AE33 and C_F=2.9 for AE31), resulted in relatively low MAC_{EC} values at all wavelengths, which are consistent with previously reported values for fresh BC at urban background sites (i.e. BC particles that had not had enough time to build a coating layer big enough to modify largely its absorptive properties) (Table 3).

The average of the daily MAC_{EC} values found at both cities La Paz and El Alto are within those reported for urban and urban background areas where the absorbing particles had already undergone little mixing/aging processes (Chen et al., 2017; Cui et al., 2016; Kondo et al., 2009; You et al., 2016). Despite intense radiation, the ageing process does not appear faster in the high altitude as respect to other places. Similar average MAC_{rBC} values were obtained from the hourly ratios of absorption coefficients over rBC mass concentrations in the city of EA (eq. [3]), conversely, much higher values were obtained for the city of LP. The latter phenomenon resulted from an instrumental limitation. The detection capability of SP2 outside the size range 80-650 nm is very limited (Pileci et al., 2021) thus the rBC mass is typically underestimated in particular when the rBC mass distribution peaks below the 80 nm lower detection limit of the SP2-XR. This was the case for 90% of samples in La Paz, while in El Alto, rBC mass distributions were normally monomodal with a peak around 180 - 200 nm.

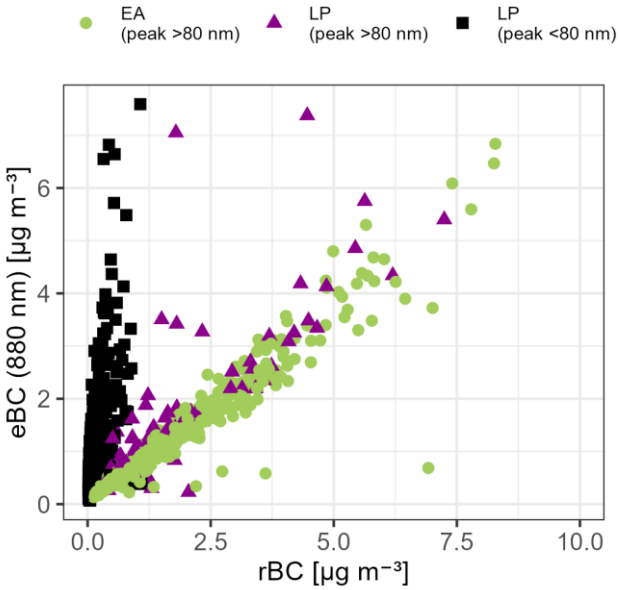

Figure 5. BC concentrations vs rBC concentrations measured during Apr-May 2018 at both sites. Color and shape distinguish mass size distributions of rBC that peaked within (LP: purple triangles and EA: green circles) or outside the size range of the SP2-XR (black squares).

Figure 5 displays the comparison of the simultaneous integrated mass concentrations of rBC and the optically estimated BC concentrations in LP and EA. In color are displayed the cases when in LP (green circles) and in El Alto (purple circles) the mass size distributions peaked above 80 nm. In black (squares) the cases in LP where the distribution peaked below 80 nm. In the latter case, the rBC mass concentrations are highly underestimated, accounting for less than 15% of the mass of absorbing aerosol. Reliable MAC_{rBC} coefficients for LP cannot be calculated due to the large fraction of the mass missed below the detection limit (Table 3).

No evident relation between meteorological parameters and the particle's aging state was observed in La Paz. Modini et al. (in prep) will further discuss rBC concentrations in both cities. In the context of the present study, we restricted the calculation of MAC_{rBC} to the cases when the size distribution of rBC peaked within the detection limit of the SP2-XR. Given the low number of datapoints that meet this criterion in LP, mean values of MAC_{rBC} are strongly influenced by the few extreme events, resulting in very high MAC_{rBC} values. No substantial variability in MAC_{rBC} values was observed on hourly timescales. This suggests that the emission sources and transport pathways to the LP and EA sites were relatively constant throughout the measurement period. Again, this is consistent with the dominant source of BC being local vehicular emissions.

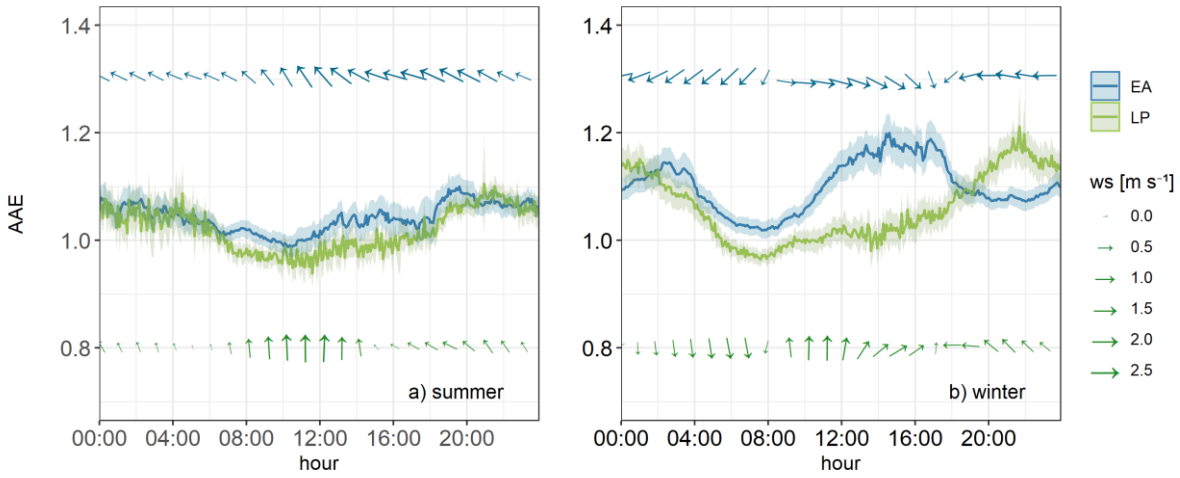

Figure 6. Average diurnal variation of the AAE (solid lines), wind speed and wind direction (arrows above and below the solid lines) at both sites during a) winter and b) summer. The shaded area behind the solid curves represents the 95% CI.

Average AAE coefficients of 1.1±0.2 were found for both La Paz and El Alto and of 1.0±0.3 in CHC-GAW. The diurnal variability of AAE in the urban sites shows an overall decrease around the morning rush-hour peak towards the minimum values for both sites (Figure 6.a and 6.b). However, a difference in the evolution of this parameter throughout the day can be noticed between the sites during winter, the driest season of the year (Figure 6.b).

At EA, between 9:00 and 18:00, a slight increase of the average AAE can be observed only in El Alto. During the same period, in winter (Figure 6.b), average wind direction changes in El Alto from being mostly easterly to north-westerly winds. This change in the wind direction allows the incursion of particles with different optical properties coming from the altiplano, like dust. It is worth emphasizing that the change in the AAE during this period of the day is not substantial and takes place when BC concentrations are at their lowest levels, thus, no significant impact in absorption was observed at 880 nm. However, this reveals the possible influence of multiple sources of absorbing particles in El Alto besides traffic and biomass burning. This should come as no surprise, since dust is the major source of PM_{10} particles in El Alto, being responsible for 46% of the mass during winter (Mardoñez et al., 2022).

In La Paz, winds are practically bidirectional throughout the year due to the topography of the city, Winds typically follow the direction of the canyon, blowing mainly from the south. No change in the AAE is observed at this site besides the decrease of AAE during daytime resulting from fresh vehicular emissions.

3.3. Source apportionment of BC

3.3.1. Aethalometer method

The apportionment of the contribution of vehicular emissions and biomass burning to absorption was calculated following the methodology described in section 2.5.1. Average contributions attributed to BB emissions present highest values during the BB season (Jul-Nov) and minimum values during the beginning of the wet season (Dec-Jan). The median contribution of BB to BC concentrations based on the Aethalometer method was estimated to be roughly 30% at the three sites during the BB season (Figure 7, top), and it decreases to 19%, 16% and 4% in LP, EA and CHC-GAW, respectively, outside this period. Extremally low BC mass concentrations measured in the mountain station make the dispersion of the apportioned BB contributions to BC to be widely dispersed around the median values in CHC-GAW. In Figure 7 (bottom) are shown the resulting time series of the apportioned BC mass concentrations attributed to biomass burning practices, which display similar seasonal trends throughout the years at the three sites.

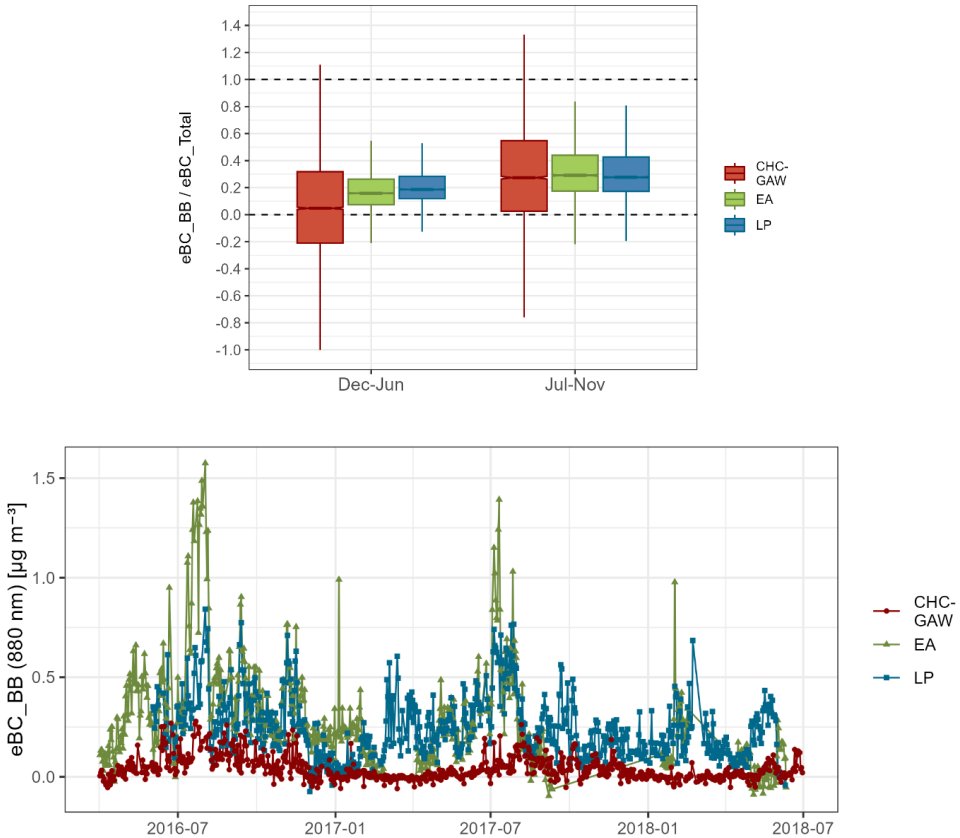

Figure 7. Boxplot of the hourly BC_WB/BC resulting from the bilinear aethalometer method displaying maximum contributions during the biomass burning season (Jul-Nov) (top), time series of the daily apportioned BC mass concentrations (excluding outliers) (bottom).

3.3.2. Source deconvolution of absorption through multilinear regression

One of the limitations of the Aethalometer bilinear method is that it only allows the differentiation of two emission sources, which is suited for most cities in OECD countries. In La Paz/El Alto, this assumption does not necessarily hold, as other sources of BC may be impacting the urban air quality. Hence, we used the results from Mardoñez et al. (2022) where an integrated PMF approach was employed and 11 different sources of PM_{10} were identified. In the present study, only the sources that significantly contributed to absorption were included in the multilinear ordinary least-square regression (MLR) to determine how absorption can be attributed to given sources at different wavelengths (section 2.5.2).

The regressions laid out R^2>0.8 for all wavelengths, with a reconstruction > 80% of the observed absorption coefficients. The obtained source-specific MAC values (absorption per mass unit of each source) are displayed in Figure 8. Waste burning stands out as the most efficient source in terms of absorption, followed by sources directly or indirectly linked to traffic (TR1, TR2, Secondary nitrate, secondary sulfate), and biomass burning.

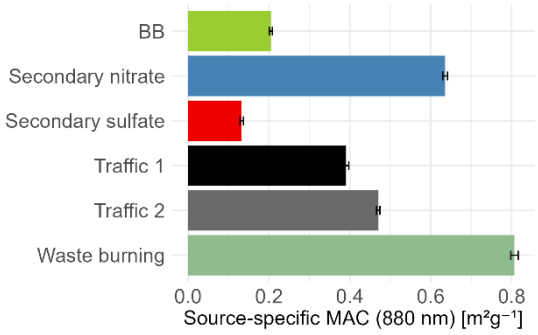

Figure 8. Median source-specific mass absorption cross sections (ß) obtained from the multisite MLR between b_{abs} (880 nm) and the mass contribution of the six sources of PM_{10}, resolved by Mardoñez et al. (2022), that significantly contributed to the measured absorption coefficients. The black error bars represent the 95% CI of the median.

In terms of their contribution to absorption at 880 nm (Figure 9), TR2 and secondary nitrate stand out as the two major sources of absorbing aerosols at both sites. It is important to highlight that the chemical profile of the secondary nitrate factor, contained 10-20% of the total measured EC and OC, and some alkanes. These components, tracers of traffic emissions, were not successfully separated from the tracers of secondary nitrate (ammonium and nitrate), thus, revealing its association to primary vehicular emissions. Having traffic and traffic related factors as the major sources responsible for absorbing aerosol particles is coherent with the results obtained by the aethalometer method, and with the mean AAEs~1 obtained at each site.

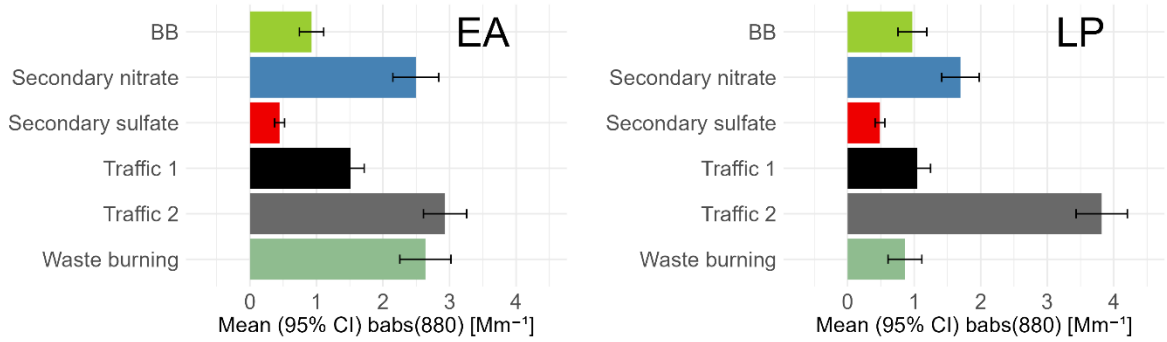

Figure 9. Mean contribution to absorption of the six sources of PM_{10} resolved by Mardoñez et al. (2022) (left: EA, right: LP) that presented a p-value <0.05 in the multilinear ordinary least-squares regression.

The third and fourth sources responsible for the measured absorption coefficients in the city of El Alto are waste burning and TR1, whereas the inverse is observed in the city of La Paz. Regional BB comes as the fifth source at EA and fourth at LP (tying with TR1) and Secondary sulfate presented the smallest contributions to absorption. It should be emphasized that Waste burning represented less than 5% of the total PM_{10} mass concentrations at both sites (Mardoñez et al. 2022), however, it becomes one of the leading sources contributing to absorption in EA.

Moreover, Table 4 presents the mean source-specific AAE calculated, as described in Section 2.5.2, including all seven wavelengths and also excluding the shortest one (370 nm). The highest AAE found corresponds to BB, which is at the lower end of the reported literature values. The AAE for BB including 370 nm coincides with the value recommended by Zotter et al. (2017). The value obtained excluding the shortest wavelength confirms the AAE_{BB} selected for the aethalometer method in section 2.5.1 and is comparable to the lower end of AAE values found by (Rizzo et al., 2011) during the BB season in a Brazilian pasture site located in the Amazon. The remaining sources, influenced by local anthropogenic activities including vehicular emissions and waste burning present an AAE close to 1, corresponding to freshly emitted, relatively pure, BC particles. Particularly, the average of the AAE for the traffic sources also coincides with the AAE selected as representative of traffic in section 2.5.1.

Although the average AAE for the two traffic profiles TR2 presents a lower AAE than TR1. Given that TR1 and TR2 presented different chemical profiles, this difference in the wavelength dependency of their contributions to absorption could also give insights of a difference in the nature or the state of the absorbing aerosol particles emitted by these two sources. Based on the experiments of Schnaiter et al. (2005), Liu et al. (2018) has estimated AAE<1 for aged diesel BC particles (compact and coated). Other European studies have also reported low AAE in experiments that involved diesel buses (accelerating) (Helin et al., 2021) or diesel dominated regions (Zotter et al., 2017). Nevertheless, given that the vehicle fleet, the fuel and the combustion conditions in LP-EA are different than the ones in the mentioned studies, only an in-situ characterization of the exhaust emissions would unveil the identity of each factor.

The presence of EC in the chemical profile of the waste burning factor, as described in Mardoñez et al. (2022), and the AAE=1.1-1.2 associated to it suggest that this source could result from combustion processes at high temperatures.

Table 4. Source-specific AAE obtained from the non-linear regression of the source-specific mass absorption MAC (λ) cross-sections and wavelength

	AAE (370 - 950 nm)	AAE (470 - 950 nm)
BIOMASS BURNING	1.68±0.08	1.43±0.05
TRAFFIC 1	1.05±0.06	0.97±0.08
TRAFFIC 2	0.84±0.06	0.86±0.04
SECONDARY NITRATE	0.96±0.02	1.00±0.05
SECONDARY SULFATE	1.06±0.04	1.11±0.02
WASTE BURNING	1.17±0.04	1.14±0.06

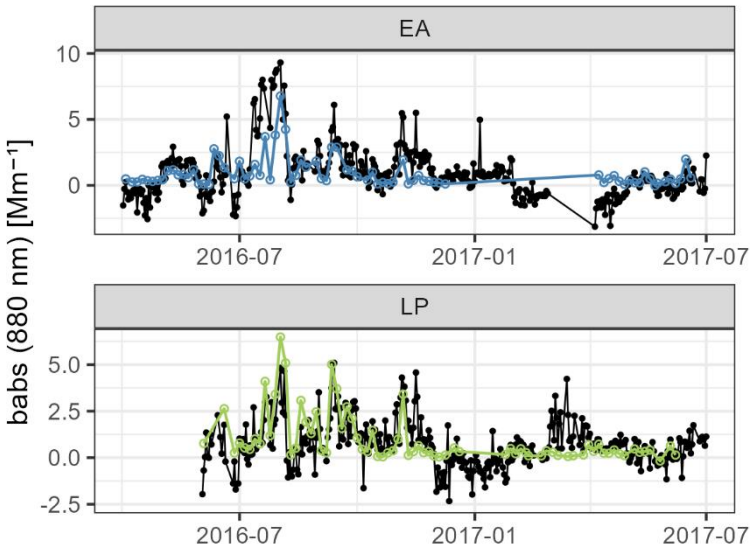

Figure 10. Timeseries of the contribution of agricultural biomass burning to the absorption coefficients measured at the two urban background sites (LP and EA) using two different apportioning methods: Aethalometer method (black lines) and MLR deconvolution from the mass contribution of PM_{10} sources resolved by Mardoñez et al. (2022) (colored lines).

The apportioned absorption coefficients calculated through the aethalometer method are clearly higher than those obtained from the MLR. However, when AAE_{TR} is increased to 1 (the average AAE of the non-BB sources) the apportioned absorption coefficients attributed to biomass burning obtained from both methods are brought closer together (Figure 10). This change decreased the previously calculated median contribution of BB to absorption by 5% during the BB season and resulted in a general agreement between the apportioning methods at both sites (except for the maximum contributions obtained by the aethalometer method at EA in

2016, and at LP in March 2017). These discrepancies could be influenced by the presence of other confluent sources that have AAE>1 and that its contribution increase during the same periods. It is possible to observed that the efficiency of predicting low contributions of BB by the Aethalometer method results in noisy absorption coefficients below 0.

We can conclude that both source apportionment methods highlight local anthropogenic activities as the main sources responsible for the observed absorption, dominated by sources influenced by primary and secondary vehicular emissions. However, the contributions of coexisting sources of absorbing particles can be masked in the two-source aethalometer model, leading to an overestimation of the contribution of BB to total absorption. In addition, BB is responsible for a small but significant fraction of the absorption despite the fact that the emitting sources are located hundreds of kilometers away from the urban centers, to the other side of the Andes. Despite the large contribution of dust to PM mass concentrations, the chemical and optical properties of dust make its contribution to total absorption almost insignificant.

4. Conclusions

The average background concentrations of BC in La Paz (LP) and El Alto (EA) are comparable amongst the sites and lower than the concentrations reported for other high-altitude Latin-American megacities. The different local meteorological conditions make the concentrations of BC in EA much higher during the evening compared to LP. A factor two difference in magnitude can be observed between working and non-working days at both sites, as well as between the dry and the wet season, indicating the important role weekly human activities and meteorology play in modulating the BC concentrations. The influence of the conurbation can also be observed at the global station CHC-GAW, located ~20 km away, showing concentrations that are roughly 35% of what is measured in the urban area (within the hours CHC-GAW is influenced by the urban mixing layer, ~10-16h).

Despite the specific conditions of the sites, the intrinsic properties of BC are not fundamentally different than at other places. The MAC values and the AAE estimated for both cities show that at an urban background level, BC concentrations are dominated by relatively fresh vehicular emissions that do not undergo drastic ageing processes. Nevertheless, the peaking at low diameters of the BC mass size distributions in the city of La Paz is a phenomenon that is not expected at an urban background site, and remains to be further investigated.

The main sources of absorbing particulate matter in LP-EA are rather local. Vehicular emissions are the first target to tackle from an air quality perspective as well as to reduce the impact these emissions can have on climate. Other sources that contribute to BC are open waste burning (particularly in EA) and biomass burning. This is noteworthy since open waste burning occurs in many cities, in Bolivia and elsewhere.

It was observed that the aethalometer method can overestimate the contributions of biomass burning in the presence of a third source of absorbing aerosol particles, such as waste burning. The multilinear regression

allowed the estimation of the source-specific MAC values, the source contribution to total absorption and the source-specific absorption Ångström exponent (AAE) of the sources directly or indirectly associated to vehicular emissions, biomass burning and open waste burning.

Rigorous policies controlling the open waste burning and the size/state of the circulating vehicle fleet are therefore imperative in order to reduce the impact of BC on climate and on health of the inhabitants of the conurbation. In addition, the observation of BC particles with very low diameters at an urban background site is a phenomenon that requires further investigation since it represents a potential higher risk of exposure to ultrafine particles of the local population. This represent an alarming threat to the health of the residents of the conurbation, for which prompt actions need to be taken in order to preserve the health of their inhabitants.

Code availability

All calculations were performed in R version 4.1.0 and the code is available upon request.

Acknowledgments

Authors wish to thank all the many people from the different laboratories (LFA, Idaea-CSIC, IGE, Air O Sol analytical platform, EDYTEM) who actively contributed over the years in filter sampling and/or analysis.

S. Rios and E. Miranda of GAMLP (Gobierno Autónomo Municipal de La Paz) who provided access and facilitated tasks at Pipiripi; IIF personnel that helped in logistics during the campaign; Undergrad students who collected samples: Y. Laura, G. Salvatierra, M. Roca, D. Calasich, E. Huanca, Z. Tuco, S.Herrera, M. Vicente, M. Zapata, R. Copa.

Financial support

This research has been supported by the Institute de Recherche pour le Développement (IRD) France and IRD delegation in Bolivia, by The Labex OSUG@2020 (ANR10 LABX56) to, EU H2020 MSCA-RISE project PAPILA (Grant #: 777544) and by CNRS/INSU and Ministère de l'Enseignement SUpérieur et de la Recherche with contribution to ACTRIS-FR and SNO-CLAP.

Air Pollution and its Association to Health Outcomes

One of the main reasons for monitoring air quality parameters is to be able to describe the link between air pollution and its health effects. As previously discussed, despite the numerous studies that have been able to find associations between exposure to particles smaller than 10 or 2.5 µm in diameter, this metric does not describe the mechanism by which these associations occur. Moreover, this metric is highly influenced by the mass of bigger particles that typically represent the least threat for human health. On the other hand, oxidative potential, the newly proposed air quality metric, aims to quantify the toxicity of the inhaled particles that are responsible for the oxidation of the lung tissue. The following chapter will describe the results of two assays measuring the oxidative potential associated with the particulate matter collected in La Paz and El Alto.

Up to this point we have managed to analyze, comprehensively and from different perspectives, the main sources that affect air quality in the conurbation. The objective of the following chapter is to study the impact that each of them has on health from the perspective of oxidative potential. Finally, this impact will be evaluated by looking at the main associations between the air quality parameters reviewed and each of the resolved sources, with two respiratory health outcomes. This chapter is also presented in the form of a scientific article since it is currently being prepared to be submitted to a scientific journal. The manuscript is currently under review by the co-authors.

Oxidative potential of particulate matter and its association to respiratory health endpoints in high-altitude cities in Bolivia

Lucille Joanna S. Borlaza[1], Valeria Mardoñez[1,2], Anouk Marsal[1], Ian Hough[1], Dinh Ngoc Thuy Vy[1], Marcos Andrade[2], Jean-Luc Jaffrezo[1], Andrés Alastuey[3], Jean-Luc Besombes[4], Griša Močnik[5,6,7,] Isabel Moreno[2], Fernando Velarde[2], Jacques Gardon[8], Alex Cornejo[9], Paolo Laj[1,10], and Gaëlle Uzu[1]

[1]Institute des Géosciences de l'Environnement, Université Grenoble Alpes, CNRS, IRD, Grenoble INP, Grenoble, France
[2]Laboratorio de Física de la Atmósfera, Instituto de Investigaciones Físicas, Universidad Mayor de San Andrés, La Paz, Bolivia
[3]Institute of Environmental Assessment and Water Research (IDAEA), CSIC, Barcelona, Spain
[4]Université Savoie Mont Blanc, CNRS, EDYTEM (UMR 5204), Chambéry 73000, France
[5] Center for Atmospheric Research, University of Nova Gorica, 5270 Ajdovščina, Slovenia
[6] Haze Instruments d.o.o., 1000 Ljubljana, Slovenia
[7] Department of Condensed Matter Physics, Jozef Stefan Institute, 1000 Ljubljana, Slovenia
[8]Hydrosciences Montpellier, Université de Montpellier, IRD, CNRS, Montpellier, France
[9]Viceministerio de Promoción, Vigilancia Epidemiológica y Medicina Tradicional (VPVEyMT), La Paz, Bolivia
[10] Institute for Atmospheric and Earth System Research (INAR), and Department of Physics, University of Helsinki, 00014 Helsinki, Finland

Correspondence to: G Uzu (gaelle.uzu@ird.fr)

Abstract. Air pollution has been demonstrated to pose a hidden threat and leading risk to human health, prompting a quest for novel air quality metrics that can more accurately evaluate the potential harm caused by exposure to it. The objective of this study was to determine the most oxidizing sources of particulate matter (PM) in the lungs in two high-altitude Bolivian cities, by evaluating their relative contribution to the oxidative potential (OP) of PM, as measured by two tests (OPDTT and OPDCFH). Moreover, it was sought to investigate the associations between three exposures (PM, OP and BC) vs. the number of weekly medical visits due to two respiratory outcomes (acute respiratory infections, ARI, and pneumonia). Association analysis was performed using a Poisson regression model, adjusting for potential meteorological confounders and exploring associations occurring with a 0- to 2-week lag between health effects and exposures. Health associations with the 11 emission sources of PM resolved by PMF in a previous source apportionment study on the site were also analyzed. Anthropogenic combustion (traffic and biomass burning) and its related sources represent the major contributors to oxidative potential. The strongest associations between exposures and health outcomes were found between OPDTT and $PM_{2.5}$ vs pneumonia and ARI. This suggests that OPDTT is a good candidate as a predictor of the health impact polluting anthropogenic sources for the two investigated respiratory outcomes. Traffic emissions, beyond being found as one of the most important sources of PM, BC and OPDTT activity in the conurbation, also showed significant positive associations with both respiratory outcomes at lag 0.

1. Introduction

Ambient particulate matter (PM) air pollution has been linked to millions of premature deaths globally (WHO, 2021a) and remains a critical issue in many areas due to anthropogenic emissions from traffic, industry, and other sources (Borlaza et al., 2018, 2021a). The situation becomes even more complex in high-altitude cities (> 2000 m above sea level (a.s.l.)) due to limited oxygen in the air and its effect on breath volume (Beall, 2007; Julian & Moore, 2019; U.S. EPA, 2011). Particulate matter (measured as PM_{10} or $PM_{2.5}$) has decreased due to emission control policies implemented in some areas of the world (Aas et al., 2019; Borlaza et al., 2022a; Collaud Coen et al., 2020), but many high-altitude cities located in developing countries are facing worsening air quality with growing industrial sectors and upsurges in traffic (Ramírez, et al., 2018a; Zalakeviciute, et al., 2020).

Much work remains to elucidate the mechanism of PM exposure leading to adverse health effects. One of the well-recognized pathways is the capacity of certain PM components to induce oxidative stress in the lungs, leading to inflammatory responses that range from cell damage to cell death (Ayres et al., 2008; Kaur et al., 2022; Mudway et al., 2020). Some potential pathways of PM-induced oxidative stress arise from acute inflammatory responses, nucleic acid damage and repair, and energy perturbations (Tang et al., 2022). Hence, a growing number of studies have focused on assessing the oxidative potential (OP) of PM, defined as the capability of PM to generate reactive oxygen species (ROS) that deplete anti-oxidants in the lungs (Bates et al., 2019; Borlaza et al., 2018; Borlaza, et al., 2021b; Daellenbach et al., 2020; Park et al., 2018). However, there is still quite limited evidence concerning the potential of OP as a health-based metric (Borlaza et al., 2022b; Marsal et al., 2023; Weichenthal et al., 2016, 2021), especially in high-altitude cities.

An extensive study of ambient PM air pollution in two high-altitudes Bolivian cities, La Paz (approximately 3200-3600 m a.s.l.) and El Alto (4050 m a.s.l.), has been recently reported (Mardoñez et al., 2022). In that study, for the very first time, an innovative multisite Positive Matrix Factorization (PMF) modelling technique was used to apportion the sources of PM in the Altiplano area. A very key feature of the study of is that the PMF methodology uses a large set of organic markers such as levoglucosan, polycyclic aromatic hydrocarbons (PAHs), hopanes, and alkanes that were added to a common input dataset (traditionally only including ions, metals, and carbonaceous (organic and elemental carbon) components of PM). A total of 11 sources of PM were identified, both natural and anthropogenic, including two traffic-related factors, a non-exhaust factor, and commonly unresolved sources such as lubricant oil and waste burning sources.

This study evaluates the capacity of each PM source in the Bolivian Altiplano to induce oxidative stress in the lungs and explores health impacts. First, we use an advanced PMF dataset (Mardoñez et al., 2022) to identify the main PM sources that drive OP. Then, we evaluate the association of source-specific PM and OP with hospital visits due to respiratory disease. To the best of our knowledge, this is the first study linking OP and PM sources to respiratory health in high altitude cities, allowing a direct estimation of the health impact of individual PM sources.

2. Materials and methods

2.1. Study areas and sampling parameters

The study area consists of two adjacent high-altitude cities in Bolivia, La Paz (LP, 16.50°S, 68.13°W, 3600 m.a.s.l.) and El Alto (EA, 16.51° S, 68.13° W, 4025 m.a.s.l.). Each city has a single PM sampling site. The sampling site in LP lies on the rooftop of a four-story building of the Museum Pipiripi (Espacio Interactivo Memoria y Futuro Pipiripi), located on a steep hill downtown, surrounded by residential areas. The EA sampling site is located on the Altiplano plateau, in the meteorological observatory of the El Alto International Airport, surrounded by a few industrial sites and a large vehicle fleet servicing regional and international connections for the metropolis. Due to the topographical differences between the LP and EA sites, the meteorological conditions can vary greatly despite their separation of only 7 km (horizontal distance) and 0.5 km (vertical distance).

The sampling campaign was conducted between April 2016 and June 2018, with high-volume samplers (DA80, Digitel) to collect 24-hr PM_{10} (April 2016- June 2017) and $PM_{2.5}$ (June 2017- July 2018) samples onto quartz fiber filters (150 mm-diameter, Pallflex QAT and Whatman) once every three days. All filters were preheated at 500°C for 8 hours before sampling. After sample collection, all filters were safely stored in a low temperature-controlled environment until analysis.

The daily mass concentrations (µg m^{-3}) were measured by gravimetric analysis of the filters. All filters were strategically fractioned to be sufficient for all the chemical analyses considered. The chemical characterizations were: elemental carbon (EC), organic carbon (OC), sugar anhydrides (Levoglucosan, Mannosan), sugar alcohols (Arabitol, Mannitol), water-soluble ions (SO_4^{2-}, NO_3^-, Cl^-, MSA, NH_4^+, Na^+, K^+, Mg^{2+}, Ca^{2+}), metals (Al, Ca, K, Na , Mg, Fe, Ti, V, Mn, Cu, Zn, Rb, Sn, Sb, Pb), polycyclic aromatic hydrocarbons (PAHs: Fla, Pyr, Tri, BaA, Chr, BaP, BghiP, IP, BbF, Cor), alkanes (C21-C26), methyl PAHs, thiophens, hopanes (HP3 to HP4), alkane methoxyphenols, and methylnitrocatechols. Field blank samples (52) were also collected and used to calculate the limits of quantification, which were subtracted from the samples before calculating atmospheric concentrations. An intensive characterization study on the PM chemistry and sources in the area has been reported elsewhere (Mardoñez et al., 2022). Equivalent black carbon (BC) mass concentrations were also measured during the same period at both sites using an aethalometer model AE33 in EA and an aethalometer model AE31 in LP (April 2016- June 2018). However, due to the intermittence of data availability resulting from technical problems in EA, only the period of data May 2016- Aug 2017 is considered in the present analysis. Wind speed and wind direction were measured at both sites with a 15-min time resolution using anemometers placed on the sites. Other meteorological variables were provided by the Airport's air navigation administration (Administración de Aeropuertos y Servicios Auxiliares a la Navegación Aérea, AASANA) with a 1-hour time resolution, for El Alto, and from the National Meteorology and Hydrology Service

(Servicio Nacional de Meteorología e Hidrología, SENAMHI) (*SENAMHI*, n.d.) for La Paz on a daily time resolution.

2.2. Oxidative potential (OP) analysis

The OP of PM_{10} and $PM_{2.5}$ was assessed by two acellular assays (using dithiothreitol (DTT), and dichlorofluorecein (DCFH) probes) with filter extraction using a simulated lung fluid (SLF) solution at 37°C and at 25 µg mL^{-1} iso-mass concentration based from the protocol proposed in (Calas et al., 2018). In the DTT assay, the probe is an anti-oxidant surrogate representing the reaction between PM and biological reducing agents. The consumption of DTT in the reaction corresponds to the capacity of PM to generate reactive oxygen species (ROS) (Cho et al., 2005).The remaining DTT is reacted with 5,5-dithio-bis-(2-nitrobenzoic acid) (DTNB) to produce 5-mercapto-2-nitrobenzoic acid (TNB). This solution is then analyzed under a spectrometer (absorbance at 412 nm wavelength using a TECAN spectrophotometer Infinite M200 Pro plate-reader in 96-well multiwall plate (Greiner-Bio) for a total of 30 minutes of analysis time with a 10-minute interval. In the DCFH assay, a particle-bound ROS method is based on the reaction of the ROS in PM with DCFH, a non-fluorescent reagent, with horseradish peroxidase. This reaction produces a fluorescent compound, 2,7-dichlorofluorescein (DCF). The DCF formation is also analyzed under a spectrometer (excitation at 485 nm, emission at 530 nm wavelength using the same plate-reader as the DTT-assay) in a black 96-well multiwall plate for a total of 30 minutes of analysis time with a 2-minute interval under constant agitation at 37°C.

To ensure the stability of analysis, a positive control is analysed in every experiment using a 1,4-naphthoquinone (1,4-NQ) solution for analysis using DTT (40 µl of 24.7 µM stock solution) and DCFH (80 µl of 24.7 µM 1,4-NQ solution) assays. There is a ≤3% coefficient of variation (CV) in the positive control analysis for both assays. Finally, the OP activity of PM is calculated based on a volume-normalized metric (OP_v) representing the OP consumption (nmol min^{-1}) of PM normalized by the air volume (m^3) during sampling. All samples were analysed in triplicate with a CV between 0 and 10% for each assay.

We aggregated the OP measures to match our health outcome data by averaging all measures in each week.

2.3. Source apportionment of PM

Source apportionment of PM_{10} was performed using the Positive Matrix Factor PMF 5.0 model, developed by the U.S. Environmental Protection Agency (EPA). The improved multi-site database used for the PMF model is detailed in Mardoñez et al. (2022). Briefly, the PMF applies a weighted least-squares fit algorithm as described in Eq. 1:

$$x_{ij} = \sum_{k=1}^{p} g_{ik} f_{kj} + e_{ij} \quad [1]$$

where x_{ij} represents the *j*th measured chemical species in the *i*th PM sample, *p* is the number of sources, g_{ik} is the contribution of the *k*th source to the *i*th sample, f_{kj} is the contribution of the *k*th source to the *j*th

chemical species (obtained source chemical profiles), e_{ij} are the model residuals. The final solution selected with good statistical indicators and sound geochemical properties resulted in 11 resolved sources: dust, secondary sulfate, secondary nitrate, primary biogenic aerosols (PBA), MSA-rich, biomass burning (BB), traffic 1 (TR1), traffic 2 (TR2), lubricant, non-exhaust emissions, and waste burning. A complete description of each PM source is presented in Mardoñez et al. (2022).

2.4. Source apportionment of OP

The OP contribution of each PM_{10} source was apportioned using multiple linear regression (MLR) based on the procedure proposed in Weber et al. (2018). Briefly, the OP activity measured in each PM sample was used as the dependent variable while the mass contributions of each PMF-resolved source (μg m^3) were used as the independent variables, as shown in Eq. 2:

$$OP_{obs} = (G \times \beta) + \varepsilon \; [2]$$

where OP_{obs} are the observed OP_v measured either by DTT or DCFH assay (nmol min^{-1} m^{-3}), G are the source contributions (μg m^{-3}) obtained from the PMF model, β are the regression coefficients representing the mass-normalized ("intrinsic") OP (OP_m) (nmol min^{-1} μg^{-1}) of each source, and ε are the model residuals. The uncertainties of β were estimated by a bootstrapping method (*n*=500) using random selection of samples to account for outliers and seasonal variation in each source-specific OP_m. The OP contribution of each source was calculated by multiplying β of each source by the mass contribution of the source.

2.5. Linking OP of sources to respiratory health endpoints

Weekly medical visits at all health care centers in La Paz and El Alto due to either (1) pneumonia (Pneu) or (2) acute respiratory infections other than pneumonia (ARI) was obtained from the Bolivian Ministry of Health and Sports. Pneumonia is an infection of the distal bronchi that may be caused by bacteria, viruses, fungi, or other chemical irritants. Acute respiratory infections are infections of the airways, that can occur in the upper (from the nostrils to the larynx) or the lower respiratory tract (from the trachea to the alveoli), such as laryngitis or bronchitis.

The adjusted associations of observed exposures (PM, OP_{DTT}, $OP_{DCFH,}$ BC), normalized by their respective interquartile range (IQR), with the health endpoints were estimated using quasi-Poisson regression models separately for each exposure, in each size fraction (PM_{10} and $PM_{2.5}$), for each of Pneu and ARI (single-exposure models). The adjustment factors considered in the models were chosen based on the literature: time, meteorological conditions (temperature, relative humidity, wind speed), and a random effect representing the city (El Alto and La Paz). We modelled time as a natural spline with 6 degrees of freedom per year, representing time-varying unmeasured confounders having a period of two months or more. We modelled each meteorological variable as a natural spline with three degrees of freedom to capture potentially non-linear associations with the health outcomes. We fit a separate model for each of lags 0, 1, and 2 weeks where lag 0 is the week of the medical visit count and lag 1 is the previous week. This approach was driven by the possibility

that there may be a time lag between exposure, the manifestation of biological effects, and an individual seeking medical care. A similar analysis was also applied to the sources of PM resolved by Mardoñez et al. (2022), with the difference that for this model a multi-pollutant approach was followed i.e. the linearly independent contributions of each source to PM_{10} were simultaneously included as additive terms in the model.

As a preliminary analysis, unadjusted associations were also estimated for each exposure using univariate regression models (provided in the SI, S1). A stratified analysis was also performed by repeating the same analysis for each of three age groups (adults age ≥20 years, children-teenagers age 1 to 19 years old, and infants age < 1 year) (provided in the SI, S2). All statistical analyses were performed using R (R Core Team, 2021) ; adjusted analyses used the glmmPQL function from the MASS package (Venables & Ripley, 2002).

3. Results and discussion

3.1. Study population and the characteristics of particulate matter and its oxidative potential (OP)

El Alto and La Paz have a surface area of 370 and 475 km2, respectively, and a projected population of 1 030 151 and 912 960 inhabitants in 2018, respectively (Red MoniCA, 2021). The highest number of medical visits were during the months of April to June (average temperatures of 6.8°C in EA and 12.3°C in LP), highlighting the potential influence of meteorological conditions, with a second smaller mode between September and November for both health endpoints (Figure 1).

The median (25^{th} – 75^{th} percentile) mass concentrations of PM_{10} and $PM_{2.5}$ during the study period were 28.9 (21.2 – 39.3) and 15.6 (11.9-19.5) µg m^{-3}, respectively, in El Alto and 24.4 (19.4 – 31.6) and 14.7 (11.9-18.0) µg m^{-3}, respectively, in La Paz, with a distinct seasonal variability (high during colder months with minimum precipitation (dry season), May-Aug, and low during the wet season, Dec-Mar) (Figure 1). During the study period, 13% of days in EA and 4% of days in LP exceeded the WHO air quality guideline level for PM_{10} of 45 µg m^{-3}. All exceedances occurred during the dry season, which overlaps with the austral winter months. In contrast, roughly 50% of days in both cities exceeded the WHO AQ guideline level for $PM_{2.5}$ of 15 µg m^{-3}. It is important to note that these exceedances were observed in urban background stations, where the minimum levels of pollution are expected. It can be expected that values vary greatly above these concentrations across the cities, especially closer to local sources, likely reaching the local air quality regulatory levels (150 µg m^{-3}). The median (25^{th} – 75^{th} percentile) OP_{DTT} was 1.93 (1.34-2.58) nmol min^{-1} m^{-3} for PM_{10} and 1.35 (0.90-1.88) nmol min^{-1} m^{-3} for $PM_{2.5}$; for OP_{DCFH} it was 0.54 (0.31-0.82) nmol min^{-1} m^{-3} for PM_{10} and 0.26 (0.14-0.53) nmol min^{-1} m^{-3} for $PM_{2.5}$, following the same seasonality as PM (Figure 1). The annual median (25^{th} – 75^{th} percentile) BC mass concentration was 1.0 (0.5-1.9) and 0.8 (0.5-1.4) µg m^{-3} in El Alto and La Paz, respectively, with a similar seasonality as PM (Figure 1).

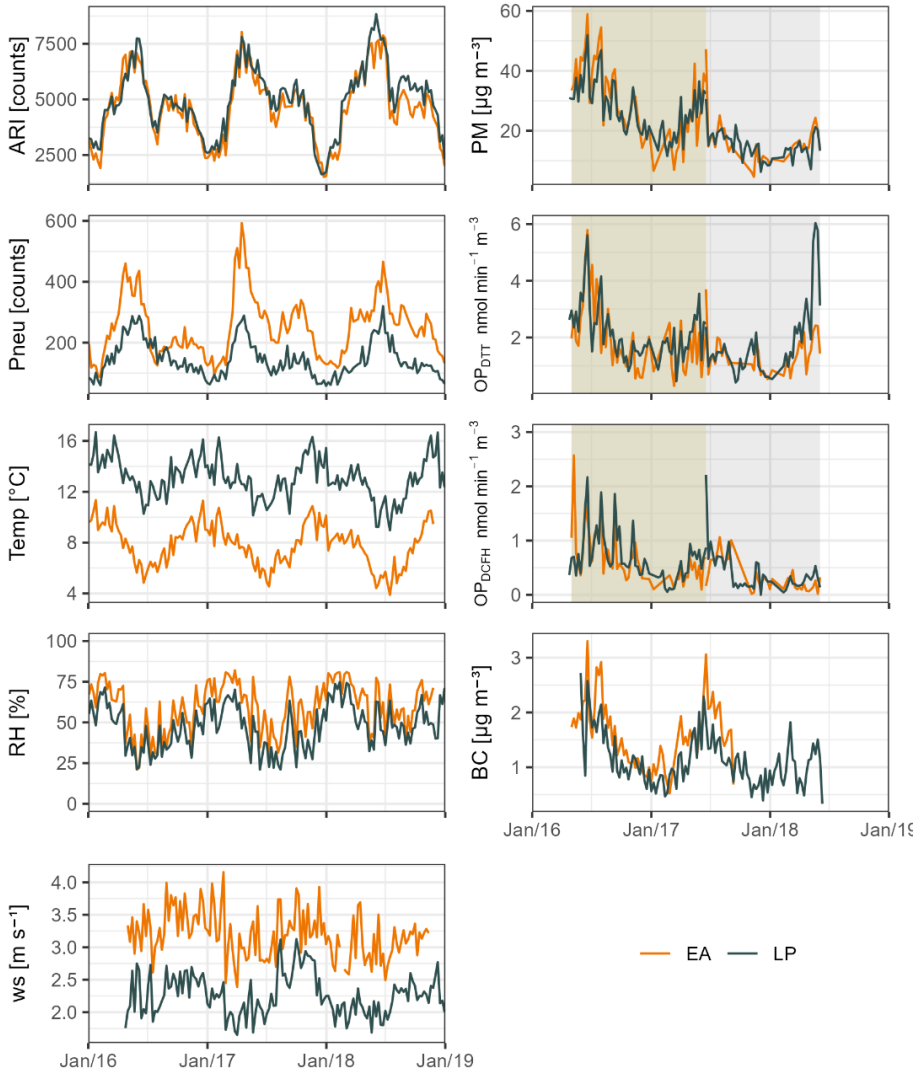

Figure 1: Temporal variation of the number of medical visits due to acute respiratory infection (ARI) and pneumonia (Pneu); meteorological variables: mean temperature (Temp), relative humidity (RH), and wind speed (ws); and exposures: particulate matter (PM), oxidative potential (OP_{DTT} & OP_{DCFH}), black carbon (BC) in La Paz (LP) an El Alto (EA) during the measurements campaign. Note: green and grey background respectively refer to measurements in the PM_{10} and $PM_{2.5}$ fractions.

3.2. Sources of OP of PM_{10}

Sources of PM_{10} in terms of mass concentration were previously identified and apportioned using PMF 5.0 (Mardoñez et al., 2022) (Figure 2). These PMF-resolved sources were used to apportion the corresponding OP of PM_{10} using MLR, resulting in a deconvolution with an R^2 (coefficient of determination) 0.48 for OP_{DTT} and 0.67 OP_{DCFH}, respectively. Spearman correlation coefficients (r_s) for measured OP and the PMF-resolved sources were also calculated for each assay and season (see Table S1 in the SI). Generally, the estimated source-specific OP is well within the range of the observed OP. There are some local events, possibly a high-PM_{10} event, that were not captured in the MLR-modelled OP. The two assays used in this study allowed a wider sensitivity towards various sources, but ultimately focused on the impact of anthropogenic sources to OP of PM_{10}.

The intrinsic characteristic of PM_{10} to induce oxidative stress, represented by the mass-normalized OP (OP_m, nmol min^{-1} μg^{-1}) of each source is provided in Figure S4 in the SI. The PM_{10} sources with higher OP_m contain more redox-active species. In terms of daily mean contribution to volume-normalized OP (OP_{DTT}: lubricant, non-exhaust emissions, traffic 1 and traffic 2; OP_{DCFH}: biomass burning, waste burning, secondary sulfate, secondary nitrate). In terms of daily mean OP_v contribution, the top three sources of OP_{DTT} are all traffic-related sources, namely: traffic 2 (0.5±0.3 nmol min^{-1} m^{-3}), non-exhaust (0.3±0.4 nmol min^{-1} m^{-3}), and traffic 1 (0.2±0.2 nmol min^{-1} m^{-3}) (Figure 2). These results highlight the impact of sources driven by anthropogenic emissions on OP of PM_{10}. For OP_{DCFH}, the top three sources are biomass burning (0.2±0.3 nmol min^{-1} m^{-3}), sulfate rich (0.1±0.1 nmol min^{-1} m^{-3}), and secondary nitrate (0.1±0.1 nmol min^{-1} m^{-3}) (Figure 2) which are secondary sources that are also linked to anthropogenic emissions. The sulfate-rich source was generally associated with long-range transport of pollutants, and the nitrate-rich source with oxidation of nitrogen oxides from traffic emissions (Mardoñez et al., 2022). These sources accounted in average for 58% of the total OP_{DCFH}, confirming the importance of anthropogenic emissions.

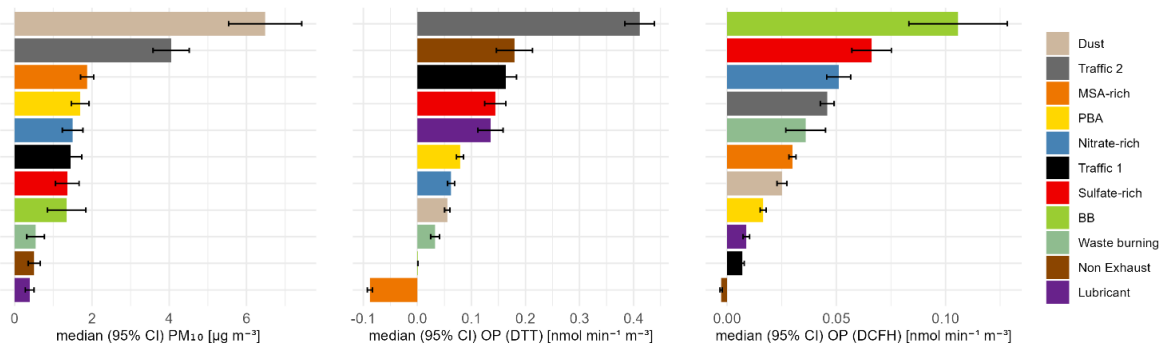

Figure 2. Median source contribution to PM mass concentrations (obtained from PMF, left), reconstructed volume-normalized OP_{DTT} of PM_{10} (middle), and reconstructed volume-normalized OP_{DCFH} of PM_{10} (right). The black error bars represent the 95% confidence interval. Note: PBA – primary biogenic aerosols, BB – biomass burning.

Although it is clear that anthropogenic sources are important drivers of OP of PM_{10}, there are also contributions from biogenic sources (MSA-rich and primary biogenic aerosols (PBA)). These sources, identified by key organic tracers, play in important role in the dynamics of OP in PM_{10} (Borlaza et al., 2022b; Daellenbach et al., 2020) based on their ability to modulate the redox-active species in PM (Samake et al., 2017).

Figure 2 highlights the variation in source impacts based on PM_{10} mass concentration vs OP. The top sources of PM_{10} are dust, traffic 2, accounting for a combined 43% of total PM_{10}. Traffic 2 is also top ranking for OP_{DTT} and is fourth for OP_{DCFH}, however, the dust contributes much less to the capability of PM_{10} to induce oxidative stress in both assays. This is explained by a low intrinsic OP for dust factor, for instance 8 times lower than intrinsic OP for Traffic 2 in OP_{DDT}. In contrast, the non-exhaust traffic source, traffic 1, lubricant, sulfate-rich, and nitrate-rich contribute relatively little to PM_{10} mass but are among the top sources of the OP when considering both assays. It is important to note these differences when assessing PM_{10}'s potential health

impacts. Differences in sources' ranking according to the assay is due the different sensitivity to both probe (Pietrogrande et al., 2019). DDT, is a thiol with a broad and balanced sensitivity to organics (mainly OC and quinones) and inorganic (mainly metal traffic-related) PM components. Whereas DCFH is sensitive to OC, TC and secondaries component as SO_4^{2-} and NO_3^- (Borlaza, et al., 2021b; Pietrogrande et al., 2019) for targeting particle-bound ROS but also reactive nitrogen (Crow, 1997; Venkatachari et al., 2005). The traffic 2 source contributes strongly both to mass and OP_{DTT}, supporting the mitigation of this source to alleviate the health impacts of PM_{10} exposure. It can be observed as well that agricultural BB is an important source of oxidative potential from the perspective of $OP_{DCFH.}$ A reduction in the emissions of this seasonal practice would result in the improvement of the air quality at a regional level.

3.3. Linking PM exposure to respiratory health endpoints

The adjusted associations of $PM_{2.5}$, OP_{DTT}, OP_{DCFH}, and BC with ARI and Pneu are illustrated in Figures 3. An IQR increase in $PM_{2.5}$ mass concentration during the study period was associated with a 3% (95% CI: -1%–8%) increase in hospital visits for Pneu two weeks later (Figure 3, left panel). A similar association was found for ARI, which increased hospital visits by 3% (95% CI: 0%–7%) two weeks after an IQR increase in $PM_{2.5}$ mass concentration (Figure 3, right panel). Very similar associations were found for BC mass concentration. Associations were strongest at lag 2 weeks and weaker at lag 1 and lag 0 weeks, except for BC and ARI which showed a similar association at lag 1 and lag 2 weeks. The baseline analysis using univariate (unadjusted) showed stronger association, as presented in Figure S1 in the SI.

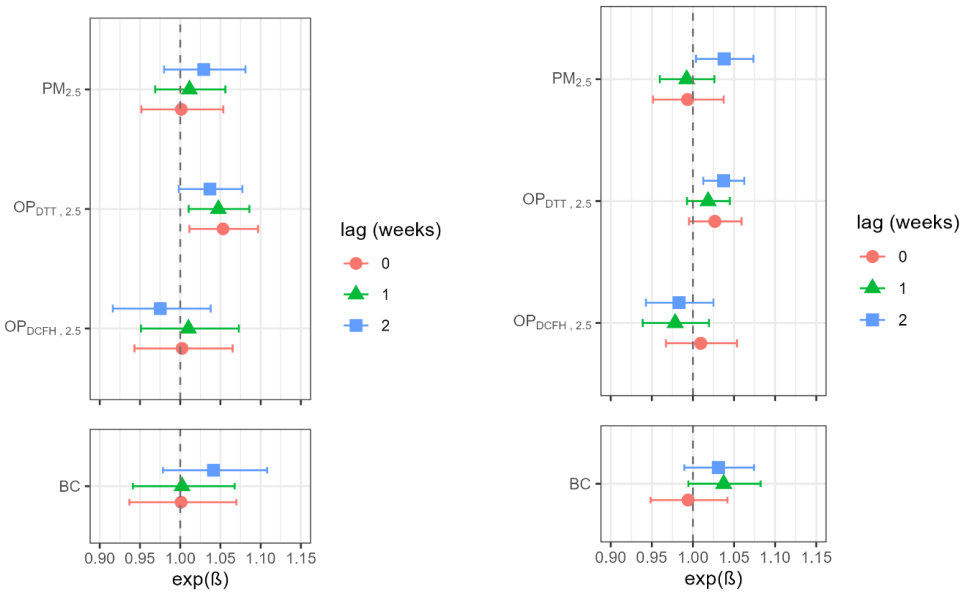

Figure 3: Associations between weekly medical visits for acute respiratory infection (Pneu, left panel) and pneumonia (ARI, right panel) PM, OP_{DTT}, OP_{DCFH} in the $PM_{2.5}$ fraction, and BC. Note: All estimates are normalized by their IQR increase, and adjusted for time trend, temperature, relative humidity, wind speed, and with a random effect representing the city (El Alto and La Paz).

Associations of OP of $PM_{2.5}$ were generally seen at lag 0 and 1 week for Pneu and at lag 2 weeks for ARI. For each IQR increase in OP_{DTT} for Pneu (1.05 change in medical visits for each increase in OP_{DTT} by one IQR after adjustment, 95%CI, 1.01 to 1.10 medical visits, p = 0.01, lag 0 weeks, Figure 3, left panel) and ARI (1.04 change in medical visits for each increase in OP_{DTT} by one IQR after adjustment, 95%CI, 1.01 to 1.06 medical visits, p = 0.004, lag 2 weeks, Figure 3, right panel). OP_{DCFH} was not clearly associated with hospital visits.

There were no clear associations of PM_{10} mass concentration and its OP with medical visits (Figure S5 in the SI). This might be due to residual confounding, possibly related to the fact that PM_{10} was sampled during a different time period (April 2016 to June 2017) than $PM_{2.5}$ (June 2017 to July 2018). In the literature, stronger associations are typically found for $PM_{2.5}$ compared to PM_{10} (Kim et al., 2018; Yin & Xu, 2018).

Thanks to the previous study apportioning the sources of PM_{10} in the same sites (Mardoñez et al., 2022) we were also able to examine associations of PM_{10} sources with respiratory health (Figure 4). PM_{10} is more suited for an exhaustive and comprehensive source apportionment, especially when accounting for non-exhaust emissions that are mostly emitted in the coarse mode.

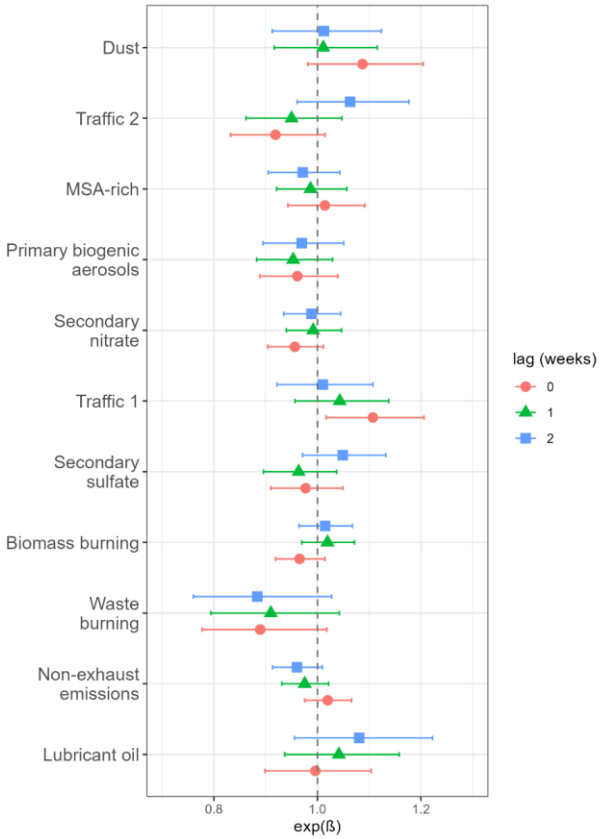

Figure 4: Associations between weekly medical visits for acute respiratory infection (Pneu) and the PMF-resolved sources of PM in a multi-pollutant model. Note: All estimates are normalized by their IQR increase, and adjusted for time trend, temperature, relative humidity, wind speed, and with a random effect representing the city (El Alto and La Paz).

Generally, the PMF-resolved dust and traffic 1 factors showed positive associations in all lags considered for both Pneu and ARI. An IQR increase in PM_{10} from the traffic 1 factor was associated with 11% (95% CI: 2%–21%) increase in hospital visits for Pneu during the same week (Figure 4). An IQR increase in PM_{10} from the dust source was associated with a 5% (95% CI: -1%–11%) increase in hospital visits for ARI during the same week (Figure 5). Most other PM_{10} sources did not show clear associations with hospital visits. However, an IQR increase in PM_{10} from traffic 1 and lubricant oil was associated with a decrease in hospital visits for ARI (-7%, 95% CI: -12% – -1% for traffic 1 PM_{10} at lag 1 week; -9%, 95% CI: -14% – -3% for lubricant oil PM_{10} at lag 0 weeks). Waste burning was negatively associated to Pneu at all lags, although the association did not clearly differ from null. These associations are biologically implausible and may be due to residual confounding.

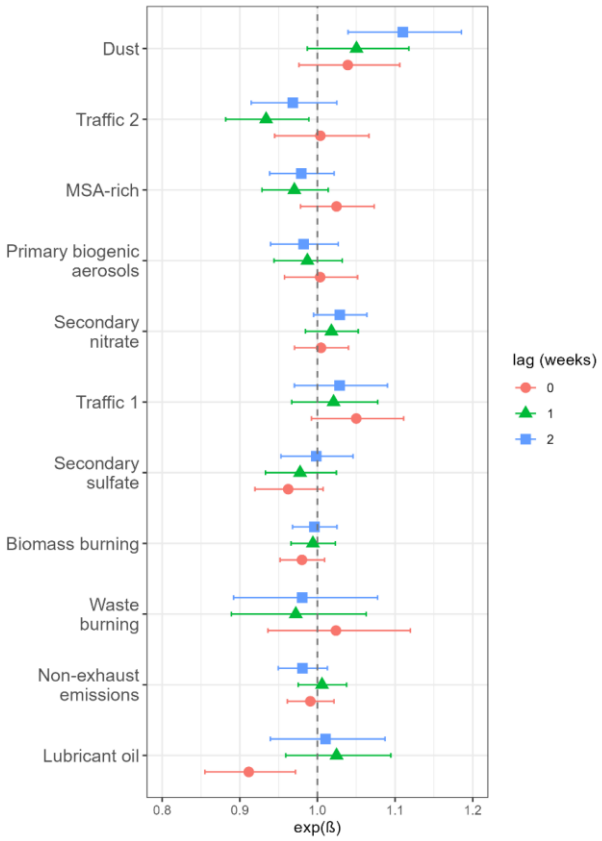

Figure 5: Associations between weekly medical visits for pneumonia (ARI) and the PMF-resolved sources of PM in a multi-pollutant model. Note: All estimates are normalized by their IQR increase, and adjusted for time trend, temperature, relative humidity, wind speed, and with a random effect representing the city (El Alto and La Paz).

Overall, these findings suggest that $PM_{2.5}$ and its OP may contribute to respiratory disease in El Alto and La Paz. Traffic 1 may be a driver of this association since PM^{10} from traffic 1 was associated with Pneu and seemed to increase hospital visits for ARI. Traffic 1 was also one of the top sources of OP of PM_{10}. Most traffic exhaust emissions are in the fine mode so its effects are likely included in the associations observed for $PM_{2.5}$. Dust is associated to respiratory diseases, but possibly through an additional biological pathway than oxidative stress or indirect one since it was only a minor contributor to the OP of PM_{10}. In fact, mineral dust and dust sand have

been found to have a direct physical effect on epithelial cells by causing damage based on the particles' composition and shape (Fussell & Kelly, 2021). This damage triggers the release of secondary cytokines and the generation of oxidative stress within the lesion, which may contribute to the onset of acute lung toxicity (Naota et al., 2010). This information could explain its low OP intrinsic reactivity because the OP response is only affected by exogenous ROS in an acellular assay. Furthermore, an additional interesting point was found in studies investigating the link between meningitis season and dust events in Africa where the extreme dryness combined with high dust loads during the dry season was proposed as a combined mechanism to explain the damage the pharyngeal mucosa, making the epithelium more vulnerable to bacterial invasion and potentially leading to meningitis. The Altiplano area exhibits also low humidity levels (<60% annual average) that can exacerbate high dust content health effects (Deroubaix et al., 2013).

Finally, different lags in associations for pneumonia vs. ARI may be explained by different rates of progression or symptom severity for the two diseases.

3.4. Strengths and limitations of the study

In this study, the OP of PM in both the fine and coarse fractions ($PM_{2.5}$ and PM_{10}) were assessed by DTT and DCFH assays. The sources of OP of PM_{10} were estimated from PMF-resolved sources in a previous study (Mardoñez et al., 2022). The measured air quality parameters and the PM_{10} sources were associated with health endpoints represented by hospital visits due to pneumonia and acute respiratory infections. To the best of our knowledge, this is the first attempt to link these parameters in Bolivia using long term measurements, especially in a high-altitude site as is the metropolitan area of La Paz and El Alto.

The strength of this study relies on the unique opportunity to associate multiple air quality parameters and specific PM sources with respiratory health. Our findings showed clear associations of $PM_{2.5}$, both in terms of mass and OP, with respiratory endpoints, possibly driven by traffic emissions. Additionally, associations of OP of $PM_{2.5}$ with respiratory health were seen as early as the week of exposure, whereas for $PM_{2.5}$ associations were only seen two weeks following exposure. This highlights the usefulness of OP as a health-based metric of PM exposure, consistent with previous studies examining different health outcomes (Bates et al., 2019; Borlaza, et al., 2021b; Lavigne et al., 2018; Marsal et al., 2023; Mataveli et al., 2021; Strak et al., 2017)

We acknowledge that the sampling periods of PM_{10} and $PM_{2.5}$ were consecutive not in parallel (Figure 1). We do not expect that PM composition or unmeasured confounders varied substantially between 2016 and 2017, although if it did it might help explain the fact that we observed clearer associations with respiratory health for $PM_{2.5}$ than for PM_{10}. We were unable to collect data on possible confounding factors other than meteorology, although we controlled for temporal trends with a period longer than two months. This however means we were only able to detect the effects of acute not chronic PM exposure. At the same time, our health data was only available weekly, which limited our ability to detect effects at timescales of a few days. PM samples were collected every third day, which may have led us to underestimate exposure due to missed

short-term air pollution peaks. We estimated exposure based on PM samples from two locations which may not be representative of individuals' exposure. The resulting exposure measurement error may have biased our estimates towards the null or decreased our power to detect associations.

We chose to focus on PM_{10} sources rather than source-specific OP because the PM_{10} source apportionment model had much better performance (R^2=0.99) than the OP deconvolution (R^2=0.48 for OP_{DTT} and R^2=0.68 for OP_{DCFH}). We tested a high number of associations (n= 46) without any formal correction for multiple comparisons, so our findings should be interpreted with caution as some reported associations could be due to chance.

Despite these limitations, this study adds to our understanding of the health effects of specific PM sources and the relevance of oxidative potential as a health-related air quality metric. It supports previous work pointing to the importance of anthropogenic emissions, particularly from traffic, and suggests a link between the oxidative potential of $PM_{2.5}$ and respiratory disease in a little-studied high-altitude setting.

4. Conclusions

This study takes advantage of a unique opportunity to assess the OP of PM in high-altitude cities in Bolivia with a complex topography and meteorology, and to find the link between PM sources and its OP with medical admission for pneumonia and acute respiratory infection. The main sources contributing to OP originate from anthropogenically-derived sources. Epidemiological models between sources and hospital admissions for respiratory outcomes revealed that OP_{DTT} was able to detect positive association between with both pneumonia and acute respiratory diseases already in the first week of exposure, whereas 2 weeks lags were necessary for PM mass. OP_{DTT} source deconvolution showed that the most oxidizing sources in the conurbation are traffic related, while dust is of second order despite its large contribution to the mass of PM. In contrast, positive associations for the dust and traffic sources where obtained from the epidemiological models. We find this consistent with the different biological pathways through which dust and vehicular emissions can cause oxidative stress. Being an acellular assay, OP_{DTT} is only capable to predict the exogenous oxidative stress caused by the reactive oxygen species (ROS) carried or produced by the particulate matter. We consider secondary and endogenous oxidative stress is produced by dust as a result of physical damage in the lung.

These findings could help target traffic and dust emission sources that are critical to control the health effects of PM pollution

Acknowledgements

The authours would like to thank the Viceministerio de Promoción, Vigilancia Epidemiológica y Medicina Tradicional del Ministerio de Salud y Deportes (Vice ministry of Promotion, Epidemiologic surveillance and Traditional Medicine, from the Ministry of Health and Sport) for providing the health endpoints data.

The long-term observations are performed within the framework of GAW and ACTRIS, receiving support from the Universidad Mayor de San Andrés and from the international stakeholders. In France, support from the Centre national de la recherche scientifique through ACTRIS-FR/SNO CLAP as well as the Institut de Recherche et Développement (IRD) and Observatoire des Sciences de l'Univers de Grenoble (OSUG) through the French National Research Agency's Laboratories of Excellence in particular, is greatly acknowledged. In Spain, support from the CSIC is acknowledged.

Financial support

The postdoc of Lucille Joanna Borlaza is funded by the Predict'air project (grant Fondation UGA-UGA 2022-16 and grant PR-PRE-2021 FUGA-Fondation Air Liquide). The PhD of Valeria Mardonez was supported by IRD/CNRS, ARTS Grant. The work on Oxidative Potential measurements is also supported by the French National Research Agency in the framework of the Get OP Stand OP (ANR-19-CE34-0002-01) and ACME (ANR-15-IDEX-02). Maintenance of measurements on site and chemical analysis on the Air-O-Sol facility at IGE was made possible with the funding of some of the equipment by the Labex OSUG@2020 (ANR10 LABX56).

Code availability

The software code could be made available upon request by contacting the corresponding author.

Data availability

The OP and health datasets could be made available upon request by contacting the corresponding author.

Author contributions

GU designed the study, developed the OP assays and gathered health data. MA, PL, AA, JLB made the project and sampling possible in Bolivia (High-volume sampler donation). IM performed the air sampling. JLJ, AA, JLB, GU produced the air quality data. LJSB, VM, AM, IH, processed the data of the study. LJSB wrote the paper. GU, revised the original draft. All authors reviewed and edited the manuscript.

Competing interests

The authors declare that they have no conflict of interest.

CONCLUSIONS

The overall objectives of this study were to document the levels of particulate pollutants affecting air quality in the metropolitan region of La Paz and El Alto, to identify their sources of emission and to assess the potential impact of exposure to air pollution on the health of the inhabitants in the conurbation. In a longer prospective, the aim of the study is to provide baseline information on drivers for air quality in this area onto which policy making and air quality regulations can be advised.

While some studies have characterized pollution levels in large Latin American cities, very few have addressed the links between air pollutants and health information provided by municipal health services, let alone the inclusion of oxidation potential as a measure. The present study is unique, not only because it documents for the first time the nature of particulate pollution in La Paz-El Alto, but also because of the peculiarities of the region: high altitude (3200 m to 4100 m above sea level), complex topography, intense solar radiation during the day, and distinct physiological adaptive responses of the inhabitants to low pressure conditions.

Throughout this work, a detailed description of the state of air quality in terms of airborne particulate matter was presented, as well as their main emitting sources. This information coupled with local health data formed the basis for a first assessment of the potential impact of particulate matter on the health of the inhabitants of the area. This work focused on three parameters typically used for the description of air quality: particulate matter (PM) and its chemical speciation, black carbon (BC) and oxidative potential (OP).

In the conurbation of La Paz-El Alto, PM_{10} concentrations measured throughout the study period rarely exceeded the guidelines recommended by the World Health Organization (WHO). These episodes occurred mostly within the dry season. It should be considered however that background levels of particulate pollutants may differ significantly from roadside concentrations, and that the background levels are sufficiently high to consider that many inhabitants in the cities are exposed to harmful levels of pollutants.

By using different mathematical and statistical tools, it was possible to identify the main sources of each of these parameters and their temporal variability, finding that the emitting sources are mostly local and strongly modulated by the local meteorology. By the use of the US EPA Positive Matrix Factorization (PMF) tool and thanks to the wide range of chemical compounds analyzed from the PM_{10} filter samples collected in both cities, it was possible to identify 11 major sources affecting the air quality of the conurbation. The proximity between the two cities made it possible to apportion the sources of PM following a multisite approach, an increasingly used technique due to the robustness it provides to the analysis.

Results from the PMF study showed that almost 50% of the PM mass concentrations measured at both sites can be attributed to mineral dust (naturally and anthropogenically resuspended) and vehicular emissions. Vehicular emissions are also connected to secondary sources influenced by the precursor gases emitted by cars (Secondary Nitrate and Secondary Sulfate). The third outstanding source of pollution found was biomass burning (BB) linked to agriculture practices and land use changes in the lowlands. The highest emissions of BB

typically occur at the end of the dry season and contribute to the exceedance of the threshold levels recommended by the WHO for exposure to PM_{10}. Finally, the remaining mass concentrations were attributed to natural sources (Primary Biogenic Organic Aerosols and Secondary Biogenic Organic Aerosols). A very interesting finding of the study, based on the inclusion of organic tracers in the PMF was to allow the resolution of a small source in terms of mass contribution, associated to the open combustion of waste, which is responsible for a large fraction of the organic tracers that are known to be harmful to health.

It is interesting to note that use of positive matrix factorization was not straightforward when source profiles are pretty much unknown, contrary to the case of cities in the OECD regions. In fact, the 11-factor model was finally selected as the most satisfactory source profiles after many attempts. Directly transposing source profiles from the specific situations in European cities may lead to errors in the identification of emission sources and this must be considered in future studies.

The second air quality parameter analyzed in the present study was the mass concentration of BC, more precisely, the mass concentration of equivalent black carbon (eBC), due to the optical technique employed to measure it. Beyond the important role BC plays on Climate, its importance lies in the small size of given particles and their potential to carry hazardous compounds deep into the lung. Very few studies describe this parameter in the South American region, and even fewer were performed in high altitude conditions. In La Paz and El Alto, the different meteorological conditions experienced by each city make the diurnal variability of BC distinct, however, no significant difference was observed in the average concentrations of BC between the sites. Moreover, the particular conditions for combustion in these cities result in the emission of finer particles than what is usually observed at sea level. The mass absorption cross sections (MAC) associated with these particles were found to be consistent with previously reported MAC values corresponding to freshly emitted BC at urban background stations.

The optical properties of BC in the conurbation point to vehicular emissions as the main source of BC, supporting the PMF study. Moreover, the execution of a two-source model, based on the wavelength dependence of the absorption coefficients, indicated BB as the other significantly contributing source during the dry season. A BC source deconvolution method was implemented based on the association of the multiwavelength absorption coefficients and the mass contribution to PM of the resolved sources from the PMF analysis. The association was made through a simple multilinear regression (MLR) which confirmed the results obtained by the bilinear model. This constitutes an innovative complementary and statistically valid method to characterize the source-specific optical properties of aerosol particles at sites where source apportionment studies of PM have been carried out.

PM mass concentrations are mainly dominated by the mass of the bigger particles, which pose less of a health threat and mostly originate from natural sources. Thus, there is an inherent need to establish air quality parameters that rather assess the toxicity of particulate matter. One of the parameters proposed to accomplish this purpose and which has shown significant associations with health effects is OP. In the present

work, we mainly addressed the OP activity of PM measured by two acellular assays: OP_{DTT} and OP_{DCFH}. Following the same multilinear regression method described in the previous paragraph, we proceeded to deconvolute the main sources of the observed OP activity in both cities. The reconstructed activity of OP_{DTT} and OP_{DCFH} was mostly attributed to anthropogenic sources of PM, particularly: vehicular emissions, biomass burning and open waste burning, as well as to secondary sources of aerosols whose precursors originate in the combustion of fossil fuels.

Finally, this work investigated the possible associations between the previously described air quality parameters and two respiratory health outcomes: acute respiratory infections (ARI) and pneumonia. The number of medical visits due to these two conditions was provided by the Bolivian Ministry of Health with a weekly time resolution. The associations were then analyzed using epidemiological models (Poisson regression) after controlling for the seasonal variability and possible meteorological confounding meteorological factors through a multisite approach. Despite the limitations of the methodology applied to such a short time series (approximately one year per site) with a low temporal resolution, significant positive associations were found between both health outcomes and OP_{DTT} activity measured in the $PM_{2.5}$ fraction. Similarly, a trend towards a lagged positive association can be observed between $PM_{2.5}$ and eBC mass concentrations with the number of reported cases of ARI, and between eBC mass concentrations and the number of reported cases of pneumonia. These results support that OP_{DTT} is a good predictor of the health effects of air quality with respect to the two health outcomes investigated in this work. All the more, such positive associations between respiratory outcomes and air quality parameters highlight the harmful effects of particulate pollutants on health in the conurbation.

We believe that controlled studies of direct emissions from vehicles fueled by different fuel types under different conditions of elevation, slope gradient, load, and speed could help elucidate the identity of the two traffic profiles resolved by the PMF. Given that $PM_{2.5}$ was found to have the strongest associations with health effects, a source apportionment study on the $PM_{2.5}$ fraction is the next step needed to learn the composition of the smaller PM fraction and further investigate possible antagonistic effects that mask the observed associations between health effects and $PM_{2.5}$ but not PM_{10}. Similarly, further analysis of the dynamics of the mixing layer on short time scales (diurnal variations) could provide a better understanding of the influence that cities have on each other and on the GAW global station at Chacaltaya. Finally, the lack of emission inventories and up-to-date statistical information available in the region limited the interpretation of the results in the further identification of traffic sources. This also made the interpretation of the PMF results more difficult and limited the potential power of the PMF tool's constraint function.

We are aware of the limitations of our study. Clearly, our monitoring strategy would have been more robust if it had been supplemented with gaseous components (NO_x and specific volatile organic compounds) to obtain a holistic description of the air quality status in the region. This is not so simple in Bolivia, especially because of the difficulties in accessing reference gases for instrument calibration. We are also aware of all the

difficulties encountered to maintain a long-term monitoring station in La Paz El Alto: Instrument functioning at low pressure can be problematic, replacing technical parts is not immediate, regular maintenance by UMSA-LFA staff is demanding, but this study is also an opportunity to propose some improvements in the logistic organization. A first recommendation we can make for the continuity of activities is to avoid changes in the sampling methodologies and to make sure any change is documented with a period of parallel measurements so that continuity is ensured and discrepancies eventually corrected. In our study, these changes resulted in a reduction in the time series available, which reduced the statistical power of the analysis given the reduced number of data points. Additional uncertainty was also introduced by the difference in instrumentation within sites and the lack of inter-comparison periods for online instruments measuring under the same conditions.

We consider that the results of the rigorous analysis of the three different air quality parameters presented in this document stablish a base line of the general exposure of the inhabitants of La Paz-El Alto to particulate atmospheric pollutants. Moreover, this study contributes to the documentation of air quality studies in the understudied South American region. We hope that this work can be used for advising future policy making, and that the different sampling and data analysis methodologies implemented can serve as a reference that facilitates the replication of this study in other parts of the country and the region. We consider that the description of the chemical composition of the particulate matter emitted by the different resolved sources can also complement the existing emissions inventories. Also, this study can be considered as a firm basis for the implementation and evaluation/validation of a chemical transport model that could allow the forecast of air quality in the area. Finally, to the best of our knowledge, this is the first long term epidemiological study to investigate the existing associations between air quality parameters and the observed health outcomes in Bolivia.

This work provided a description of the urban background state of air quality, i.e. the minimum concentrations of particulate matter to which the inhabitants of the conurbation are exposed to. Nevertheless, people are often exposed to much higher concentrations on a daily life basis. This calls for imperative measures to improve the air quality in the city given the added vulnerability that comes from living in high-altitude conditions. As it has been observed from different perspectives, the main responsible for pollution in La Paz-El Alto are vehicular emissions. We consider that more rigorous control of the state of vehicles circulating in the city is of utmost importance. Secondly, the implementation of massive transportation systems to reduce the size of the vehicle fleet, or transportation systems that use alternative energy sources, are crucial. Similarly, waste burning should be prohibited as it is a major source of hazardous pollutants associated with high human health risk factors. Moreover, it is essential to update the policies of pollutant emissions to regulate the growing industry factor. A decrease in the emissions of agricultural BB would also result in a significant improvement in the air quality of the entire country.

Only reliable, comprehensive, long-term air quality monitoring will allow the effectiveness of current and future air quality policies to be evaluated. A single sampling point is not sufficient for spatial characterization

of the air quality status in different parts of the city. Therefore, proper maintenance and better equipping of existing air quality monitoring networks would significantly contribute to efforts to improve air quality in Bolivia's metropolitan areas. In addition, the implementation of an interactive air quality status tool could be beneficial in alerting the population of pollution peaks so that they can take actions to reduce their own exposure. Finally, it is important to raise awareness of the health risk of air pollution so that the public can actively participate in reducing air pollutant emissions.

ANEX I: Supplementary Information Chapter IV

Source Apportionment of Airborne Particulate Matter in the Bolivian Cities of La Paz and El Alto

Table S1. Bolivian air quality guidelines[13]

Pollutant	***Concentration***	***Period/ statistic characterization***
Carbon Monoxide (CO)	10 mg m^{-3}	8h mean
	40 mg m^{-3}	1h mean
Sulfur dioxide (SO_2)	80 µg m^{-3}	annual mean
	365 µg m^{-3}	24h mean
Nitrogen dioxide (NO_2)	150 µg m^{-3}	24h mean
	400 µg m^{-3}	1h mean
Total suspended particles (TSP)	260 µg m^{-3}	24h mean
	75 µg m^{-3}	annual mean
Particles smaller than 10 µm (PM10)	150 µg m^{-3}	24h mean
	50 µg m^{-3}	annual mean
Ozone (O3)	236 µg m^{-3}	1h mean
Lead (Pb)	1.5 µg m^{-3}	3-month mean

[13] The concentration values are referred to normal concentrations of pressure and temperature ($\bar{T} = 298\ K$, $\bar{P} = 1013.5\ hPa$)

Figure S1. Photographs taken at the sampling sites (Left: El Alto sampling site; right: La Paz sampling site)

Figure S2. Sampling sites. ©OpenStreetMap contributors 2020. Distributed under a Creative Commons BY-SA License

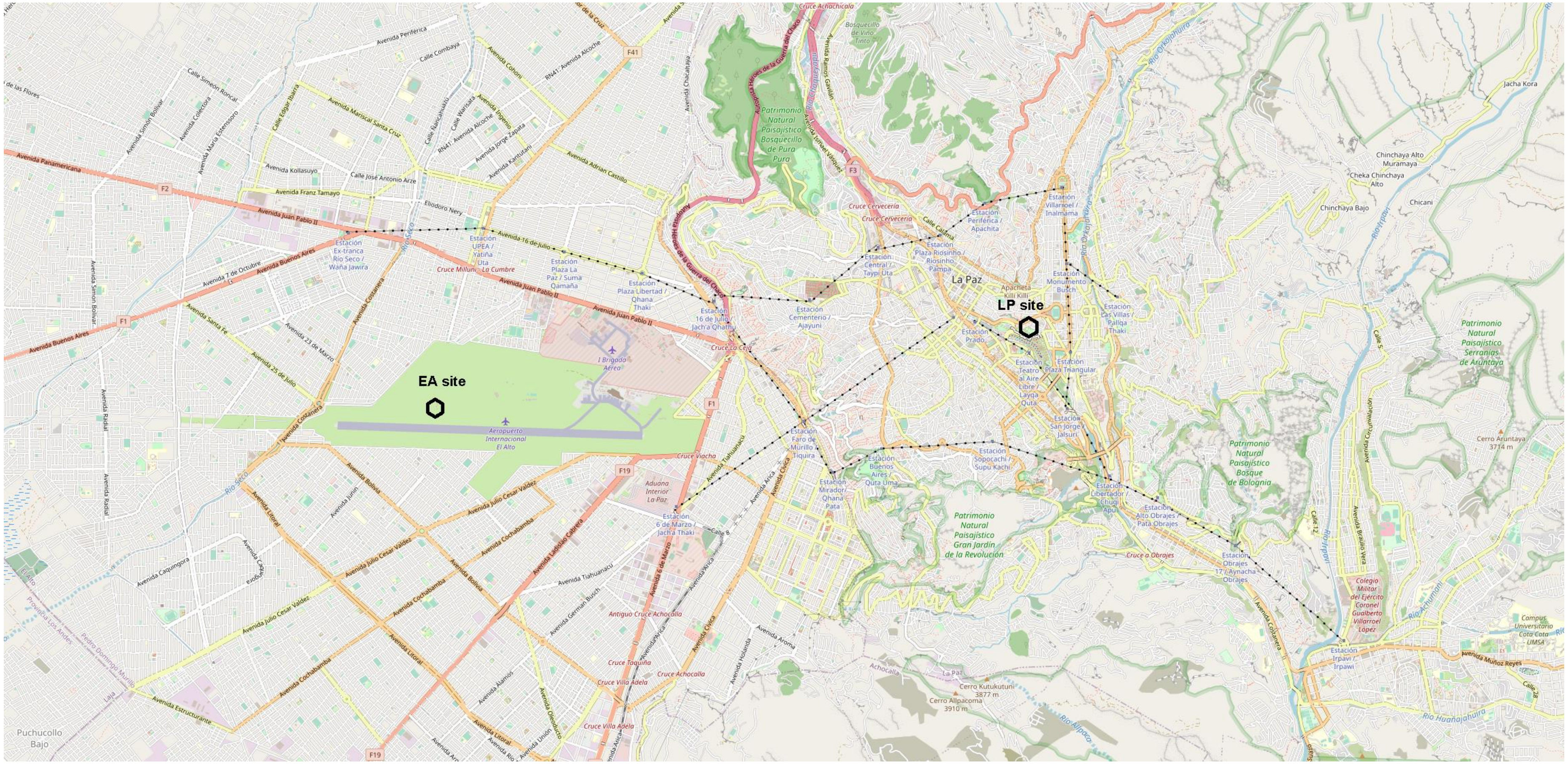

Table S2. Mean, median and standard deviation (sd) of the measured ambient concentrations (above the mean QL, after excluding outliers and samples collected during festivities or the day after, e.g. San Juan, Christmas and New Year). For STP concentrations, ambient concentrations in El Alto must be multiplied by a factor 1.52 and 1.46 for La Paz.

					El Alto (EA)				La Paz (LP)			
Group	**Specie**	**Analysis**	**Units**	**mean QL**	**mean**	**median**	**sd**	**n**	**mean**	**median**	**sd**	**n**
	particulate matter (PM)	gravimetry	[µg m^{-3}]	---	29.9	28.9	12.0	93	27.18	27.07	8.91	103
carbonaceous aerosols	**organic carbon (OC)**	thermal-optical analysis (Cavalli et al., 2010)	[µg m^{-3}]	0.21	3.51	3.48	1.57	93	3.85	3.68	1.78	103
	elemental carbon (EC)		[µg m^{-3}]	0.02	1.46	1.41	0.60	93	1.59	1.57	0.78	103
polyhydric alcohols	**arabitol**	high performance liquid chromatography (HPLC) (Piot et al., 2012)	[ng m^{-3}]	0.77	2.09	1.79	1.08	83	3.75	3.18	2.28	100
	sorbitol		[ng m^{-3}]	0.79	9.13	5.34	10.77	75	13.88	7.75	17.38	87
	mannitol		[ng m^{-3}]	0.77	3.82	3.37	2.67	88	6.73	5.30	4.53	97
monosaccharide anhydrides	**levoglucosan**		[ng m^{-3}]	0.62	87.73	66.47	76.80	93	79.00	46.26	83.15	101
	mannosan		[ng m^{-3}]	0.77	7.52	4.32	9.02	89	7.46	3.33	10.08	98
	galactosan		[ng m^{-3}]	0.31	3.91	1.65	5.74	91	4.31	1.86	6.09	95
saccharides	**glucose**		[ng m^{-3}]	0.77	14.35	13.81	5.84	93	22.07	22.33	8.81	102
ions	**methanesulfonic acid (MSA^-)**	ionic chromatography (IC) (Jaffrezo, Aymoz, & Cozic, 2005)	[ng m^{-3}]	0.06	3.93	3.57	1.87	93	4.38	4.05	2.48	88
	chloride (Cl^-)		[ng m^{-3}]	5.56	217.51	152.27	235.80	93	65.24	52.56	52.79	102
	nitrate (NO_3^-)		[ng m^{-3}]	11.02	609.72	551.21	359.84	92	555.16	482.23	321.65	102
	sulfate (SO_4^{2-})		[ng m^{-3}]	5.29	1247.06	1068.66	723.87	93	1252.77	1098.03	769.54	102
	oxalate (Ox^-)		[ng m^{-3}]	1.64	50.07	45.75	43.71	73	44.95	24.11	58.18	91
	sodium (Na^+)		[ng m^{-3}]	10.47	52.05	46.35	32.64	86	40.94	39.59	21.10	95
	ammonium (NH_4^+)		[ng m^{-3}]	8.74	511.29	451.65	399.06	93	403.81	333.12	308.04	102
	potassium (K^+)		[ng m^{-3}]	2.76	77.41	68.44	52.61	93	73.34	56.82	55.77	102
	magnesium (Mg^+)		[ng m^{-3}]	0.62	25.14	22.72	12.72	93	24.33	22.45	12.77	102
	calcium (Ca^+)		[ng m^{-3}]	3.53	362.51	312.20	201.63	93	256.30	222.58	136.51	102
metals	**aluminum (Al)**		[µg m^{-3}]	0.003	1.681	1.582	0.928	93	1.133	1.035	0.563	101

	calcium (Ca)	inductively coupled plasma atomic emission spectrometry (ICP-AES)	[µg m^{-3}]	0.001	0.428	0.386	0.218	93	0.350	0.328	0.181	101
	potassium (K)		[µg m^{-3}]	0.001	0.529	0.527	0.287	93	0.394	0.361	0.196	101
	sodium (Na)		[µg m^{-3}]	0.001	0.137	0.135	0.078	93	0.110	0.106	0.060	101
	magnesium (Mg)		[µg m^{-3}]	0.001	0.160	0.156	0.083	93	0.125	0.125	0.059	101
	iron (Fe)		[µg m^{-3}]	0.001	0.932	0.900	0.501	93	0.669	0.590	0.357	101
	lithium (Li)	inductively coupled plasma mass spectrometry (ICP-MS) (Xavier Querol et al., 2001)	[ng m^{-3}]	0.05	1.60	1.42	0.96	93	1.04	0.92	0.57	101
	beryllium (Be)		[ng m^{-3}]	0.05	0.10	0.10	0.02	49	0.08	0.08	0.02	27
	phosphor (P)		[ng m^{-3}]	0.05	37.08	34.43	17.91	93	25.48	22.66	11.94	101
	scandium (Sc)		[ng m^{-3}]	0.05	0.24	0.21	0.13	35	0.20	0.20	0.09	25
	titanium (Ti)		[ng m^{-3}]	0.05	80.15	74.41	44.71	93	55.83	50.55	27.76	101
	vanadium (V)		[ng m^{-3}]	0.05	2.04	2.01	1.08	88	1.54	1.49	0.73	97
	chromium (Cr)		[ng m^{-3}]	0.05	2.66	1.84	4.52	78	2.36	2.02	1.45	97
	manganese (Mn)		[ng m^{-3}]	0.05	16.48	15.75	8.71	93	12.69	11.90	6.19	101
	cobalt (Co)		[ng m^{-3}]	0.05	0.36	0.32	0.18	91	0.24	0.22	0.11	99
	nickel (Ni)		[ng m^{-3}]	0.05	1.18	0.96	1.29	83	1.12	0.86	0.84	99
	cupper (Cu)		[ng m^{-3}]	0.05	2.89	2.51	1.89	90	4.25	3.91	2.52	101
	zinc (Zn)		[ng m^{-3}]	0.05	12.72	12.63	5.51	93	11.68	11.24	5.47	100
	gallium (Ga)		[ng m^{-3}]	0.05	0.40	0.39	0.23	90	0.29	0.26	0.15	101
	germanium (Ge)		[ng m^{-3}]	0.05	0.11	0.11	0.04	21	0.13	0.11	0.07	8
	arsenic (As)		[ng m^{-3}]	0.05	1.81	1.53	1.07	93	1.03	0.98	0.46	101
	selenium (Se)		[ng m^{-3}]	0.05	0.09	0.10	0.02	16	0.10	0.09	0.03	17
	rubidium (Rb)		[ng m^{-3}]	0.05	3.12	2.88	1.76	93	2.11	1.88	1.10	101
	strontium (Sr)		[ng m^{-3}]	0.05	3.45	3.36	1.90	93	2.64	2.42	1.33	101
	yttrium (Y)		[ng m^{-3}]	0.05	0.43	0.42	0.23	83	0.37	0.31	0.26	85
	zirconium (Zr)		[ng m^{-3}]	0.40	7.49	7.63	1.88	93	6.25	5.99	1.86	100
	niobium (Nb)		[ng m^{-3}]	0.05	0.30	0.29	0.13	93	0.23	0.23	0.09	101
	molibdene (Mo)		[ng m^{-3}]	0.05	1.21	1.09	0.74	49	1.39	1.00	1.13	29

	cadmium (Cd)		[ng m^{-3}]	0.05	0.14	0.13	0.06	90	0.09	0.08	0.02	57
	tin (Sn)		[ng m^{-3}]	0.05	0.58	0.44	0.43	92	0.40	0.36	0.22	101
	antimony (Sb)		[ng m^{-3}]	0.05	1.05	0.80	0.83	91	0.95	0.78	0.67	101
	cesium (Cs)		[ng m^{-3}]	0.05	0.34	0.29	0.19	90	0.22	0.21	0.12	97
	barium (Ba)		[ng m^{-3}]	0.05	14.60	14.48	7.24	90	15.64	15.58	7.46	101
	lanthanum (La)		[ng m^{-3}]	0.05	0.82	0.81	0.42	92	0.58	0.54	0.27	101
	cerium (Ce)		[ng m^{-3}]	0.05	1.65	1.62	0.90	93	1.22	1.16	0.67	101
	praseodymium (Pr)		[ng m^{-3}]	0.05	0.20	0.20	0.10	86	0.17	0.17	0.06	94
	neodymium (Nd)		[ng m^{-3}]	0.05	0.75	0.73	0.41	92	0.52	0.49	0.25	101
	samarium (Sm)		[ng m^{-3}]	0.05	0.15	0.15	0.07	79	0.11	0.12	0.04	73
	europium (Eu)		[ng m^{-3}]	0.05	0.07	0.07	0.01	26	0.07	0.07		1
	gadolinium (Gd)		[ng m^{-3}]	0.05	0.14	0.14	0.06	73	0.11	0.10	0.05	73
	terbium (Tb)		[ng m^{-3}]	0.05	0.07	0.07	0.01	46	0.07	0.07	0.01	18
	dysprosium (Dy)		[ng m^{-3}]	0.05	0.12	0.11	0.04	61	0.10	0.08	0.05	59
	holmium (Ho)		[ng m^{-3}]	0.05	0.07	0.07	0.01	47	0.07	0.07	0.00	6
	erbium (Er)		[ng m^{-3}]	0.05	0.07	0.07	0.01	35	0.07	0.07	0.01	34
	thulium (Tm)		[ng m^{-3}]	0.05				0				0
	ytterbium (Yb)		[ng m^{-3}]	0.05	0.07	0.07	0.01	34	0.07	0.07	0.02	57
	lutetium (Lu)		[ng m^{-3}]	0.05				0				0
	hafnium (Hf)		[ng m^{-3}]	0.40	0.40	0.40		1	0.42	0.41	0.01	9
	tantalum (Ta)		[ng m^{-3}]	0.05				0				0
	tungsten (W)		[ng m^{-3}]	0.05	0.24	0.16	0.23	84	0.20	0.13	0.15	81
	thallium (Tl)		[ng m^{-3}]	0.05	0.07	0.07	0.01	2				0
	lead (Pb)		[ng m^{-3}]	0.05	2.87	2.52	1.61	93	2.05	1.84	1.17	100
	bismuth (Bi)		[ng m^{-3}]	0.05	0.26	0.12	0.46	29	0.19	0.12	0.19	19
	thorium (Th)		[ng m^{-3}]	0.05	0.40	0.34	0.28	89	0.26	0.22	0.18	97
	uranium (U)		[ng m^{-3}]	0.05	0.09	0.09	0.03	48	0.10	0.08	0.06	36

polyaromatic hydrocarbons (PAH)	**phenanthrene (Phe)**	high performance liquid chromatography (HPLC- Fluo) (Besombes et al., 2001)	[ng m^{-3}]	0.008	0.036	0.032	0.021	88	0.045	0.040	0.025	100
	anthracene (An)		[ng m^{-3}]	0.001	0.004	0.003	0.002	90	0.005	0.004	0.003	99
	fluoranthene (Fla)		[ng m^{-3}]	0.002	0.102	0.069	0.097	90	0.083	0.052	0.086	102
	pyrene (Pyr)		[ng m^{-3}]	0.003	0.123	0.082	0.119	91	0.105	0.070	0.107	102
	triphenylene (Tri)		[ng m^{-3}]	0.002	0.080	0.063	0.070	91	0.052	0.036	0.052	101
	retene (Ret)		[ng m^{-3}]	0.000	0.103	0.039	0.152	87	0.045	0.019	0.054	91
	benzo(a)anthracene (BaA)		[ng m^{-3}]	0.008	0.196	0.132	0.171	90	0.147	0.092	0.152	97
	chrysene (Chr)		[ng m^{-3}]	0.004	0.235	0.200	0.182	91	0.165	0.115	0.165	102
	benzo(e)pyrene (BeP)		[ng m^{-3}]	0.005	0.273	0.215	0.282	91	0.228	0.170	0.235	102
	benzo(b)fluoranthene (BbF)		[ng m^{-3}]	0.005	0.250	0.221	0.164	90	0.202	0.165	0.162	102
	benzo(k)fluoranthene (BkF)		[ng m^{-3}]	0.002	0.104	0.096	0.070	90	0.081	0.063	0.067	100
	benzo(a)pyrene (BaP)		[ng m^{-3}]	0.002	0.122	0.094	0.108	90	0.124	0.085	0.116	101
	benzo(g,h,i)perylene (BghiP)		[ng m^{-3}]	0.008	0.410	0.387	0.228	90	0.404	0.351	0.291	101
	dibenzo(a,h)anthracene (DBahA)		[ng m^{-3}]	0.000	0.010	0.006	0.010	88	0.008	0.005	0.009	101
	indeno(1,2,3-cd)pyrene (IP)		[ng m^{-3}]	0.005	0.218	0.214	0.136	91	0.196	0.155	0.144	102
	coronene (Cor)		[ng m^{-3}]	0.002	0.251	0.237	0.143	91	0.268	0.216	0.190	100
alkanes	**C11**	gas chromatography–mass spectrometry (GS-MS) (Golly, 2014)	[ng m^{-3}]	0.070	0.698	0.712	0.358	16	0.559	0.455	0.431	20
	C12		[ng m^{-3}]	0.170	0.254	0.254	0.052	4	1.588	0.865	1.846	3
	C13		[ng m^{-3}]	0.115	0.217	0.184	0.095	19	0.284	0.231	0.244	14
	C14		[ng m^{-3}]	0.070	0.126	0.107	0.036	7	0.121	0.108	0.024	3
	C15		[ng m^{-3}]	0.070	0.381	0.103	0.686	6	0.253	0.124	0.385	12
	C16		[ng m^{-3}]	0.115	0.194	0.170	0.049	3	0.224	0.176	0.119	6
	C17		[ng m^{-3}]	0.138	0.228	0.219	0.061	33	0.236	0.229	0.058	20
	C18		[ng m^{-3}]	0.128	0.279	0.273	0.117	47	0.292	0.273	0.198	39
	C19		[ng m^{-3}]	0.109	0.571	0.548	0.404	62	0.449	0.376	0.271	55
	C20		[ng m^{-3}]	0.110	1.302	1.093	1.106	71	0.908	0.718	0.783	74
	C21		[ng m^{-3}]	0.339	2.375	1.691	2.056	75	1.674	0.923	1.611	93

	C22		[ng m^{-3}]	0.186	3.118	2.595	2.762	87	2.060	1.128	2.139	101
	C23		[ng m^{-3}]	0.314	3.149	2.634	2.552	86	2.482	1.398	2.443	100
	C24		[ng m^{-3}]	0.231	2.760	2.240	2.157	89	2.278	1.414	2.168	100
	C25		[ng m^{-3}]	0.598	2.849	2.265	1.889	83	2.500	1.692	1.991	97
	C26		[ng m^{-3}]	0.175	2.229	1.917	1.394	90	2.091	1.479	1.627	101
	C27		[ng m^{-3}]	0.580	2.678	2.148	1.847	84	2.714	1.982	2.255	100
	C28		[ng m^{-3}]	0.292	1.719	1.555	1.049	88	1.725	1.251	1.320	100
	C29		[ng m^{-3}]	0.841	2.891	2.306	2.015	83	2.920	1.861	3.077	93
	C30		[ng m^{-3}]	0.288	1.254	1.048	0.810	86	1.205	0.846	0.967	95
	C31		[ng m^{-3}]	0.570	2.348	1.647	1.785	82	2.300	1.429	2.464	83
	C32		[ng m^{-3}]	0.070	0.807	0.652	0.584	84	0.747	0.540	0.669	97
	C33		[ng m^{-3}]	0.070	0.755	0.658	0.538	84	0.825	0.577	0.830	89
	C34		[ng m^{-3}]	0.070	0.564	0.429	0.423	73	0.480	0.359	0.392	82
	C35		[ng m^{-3}]	0.070	0.629	0.429	0.556	68	0.484	0.293	0.474	77
	C36		[ng m^{-3}]	0.070	0.381	0.249	0.358	53	0.357	0.271	0.321	52
	C37		[ng m^{-3}]	0.070	0.394	0.255	0.468	36	0.198	0.166	0.151	24
	C38		[ng m^{-3}]	0.070	0.281	0.187	0.258	15	0.175	0.128	0.126	18
	C39		[ng m^{-3}]	0.070	0.351	0.224	0.362	17	0.164	0.114	0.122	24
	C40		[ng m^{-3}]	0.070	0.319	0.259	0.231	12	0.106	0.100	0.025	9
	Pristane		[ng m^{-3}]	0.070	0.189	0.147	0.164	25	0.258	0.163	0.204	24
	Phytane		[ng m^{-3}]	0.070	0.180	0.161	0.082	23	0.196	0.150	0.139	36
Methyl PAH	**2-methyl-naphthalene**		[ng m^{-3}]	0.019				0				0
	1-methyl-fluorene		[ng m^{-3}]	0.007				0	0.040	0.011	0.051	3
	3-methyl-phenanthrene		[ng m^{-3}]	0.025				0	0.125	0.125	0.141	2
	2-methyl-phenanthrene		[ng m^{-3}]	0.014				0	0.018	0.017	0.005	7
	2-methyl-anthracene		[ng m^{-3}]	0.014				0	0.041	0.041	0.035	2
	4/9-methyl-phenanthrene		[ng m^{-3}]	0.014				0	0.040	0.040		1

	1-methyl-phenanthrene		[ng m^{-3}]	0.007	0.010	0.010		1	0.022	0.013	0.029	9
	4-methyl-pyrene		[ng m^{-3}]	0.007	0.019	0.015	0.012	25	0.022	0.015	0.015	32
	1-methyl-pyrene		[ng m^{-3}]	0.007	0.024	0.017	0.016	27	0.025	0.017	0.018	37
	1+3-Methyl-fluorene		[ng m^{-3}]	0.007	0.016	0.015	0.005	13	0.017	0.014	0.006	14
	Methyl-fluorene/pyrene		[ng m^{-3}]	0.007	0.015	0.011	0.008	20	0.016	0.016	0.007	21
	1-methylfluoranthene		[ng m^{-3}]	0.007	0.017	0.015	0.009	21	0.020	0.014	0.013	26
	3-methyl-chrysene		[ng m^{-3}]	0.008	0.034	0.031	0.022	32	0.039	0.026	0.037	54
	Methyl-chrysene/BenzoAnthracene		[ng m^{-3}]	0.007	0.016	0.014	0.008	28	0.022	0.016	0.016	39
thiophens	**DBT (DiBenzoThiophen)**		[ng m^{-3}]	0.007	0.011	0.011	0.003	4	0.024	0.013	0.022	7
	PheT(4,5) (Phenanthro(4,5 bcd)Thiophen)		[ng m^{-3}]	0.007	0.012	0.011	0.004	4	0.016	0.011	0.016	16
	BNT(2,1) (Benzo(b)Naphto(2,1 d)Thiophen)		[ng m^{-3}]	0.027	0.027	0.027	0.006	7	0.040	0.039	0.020	14
	BNT(1,2) (Benzo(b)Naphto(1,2 d)Thiophen)		[ng m^{-3}]	0.007	0.009	0.010	0.001	3	0.016	0.010	0.009	9
	BNT(2,3) (Benzo(b)Naphto(2,3 d)Thiophen)		[ng m^{-3}]	0.007	0.010	0.010	0.002	12	0.017	0.015	0.009	12
	DNT(2,1) (Dinaphto (2,1) Thiophen)		[ng m^{-3}]	0.007	0.014	0.011	0.008	3	0.014	0.012	0.006	3
	BPT(2,1) (Benzo(b)Phenanto(2,1d)thiophen)		[ng m^{-3}]	0.007				0				0
hopanes	**HP1 (Trisnorneohopane)**		[ng m^{-3}]	0.012	0.060	0.041	0.048	46	0.074	0.049	0.065	64
	HP2 (17α(H)-Trisnorhopane)		[ng m^{-3}]	0.013	0.047	0.038	0.031	54	0.056	0.039	0.044	94
	HP3 (17α(H)-21β(H)-Norhopane)		[ng m^{-3}]	0.007	0.143	0.097	0.122	87	0.215	0.147	0.183	99
	HP4 (17α(H)-21β(H)-Hopane)		[ng m^{-3}]	0.011	0.179	0.119	0.150	83	0.255	0.168	0.212	99
	HP5 (17α(H)-21β(H)-22S-Homohopane)		[ng m^{-3}]	0.007	0.077	0.050	0.064	77	0.109	0.069	0.093	98
	HP6 (17α(H)-21β(H)-22R-Homohopane)		[ng m^{-3}]	0.007	0.059	0.035	0.053	72	0.081	0.050	0.074	99
	HP7 (17α(H)-21β(H)-22S-Bishomohopane)		[ng m^{-3}]	0.007	0.057	0.036	0.053	73	0.077	0.043	0.072	100
	HP8 (17α(H)-21β(H)-22R-Bishomohopane)		[ng m^{-3}]	0.007	0.042	0.026	0.034	66	0.058	0.037	0.051	94
	HP9 (17α(H)-21β(H)-22S-Trishomohopane)		[ng m^{-3}]	0.007	0.044	0.023	0.043	68	0.057	0.031	0.055	89
	HP10 (17α(H)-21β(H)-22R-Trishomohopane)		[ng m^{-3}]	0.007	0.038	0.024	0.028	57	0.043	0.024	0.039	77
	DMPT (6,10,14-trimethyl-2-pentadecanone)		[ng m^{-3}]	0.055	0.749	0.524	0.637	89	0.984	0.631	1.345	102

methoxyphenols	**Vanillin**		[ng m^{-3}]	0.017	0.199	0.162	0.119	22	0.172	0.144	0.101	22
	Acetovanillone		[ng m^{-3}]	0.055	0.280	0.236	0.169	27	0.272	0.095	0.520	16
	Guaiacyl acetone		[ng m^{-3}]	0.057	0.239	0.226	0.117	15	0.161	0.143	0.086	14
	Coniferylaldehyde		[ng m^{-3}]	0.056	0.260	0.224	0.137	4	0.352	0.281	0.199	4
	Vanillic acid		[ng m^{-3}]	0.018	0.577	0.423	0.449	46	0.713	0.533	0.723	40
	Homovanillic acid		[ng m^{-3}]	0.014	0.218	0.175	0.079	3	0.087	0.087	0.034	2
	Syringol		[ng m^{-3}]	0.006				0	0.066	0.066		1
	4-methylsyringol		[ng m^{-3}]	0.006				0	0.032	0.032		1
	4-propenylsyringol		[ng m^{-3}]	0.028				0	0.093	0.093		1
	Acetosyringone		[ng m^{-3}]	0.028	0.398	0.353	0.227	33	0.420	0.409	0.220	31
	Syringyl acetone		[ng m^{-3}]	0.017	0.181	0.181		1	0.089	0.089		1
	Sinapyl aldehyde		[ng m^{-3}]	0.056	0.160	0.160		1	0.348	0.348	0.204	2
	Syringic acid		[ng m^{-3}]	0.018	0.322	0.283	0.182	34	0.442	0.331	0.328	33
sterols	**Cholesterol**		[ng m^{-3}]	0.056	2.300	1.926	1.412	11	1.534	1.413	0.858	22
methyl-nitricatechols	**3methylcatechol**		[ng m^{-3}]	0.070				0	0.133	0.133		1
	4-methylcatechol		[ng m^{-3}]	0.084				0				0
	4nitroguaiacol		[ng m^{-3}]	0.300	0.414	0.414		1				0
	4nitrocatechol		[ng m^{-3}]	0.140	1.001	0.806	0.601	14	1.602	1.458	1.130	22
	3-methyl-6-nitrocatechol		[ng m^{-3}]	0.124				0				0
	4-methyl-5-nitrocatechol		[ng m^{-3}]	0.140	0.236	0.248	0.022	3	0.381	0.334	0.165	12
	3-methyl-5-nitrocatechol		[ng m^{-3}]	0.070	0.355	0.292	0.122	3	0.523	0.581	0.245	13
	3methyl4nitrocatechol		[ng m^{-3}]	0.124	0.195	0.195		1	0.925	0.281	1.096	7

Table S3. Species analyzed from fuel samples collected at La Paz and El Alto

	Sample#	***Al***	***Cr***	***Mn***	***Fe***	***Co***	***Ni***	***Cu***	***Zn***	***As***	***Ag***	***Cd***	***Pb***
		mg/l	mg/l	mg/l	mg/l	mg/l	mg/l	mg/l	mg/l	mg/l	mg/l	mg/l	mg/l
gasoline	1	1374	396	6299	281	4.58	23.1	0	84.8	400	12.3	0.15	9.6
gasoline	2	823	384	6732	0	2.50	10.1	0	168	347	9.349	0.29	9.9
gasoline	3	854	351	6166	0	2.83	7.0	0	171	307	1.215	0.43	9.7
diesel	4	1491	982	66.2	0	2.02	13.0	0	785	400	1.465	0.50	25.2
diesel	5	1581	881	41.4	0	2.33	13.5	0	655	374	0.464	0.72	26.5
diesel	6	3497	1018	91.0	1162	2.23	11.5	0	749	436	0.624	1.10	28.4

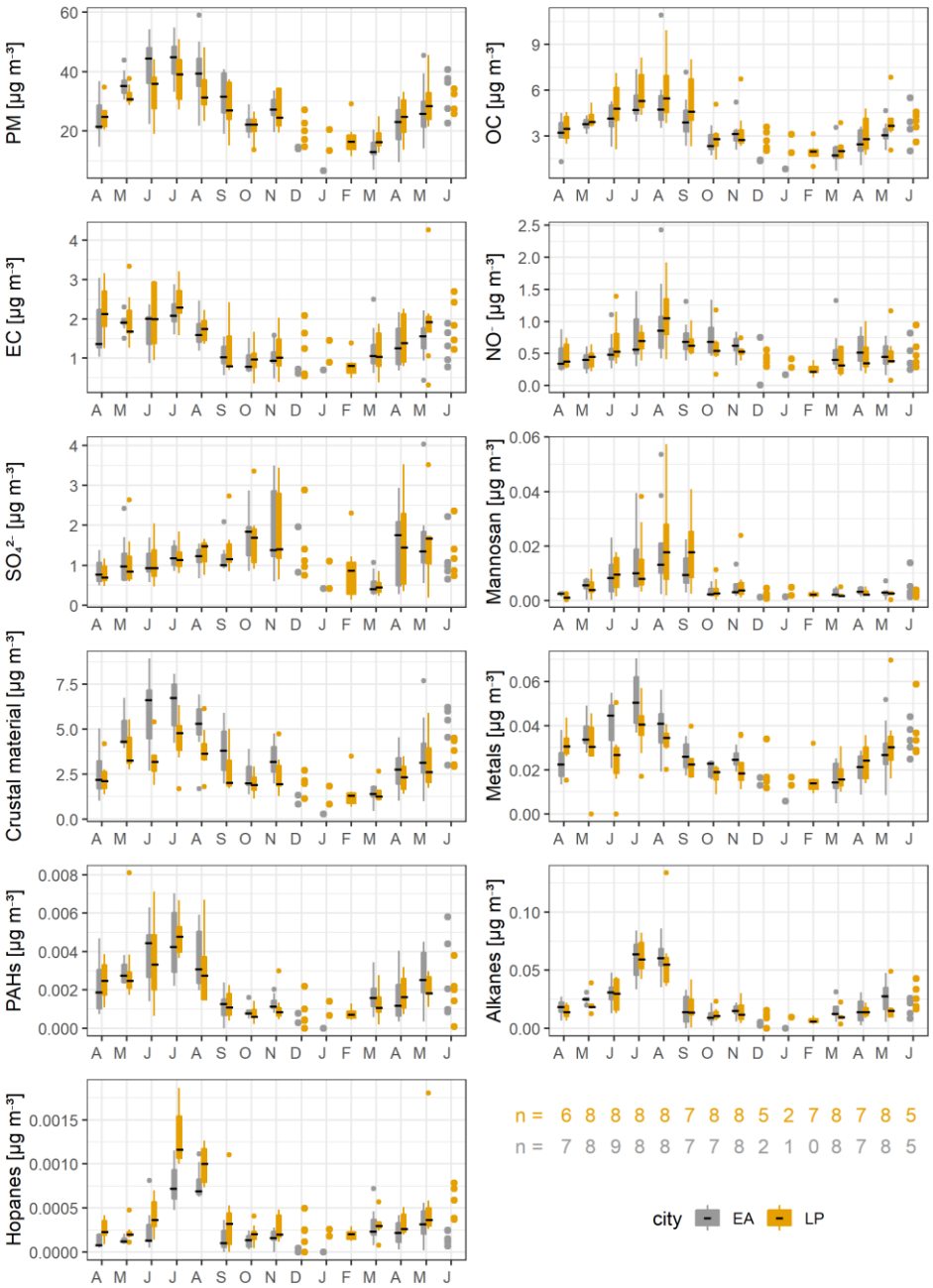

Figure S3. Monthly variation of major contributor species to PM10, crustal material comprises: Al, Fe, Ti, Ca, Mg, K, Mn, P; metals comprises: Co, Ni, Cu, Zn, As, Rb, Sr, Cd, Sn, Sb, Pb; PAHs is the sum of: Phe, An, Fla, Pyr, Tri, Ret, BaA, Chr, BeP, BbF, BkF, BaP, BghiP, DBahA, IP, Cor; alkanes are the sum of C20-C31, hopanes the sum of HP3 and HP4; and n is the number of filters collected in the corresponding month at each site.

Figure S4. Chemical profile of single-site sources of PM10

El Alto

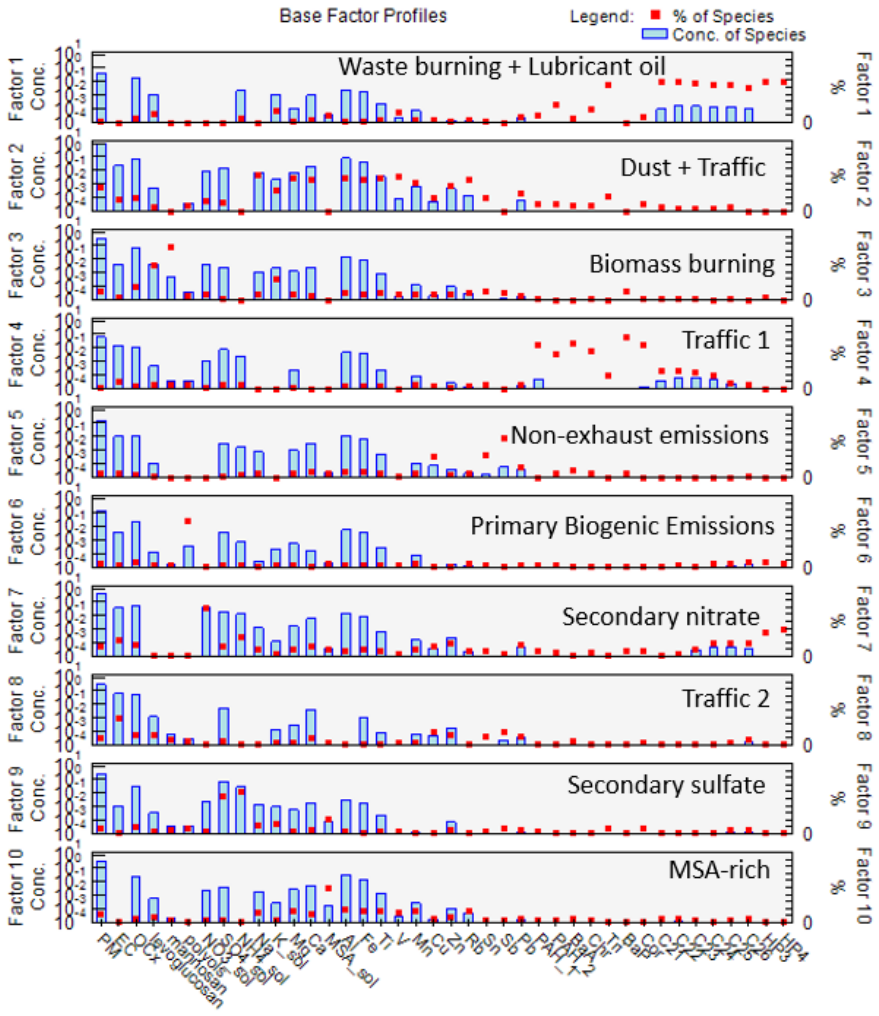

La Paz

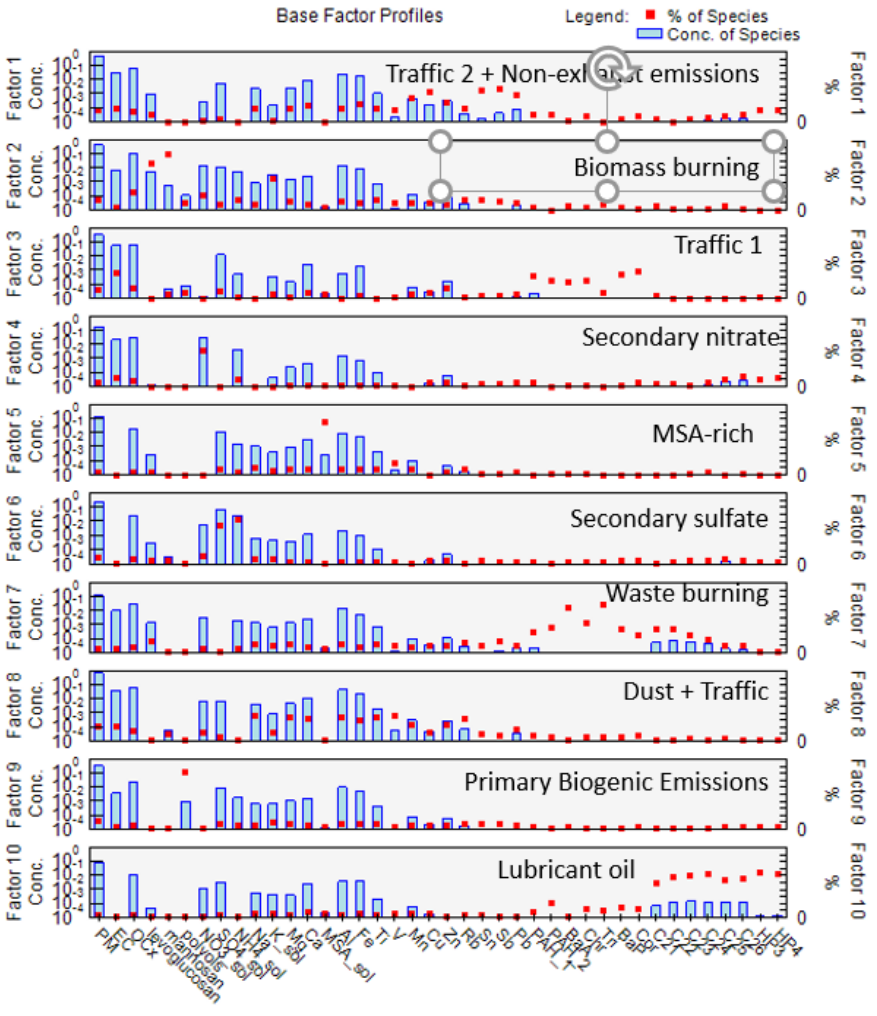

Figure S5. Percentage contribution of sources to total ambient PM (single site approach)

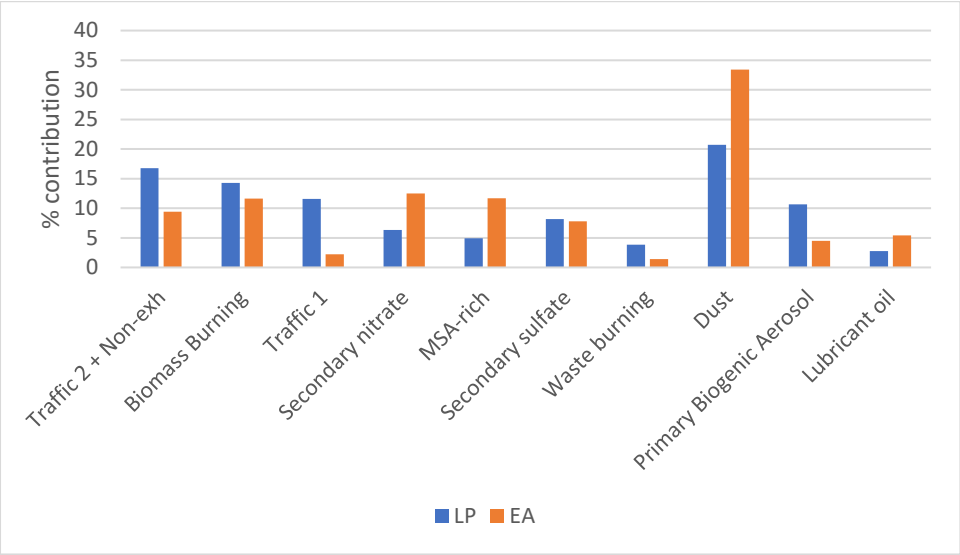

Table S4. Bootstrap mapping of single site solution El Alto

	Waste burning + Lubricant oil	Dust	Biomass burning	Traffic 1	Non-exhaust emissions	Primary Biogenic Aerosols	Secondary nitrate	Traffic 2	Secondary sulfate	MSA-rich	Unmapped
Boot Factor 1	98	0	0	2	0	0	0	0	0	0	0
Boot Factor 2	0	100	0	0	0	0	0	0	0	0	0
Boot Factor 3	0	0	100	0	0	0	0	0	0	0	0
Boot Factor 4	5	0	0	95	0	0	0	0	0	0	0
Boot Factor 5	0	0	0	0	98	1	0	0	1	0	0
Boot Factor 6	2	0	0	0	0	98	0	0	0	0	0
Boot Factor 7	0	0	0	0	0	0	100	0	0	0	0
Boot Factor 8	20	3	0	8	2	0	5	61	1	0	0
Boot Factor 9	0	0	0	0	0	0	0	0	100	0	0
Boot Factor 10	0	0	0	0	0	0	0	0	0	100	0

Table S5. Bootstrap mapping of single site solution La Paz

	Traffic 2 + Non-exhaust	Biomass Burning	Traffic 1	Secondary nitrate	MSA-rich	Secondary sulfate	Waste burning	Dust	Primary Biogenic Aerosols	Lubricant oil	Unmapped
Boot Factor 1	84	1	3	1	1	0	4	3	0	3	0
Boot Factor 2	0	100	0	0	0	0	0	0	0	0	0
Boot Factor 3	11	0	80	0	0	1	5	1	0	2	0
Boot Factor 4	0	0	0	99	0	0	0	0	0	1	0
Boot Factor 5	0	0	0	0	100	0	0	0	0	0	0
Boot Factor 6	0	0	0	0	0	100	0	0	0	0	0
Boot Factor 7	2	0	2	0	0	0	94	1	0	1	0
Boot Factor 8	0	0	0	0	0	0	1	98	0	1	0
Boot Factor 9	0	0	0	0	0	0	0	0	100	0	0
Boot Factor 10	3	0	1	0	0	0	3	1	0	92	0

Table S6. Spearman correlations between chloride and each of the resolved sources of PM. Strongest correlations are found between Cl- and Waste burning, secondly with TR1 and Non-exhaust.

		Waste burning	Sec. sulfate	TR1	MSA-rich	Lubricant	BB	Dust	Sec. Nitrate	Non-Exhaust	PBA	TR2
Spearman	Cl- EA	0.75	-0.22	0.57	0.34	0.28	0.47	0.59	-0.24	0.67	-0.19	0.25
	Cl- LP	0.67	0.01	0.61	0.39	0.49	0.53	0.45	0.19	0.57	-0.25	0.44

Test of Similarity of Chemical Profiles

In source apportionment studies, factors are labeled according to their chemical profile and its similarity to what was previously reported in the literature. Although the source identification is based on the specific tracers of the different sources, the exact chemical profile of sources with the same name could vary from site to site. Thus, a metric to quantitively evaluate the similarity

between two factors was proposed by Belis et al. 2015 and Pernigotti & Belis, 2018. Two parameters are considered to establish given similarity: the Pearson distance (PD) and the similarity Identity distance (SID), defined as follows:

$$PD = 1 - r^2 \quad [S1]$$

$$SID = \frac{\sqrt{2}}{m} \sum_{j=1}^{m} \frac{|x_j - y_j|}{x_j + y_j} \quad [S2]$$

Where m is the number of common species existing between the two compared profiles and, x and y are the relative mass of the specie j in each factor profile. According to Pernigotti & Belis, 2018, PD < 0.4 and SID < 1 are considered as acceptable criteria for profile similarity.

This method was used to evaluate the similarity of the resolved factors in La Paz-El Alto with what was found in France by Borlaza et al., 2021a and Weber et al., 2019 (Figure S6). From the 11 resolved sources, only 8 were comparable with was obtained from the French-sites source apportionment, out of which 4 resulted to be significantly similar to what was observed in France: primary biogenic aerosols, biomass burning, secondary sulfate and traffic 2. Although waste burning was not among the identified sources in France, this factor was compared to the industrial emissions observed in France. The disparities between the remaining factors (dust, secondary nitrate, MSA-rich and traffic 1) was largest in the PD parameter, which is highly sensitive to variation in the major mass fractions of the PM, and will be discussed below.

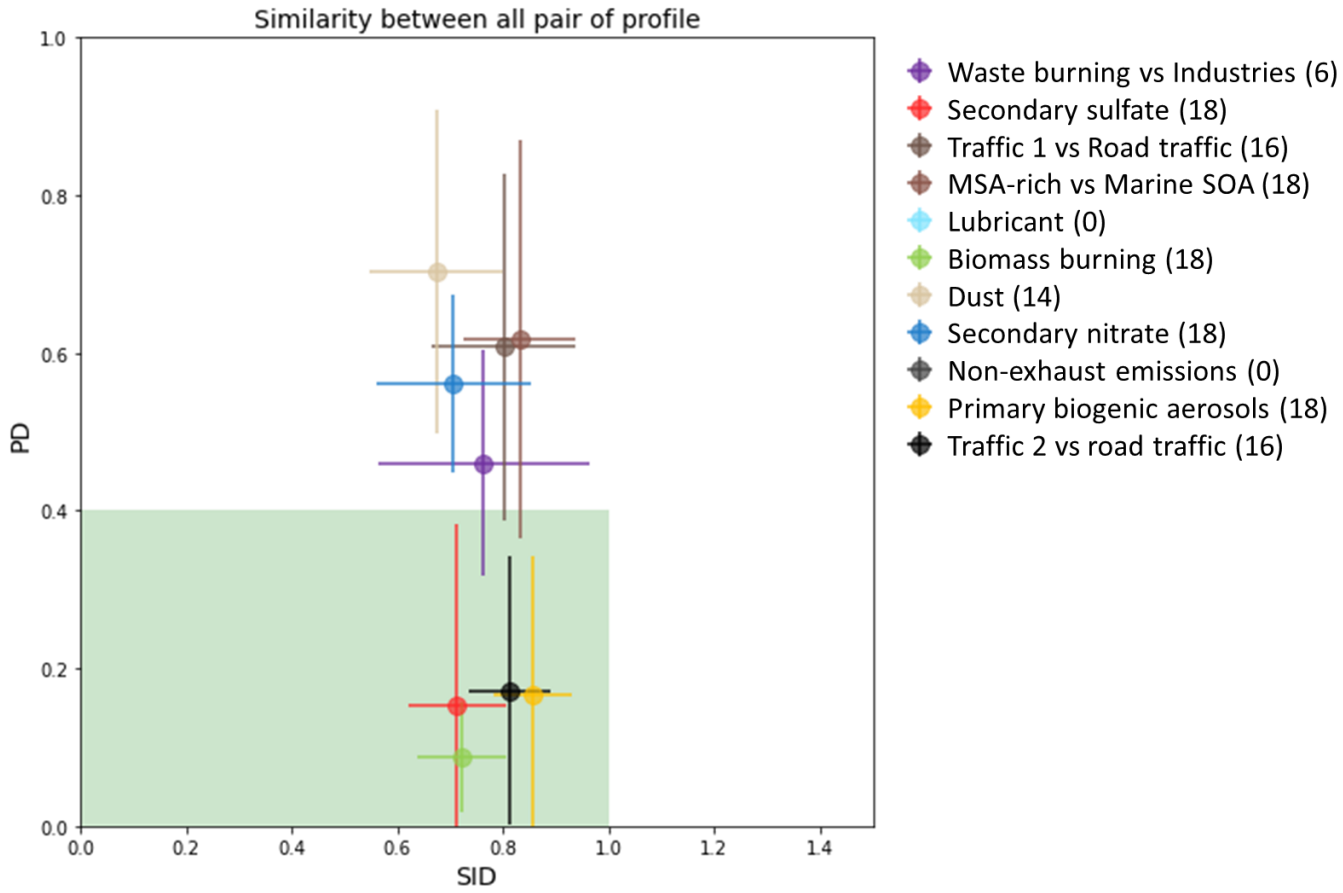

Figure S6. Similarity plot of the sources of PM10 in La Paz-El Alto and the sources identified by Borlaza et al. 2021a and Weber et al. 2019, by pairs, of profiles belonging to the same factor/source category. The mean ± standard deviation (sd) for each source category are plotted (circles correspond to the mean and lines to the sd on both axis). The green box highlights the acceptable area for profile similarity according to Pernigotti & Belis, 2018.

It was observed that the largest difference between the dust profiles, was the relative abundance of EC, OC, sulfate and nitrate assigned to the factors. The abundance of such species in the dust profiles in France was considerably higher compared to La Paz. In contrast, the relative concentrations of Al and Fe were generally higher for LP-EA. This shows that not only the composition of dust but the aging of the air masses carrying it are different. Similarly, for secondary nitrate, the OC and EC relative concentrations found in the secondary nitrate factor in LP-EA was generally higher than in France. This is likely because the main source of secondary-nitrate precursors in LP-EA are vehicular gaseous emissions and since the process through which secondary nitrate is formed is a relatively fast chemical process, the PMF was not able to fully separate both factors. On the other hand, nitrate relative concentrations were 2 to 4 times higher than what was observed

in LP_EA. The largest difference observed in the MSA-rich chemical profiles, that led to high PD values, were the relative abundances of OC, sulfate, Al and Fe. Specifically, OC and sulfate where repeatedly higher in France, which gives an idea of the aging processes that secondary marine organic aerosols undergo. In contrast, in LP-EA, Al and Fe relative masses were significantly higher than in France. This is likely due to the mixing that takes place during the transport of this secondary aerosols across the Altiplano until reaching the metropolis. Traffic 1 had noticeably higher concentrations of Al and Fe in LP-EA but lower OC, sulfates and nitrates. In contrast, high OC relative concentrations in traffic 2, primary biogenic emissions, secondary sulfate and biomass burning, in both LP-EA and France pull the PD towards lower values.

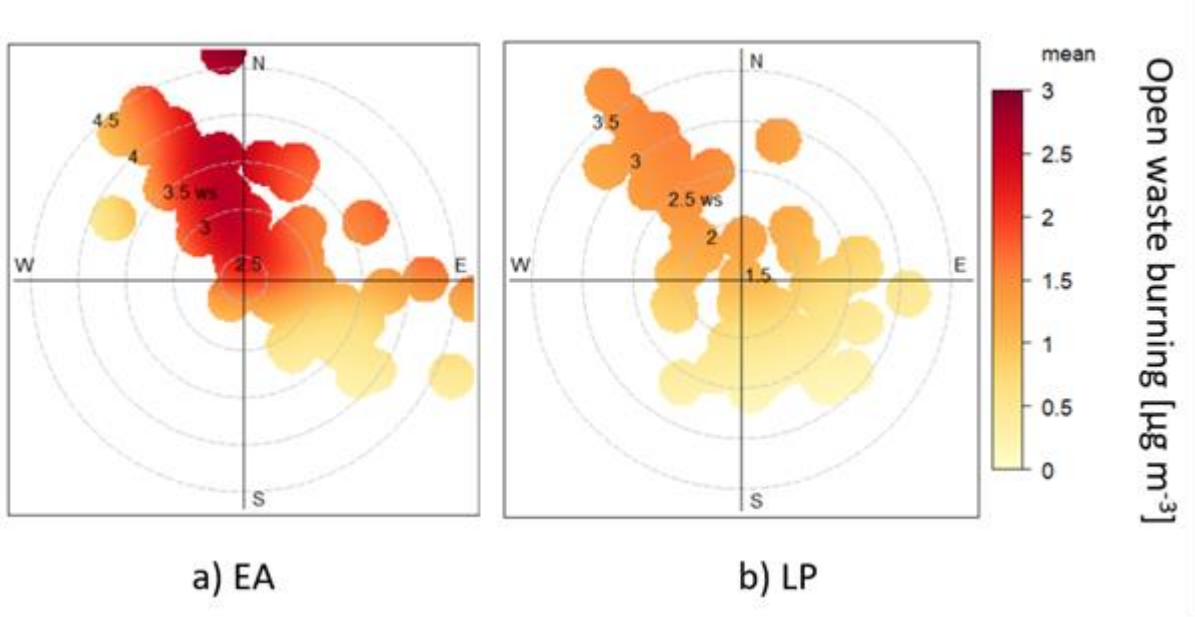

Figure S7. Polar plot showing the mean concentrations attributed to open waste burning and the associated wind speed (m s-1) and wind direction.

ANNEX II: Ground-level O_3 concentrations

As mentioned in the Conclusions section, the gaseous component of atmospheric pollution was not included in the measurements campaign. However, it plays a very important role in air pollution and remains to be studied in the analysis of air quality in La Paz and El Alto. During my thesis, I had the opportunity to collaborate with the Laboratory for Atmospheric Physics (LFA) on the installation and maintenance of the two ozone (O_3) analyzers (Thermo Scientific Fisher Model 49i) at the La Paz (LP) and El Alto (EA) stations, as well as with the quality control of the data. Preliminary results of the first data exploration of the continuous O_3 measurements taken post-campaign will be presented in this section. The importance of monitoring this gaseous compound lies in both the health threat it represents for public health, as well as the role it plays as a greenhouse gas.

As mentioned in Chapter 2, the O_3 analyzers were implemented at the sampling sites in May 2021 and continue to operate until present. It is worth mentioning that these measurements still need to be validated by calibration controls, which so far could not be performed. However, at the beginning of the campaign an inter-comparison phase was performed with a recently calibrated O_3 analyzer that had just gotten back from an international calibration center, and that measures continuously at the Chacaltaya station. In addition, the drift of the zero value in the measurements is monitored every two weeks. No drift has been observed so far. Therefore, it is considered that the measurements under the conditions presented below are valid for a first exploratory analysis of the volume mixing ratio of O_3 in the three sampling sites.

The first thing to note is that the average O_3 volume mixing ratio at the urban sampling sites is lower than expected, considering that traffic is the dominant source of pollution and that they are located in a region that receives high doses of ultraviolet radiation due to its geographic location (Table 1). It can also be observed that while the dispersion around the mean in CHC-GAW is very low, the values fairly vary in the urban regions. Having higher volume mixing ratios in regional background conditions than in urban areas is consistent with what is reported in the literature (Guerreiro et al., 2014; Paoletti et al., 2014; Sicard et al., 2013, 2016). No significant difference is observed between the O_3 levels recorded in the cities of La Paz and El Alto.

Table 1. Mean, median and standard deviation of the volume mixing ratios of O_3 at the three sampling sites.

SITE	MEAN [PPB]	MEDIAN [PPB]	SD [PPB]
CHC-GAW	32.4	32.4	6.35
EA	23.4	22.9	15.9
LP	22.1	21.3	14.6

Figure 1 (left panel) shows the summary of the diurnal and monthly variability of the ozone volume mixing ratio at the La Paz (LP) and El Alto (EA) sampling sites between May 2021 and November 2022 (with a temporal resolution of 1 minute), and at the Chacaltaya (CHC-GAW) sampling station during the year 2022 (with an hourly temporal resolution). While there is almost no diurnal variation at the regional monitoring station, a stable maximum is observed around noon in the metropolitan area, which corresponds to the diurnal ozone production driven by solar radiation (Ahrens & Henson, 2016; Seinfeld & Pandis, 2016). Slightly higher mixing

ratios are observed in EA with a wider maximum mode than in La Paz. It can also be observed that during the early morning, in the city of El Alto, a smaller peak of ozone production takes place around 3 am, and that concentrations in both cities decrease rapidly towards minimum levels around 6 am. These early morning phenomena remains to be explained.

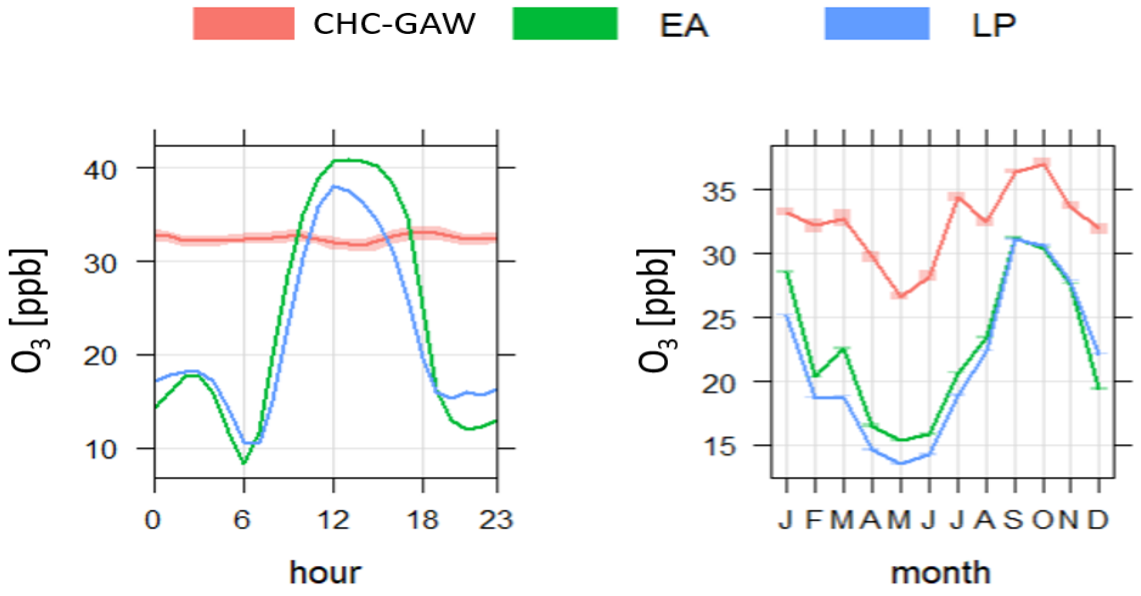

Figure S1. Diurnal (left panel) and monthly (right panel) variation of O3 levels in the urban areas of La Paz (LP) and El Alto (1-min time resolution, May, 2021 to Nov, 2022) and the regional background station in Mount Chacaltaya (CHC-GAW) (1-h time resolution).

Figure S1 (right panel) shows how the mixing ratios of O_3 vary considerably throughout the year. The lowest values are observed between the months of April and June, and comprise the wet-to-dry transition period together with the beginning of the dry season, which coincides with the beginning of the austral winter. During the winter, the lowest yearly solar radiation doses are observed, where clear-sky days can be expected for the most part. This is consistent with the minimum O_3 levels observed. In contrast, the annual maximum levels of O_3 is between September and December. This period corresponds to the transition from the dry to the wet season. The latter coincides with the austral summer, when the maximum ultraviolet radiation is recorded. It can be argued that this maximum take place due to the gradual increase in solar radiation doses experienced in the region, combined with frequent clear-sky days. However, this increase begins in the month of July, whose meteorological conditions are not significantly different from those of June. Moreover, based on the results of the previous chapters, it is known that this period (Aug-Oct) coincides with the maximum influence of agricultural biomass burning in the region. Similarly, this period also coincides with the austral spring. The possible association between the increased levels of O_3 in the last months of the year and other confluent factors during this period remains to be investigated.

As mentioned in previous chapters, the air quality monitoring network (Red MoniCA) regularly monitors some gaseous compounds using passive methods in several sampling points across the city. Although the time resolution of these measurements is very low (monthly basis), and the uncertainty of the values is very high, this database counts with a large temporal and spatial coverage. Figure S2 shows the average annual variation of O_3 and NOx levels (one of the most important drivers of O_3 in urban areas, that is mainly emitted by traffic) measured between 2004 and 2016 at 13 measurement sites deployed throughout the city of La Paz. These data provided by Red Monica, qualitatively describe that a similar annual average behavior was observed to a greater or lesser extent at all sampling sites across the years. In contrast, no significant seasonal change was observed in NOx levels.

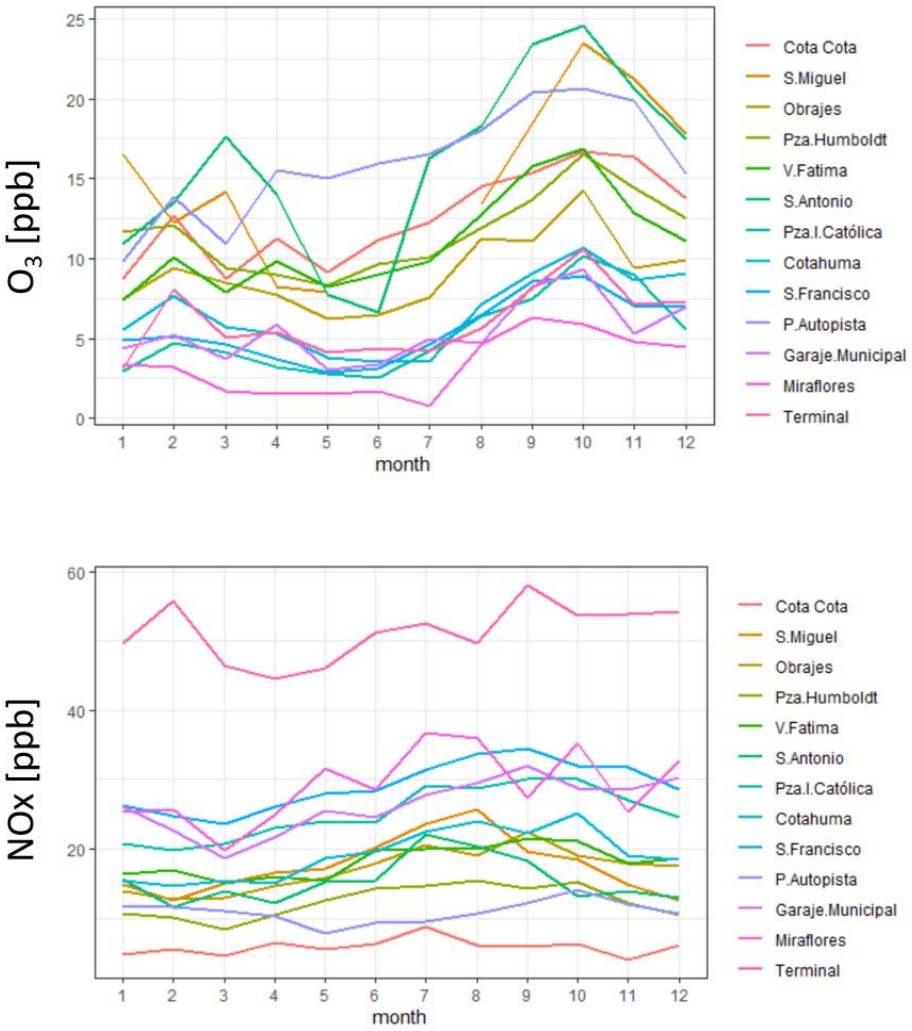

Figure S2. Monthly variation of O_3 (upper panel) and NOx (lower panel) levels reported by Red MoniCa between 2004 and 2016 at 13 sampling points in the city of La Paz.

Figure S2 also shows that both O_3 and NOx levels are overall low, and it can be derived that the increase in O_3 concentrations in the conurbation from August to November is not associated to a change in the availability of NOx. Since O_3 production is limited by two the availability of NOx and volatile organic compounds (VOCs)

(Seinfeld & Pandis, 2016), it can be inferred that the increase is likely driven by a seasonal increase in the dose of solar radiation or increase in the availability of VOC's.

The next steps to be taken in this research include validating the O_3 measurements by checking the instruments calibration, investigating the radiation doses measured in both cities during the same period, and investigating possible sources of VOCs in the region. It would also be of great benefit to include continuous NOx measurements at the sampling sites. Finally, an analysis of the effect of O_3 on the respiratory outcomes as investigated in this work can be conducted.

ANNEX III: Supplementary Information Chapter VI

Air Pollution and its Association to Health Outcomes

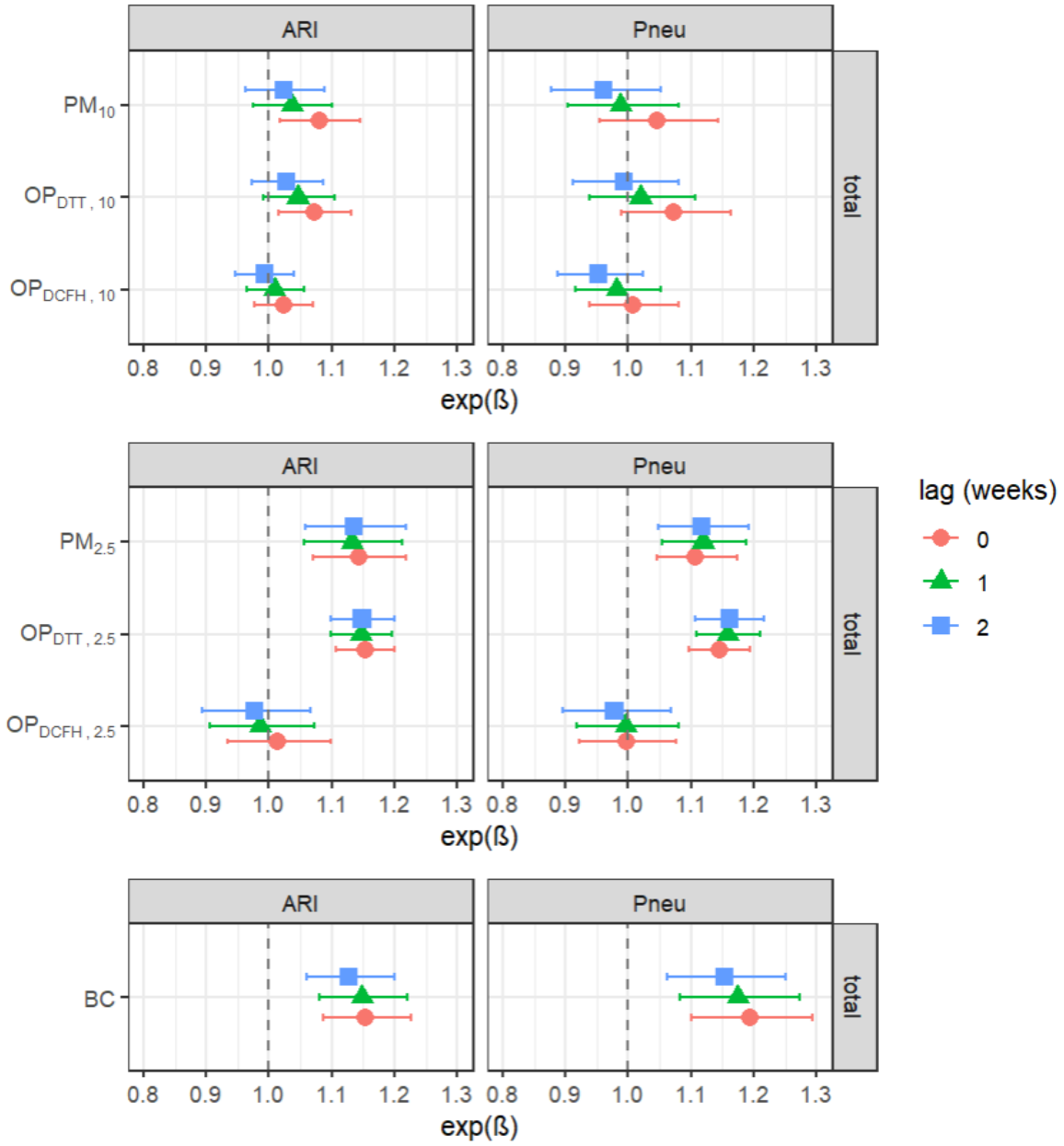

Figure S1. Univariate regression model results between both outcomes and all the exposures at lags 0, 1 and 2 weeks

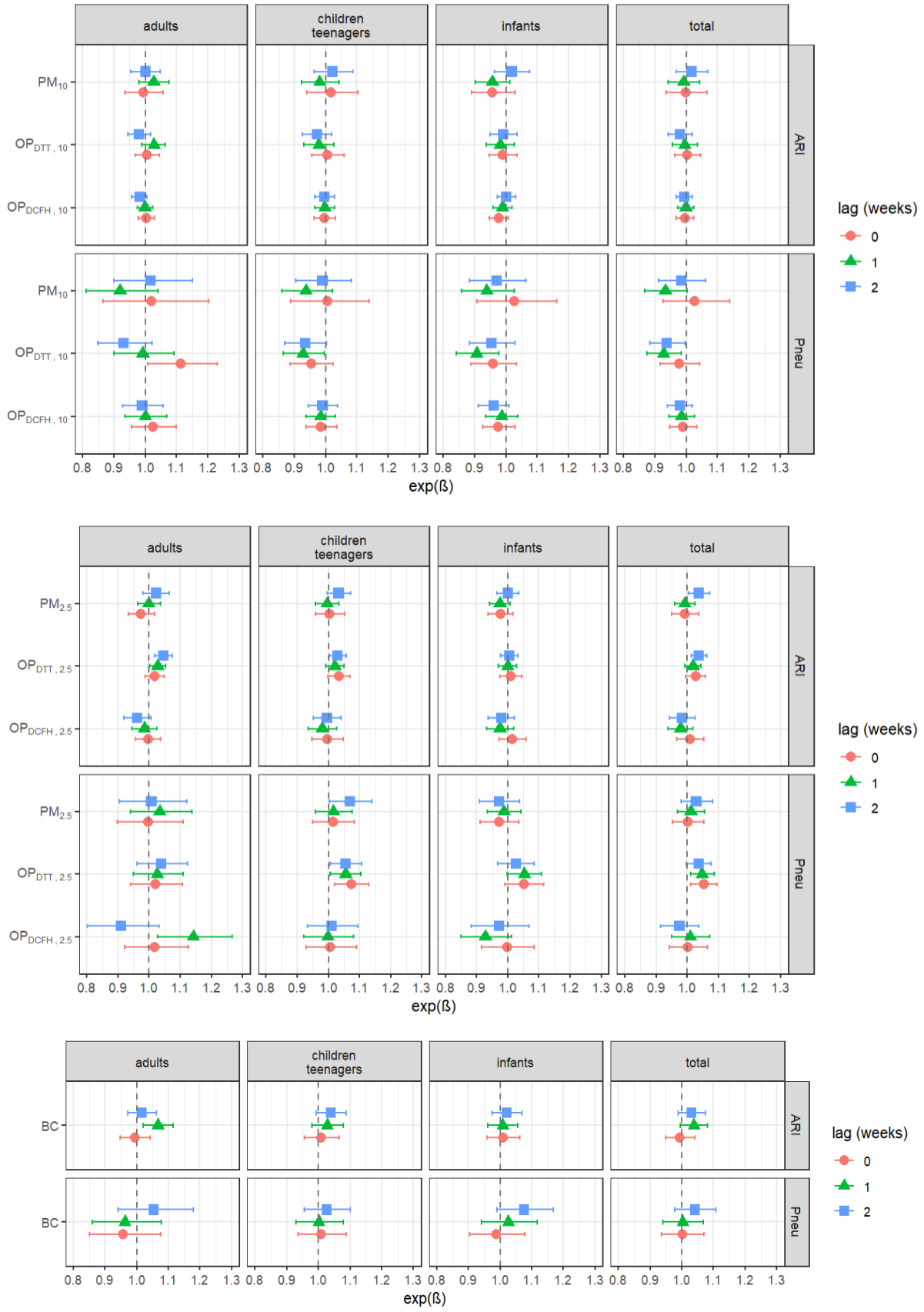

Figure S2. Main model stratified by age group for both respiratory outcomes

Table S1. Spearman correlation coefficients between measured OP and PMF resolved sources.

	OP_{DTT}	OP_{DCFH}
BIOMASS BURNING	0.39	0.74
DUST	0.38	0.49
LUBRICANT OIL	0.36	0.22
MSA-RICH	0.27	0.32
SECONDARY NITRATE	0.01	0.25
NON-EXHAUST EMISSIONS	0.48	0.20
PRIMARY BIOGENIC AEROSOL	-0.06	-0.05
SECUNDARY SULFATE	-0.04	0.24
TRAFFIC 1	0.46	0.36
TRAFFIC 2	0.32	0.00
WASTE BURNING	0.51	0.51

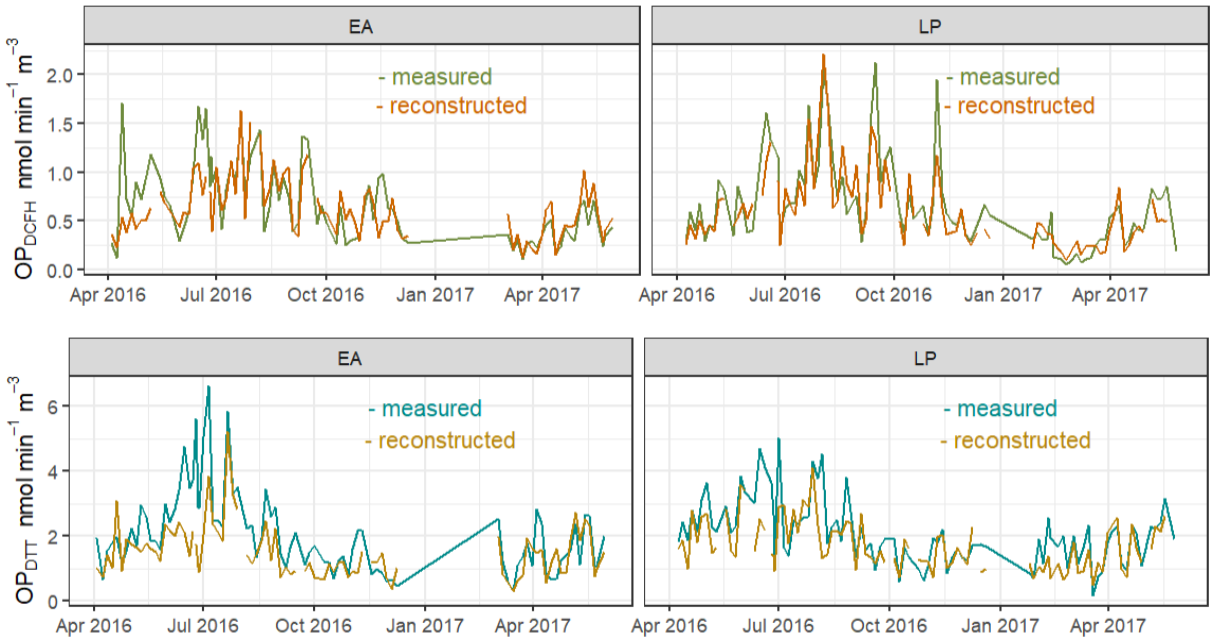

Figure S3. Time series of measured OP vs reconstructed OP (from the results of the MLR OP source deconvolution)

Table S2. Obtained associations for all the AQ parameters presented in the main analysis

AQ	group		lag	beta	SE	t-value	p-value	ll	up	exp(b)	exp(ll)	exp(ul)
BC	total	ARI	0	-0.01	0.02	-0.248	0.805	-0.05	0.04	0.99	0.95	1.04
BC	total	ARI	1	0.04	0.02	1.702	0.091	-0.01	0.08	1.04	0.99	1.08
BC	total	ARI	2	0.03	0.02	1.452	0.149	-0.01	0.07	1.03	0.99	1.07
PM	total	ARI	0	-0.01	0.02	-0.296	0.768	-0.05	0.04	0.99	0.95	1.04
OP_DTT_m3	total	ARI	0	0.03	0.02	1.659	0.102	0.00	0.06	1.03	1.00	1.06
OP_DCFH_m3	total	ARI	0	0.01	0.02	0.430	0.669	-0.03	0.05	1.01	0.97	1.05
PM	total	ARI	1	-0.01	0.02	-0.451	0.654	-0.04	0.03	0.99	0.96	1.03
OP_DTT_m3	total	ARI	1	0.02	0.01	1.406	0.165	-0.01	0.04	1.02	0.99	1.04
OP_DCFH_m3	total	ARI	1	-0.02	0.02	-1.041	0.302	-0.06	0.02	0.98	0.94	1.02
PM	total	ARI	2	0.04	0.02	2.176	0.033	0.00	0.07	1.04	1.00	1.07
OP_DTT_m3	total	ARI	2	0.04	0.01	2.984	0.004	0.01	0.06	1.04	1.01	1.06
OP_DCFH_m3	total	ARI	2	-0.02	0.02	-0.803	0.425	-0.06	0.02	0.98	0.94	1.02
BC	total	Pneu	0	0.00	0.03	0.033	0.974	-0.07	0.07	1.00	0.94	1.07
BC	total	Pneu	1	0.00	0.03	0.073	0.942	-0.06	0.07	1.00	0.94	1.07
BC	total	Pneu	2	0.04	0.03	1.277	0.204	-0.02	0.10	1.04	0.98	1.11
PM	total	Pneu	0	0.00	0.03	0.050	0.961	-0.05	0.05	1.00	0.95	1.05
OP_DTT_m3	total	Pneu	0	0.05	0.02	2.501	0.015	0.01	0.09	1.05	1.01	1.10
OP_DCFH_m3	total	Pneu	0	0.00	0.03	0.073	0.942	-0.06	0.06	1.00	0.94	1.07
PM	total	Pneu	1	0.01	0.02	0.522	0.604	-0.03	0.05	1.01	0.97	1.06
OP_DTT_m3	total	Pneu	1	0.05	0.02	2.524	0.014	0.01	0.08	1.05	1.01	1.09
OP_DCFH_m3	total	Pneu	1	0.01	0.03	0.329	0.743	-0.05	0.07	1.01	0.95	1.07
PM	total	Pneu	2	0.03	0.03	1.150	0.254	-0.02	0.08	1.03	0.98	1.08
OP_DTT_m3	total	Pneu	2	0.04	0.02	1.864	0.067	0.00	0.07	1.04	1.00	1.08
OP_DCFH_m3	total	Pneu	2	-0.03	0.03	-0.790	0.432	-0.09	0.04	0.98	0.92	1.04

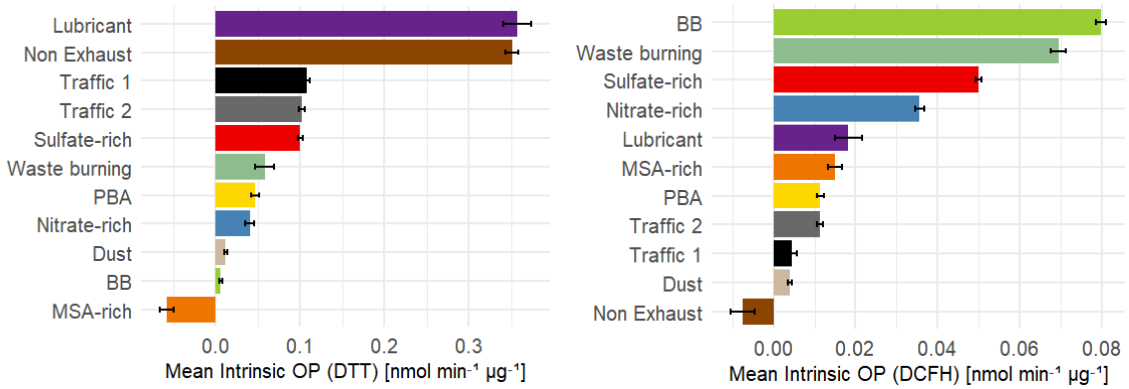

Figure S4. Source-specific intrinsic OP obtained from the MLR OP deconvolution based on the 11 PMF resolved sources

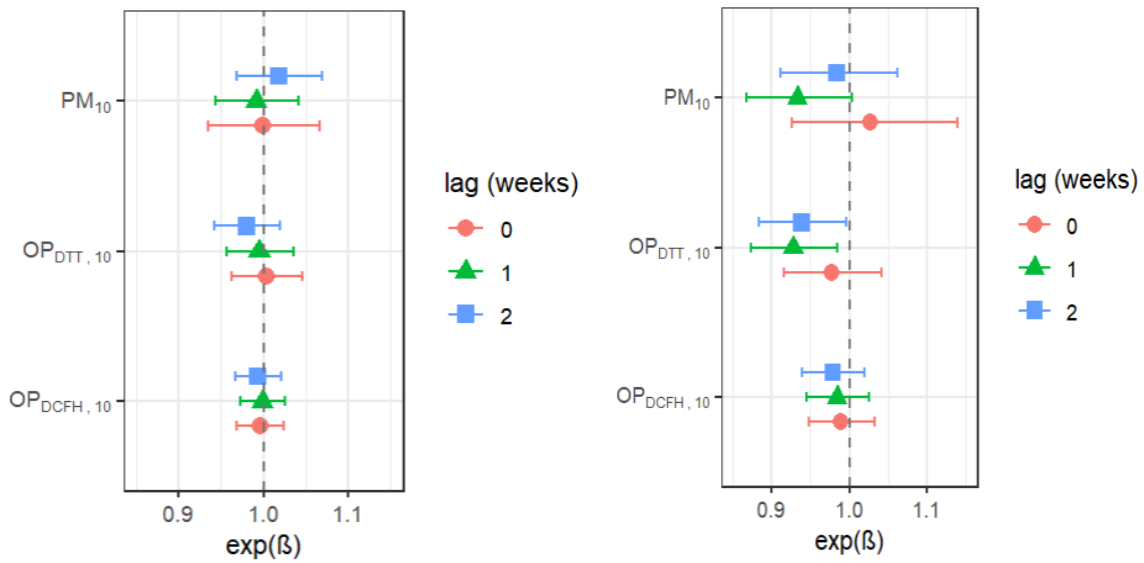

Figure S5. Associations obtained between ARI (left pannel) and Pneu (right pannel) vs PM, OP_{DTT}, OP_{DCFH} in the PM_{10} fraction.

RESUMÉ EN FRANÇAIS

Introduction

La pollution de l'air, telle que définie par Seinfeld & Pandis (2016), est une situation dans laquelle des substances émises par les activités anthropiques sont présentes en concentrations suffisamment élevées par rapport aux valeurs ambiantes normales pour générer des effets négatifs sur l'homme, la faune, la végétation ou certains matériaux. Ces substances sont appelées polluants atmosphériques. La pollution de l'air est considérée comme le deuxième facteur de risque le plus important pour les maladies non transmissibles, puisqu'on estime qu'en 2019, la pollution de l'air ambiant extérieur était responsable de 4,2 millions de décès prématurés dans le monde, un chiffre qui passe à 6,7 millions si l'on prend également en compte la pollution de l'air à l'intérieur des habitations (WHO, 2021a).

L'Organisation mondiale de la santé (OMS) a estimé qu'environ 99 % de la population mondiale vit dans des conditions qui ne satisfont pas les lignes directrices proposées en matière de qualité de l'air. En outre, bien que la pollution de l'air soit principalement une question locale, les gens sont souvent exposés à des émissions plus ou moins éloignées géographiquement en raison du transport régional de la masse d'air. Enfin, l'exposition n'est pas la même à tous les niveaux socio-économiques. L'OMS a estimé qu'environ 89 % des décès prématurés causés par la pollution de l'air extérieur dans le monde ont lieu dans des pays à revenu faible ou intermédiaire, ce qui fait de la pollution de l'air un problème d'injustice sociale (WHO, 2021a).

La plupart des pays d'Amérique Latine (AL) sont classés parmi les pays à revenu moyen dont la qualité de l'air se dégrade de plus en plus en raison de la croissance rapide de la population, de l'urbanisation et de l'industrie, ainsi que de l'absence de politiques rigoureuses en matière de protection de l'environnement. Bien que la densité de population soit relativement faible dans cette région, près de 80 % de la population de l'AL vit dans des centres urbains autour desquels l'industrie est souvent concentrée (Bravo & Torres, 2000; Husaini et al., 2022; UNEP & CCAC, 2016, 2018). Ainsi, on trouve en Amérique Latine 5 des 21 plus grandes zones métropolitaines du monde : Mexico (Mexique), Sao Paulo (Brésil), Buenos Aires (Argentine), Rio de Janeiro (Brésil) et Bogota (Colombie).

La combustion de la biomasse est l'un des plus grands problèmes climatiques et de qualité de l'air auxquels la région de l'Amérique Latine est confrontée. La combustion peut être induite par des changements d'usage des sols ou par le défrichage des sols agricoles, mais aussi par les incendies de forêt accidentels qui deviennent de plus en plus fréquents, en particulier dans le contexte du changement climatique (Barlow et al., 2020; Mataveli et al., 2021). Bien qu'il n'y ait pas beaucoup d'études à grande échelle dans la région, certaines études estiment que 48 % des émissions de $PM_{2.5}$ provenant de la combustion de la biomasse en Amérique du Sud trouvent leur origine en Amazonie, où une surface de 16 686 km^2 est brûlée chaque année (Mataveli et al., 2021). La portée de ces émissions peut s'étendre à l'échelle régionale et elles ont non seulement un impact

énorme sur le climat et les écosystèmes, mais aussi un impact direct sur la santé humaine (Alves et al., 2017; Marlier et al., 2020; Nawaz & Henze, 2020).

Malgré la grande superficie de la région de l'Amérique Latine, le nombre d'études sur la qualité de l'air reste réduit par rapport à l'Amérique du Nord ou à l'Europe. Comme il n'y a pas assez d'études pour décrire entièrement cette région, il est difficile d'estimer l'impact réel de la pollution de l'air. Néanmoins, les études existantes montrent que les émissions des véhicules représentent la principale source de pollution directe et indirecte. Bien qu'à plus petite échelle, c'est aussi la réalité à laquelle sont confrontées les villes moyennes de l'Amérique Latine.

Pollution atmosphérique dans les villes latino-américaines de haute altitude

Plusieurs grandes villes d'Amérique Latine ont été construites à haute altitude (>2000 m au-dessus du niveau de la mer), ce qui représente un défi supplémentaire en termes de qualité de l'air. La pression atmosphérique diminue de manière exponentielle avec l'altitude, tout comme la disponibilité de l'oxygène. L'altitude a donc un impact direct sur les émissions et l'exposition aux polluants atmosphériques.

En raison de la faible pression atmosphérique et de la faible concentration en oxygène, des études ont montré que l'efficacité de la combustion des carburants fossiles dans les véhicules diminue. Il en résulte une augmentation de la consommation de carburant et une augmentation des particules émises. De même, les villes de haute altitude reçoivent des quantités de rayonnement solaire plus élevées que les autres régions situées à la même latitude, ce qui a un impact sur les processus photochimiques qui se déroulent dans l'atmosphère (Chaffin & Ullman, 1994; Giraldo & Huertas, 2019; Graboski & McCormick, 1996; Chao He et al., 2011; Nagpure et al., 2011; Pan et al., 2011; Wang et al., 2013a, b).

En outre, les personnes vivant en haute altitude doivent compenser la disponibilité réduite d'oxygène par volume d'air. La première réponse physiologique à de faibles concentrations d'oxygène lors d'une exposition à des conditions de haute altitude est une augmentation du métabolisme de base (la quantité d'énergie nécessaire pour maintenir le fonctionnement du corps), ce qui induit une augmentation du taux de ventilation parmi d'autres mécanismes. Le métabolisme de base augmente normalement d'environ 17 à 27 % pendant les premières semaines suivant l'exposition à des conditions d'hypoxie, puis revient progressivement au niveau de base du niveau de la mer (Beall, 2007). Toutefois, les populations vivant sur les hauts plateaux ont développé différents mécanismes physiologiques qui leur permettent de surmonter le manque d'oxygène, comme par exemple les Andins et les Tibétains, deux des plus anciennes cultures de haute altitude. Il a été observé que certaines personnes vivant dans des régions de très haute altitude partagent certains traits résultant des conditions dans lesquelles elles vivent, notamment : une taille en moyenne plus petite, une cage thoracique plus large, des gradients alvéolaires/artériels d'O_2 plus étroits, des capacités pulmonaires accrues, un débit sanguin de l'artère utérine plus important pendant la grossesse et une utilisation accrue de l'O_2 cardiaque, ce qui suggère globalement une plus grande efficacité du transfert et de l'utilisation de l'O_2 (Akunov

et al., 2018; Beall, 2007; Fierce et al., 2016; Frisancho, 1977; Frisancho, 2013; Frisancho et al., 1999; Jansen & Basnyat, 2011; Julian & Moore, 2019; Li et al., 2018; Pérez-Padilla, 2022).

Il a été démontré que les Tibétains, par exemple, ont une ventilation au repos plus élevée (15,0 L/min) que les personnes vivant au niveau de la mer (11 L/min), ce qui leur permet de faire face à l'hypoxie (Beall, 2007). En revanche, il a été démontré que les Andins ont une ventilation au repos similaire à celle des personnes vivant au niveau de la mer, mais une concentration d'hémoglobine et des taux d'érythropoïétine plus élevés. La saturation en oxygène et la concentration en hémoglobine déterminent la teneur en oxygène artériel ; par conséquent, les habitants des hauts plateaux andins semblent surcompenser l'hypoxie environnementale, en affichant une teneur en oxygène artériel plus élevée. En revanche, les Tibétains semblent souffrir d'une hypoxie profonde par rapport aux personnes vivant au niveau de la mer. En outre, il a été démontré que les femmes enceintes originaires des Andes et vivant à haute altitude augmentent l'apport d'oxygène à l'utérus et au placenta en augmentant la ventilation et la saturation en oxygène (Beall, 2007; Julian & Moore, 2019). Par conséquent, bien que l'ampleur et les mécanismes par lesquels l'altitude influe sur l'exposition à la pollution atmosphérique restent à l'étude, les conditions extrêmes d'hypoxie (entraînant une augmentation de la ventilation) augmentent les risques associés à l'exposition à la pollution atmosphérique.

Parmi les plus grandes villes d'altitude de l'AL ($\gtrsim$ 2 millions d'habitants), on peut citer : Mexico (2850 m d'altitude, Mexique), Bogota (2620 m d'altitude, Colombie), Quito (2240 m d'altitude, Équateur), La Paz (3200-3600 m d'altitude) et El Alto (4050 m d'altitude). Le nombre limité d'études existantes sur la qualité de l'air montre que les villes les plus peuplées, telles que Mexico et Bogota, ainsi que la ville plus petite de Quito, connaissent une détérioration de la qualité de l'air.

Les études sur la qualité de l'air menées dans ces villes font état de deux grandes sources communes de particules, à savoir le trafic et la poussière (Ramírez et al., 2018a; Raysoni et al., 2017; Vega et al., 2012), qui souvent un élément anthropique important dans la remise en suspension des poussières. Cependant, la mise en œuvre de stratégies de contrôle des émissions telles que la réduction de la teneur en soufre des carburants, la restriction de la circulation des véhicules et les mises à niveau technologique de l'industrie commence à produire des résultats encourageants dans les villes de Mexico et de Bogota. Par exemple, à Bogota, malgré le fait que les sources mobiles ont augmenté de 100 % au cours de la dernière décennie, les concentrations de PM_{10} ont montré une tendance constante à la baisse, et les concentrations de $PM_{2.5}$ ne semblent pas s'être aggravées selon Mura et al. (2020). D'autre part, à Mexico, bien que les concentrations de PM_{10} n'aient pas montré d'amélioration significative, Morton-Bermea et al. (2021) a signalé que les concentrations de plomb (Pb), cobalt (Co), mercure (Hg), manganèse (Mn), arsenic (As) et cadmium (Cd) affichaient une tendance à la baisse. Cela prouve l'impact bénéfique encourageant que les actions propulsées par les politiques de qualité de l'air peuvent avoir sur les émissions de PM et la qualité de l'air dans une ville.

Objectifs de la présente étude

La Paz et El Alto forment la deuxième région métropolitaine de Bolivie qui est considérée comme l'une des régions métropolitaines les plus élevées du monde (3000-4000 m d'altitude). Cette conurbation compte actuellement près de 2 millions d'habitants (INE, 2020c). Au cours de la dernière décennie, le gouvernement, les municipalités et la communauté scientifique se sont efforcés d'évaluer la qualité de l'air dans cette région. Les réglementations concernant l'âge des voitures importées, la mise en place de moyens de transport public alternatifs, l'établissement de réseaux de surveillance de la qualité de l'air, les restrictions sur les véhicules dans les centres-villes sont quelques exemples de ces efforts. Cependant, à notre connaissance, aucune étude à long terme sur la qualité de l'air n'a été réalisée pour étudier la masse et la composition chimique des particules dans cette région aux conditions extrêmes et difficiles pour ses habitants.

Dans ce contexte, cette thèse cherche à identifier et à caractériser les sources de particules affectant la qualité de l'air dans la région métropolitaine de La Paz et El Alto, ainsi qu'à étudier la dynamique et le transport des polluants depuis/vers/entre les deux villes. L'objectif est également d'évaluer l'impact de l'exposition à la pollution atmosphérique sur la santé des habitants de la conurbation et de fournir une base de référence pour la qualité de l'air dans cette zone, sur laquelle les politiques et les réglementations en matière de qualité de l'air pourront s'appuyer.

Ce travail se fonde sur les données relatives à la qualité de l'air, aux paramètres météorologiques et sanitaires recueillies entre 2016 et 2019 dans les deux villes. Pour atteindre ces objectifs, il est prévu de :

- Combiner les mesures simultanées en ligne et hors ligne des propriétés physiques et chimiques des particules d'aérosols mesurées à La Paz et El Alto.
- Appliquer différentes méthodes de répartition des sources.
- Inclure les inventaires d'émissions existants
- Combiner les données sur la qualité de l'air avec les réponses épidémiologiques pour évaluer la présence éventuelle et l'ampleur d'une association entre les deux.

Méthodologie

Sites d'échantillonnage.

Afin d'évaluer les propriétés de la pollution de fond urbaine, un site d'échantillonnage de la pollution de fond urbaine a été installé dans chaque ville, où plusieurs paramètres ambiants et météorologiques ont été mesurés simultanément. Les sites d'échantillonnage étaient situés à 7 km l'un de l'autre, avec une différence d'altitude de plus de 400 m, et à une distance d'environ 20 km de la station de surveillance de la Veille de l'atmosphère globale de Chacaltaya (CHC-GAW).

Le site de mesure d'El Alto (EA) a été installé à l'intérieur de l'aéroport international d'El Alto, dans les installations de l'observatoire météorologique (16.5100° S, 68.1987° W, 4025 m d'altitude). L'observatoire se trouvait à une distance d'environ 300 m de la piste de l'aéroport et de 500 m de la route principale la plus

proche. Le trafic aéroportuaire est généralement faible, surtout pendant la journée, et aucun pic significatif des paramètres mesurés (CO_2, PM) n'a été observé pendant le décollage ou l'atterrissage des avions. Le trafic routier dans le périmètre de l'aéroport est pratiquement inexistant. La zone autour du site d'échantillonnage n'est pas asphaltée, donc poussiéreuse, et il n'y a pas d'autres bâtiments à proximité de l'observatoire.

Le site de mesure de La Paz (LP) a été placé sur le toit du musée Pipiripi de la ville (Espacio Interactivo Memoria y Futuro Pipiripi : 16.5013°S, 68.1259°W, 3600 m d'altitude). Ce bâtiment municipal est situé sur une petite colline au centre de La Paz. Contrairement au site de EA, dans un rayon de 1 km, le site de la LP est entouré de nombreuses routes très fréquentées et de zones résidentielles denses, avec une distance minimale horizontale et verticale par rapport à la route la plus proche d'environ 70 et 45 m, respectivement. Par ailleurs, les environs immédiats du site (dans un rayon d'environ 100 m) sont couverts d'espaces verts et d'un parking pour les bus de la municipalité au pied de la colline. Le site d'échantillonnage étant situé dans le centre-ville, le transit des véhicules lourds (hormis les bus publics) est limité.

Tableau 1. Résumé de l'instrumentation placée dans chacune des stations urbaines, de leur période de fonctionnement et de leur résolution temporelle

	El Alto	*La Paz*
Aethalomètre AE33	Avril 2016 - septembre 2017 (1-min)	X
Aethalomètre AE31	Jan 2018 - Juin 2018 (5-min)	Avril 2016 - Juin 2018 (5-min)
PM_{10} échantillons	Avril 2016 - juin 2017 (24 heures tous les 3 jours)	Avril 2016 - juin 2018 (24 heures tous les 3 jours)[14]
$PM_{2.5}$ échantillons	Juin 2017 - Juin 2018 (24 heures tous les 3 jours)	Juin 2017 - Juin 2018 (24 heures tous les 3 jours)
SP2-XR	Avril 2018 - Mai 2018 (1-min)	Avril 2018 - Mai 2018 (1-min)
Météorologie	Avril 2016 - Juin 2018 (1 heure)	Avril 2016 - Juin 2018 (1 jour)

La campagne d'échantillonnage des particules s'est déroulée entre avril 2016 et novembre 2018, avec une prolongation de l'échantillonnage des PM à La Paz jusqu'en mars 2019. En outre, la surveillance en ligne de l'ozone (O_3) a débuté en 2021. La campagne a combiné des techniques en ligne et hors ligne pour la caractérisation chimique et physique des particules d'aérosols atmosphériques. Ainsi, étant donné que le début et la fin de l'échantillonnage des différents instruments situés sur chaque site n'étaient pas les mêmes, le tableau 1 présente les instruments installés pendant la campagne et la figure 1 montre la disponibilité des

[14] Après juin 2017, seuls 25 échantillons du filtre PM_{10} ont été collectés par intermittence en raison de problèmes techniques.

données tout au long des années 2016 à 2019 sur une base hebdomadaire. Le fait d'avoir une idée claire de la disponibilité des données facilitera la discussion sur les avantages et les limites de l'ensemble de données dans les sections suivantes.

Figure 1. Description graphique des données disponibles de tous les paramètres atmosphériques, météorologiques et épidémiologiques mesurés tout au long de la campagne sur chaque site.

Conclusions

Les objectifs généraux de cette étude étaient de documenter les niveaux de polluants particulaires affectant la qualité de l'air dans la région métropolitaine de La Paz et El Alto, d'identifier leurs sources d'émission et d'évaluer l'impact potentiel de l'exposition à la pollution de l'air sur la santé des habitants de la l'agglomération. À plus long terme, l'objectif de l'étude est de fournir des informations sur les facteurs influençant la qualité de l'air dans cette région, sur la base desquelles l'élaboration de politiques et de réglementations en matière de qualité de l'air pourra être développée.

Si certaines études ont caractérisé les niveaux de pollution dans les grandes agglomérations d'Amérique latine, très peu ont abordé les liens entre les polluants atmosphériques et les issues de santé recensées par les services de santé municipaux, sans parler de l'inclusion du potentiel d'oxydation des particules en tant que métrique. La présente étude est unique, non seulement parce qu'elle documente pour la première fois la nature de la pollution particulaire à La Paz-El Alto, mais aussi en raison des particularités de la région : haute

altitude (3200 m à 4100 m au-dessus du niveau de la mer), topographie complexe, rayonnement solaire intense pendant la journée et réponses physiologiques distinctes d'adaptation des habitants aux conditions de basse pression.

Tout au long de ce travail, une description détaillée de l'état de la qualité de l'air en termes de particules en suspension a été présentée, ainsi que leurs principales sources d'émission. Ces informations, associées aux données sanitaires locales, ont servi de base à une première évaluation de l'impact potentiel des particules sur la santé des habitants de la région. L'étude s'est concentrée sur trois paramètres généralement utilisés pour décrire la qualité de l'air : les particules (PM) et leur spéciation chimique, le carbone suie (BC) et le potentiel d'oxydation (PO).

Dans l'agglomération de La Paz-El Alto, les concentrations de PM_{10} mesurées tout au long de la période d'étude ont rarement dépassé les recommandations de l'Organisation Mondiale de la Santé (OMS). Ces épisodes se sont produits principalement pendant la saison sèche. Il faut toutefois tenir compte du fait que les niveaux de fond des polluants particulaires peuvent différer sensiblement des concentrations en bord de route, et que les niveaux de fond sont suffisamment élevés pour considérer que de nombreux habitants des villes sont exposés à des niveaux nocifs de polluants.

En utilisant différents outils mathématiques et statistiques, il a été possible d'identifier les principales sources de chacun de ces paramètres et leur variabilité temporelle, en constatant que les sources d'émission sont principalement locales et fortement modulées par la météorologie du site. Grâce à l'utilisation de l'outil *positive matrix factorization* (PMF) de l'agence de protection de l'environnement des Etats-Unis (US EPA) et à la large gamme de composés chimiques analysés à partir des échantillons de PM_{10} collectés sur filtres dans les deux villes, il a été possible d'identifier 11 sources majeures affectant la qualité de l'air de l'agglomération. La proximité entre les deux villes a permis de répartir les sources de PM selon une approche multisite, une technique de plus en plus utilisée en raison de la robustesse qu'elle confère à l'analyse.

Les résultats de l'étude PMF ont montré que près de 50 % des concentrations massiques de particules mesurées sur les deux sites peuvent être attribuées à la poussière minérale (remise en suspension de manière naturelle et anthropique) et aux émissions des véhicules. Les émissions des véhicules sont également liées à des sources secondaires influencées par les gaz précurseurs émis par les voitures (nitrate secondaire et sulfate secondaire). La troisième source de pollution la plus importante est la combustion de la biomasse (BB), liée aux pratiques agricoles et aux changements d'affectation des sols dans les terres basses. Les émissions les plus élevées de BB se produisent généralement à la fin de la saison sèche et contribuent au dépassement des seuils recommandés par l'OMS pour l'exposition aux PM_{10}. Enfin, les autres contributions aux concentrations de particules ont été attribuées à des sources naturelles (aérosols organiques biogéniques primaires et secondaires). Un résultat très intéressant de l'étude, basé sur l'inclusion de traceurs organiques dans la PMF, a été de permettre la résolution d'une source contribuant à une faible partie de la masse de particules,

associée à la combustion à l'air libre de déchets, mais qui est responsable d'une grande partie des traceurs organiques qui sont connus pour être nocifs pour la santé.

Il est intéressant de noter que l'utilisation de la PMF a été rendue complexe par le manque de connaissance des profils de sources dans cette région, contrairement aux villes des régions de l'OCDE. Finalement, le modèle à 11 facteurs a été sélectionné comme le profil de source le plus satisfaisant après de nombreuses tentatives. La transposition directe des profils de sources des études précédentes dans les villes européennes peut conduire à des erreurs dans l'identification des sources d'émissions, ce qui doit être pris en compte dans les études futures.

Le deuxième paramètre de qualité de l'air analysé dans la présente étude est la concentration de BC, plus précisément la concentration de carbone suie équivalent (eBC), en raison de la technique optique employée pour le mesurer. Au-delà du rôle important que joue le BC sur le climat, son importance réside dans la petite taille de ses particules et dans leur potentiel à transporter des composés dangereux au plus profond des poumons. Très peu d'études décrivent ce paramètre dans la région de l'Amérique du Sud, et encore moins ont été réalisées dans des conditions de haute altitude. À La Paz et El Alto, les différentes conditions météorologiques rencontrées dans chaque ville rendent la variabilité diurne du BC distincte, mais aucune différence significative n'a été observée dans les concentrations moyennes de BC entre les sites. De plus, les conditions particulières de combustion dans ces villes entraînent l'émission de particules plus fines que ce qui est habituellement observé au niveau de la mer. Les sections transversales d'absorption de masse (MAC) associées à ces particules se sont avérées cohérentes avec les valeurs précédemment rapportées de MAC correspondant au BC fraîchement émis dans les stations de fond urbain.

Les propriétés optiques du BC dans la l'agglomération indiquent que les émissions des véhicules sont la principale source de BC, ce qui confirme l'étude PMF. En outre, l'exécution d'un modèle à deux sources, basé sur la dépendance en longueur d'onde des coefficients d'absorption, a indiqué que le BB était également une source contribuant de manière significative pendant la saison sèche. En outre, une méthode de déconvolution de la source BC a été mise en œuvre sur la base de l'association des coefficients d'absorption multi-longueur d'onde avec la contribution à la masse de PM des sources résolues par l'analyse PMF. L'analyse a été réalisée par une régression linéaire multiple (MLR) qui a confirmé les résultats obtenus à partir du modèle bilinéaire. Il s'agit d'une méthode complémentaire innovante et statistiquement valide pour caractériser les propriétés optiques des particules d'aérosol spécifiques à la source sur des sites où des études de répartition des sources de particules ont été réalisées.

Les concentrations massiques de particules sont principalement dominées par la masse des particules les plus grosses, qui représentent une menace moindre pour la santé et proviennent le plus souvent de sources naturelles. Il est donc nécessaire d'établir des paramètres de qualité de l'air qui permettent d'évaluer la toxicité des particules. L'un des paramètres proposés pour atteindre cet objectif et qui a montré des associations significatives avec les effets sur la santé est le PO. Dans le présent travail, nous nous sommes

principalement intéressés au PO des particules, mesuré par deux tests acellulaires : PO_{DTT} (dithiothréitol) et PO_{DCFH} (dichlorofluorescéine). En suivant la même méthode de régression linéaire multiple décrite dans le paragraphe précédent, nous avons procédé à la déconvolution des principales sources de l'activité du PO observée dans les deux villes. L'activité reconstituée des PO_{DTT} et PO_{DCFH} a été principalement attribuée à des sources anthropogéniques de PM, en particulier : les émissions des véhicules, la combustion de la biomasse et la combustion des déchets à l'air libre, ainsi qu'à des sources secondaires d'aérosols dont les précurseurs proviennent de la combustion de combustibles fossiles.

Enfin, ce travail a étudié les associations possibles entre les paramètres de qualité de l'air décrits précédemment et deux issues de santé : les infections respiratoires aiguës (IRA) et la pneumonie. Le nombre de visites à l'hôpital dues à ces deux pathologies a été fourni par le ministère bolivien de la santé avec une résolution temporelle hebdomadaire. Les associations ont ensuite été analysées à l'aide de modèles épidémiologiques (régression de Poisson) après contrôle de la variabilité saisonnière et des éventuels facteurs météorologiques confondants dans le cadre d'une approche multisite. Malgré les limites de la méthodologie appliquée à une série temporelle aussi courte (environ un an par site), avec une faible résolution temporelle, des associations positives significatives ont été trouvées entre l'exposition au PO_{DTT} (mesuré dans la fraction $PM_{2.5}$) et les deux affections. De même, une tendance positive peut être observée entre l'exposition aux $PM_{2.5}$ et au BC et le nombre de cas déclarés d'IRA, et entre l'exposition à l'eBC et le nombre de cas déclarés de pneumonies. Ces résultats confirment que le PO_{DTT} est un bon indicateur des effets de la qualité de l'air sur la santé en ce qui concerne les deux issues de santé étudiées dans le cadre de ce travail. En outre, ces associations positives entre les problèmes respiratoires et les paramètres de la qualité de l'air mettent en évidence les effets nocifs des polluants particulaires sur la santé dans l'agglomération.

Nous estimons que des études contrôlées des émissions directes de véhicules alimentés par différents types de carburant dans différentes conditions d'altitude, de pente de la route, de charge et de vitesse pourraient aider à élucider l'identité des deux profils de trafic résolus par le PMF Étant donné qu'il a été constaté que les $PM_{2.5}$ présentaient les associations les plus fortes avec les effets sur la santé, une étude de répartition des sources sur la fraction des $PM_{2.5}$ est la prochaine étape nécessaire pour connaître la composition de la plus petite fraction des PM et étudier plus amplement les éventuels effets antagonistes qui masqueraient les associations observées entre les effets sur la santé et les $PM_{2.5}$, mais pas avec les PM_{10}. De même, une analyse plus poussée de la dynamique de la couche de mélange sur de courtes échelles de temps (variations diurnes) pourrait permettre de mieux comprendre l'influence que les villes exercent les unes sur les autres et sur la station mondiale Global Atmospheric Watch (GAW) à Chacaltaya. Enfin, le manque d'inventaires d'émissions et d'informations statistiques actualisées disponibles dans la région a limité l'interprétation des résultats dans la poursuite de l'identification des sources de trafic. Cela a également rendu l'interprétation des résultats obtenus par la PMF plus difficile et a limité la puissance potentielle de la fonction de contrainte de l'outil PMF.

Nous sommes conscients des limites de notre étude. Notre stratégie de surveillance aurait certainement été plus robuste si elle avait été complétée par l'analyse de composants gazeux (NOx et composés organiques

volatils spécifiques) afin d'obtenir une description holistique de l'état de la qualité de l'air dans la région. Cela n'est cependant pas simple en Bolivie, notamment en raison des difficultés d'accès aux gaz de référence pour l'étalonnage des instruments. Nous sommes également conscients de toutes les difficultés rencontrées pour maintenir une surveillance à long terme à La Paz El Alto : le fonctionnement des instruments à basse pression est toujours problématique, le remplacement des pièces techniques n'est pas immédiat, la maintenance régulière par le personnel du laboratoire de physique de l'atmosphère de l'université Mayor de San Andrés (UMSA-LFA) est exigeante, mais cette étude est aussi l'occasion de proposer quelques améliorations dans l'organisation logistique. Une première recommandation que nous pouvons faire pour la continuité des activités est d'éviter les changements dans les méthodologies d'échantillonnage et de s'assurer que tout changement soit documenté avec une période de mesures parallèles afin que la continuité soit assurée et que les divergences soient éventuellement corrigées. Dans notre étude, ces changements ont entraîné une réduction des séries temporelles disponibles, ce qui a réduit la puissance statistique de l'analyse. Une incertitude supplémentaire a également été introduite par la différence d'instrumentation au sein des sites et le manque de périodes d'inter-comparaison pour les instruments en ligne mesurant dans les mêmes conditions.

Nous considérons que les résultats de l'analyse rigoureuse des trois différents paramètres de qualité de l'air présentés dans ce document établissent une ligne de base de l'exposition générale des habitants de La Paz-El Alto aux polluants atmosphériques particulaires. En outre, cette étude contribue à la documentation des études sur la qualité de l'air dans cette région peu étudiée d'Amérique du Sud. Nous espérons que ce travail pourra être utilisé pour conseiller les futures décisions politiques et que les différentes méthodologies d'échantillonnage et d'analyse des données mises en œuvre pourront servir de référence pour faciliter la reproduction de cette étude dans d'autres parties du pays et de la région. Nous considérons que la description de la composition chimique des particules émises par les différentes sources résolues peut également compléter les inventaires d'émissions existants. De même, cette étude peut être considérée comme une base solide pour la mise en œuvre et l'évaluation/validation d'un modèle de transport chimique qui pourrait permettre la prévision de la qualité de l'air dans la région. Enfin, à notre connaissance, il s'agit de la première étude épidémiologique de série temporelle qui examine les associations existantes entre les paramètres de la qualité de l'air et les effets observés sur la santé en Bolivie.

Ce travail a permis de décrire l'état de la qualité de l'air en milieu urbain, c'est-à-dire les concentrations minimales de particules auxquelles les habitants de l'agglomération sont exposés. Néanmoins, les gens sont souvent exposés à des concentrations beaucoup plus élevées au quotidien. Il est donc impératif de prendre des mesures pour améliorer la qualité de l'air dans la ville, compte tenu de la vulnérabilité supplémentaire liée à la vie en haute altitude. Comme cela a été observé de différents points de vue, les principaux responsables de la pollution à La Paz-El Alto sont les émissions des véhicules. Nous considérons qu'un contrôle plus rigoureux de l'état des véhicules circulant dans la ville est de la plus haute importance. Deuxièmement, la mise en œuvre de systèmes de transport massifs pour réduire la taille de la flotte de véhicules, ou de systèmes de

transport utilisant des sources d'énergie alternatives, est cruciale. De même, l'incinération des déchets devrait être interdite, car il s'agit d'une source majeure de polluants dangereux associés à des facteurs de risque élevés pour la santé humaine. En outre, il est essentiel d'actualiser les politiques relatives aux émissions de polluants afin de réguler le facteur industriel croissant. Une diminution des émissions de BB agricoles entraînerait également une amélioration significative de la qualité de l'air dans l'ensemble du pays.

Seule une surveillance fiable, complète et à long terme de la qualité de l'air permettra d'évaluer l'efficacité des politiques actuelles et futures en matière de qualité de l'air. Un seul point de prélèvement n'est pas suffisant pour la caractérisation spatiale de l'état de la qualité de l'air dans les différentes parties de la ville. Par conséquent, une bonne maintenance et un meilleur équipement des réseaux de surveillance de la qualité de l'air existants contribueraient de manière significative aux efforts d'amélioration de la qualité de l'air dans les zones métropolitaines de Bolivie. En outre, la mise en place d'un outil interactif de l'état de la qualité de l'air pourrait être bénéfique pour avertir la population des pics de pollution afin qu'elle puisse prendre des mesures pour réduire sa propre exposition. Enfin, il est important de sensibiliser la population au risque sanitaire que représente la pollution de l'air afin qu'elle participe activement à la réduction des émissions de polluants atmosphériques.

RESUMEN EN ESPAÑOL

Introducción

La contaminación atmosférica, según la definición de Seinfeld & Pandis (2016), es la situación en la que sustancias emitidas por actividades antropogénicas están presentes en concentraciones suficientemente elevadas en comparación con los valores ambientales normales como para generar efectos negativos en los seres humanos, la fauna, la vegetación o determinados materiales. Estas sustancias se conocen como contaminantes atmosféricos. La contaminación atmosférica se considera el segundo factor de riesgo más importante de las enfermedades no transmisibles, ya que se estima que en 2019 la contaminación del aire ambiente exterior fue responsable de 4,2 millones de muertes prematuras en todo el mundo, cifra que se eleva a 6,7 millones si se tiene en cuenta también la contaminación del aire interior (WHO, 2021a).

La Organización Mundial de la Salud (OMS) ha estimado que alrededor del 99% de la población mundial vive en condiciones que no cumplen las directrices propuestas de calidad del aire. Además, aunque la contaminación atmosférica es principalmente un problema local, las personas suelen estar expuestas a emisiones que tuvieron lugar en regiones alejadas geográficamente, debido al transporte regional de las masas de aire. Por último, la exposición no es la misma en todos los niveles socioeconómicos. La OMS ha estimado que alrededor del 89% de las muertes prematuras causadas por la contaminación del aire exterior en el mundo ocurren en países de ingresos bajos y medios, lo que convierte a la contaminación del aire en un problema de injusticia social (WHO, 2021a).

La mayoría de los países de América Latina (LA) están clasificados como países de ingresos bajos a medios, cuya calidad del aire se está degradando cada vez más debido al rápido crecimiento de la población, la urbanización y la industria, así como debido a la ausencia de políticas medioambientales rigurosas. Aunque la densidad de población es relativamente baja en esta región, casi el 80% de la población de LA vive en centros urbanos, alrededor de los cuales se suele concentrar la industria (Bravo & Torres, 2000; Husaini et al., 2022; UNEP & CCAC, 2016, 2018). De hecho, América Latina alberga 5 de las 21 áreas metropolitanas más grandes del mundo: Ciudad de México (México), Sao Paulo (Brasil), Buenos Aires (Argentina), Río de Janeiro (Brasil) y Bogotá (Colombia).

La combustión de biomasa es uno de los mayores problemas climáticos y de calidad del aire a los que se enfrenta la región latinoamericana. La combustión puede ser inducida por cambios en el uso del suelo o por el desmonte de tierras agrícolas, pero también por incendios forestales accidentales que son cada vez más frecuentes debido al cambio climático (Barlow et al., 2020; Mataveli et al., 2021). Aunque no hay muchos estudios a gran escala en la región, algunos estudios estiman que el 48% de las emisiones de $PM_{2.5}$ procedentes de la combustión de biomasa en América del Sur se originan en la Amazonia, donde se quema una superficie de 16.686 km2 cada año (Mataveli et al., 2021). El alcance de estas emisiones puede extenderse regionalmente,

y no sólo tienen un enorme impacto en el clima y los ecosistemas, sino también un impacto directo en la salud humana (Alves et al., 2017; Marlier et al., 2020; Nawaz & Henze, 2020).

A pesar de la gran superficie de la región latinoamericana, el número de estudios sobre la calidad del aire sigue siendo pequeño en comparación con América del Norte o Europa. Dado que no existen suficientes estudios para describir completamente esta región, es difícil estimar el impacto real de la contaminación atmosférica. No obstante, los estudios existentes muestran que las emisiones vehiculares son la principal fuente de contaminación directa e indirecta. Aunque a menor escala, ésta es también la realidad a la que se enfrentan las ciudades latinoamericanas medianas.

Contaminación atmosférica en ciudades latinoamericanas de gran altitud

Varias de las grandes ciudades latinoamericanas se han construido a gran altitud (>2000 m sobre el nivel del mar), lo que representa un reto adicional en términos de calidad del aire. La presión atmosférica disminuye exponencialmente con la altitud, al igual que la disponibilidad de oxígeno. Por lo tanto, la altitud tiene un impacto directo en las emisiones y la exposición a los contaminantes atmosféricos. Debido a la baja presión atmosférica y a la baja concentración de oxígeno, los estudios han demostrado que la eficacia de la combustión de los combustibles fósiles en los vehículos disminuye. El resultado es un aumento del consumo de combustible y de las emisiones de material particulado. Del mismo modo, las ciudades situadas a gran altitud reciben mayores cantidades de radiación solar que otras regiones a la misma latitud, lo que facilita los procesos fotoquímicos que tienen lugar en la atmósfera (Chaffin & Ullman, 1994; Giraldo & Huertas, 2019; Graboski & McCormick, 1996; He et al., 2011; Nagpure et al. 2011; Pan et al., 2011; Wang et al., 2013a, b).

Las personas que viven a gran altitud tienen que compensar la menor disponibilidad de oxígeno por volumen de aire. La primera respuesta fisiológica a las bajas concentraciones de oxígeno durante la exposición a condiciones de gran altitud es un aumento de la tasa metabólica basal (la cantidad de energía necesaria para mantener la función corporal), que induce un aumento de la tasa de ventilación entre otros mecanismos. La tasa metabólica basal aumenta normalmente en un 17-27% durante las primeras semanas tras la exposición a condiciones hipóxicas, y después vuelve gradualmente a los valores normales a nivel del mar (Beall, 2007). Sin embargo, las poblaciones que viven en condiciones de gran altura han desarrollado diferentes mecanismos fisiológicos que les permiten superar la falta de oxígeno, como los andinos y los tibetanos, dos de las culturas más antiguas que viven a gran altitud. Se ha observado también que las personas que viven en regiones de gran altitud comparten generalmente ciertos rasgos fisiológicos derivados de las condiciones en las que viven, entre ellos: menor estatura media, caja torácica más grande, gradientes alveolares/arteriales de O_2 más estrechos, mayor capacidad pulmonar, mayor flujo sanguíneo de la arteria uterina durante el embarazo y mayor eficiencia en el tranporte y la utilización del O_2 (Akunov et al., 2018; Beall, 2007; Fierce et al., 2016; Frisancho, 1977; Frisancho, 2013; Frisancho et al., 1999; Jansen & Basnyat, 2011; Julian & Moore, 2019; Li et al., 2018; Pérez-Padilla, 2022).

Se ha demostrado que los tibetanos, por ejemplo, tienen una mayor ventilación en reposo (15,0 L/min) que las personas que viven a nivel del mar (11 L/min), lo que les permite hacer frente a la hipoxia (Beall, 2007). Por otra parte, se ha demostrado que los andinos tienen una ventilación en reposo similar a la de las personas que viven a nivel del mar, pero una concentración de hemoglobina más elevada. La saturación de oxígeno y la concentración de hemoglobina determinan el contenido de oxígeno arterial, por lo que los habitantes de las tierras altas andinas parecen sobre compensar la hipoxia ambiental, con un mayor contenido de oxígeno arterial. Además, se ha observado que las mujeres andinas embarazadas que viven a gran altitud aumentan la entrega de oxígeno al útero y la placenta mediante el aumento de la ventilación y la saturación de oxígeno (Beall, 2007; Julian & Moore, 2019). Por lo tanto, aunque el alcance y los mecanismos por los que la altitud influye en la exposición a la contaminación atmosférica siguen siendo objeto de investigación, las condiciones extremas de hipoxia (que conducen a un aumento de la ventilación) aumentan los riesgos asociados a la exposición a la contaminación atmosférica.

Entre las mayores ciudades de LA ($\gtrsim$ 2 millones de habitantes) se encuentran Ciudad de México (2850 m de altitud, México), Bogotá (2620 m de altitud, Colombia), Quito (2240 m de altitud, Ecuador), La Paz (3200-3600 m de altitud) y El Alto (4050 m de altitud). El número limitado de estudios existentes sobre la calidad del aire muestra que las ciudades más pobladas, como Ciudad de México y Bogotá, así como la ciudad más pequeña de Quito, están experimentando un deterioro de la calidad del aire.

Los estudios de calidad del aire realizados en estas ciudades apuntan a dos grandes fuentes comunes de material particulado, el tráfico y el polvo (Ramírez et al., 2018a; Raysoni et al., 2017; Vega et al., 2012), que suele tener una componente antropogénica. Sin embargo, la aplicación de estrategias de control de emisiones, como la reducción del contenido de azufre de los combustibles, la restricción del tráfico vehicular y las actualizaciones tecnológicas en la industria, están empezando a dar resultados alentadores en Ciudad de México y Bogotá. Por ejemplo, en Bogotá, a pesar de que las fuentes móviles han aumentado un 100% en la última década, las concentraciones de PM_{10} han mostrado una disminución constante, y las concentraciones de $PM_{2.5}$ no parecen haber empeorado según Mura et al. (2020). Por otra parte, en la Ciudad de México, aunque las concentraciones de PM_{10} no han mostrado ninguna mejora significativa, Morton-Bermea et al. (2021) informaron que las concentraciones de plomo (Pb), cobalto (Co), mercurio (Hg), manganeso (Mn), arsénico (As) y cadmio (Cd) han disminuído. Esto demuestra el alentador impacto beneficioso que las acciones impulsadas por las políticas de calidad del aire pueden tener en las emisiones de PM y en la calidad del aire de una ciudad.

Objetivos del estudio

La Paz y El Alto forman la segunda región metropolitana más grande de Bolivia, y es considerada una de las áreas metropolitanas más altas del mundo (3000-4000 m sobre el nivel del mar). Esta conurbación cuenta actualmente con una población de casi 2 millones de habitantes (INE, 2020c). Durante la última década, el gobierno, los municipios y la comunidad científica han trabajado para evaluar la calidad del aire en la región. Las normativas sobre la antigüedad de los coches importados, la introducción de medios alternativos de

transporte público, el establecimiento de redes de control de la calidad del aire y las restricciones a la circulación de vehículos en el centro de las ciudades son algunos ejemplos de estos esfuerzos. Sin embargo, a nuestro conocimiento, no se han realizado estudios a largo plazo sobre la calidad del aire para investigar la masa y la composición química de las partículas en esta región de condiciones extremas.

En este contexto, esta tesis pretende identificar y caracterizar las fuentes de partículas que afectan a la calidad del aire en la región metropolitana de La Paz y El Alto, y estudiar la dinámica y el transporte de contaminantes hacia/desde/entre ambas ciudades. El objetivo es también evaluar el impacto de la exposición a la contaminación atmosférica en la salud de los habitantes de la aglomeración, y proporcionar una línea de base de la calidad del aire en la zona en la que puedan basarse las políticas y normativas en materia de calidad del aire.

Este trabajo se basa en datos de calidad del aire, meteorológicos y sanitarios recogidos entre 2016 y 2019 en las dos ciudades. Para alcanzar estos objetivos, se prevé:

- Combinar mediciones simultáneas en línea y fuera de línea de las propiedades físicas y químicas de los aerosoles particulados medidas en La Paz y El Alto.
- Aplicar diferentes métodos de prorrateo de fuentes.
- Incluir los inventarios de emisiones existentes.
- Combinar datos de calidad del aire con respuestas epidemiológicas para evaluar la posible presencia y magnitud de una asociación entre ambos.

Metodología

Sitios de muestreo.

Para evaluar las propiedades de la contaminación urbana, se estableció en cada ciudad un lugar de muestreo de la contaminación urbana de fondo, donde se midieron simultáneamente varios parámetros ambientales y meteorológicos. Los lugares de muestreo estaban situados a 7 km de distancia entre sí, con una diferencia de altitud de más de 400 m, y a unos 20 km de la estación de vigilancia de la Atmósfera Global de Chacaltaya (CHC-GAW).

El sitio de medición de El Alto (EA) se estableció dentro del aeropuerto internacional de El Alto, en las instalaciones del observatorio meteorológico (16.5100° S, 68.1987° O, 4025 m de altitud). El observatorio se encuentra a aproximadamente 300 m de la pista del aeropuerto y a 500 m de la carretera principal más cercana. El tráfico del aeropuerto es generalmente escaso, especialmente durante el día, y no se observaron picos significativos en los parámetros medidos (CO_2, PM) durante el despegue o el aterrizaje de los aviones. El tráfico vehicular alrededor del aeropuerto es prácticamente inexistente. La zona que rodea el lugar de muestreo no está asfaltada y no existen otros edificios en las proximidades del observatorio.

El lugar de medición en La Paz (LP) se situó en el tejado del museo Pipiripi de la ciudad (Espacio Interactivo Memoria y Futuro Pipiripi: 16.5013°S, 68.1259°W, 3600 m sobre el nivel del mar). Este edificio municipal está situado en una pequeña colina en el centro de La Paz. A diferencia del emplazamiento de EA, en un radio de 1 km, el emplazamiento LP está rodeado de numerosas calles y avenidas muy transitadas, y densas zonas residenciales, con una distancia mínima horizontal y vertical desde la calle más cercana de aproximadamente 70 y 45 m, respectivamente. Por otro lado, las inmediaciones del emplazamiento (en un radio de aproximadamente 100 m) están cubiertas por zonas verdes y un parqueo para autobuses municipales al pie de la colina. Como el sitio de muestreo se encuentra situado en el centro de la ciudad, el tránsito de vehículos pesados (aparte de los autobuses públicos) es limitado.

La campaña de muestreo de PM se desarrolló entre abril de 2016 y noviembre de 2018, y el muestreo de PM en La Paz se extendió hasta marzo de 2019. Además, en 2021 se inició la vigilancia en línea del ozono (O3). La campaña combinó técnicas online y offline para la caracterización química y física de las partículas de aerosoles atmosféricos. Así, dado que el inicio y el final del muestreo de los diferentes instrumentos ubicados en cada emplazamiento no coincidieron, la Tabla 1 muestra los diferentes instrumentos instalados durante la campaña y la Figura 1 muestra la disponibilidad de datos a lo largo de los años 2016 a 2019 con periodicidad semanal.

Tabla 1. Resumen de la instrumentación instalada en cada una de las estaciones urbanas, su periodo de funcionamiento y su resolución temporal.

	El Alto	*La Paz*
Aethalometro AE33	Abril 2016 - Septiembre 2017 (1-min)	X
Aethalometro AE31	Enero 2018 - Junio 2018 (5-min)	Abril 2016 - Junio 2018 (5-min)
Muestras PM_{10}	Abril 2016 - Junio 2017 (24 h cada 3 días)	Abril 2016 - Junio 2018 (24 h cada 3 días)[15]
Muestras $PM_{2.5}$	Junio 2017 - Junio 2018 (24 h cada 3 días)	Junio 2017 - Junio 2018 (24 h cada 3 días)
SP2-XR	Abril 2018 - Mayo 2018 (1-min)	Abril 2018 - Mayo 2018 (1-min)
Meteorología	Abril 2016 - Junio 2018 (1 h)	Abril 2016 - Junio 2018 (1 día)

[15] Después de junio de 2017, solo se recogieron 25 muestras de filtro de PM_{10} de forma intermitente debido a problemas técnicos.

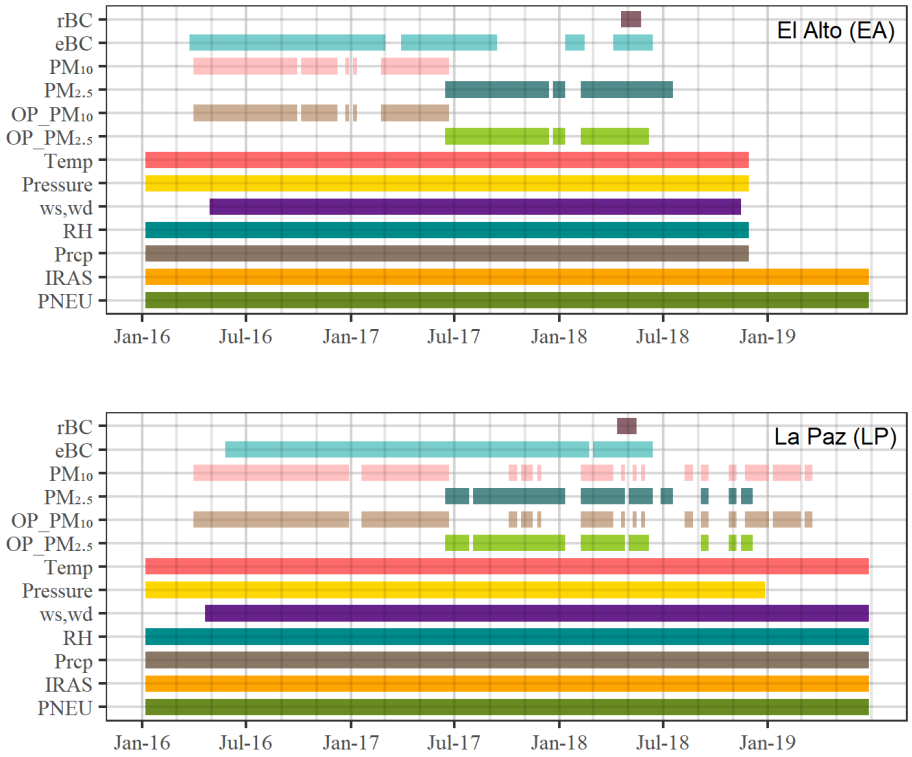

Figura 1: Descripción gráfica de los datos disponibles para todos los parámetros atmosféricos, meteorológicos y epidemiológicos medidos a lo largo de la campaña en cada emplazamiento.

Conclusiones

Los objetivos generales de este estudio fueron documentar los niveles de partículas contaminantes que afectan la calidad del aire en la región metropolitana de La Paz y El Alto, identificar sus fuentes de emisión y evaluar el impacto potencial de la exposición a la contaminación atmosférica en la salud de los habitantes de la región. A más largo plazo, el objetivo del estudio es proporcionar información sobre los factores que influyen en la calidad del aire de esta región, a partir de la cual puedan elaborarse políticas y normativas en materia de calidad del aire.

Aunque algunos estudios previos han caracterizado los niveles de contaminación en las grandes aglomeraciones urbanas de América Latina, muy pocos han abordado los vínculos entre los contaminantes atmosféricos y los resultados epidemiológicos, mucho menos utilizado el potencial oxidativo de las partículas como métrica de la calidad del aire. El presente estudio es único, no sólo porque documenta por primera vez la naturaleza de la contaminación por partículas en La Paz-El Alto, sino también por las particularidades de la región: altitud (3200 m a 4100 m sobre el nivel del mar), topografía compleja, intensa radiación solar durante el día y respuestas fisiológicas distintas de los habitantes para adaptarse a las condiciones de baja presión.

A lo largo de este trabajo se ha presentado una descripción detallada del estado de la calidad del aire en términos de partículas en suspensión, junto con sus principales fuentes de emisión. Esta información, combinada con los datos sanitarios locales, constituyó la base de una evaluación inicial del impacto potencial

de las partículas en la salud de los habitantes de la región. El estudio se centró en tres parámetros generalmente utilizados para describir la calidad del aire: las concentraciones másicas de partículas (PM) y su especiación química, el carbón negro (BC) y el potencial oxidativo (OP).

En la aglomeración La Paz-El Alto, las concentraciones de PM_{10} medidas a lo largo del periodo de estudio rara vez superaron las directrices de la Organización Mundial de la Salud (OMS). Estos episodios se produjeron principalmente durante la estación seca. Sin embargo, hay que tener en cuenta que los niveles de fondo de partículas contaminantes pueden diferir significativamente de las concentraciones cerca de las fuentes de emisión, y que los niveles de fondo son lo suficientemente altos como para considerar que muchos habitantes de ambas ciudades están expuestos a niveles nocivos de contaminación.

Utilizando diversas herramientas matemáticas y estadísticas, fue posible identificar las principales fuentes de cada uno de estos parámetros y su variabilidad temporal, observándose que las fuentes de emisión son principalmente locales y están fuertemente moduladas por la meteorología del lugar. Utilizando la herramienta de factorización matricial positiva (PMF) (US EPA) y la amplia gama de compuestos químicos analizados a partir de muestras de PM_{10}, fue posible identificar 11 fuentes principales que afectan a la calidad del aire en la aglomeración urbana. La proximidad de las dos ciudades permitió asignar las fuentes de PM mediante un enfoque multi-sitio, técnica cada vez más utilizada por la robustez que confiere al análisis.

Los resultados del estudio PMF mostraron que casi el 50% de las concentraciones másicas de partículas medidas en los dos sitios pueden atribuirse al polvo mineral (resuspendido de forma natural y antropogénica) y a las emisiones vehiculares. Las mismas también están relacionadas con fuentes secundarias de partículas que tienen su origen en los gases precursores emitidos por los automóviles (nitrato secundario y sulfato secundario). La tercera fuente de contaminación más importante es la quema de biomasa (BB), vinculada a las prácticas agrícolas y a los cambios de uso del suelo en la zona de las tierras bajas. Las mayores emisiones de quema de biomasa se producen generalmente al final de la estación seca y contribuyen a superar los umbrales de exposición a PM_{10} recomendados por la OMS. Por último, las demás contribuciones a las concentraciones de partículas se atribuyeron a fuentes naturales (aerosoles orgánicos biogénicos primarios y secundarios). Un resultado muy interesante del estudio, basado en la inclusión de trazadores orgánicos en el PMF, fue permitir la resolución de una fuente que contribuye a una pequeña parte de la masa de partículas, asociada a la combustión abierta de residuos, pero que es responsable de una gran parte de los trazadores orgánicos que se sabe que son nocivos para la salud.

Es pertinente señalar que el uso de la PMF se hizo dificultó debido a la falta de información existente sobre los perfiles químicos de emisión de las fuentes en esta región. La transposición directa de los perfiles de fuentes de estudios anteriores en ciudades europeas puede dar lugar a errores en la identificación de las fuentes de emisión, lo que debería tenerse en cuenta en futuros estudios.

El segundo parámetro de la calidad del aire analizado en este estudio es la concentración de BC. Además del importante papel que desempeña el BC en el clima, su importancia radica en el pequeño tamaño de sus

partículas y su potencial para transportar compuestos peligrosos a lo profundo de los pulmones. Muy pocos estudios describen este parámetro en la región sudamericana, y aún menos se han realizado en condiciones de gran altitud. En La Paz y El Alto, las diferentes condiciones meteorológicas encontradas en cada ciudad hacen que la variabilidad diurna de BC sea distinta, pero no se observaron diferencias significativas en las concentraciones medias de BC entre los sitios. Se observó que las condiciones particulares de combustión en estas ciudades dan lugar a la emisión de partículas más finas que las que se observan habitualmente a nivel del mar. Las secciones transversales de absorción de masa (MAC) asociadas a estas partículas resultaron ser coherentes con los valores MAC reportados en estudios previos, valores que corresponden a BC recién emitido medido en estaciones urbanas de fondo.

Las propiedades ópticas del BC en la aglomeración indican que las emisiones vehiculares son la principal fuente de BC, lo que confirma el estudio de PMF. Además, la ejecución de un modelo de dos fuentes, basado en la dependencia de la longitud de onda de los coeficientes de absorción, indicó que BB también era una fuente contribuyente significativa durante la estación seca. Se implementó también un método de deconvolución de fuentes de BC basado en la asociación de coeficientes de absorción de múltiples longitudes de onda con la contribución en masa de PM de las fuentes resueltas por el análisis PMF. El análisis se llevó a cabo mediante la regresión lineal múltiple (MLR), que confirmó los resultados obtenidos con el modelo bilineal. Se trata de un método complementario innovador y estadísticamente válido para caracterizar las propiedades ópticas específicas de las fuentes de partículas de aerosol en lugares en los que se han llevado a cabo estudios de reparto de fuentes de partículas.

Las concentraciones másicas de partículas están dominadas principalmente por la masa de las partículas de mayor tamaño, que suponen una menor amenaza para la salud y proceden con mayor frecuencia de fuentes naturales. Por lo tanto, es necesario establecer parámetros de calidad del aire que puedan utilizarse para evaluar la toxicidad de las partículas. Uno de los parámetros propuestos para alcanzar este objetivo y que ha mostrado asociaciones significativas con los efectos sobre la salud es el potencial oxidativo (OP). En el presente trabajo, nos enfocamos principalmente en el OP de las partículas, medido mediante dos pruebas acelulares: OP_{DTT} (ditiotreitol) y OP_{DCHF} (diclorofluoresceína). Utilizando el mismo método de regresión lineal múltiple descrito en el párrafo anterior, discriminamos las principales fuentes de la actividad de OP observada en ambas ciudades. La actividad reconstruida de OP_{DTT} y OP_{DCFH} se atribuyó principalmente a fuentes antropogénicas de PM, en particular: emisiones vehiculares, combustión de biomasa y combustión de residuos al aire libre, así como a fuentes secundarias de aerosoles cuyos precursores proceden de la combustión de combustibles fósiles.

Somos conscientes de las limitaciones de nuestro estudio. Sin duda, la estrategia de monitoreo hubiera sido mós robusta si se hubiese complementado con el análisis de componentes gaseosos (NOx y compuestos orgánicos volátiles específicos) para obtener una descripción holística del estado de la calidad del aire en la región. Sin embargo, esto no es una tarea fácil en Bolivia, entre otras cosas por las dificultades de acceso a los gases de referencia para la calibración de los instrumentos. También somos conscientes de todas las

dificultades encontradas para mantener un monitoreo a largo plazo en La Paz-El Alto: el funcionamiento de los instrumentos a baja presión es siempre problemático, el reemplazo de las piezas técnicas no es inmediato, el mantenimiento regular por parte del personal del laboratorio de física atmosférica de la Universidad Mayor de San Andrés (UMSA-LFA) es exigente, pero este estudio es también una oportunidad para sugerir algunas mejoras en la organización logística. Una primera recomendación que podemos hacer para la continuidad de las actividades es evitar cambios en las metodologías de muestreo y asegurar que cualquier cambio existente se documente con un período de mediciones paralelas, de manera que se asegure la continuidad de las medidas y se puedan corregir las posibles discrepancias. En nuestro estudio, estos cambios provocaron una reducción de las series temporales disponibles, lo que redujo la potencia estadística del análisis. También se introdujo incertidumbre adicional por la diferencia en la instrumentación dentro de los sitios y la falta de períodos de intercomparación para instrumentos en línea que miden en las mismas condiciones.

Consideramos que los resultados del análisis riguroso de los tres diferentes parámetros de calidad del aire presentados en este trabajo establecen una línea base de la exposición general de los habitantes de La Paz-El Alto a los contaminantes particulados. Este estudio contribuye también a la documentación de los estudios sobre la calidad del aire en la región poco estudiada de Sudamérica. Esperamos que este trabajo pueda ser utilizado para asesorar futuras decisiones políticas y que las diferentes metodologías de muestreo y análisis de datos implementadas puedan servir de referencia para facilitar la replicación de este estudio en otras partes del país y de la región. Consideramos que la descripción de la composición química de las partículas emitidas por las distintas fuentes resueltas también puede complementar los inventarios de emisiones existentes. De igual forma, este estudio puede ser considerado como una base sólida para la implementación y evaluación/validación de un modelo de transporte químico que podría permitir el pronóstico de la calidad del aire en la región. Por último, hasta donde sabemos, este es el primer estudio epidemiológico de series temporales de largo plazo que examina las asociaciones existentes entre los parámetros de calidad del aire y los efectos observados sobre la salud en Bolivia.

Estos trabajos han permitido describir el estado de la calidad del aire en el medio urbano, es decir, las concentraciones mínimas de partículas a las que están expuestos los residentes de la aglomeración. Sin embargo, las personas suelen estar expuestas diariamente a concentraciones mucho más elevadas. Por lo tanto, es imperativo adoptar medidas para mejorar la calidad del aire en la ciudad, dada la vulnerabilidad adicional asociada al hecho de vivir a gran altitud. Como se ha observado desde diversos puntos de vista, los principales responsables de la contaminación en La Paz-El Alto son las emisiones vehiculares. Consideramos de suma importancia un control más riguroso del estado de los vehículos que circulan en la ciudad. En segundo lugar, es crucial la implementación de sistemas de transporte masivo para reducir el tamaño de la flota de vehículos, o sistemas de transporte que utilicen fuentes de energía alternativas. Del mismo modo, debe prohibirse la incineración de residuos, ya que es una fuente importante de contaminantes peligrosos asociados a factores de alto riesgo para la salud humana. Finalmente, es esencial actualizar las políticas de emisiones contaminantes particulados y gaseosos para regular el impacto del creciente sector industrial. Una

reducción de las emisiones de las quemas de biomasa también supondría una mejora significativa de la calidad del aire en todo el país.

Sólo un seguimiento fiable, exhaustivo y a largo plazo de la calidad del aire permitirá evaluar la eficacia de las políticas de calidad del aire actuales y futuras. Un único punto de muestreo no basta para caracterizar espacialmente el estado de la calidad del aire en distintas partes de la ciudad. Por consiguiente, un mantenimiento adecuado y un mejor equipamiento de las redes de vigilancia de la calidad del aire existentes contribuirían significativamente a los esfuerzos por mejorar la calidad del aire en las áreas metropolitanas de Bolivia. Además, la introducción de una herramienta interactiva sobre el estado de la calidad del aire podría ser beneficiosa para advertir a la población sobre los picos de contaminación, de modo que puedan tomar medidas para reducir su propia exposición. Por último, consideramos importante sensibilizar a la población sobre los riesgos que la contaminación atmosférica significa para la salud, a fin de que pueda participar activamente en la reducción de las emisiones de contaminantes atmosféricos.

LIST OF FIGURES

LIST OF TABLES

REFERENCES

Aas, W., Mortier, A., Bowersox, V., Cherian, R., Faluvegi, G., Fagerli, H., Hand, J., Klimont, Z., Galy-Lacaux, C., Lehmann, C. M. B., Myhre, C. L., Myhre, G., Olivié, D., Sato, K., Quaas, J., Rao, P. S. P., Schulz, M., Shindell, D., Skeie, R. B., … Xu, X. (2019). Global and regional trends of atmospheric sulfur. *Scientific Reports*, *9*(1), 1–11. https://doi.org/10.1038/s41598-018-37304-0

Ahrens, C. D. (2012). *Essentials of Meteorology: An Invitation to the Atmosphere* (Sixth Edit). Cengage Learning. http://books.google.com/books?hl=en&lr=&id=2Yn29IFukbgC&oi=fnd&pg=PR15&dq=essentials+of+meteorology&ots=iBxgsf8asu&sig=7misqI0COKj-_LVyLFvWpyVuZ8o

Ahrens, C. D., & Henson, R. (2016). *Meteorology Today: An Introduction to Weather, Climate, and the Environment*. Cengage Learning.

Akunov, A., Sydykov, A., Toktash, T., & Doolotova, A. (2018). *Hemoglobin Changes After Long-Term Intermittent Work at High Altitude*. *9*(November), 1–7. https://doi.org/10.3389/fphys.2018.01552

Alas, H. D., Stöcker, A., Umlauf, N., Senaweera, O., Pfeifer, S., Greven, S., & Wiedensohler, A. (2022). Pedestrian exposure to black carbon and PM2.5 emissions in urban hot spots: new findings using mobile measurement techniques and flexible Bayesian regression models. *Journal of Exposure Science and Environmental Epidemiology*, *32*(4), 604–614. https://doi.org/10.1038/s41370-021-00379-5

Alastuey, A., Querol, X., Aas, W., Lucarelli, F., Pérez, N., Moreno, T., Cavalli, F., Areskoug, H., Balan, V., Catrambone, M., Ceburnis, D., Cerro, J. C., Conil, S., Gevorgyan, L., Hueglin, C., Imre, K., Jaffrezo, J. L., Leeson, S. R., Mihalopoulos, N., … Espen Yttri, K. (2016). Geochemistry of PM10 over Europe during the EMEP intensive measurement periods in summer 2012 and winter 2013. *Atmospheric Chemistry and Physics*, *16*(10), 6107–6129. https://doi.org/10.5194/acp-16-6107-2016

Alfaro-Moreno, E., García-Cuellar, C., De-Vizcaya-Ruiz, A., Rojas-Bracho, L., & Osornio-Vargas, A. R. (2010). Cellular Mechanisms behind Particulate Matter. In B. Gurjar, L. T. Molina, & C. S. P. Ojha (Eds.), *Air Pollution: Health and Enviromental Ipacts* (pp. 249–274). Taylor and Francis Group.

Aliaga, Di., Sinclair, V. A., Andrade, M., Artaxo, P., Carbone, S., Kadantsev, E., Laj, P., Wiedensohler, A., Krejci, R., & Bianchi, F. (2021). Identifying source regions of air masses sampled at the tropical high-altitude site of Chacaltaya using WRF-FLEXPART and cluster analysis. *Atmospheric Chemistry and Physics*, *21*(21), 16453–16477. https://doi.org/10.5194/acp-21-16453-2021

Alves, N. D. O., Vessoni, A. T., Quinet, A., Soares, R., Kajitani, G. S., Peixoto, M. S., Hacon, S. D. S., Artaxo, P., Saldiva, P., Frederico, C., Menck, M., & De, S. R. B. (2017). Biomass burning in the Amazon region causes DNA damage and cell death in human lung cells. *Scientific Reports*, 1–13. https://doi.org/10.1038/s41598-017-11024-3

Amato, F., Pandolfi, M., Escrig, A., Querol, X., Alastuey, A., Pey, J., Perez, N., & Hopke, P. K. (2009). Quantifying road dust resuspension in urban environment by Multilinear Engine: A comparison with PMF2. *Atmospheric Environment*, *43*(17), 2770–2780. https://doi.org/10.1016/j.atmosenv.2009.02.039

Amato, F., Viana, M., Richard, A., Furger, M., Prévôt, A. S. H., Nava, S., Lucarelli, F., Bukowiecki, N., Alastuey, A., Reche, C., Moreno, T., Pandolfi, M., Pey, J., & Querol, X. (2011). Size and time-resolved roadside enrichment of atmospheric particulate pollutants. *Atmospheric Chemistry and Physics*, *11*(6), 2917–2931. https://doi.org/10.5194/acp-11-2917-2011

Amato, Fulvio, Alastuey, A., Karanasiou, A., Lucarelli, F., Nava, S., Calzolai, G., Severi, M., Becagli, S., Gianelle, V. L., Colombi, C., Alves, C., Custódio, D., Nunes, T., Cerqueira, M., Pio, C., Eleftheriadis, K., Diapouli, E., Reche, C., Minguillón, M. C., … Querol, X. (2016). AIRUSE-LIFE+: A harmonized PM speciation and source apportionment in five southern European cities. *Atmospheric Chemistry and Physics*, *16*(5), 3289–3309. https://doi.org/10.5194/acp-16-3289-2016

Andrade, M., Zaratti, F., Forno, R., Gutiérrez, R., Moreno, I., Velarde, F., Ávila, F., Roca, M., Sánchez, M. F., Laj, P., Jaffrezo, J. L., Ginot, P., Sellegri, K., Ramonet, M., Laurent, O., Weinhold, K., Wiedensohler, A., Krejci, R., Bonasoni, P., … Whitema, O. (2015). Puesta en marcha de una nueva estación de monitoreo climático en los andes centrales de Bolivia: la estación Gaw/Chacaltaya. *Revista Boliviana de Física*, *26(26)*, 6–15.

Arias, P. A., Bellouin, N., Coppola, E., Jones, R. G., Krinner, G., Marotzke, J., Naik, V., Palmer, M. D., Plattner, G.-K., Rogelj, J., Rojas, M., Sillmann, J., Storelvmo, T., Thorne, P. W., Trewin, B., Rao, K. A., Adhikary, B., Allan, R. P., Armour, K., … Zickfe, K. (2021). Technical Summary. In V. Masson-Delmotte, P. Zhai, A. Pirani, S. L. Connors, C. Péan, S. Berger, N. Caud, Y. Chen, L. Goldfarb, M. I. Gomis, M. Huang, K. Leitzell, E. Lonnoy, J. B. R. Matthews, T. K. Maycock, T. Waterfield, O. Yelekçi, R. Yu, & B. Zhou (Eds.), *Climate Change 2021: The Physical Science Basis. Contribution of Working Group I to the Sixth Assessment Report of the Intergovernmental Panel on Climate Change* (pp. 22–144). Cambridge University Press. https://doi.org/10.1017/9781009157896.002

Arnott, W. P. (2003). Photoacoustic and filter-based ambient aerosol light absorption measurements: Instrument comparisons and the role of relative humidity. *Journal of Geophysical Research*, *108*(D1), 4034. https://doi.org/10.1029/2002JD002165

Arnott, W. Patrick, Hamasha, K., Moosmüller, H., Sheridan, P. J., & Ogren, J. A. (2005). Towards aerosol light-absorption measurements with a 7-wavelength aethalometer: Evaluation with a photoacoustic instrument and 3-wavelength nephelometer. *Aerosol Science and Technology*, *39*(1), 17–29. https://doi.org/10.1080/027868290901972

Arnott, W. Patrick, Moosmüller, H., Rogers, C. F., Jin, T., & Bruch, R. (1999). Photoacoustic spectrometer for measuring light absorption by aerosol: Instrument description. *Atmospheric Environment*, *33*(17), 2845–2852. https://doi.org/10.1016/S1352-2310(98)00361-6

Ayres, J. G., Borm, P., Cassee, F. R., Castranova, V., Donaldson, K., Ghio, A., Harrison, R. M., Hider, R., Kelly, F., Kooter, I. M., Marano, F., Maynard, R. L., Mudway, I., Nel, A., Sioutas, C., Smith, S., Baeza-Squiban, A., Cho, A., Duggan, S., & Froines, J. (2008). Evaluating the toxicity of airborne particulate matter and nanoparticles by measuring oxidative stress potential - A workshop report and consensus statement. *Inhalation Toxicology*, *20*(1), 75–99. https://doi.org/10.1080/08958370701665517

Backman, J., Schmeisser, L., Virkkula, A., Ogren, J. A., Asmi, E., Starkweather, S., Sharma, S., Eleftheriadis, K., Uttal, T., Jefferson, A., Bergin, M., Makshtas, A., Tunved, P., & Fiebig, M. (2017). On Aethalometer measurement uncertainties and an instrument correction factor for the Arctic. *Atmospheric Measurement Techniques*, *10*(12), 5039–5062. https://doi.org/10.5194/amt-10-5039-2017

Barlow, J., Berenguer, E., Carmenta, R., & França, F. (2020). Clarifying Amazonia's burning crisis. In *Global Change Biology* (Vol. 26, Issue 2, pp. 319–321). https://doi.org/10.1111/gcb.14872

Baron, P. A., & Willeke, K. (2005). *Atmospheric Measurement: Principles, Techniques and Applications*. Wiley.

Bates, J. T., Fang, T., Verma, V., Zeng, L., Weber, R. J., Tolbert, P. E., Abrams, J. Y., Sarnat, S. E., Klein, M., Mulholland, J. A., & Russell, A. G. (2019). Review of Acellular Assays of Ambient Particulate Matter Oxidative Potential : Methods and Relationships with Composition , Sources , and Health E ff ects. *Enviromental Science and Technology*, *53*, 4003–4019. https://doi.org/10.1021/acs.est.8b03430

Baumgardner, D., Kok, G., & Raga, G. (2004). Warming of the Arctic lower stratosphere by light absorbing particles. *Geophysical Research Letters*, *31*(6), 10–13. https://doi.org/10.1029/2003gl018883

Beall, C. M. (2007). Two routes to functional adaptation: Tibetan and Andean high-altitude natives. *Proceedings of the National Academy of Sciences of the United States of America*, *104*(SUPPL. 1), 8655–8660. https://doi.org/10.1073/pnas.0701985104

Belis, C. A., Favez, O., Mircea, M., Diapouli, E., Manousakas, M.-I., S., V., Gilardoni, S., Paglione, M., Decesari, S., Mocnik, G., Mooibroek, D., Salvador, P., Takahama, S., Vecchi, R., & Paatero, P. (2019). *European guide on air pollution source apportionment with receptor models: revised version 2019.* (Issue January). https://doi.org/10.2760/439106

Belis, C. A., Pernigotti, D., Karagulian, F., Pirovano, G., Larsen, B. R., Gerboles, M., & Hopke, P. K. (2015). A new methodology to assess the performance and uncertainty of source apportionment models in intercomparison exercises. *Atmospheric Environment*, *119*, 35–44. https://doi.org/10.1016/j.atmosenv.2015.08.002

Bergstrom, R. W., Pilewskie, P., Russell, P. B., Redemann, J., Bond, T. C., Quinn, P. K., & Sierau, B. (2007). Spectral absorption properties of atmospheric aerosols. *Atmospheric Chemistry and Physics*, *7*(23), 5937–5943. https://doi.org/10.5194/acp-7-5937-2007

Bernardoni, V., Ferrero, L., Bolzacchini, E., Corina Forello, A., Gregorič, A., Massabò, D., Mocnik, G., Prati, P.,

Rigler, M., Santagostini, L., Soldan, F., Valentini, S., Valli, G., & Vecchi, R. (2021). Determination of Aethalometer multiple-scattering enhancement parameters and impact on source apportionment during the winter 2017/18 EMEP/ACTRIS/COLOSSAL campaign in Milan. *Atmospheric Measurement Techniques*, *14*(4), 2919–2940. https://doi.org/10.5194/amt-14-2919-2021

Bernstein, D. M. (2022). The health effects of short fiber chrysotile and amphibole asbestos. *Critical Reviews in Toxicology*, *52*(2), 89–112. https://doi.org/10.1080/10408444.2022.2056430

Besombes, J. L., Maître, A., Patissier, O., Marchand, N., Chevron, N., Stoklov, M., & Masclet, P. (2001). Particulate PAHs observed in the surrounding of a municipal incinerator. *Atmospheric Environment*, *35*(35), 6093–6104. https://doi.org/10.1016/S1352-2310(01)00399-5

Bianchi, F., Sinclair, V. A., Aliaga, D., Zha, Q., Scholz, W., Wu, C., Heikkinen, L., Modini, R., Partoll, E., Velarde, F., Moreno, I., Gramlich, Y., Huang, W., Koenig, A. M., Leiminger, M., Enroth, J., Peräkylä, O., Marinoni, A., Xuemeng, C., … Mohr, C. (2022). The SALTENA Experiment. *Bulletin of the American Meteorological Society*, 212–229.

Birch, M. E., & Cary, R. A. (1996). Elemental Carbon-Based Method for Monitoring Occupational Exposures to Particulate Diesel Exhaust. *Aerosol Science and Technology*, *25*(3), 221–241. https://doi.org/10.1080/02786829608965393

Bishop, G. A., Morris, J. A., Stedman, D. H., Cohen, L. H., Countess, R. J., Countess, S. J., Maly, P., & Scherer, S. (2001). The effects of altitude on heavy-duty diesel truck on-road emissions. *Environmental Science and Technology*, *35*(8), 1574–1578. https://doi.org/10.1021/es001533a

Bockhorn, H. (2013). *Soot formation in combustion: mechanisms and models* (Vol. 59). Springer Science & Business Media.

Bond, T.C., Anderson, T. L., & Campbell, D. (1999). Calibration and Intercomparison of Filter-Based Measurements of Visible Light Absorption by Aerosols. *Aerosol Science and Technology*, *30*(6), 582–600. https://doi.org/10.1080/027868299304435

Bond, T.C., & Bergstrom, R. W. (2006). Light Absorption by Carbonaceous Particles: An Investigative Review. *Aerosol Science and Technology*, *40*(1), 27–67. https://doi.org/10.1080/02786820500421521

Bond, T.C., Doherty, S. J., Fahey, D. W., Forster, P. M., Berntsen, T., Deangelo, B. J., Flanner, M. G., Ghan, S., K??rcher, B., Koch, D., Kinne, S., Kondo, Y., Quinn, P. K., Sarofim, M. C., Schultz, M. G., Schulz, M., Venkataraman, C., Zhang, H., Zhang, S., … Zender, C. S. (2013). Bounding the role of black carbon in the climate system: A scientific assessment. *Journal of Geophysical Research Atmospheres*, *118*(11), 5380–5552. https://doi.org/10.1002/jgrd.50171

Bond, T.C., Zarzycki, C., Flanner, M. G., & Koch, D. M. (2011). Quantifying immediate radiative forcing by black carbon and organic matter with the Specific Forcing Pulse. *Atmospheric Chemistry and Physics*, *11*(4),

1505–1525. https://doi.org/10.5194/acp-11-1505-2011

Bond, Tami C, Habib, G., & Bergstrom, R. W. (2006). Limitations in the enhancement of visible light absorption due to mixing state. *Journal of Geophysical Research Atmospheres*, *111*(20), 1–13. https://doi.org/10.1029/2006JD007315

Borlaza, L. J. S., Cosep, E. M. R., Kim, S., Lee, K., Joo, H., Park, M., Bate, D., Cayetano, M. G., & Park, K. (2018). Oxidative potential of fine ambient particles in various environments. *Environmental Pollution*, *243*, 1679–1688. https://doi.org/10.1016/j.envpol.2018.09.074

Borlaza, L. J. S., Uzu, G., Ouidir, M., Lyon-Caen, S., Marsal, A., Weber, S., Siroux, V., Lepeule, J., Boudier, A., Jaffrezo, J.-L., Slama, R., & SEPAGES cohort study groupLucille Joanna S. Borlaza 1, Gaëlle Uzu1✉, Marion Ouidir2, Sarah Lyon-Caen2, Anouk Marsal1, Samuël Weber1, Valérie Siroux2, Johanna Lepeule2, Anne Boudier2, 3, Jean-Luc Jaffrezo1, R. S. and the S. cohort study group. (2022a). Personal exposure to PM 2 .5 oxidative potential and its association to birth outcomes. *Journal of Exposure Science & Environmental Epidemiology*, 1–11. https://doi.org/10.1038/s41370-022-00487-w

Borlaza, L. J. S., Weber, S., Jaffrezo, J. L., Houdier, S., Slama, R., Rieux, C., Albinet, A., Micallef, S., Trébluchon, C., & Uzu, G. (2021b). Disparities in particulate matter (PM10) origins and oxidative potential at a city scale (Grenoble, France) - Part 2: Sources of PM10 oxidative potential using multiple linear regression analysis and the predictive applicability of multilayer perceptron n. *Atmospheric Chemistry and Physics*, *21*(12), 9719–9739. https://doi.org/10.5194/acp-21-9719-2021

Borlaza, L. J. S., Weber, S., Uzu, G., Jacob, V., Cañete, T., Micallef, S., Trébuchon, C., Slama, R., Favez, O., & Jaffrezo, J. L. (2021a). Disparities in particulate matter (PM10) origins and oxidative potential at a city scale (Grenoble, France) - Part 1: Source apportionment at three neighbouring sites. *Atmospheric Chemistry and Physics*, *21*(7), 5415–5437. https://doi.org/10.5194/acp-21-5415-2021

Borlaza, L. J., Weber, S., Marsal, A., Uzu, G., Jacob, V., Besombes, J. L., Chatain, M., Conil, S., & Jaffrezo, J. L. (2022b). Nine-year trends of PM10sources and oxidative potential in a rural background site in France. *Atmospheric Chemistry and Physics*, *22*(13), 8701–8723. https://doi.org/10.5194/acp-22-8701-2022

Boulon, J., Sellegri, K., Venzac, H., Picard, D., Weingartner, E., Wehrle, G., Collaud Coen, M., Bütikofer, R., Flückiger, E., Baltensperger, U., & Laj, P. (2010). New particle formation and ultrafine charged aerosol climatology at a high altitude site in the Alps (Jungfraujoch, 3580 m a.s.l., Switzerland). *Atmospheric Chemistry and Physics*, *10*(19), 9333–9349. https://doi.org/10.5194/acp-10-9333-2010

Bourgeois, Q., Ekman, A. M. L., & Krejci, R. (2015). Aerosol transport over the andes from the amazon basin to the remote Pacific Ocean: A multiyear CALIOP assessment. *Journal of Geophysical Research*, *120*(16), 8411–8425. https://doi.org/10.1002/2015JD023254

Bravo, H. A., & Torres, R. J. (2000). The usefulness of air quality monitoring and air quality impact studies before

the introduction of reformulated gasolines in developing countries . Mexico City , a real case study. *Atmospheric Environment*, *34*(499–506).

Brines, M., Dall'Osto, M., Beddows, D. C. S., Harrison, R. M., Gómez-Moreno, F., Núñez, L., Artíñano, B., Costabile, F., Gobbi, G. P., Salimi, F., Morawska, L., Sioutas, C., & Querol, X. (2015). Traffic and nucleation events as main sources of ultrafine particles in high-insolation developed world cities. *Atmospheric Chemistry and Physics*, *15*(10), 5929–5945. https://doi.org/10.5194/acp-15-5929-2015

Brines, Mariola, Dall'Osto, M., Amato, F., Minguillón, M. C., Karanasiou, A., Grimalt, J. O., Alastuey, A., Querol, X., & van Drooge, B. L. (2019). Source apportionment of urban PM1 in Barcelona during SAPUSS using organic and inorganic components. *Environmental Science and Pollution Research*, *26*(31), 32114–32127. https://doi.org/10.1007/s11356-019-06199-3

Brito, J., Rizzo, L. V, Herckes, P., Vasconcellos, P. C., Caumo, S. E. S., Fornaro, A., Ynoue, R. Y., Artaxo, P., & Andrade, M. F. (2013). Physical–chemical characterisation of the particulate matter inside two road tunnels in the São Paulo Metropolitan Area. *Atmospheric Chemistry and Physics*, *13*(24), 12199–12213. https://doi.org/10.5194/acp-13-12199-2013

Cakmak, S., Dales, R., Kauri, L. M., Mahmud, M., Ryswyk, K. Van, Vanos, J., Liu, L., Kumarathasan, P., Thomson, E., Vincent, R., & Weichenthal, S. (2014). Metal composition of fine particulate air pollution and acute changes in cardiorespiratory physiology. *Environmental Pollution*.

Calas, A., Uzu, G., Kelly, F. J., Houdier, S., Martins, J. M. F., Thomas, F., Molton, F., Charron, A., Dunster, C., Oliete, A., Jacob, V., Besombes, J.-L., Chevrier, F., & Jaffrezo, J.-L. (2018). Comparison between five acellular oxidative potential measurement assays performed with detailed chemistry on PM₁₀ samples from the city of Chamonix (France). *Atmospheric Chemistry and Physics*, *18*(11), 7863–7875. https://doi.org/10.5194/acp-18-7863-2018

Caponi, L., Formenti, P., Massabó, D., Biagio, C. Di, Cazaunau, M., Pangui, E., Chevaillier, S., Landrot, G., Andreae, M. O., Kandler, K., Piketh, S., Saeed, T., Seibert, D., Williams, E., Balkanski, Y., Prati, P., Doussin, J., Atmosphériques, S., Cnrs, U. M. R., … Darmstadt, T. U. (2017). *Spectral- and size-resolved mass absorption efficiency of mineral dust aerosols in the shortwave spectrum : a simulation chamber study*. 7175–7191.

Cappa, C. D., Onasch, T. B., Massoli, P., Worsnop, D. R., Bates, T. S., Cross, E. S., Davidovits, P., Hakala, J., Hayden, K. L., Jobson, B. T., Kolesar, K. R., Lack, D. A., Lerner, B. M., Li, S.-M., Mellon, D., Nuaaman, I., Olfert, J. S., Petaja, T., Quinn, P. K., … Zaveri, R. A. (2012). Radiative Absorption Enhancements Due to the Mixing State of Atmospheric Black Carbon. *Science*, *337*(6098), 1078–1081. https://doi.org/10.1126/science.1223447

Cárdenas-Moreno, P. R., Moreno-Torres, L. R., Lovallo, M., Telesca, L., & Ramírez-Rojas, A. (2021). Spectral, multifractal and informational analysis of PM10 time series measured in Mexico City Metropolitan Area.

Physica A: Statistical Mechanics and Its Applications, *565*, 125545. https://doi.org/10.1016/j.physa.2020.125545

Carrese, S., Gemma, A., & La, S. (2013). Impacts of driving behaviours , slope and vehicle load factor on bus fuel consumption and emissions : a real case study in the city of Rome. *Procedia - Social and Behavioral Sciences*, *87*, 211–221. https://doi.org/10.1016/j.sbspro.2013.10.605

Cash, J. M., Langford, B., Di Marco, C., Mullinger, N. J., Allan, J., Reyes-Villegas, E., Joshi, R., Heal, M. R., Acton, W. J. F., Hewitt, C. N., Misztal, P. K., Drysdale, W., Mandal, T. K., Shivani, Gadi, R., Gurjar, B. R., & Nemitz, E. (2021). Seasonal analysis of submicron aerosol in Old Delhi using high-resolution aerosol mass spectrometry: Chemical characterisation, source apportionment and new marker identification. *Atmospheric Chemistry and Physics*, *21*(13), 10133–10158. https://doi.org/10.5194/acp-21-10133-2021

Castro Verdezoto, P. L., Vidoza, J. A., & Gallo, W. L. R. (2019). Analysis and projection of energy consumption in Ecuador: Energy efficiency policies in the transportation sector. *Energy Policy*, *134*(November 2018). https://doi.org/10.1016/j.enpol.2019.110948

Cavalli, F., Viana, M., Yttri, K. E., Genberg, J., & Putaud, J. P. (2010). Toward a standardized thermal-optical protocol for measuring atmospheric organic and elemental carbon: The eusaar protocol. *Atmospheric Measurement Techniques*, *3*, 79–89.

Cesari, D., Amato, F., Pandolfi, M., Alastuey, A., Querol, X., & Contini, D. (2016). An inter-comparison of PM10 source apportionment using PCA and PMF receptor models in three European sites. *Environmental Science and Pollution Research*, *23*(15), 15133–15148. https://doi.org/10.1007/s11356-016-6599-z

Chaffin, C. A., & Ullman, T. L. (1994). Effects of increased altitude on heavy-duty diesel engine emissions. *SAE Technical Papers*, *412*. https://doi.org/10.4271/940669

Chan, T. W., Brook, J. R., Smallwood, G. J., & Lu, G. (2011). Time-resolved measurements of black carbon light absorption enhancement in urban and near-urban locations of southern Ontario, Canada. *Atmospheric Chemistry and Physics*, *11*(20), 10407–10432. https://doi.org/10.5194/acp-11-10407-2011

Charrier, J. G., & Anastasio, C. (2012). On dithiothreitol (DTT) as a measure of oxidative potential for ambient particles: Evidence for the importance of soluble \newline transition metals. *Atmospheric Chemistry and Physics*, *12*(19), 9321–9333. https://doi.org/10.5194/acp-12-9321-2012

Charron, A., Polo-rehn, L., Besombes, J., Golly, B., Buisson, C., Chanut, H., Marchand, N., Guillaud, G., Jaffrezo, J., Savoie, U., Blanc, M., Velin, V., Auvergne-rhône-alpes, A., & Université, A. (2019). Identification and quantification of particulate tracers of exhaust and non-exhaust vehicle emissions. *Atmospheric Chemistry and Physics*, *29*, 5187–5207. https://doi.org/https://doi.org/10.5194/acp-19-5187-2019

Chauvigne, A., Aliaga, D., Sellegri, K., Montoux, N., Krejci, R., Mocnik, G., Moreno, I., Müller, T., Pandolfi, M., Velarde, F., Weinhold, K., Ginot, P., Wiedensohler, A., Andrade, M., & Laj, P. (2019). Biomass burning and

urban emission impacts in the Andes Cordillera region based on in situ measurements from the Chacaltaya observatory, Bolivia (5240a.s.l.). *Atmospheric Chemistry and Physics*, *19*(23), 14805–14824. https://doi.org/10.5194/acp-19-14805-2019

Chen, B., Bai, Z., Cui, X., Chen, J., Andersson, A., & Gustafsson, Ö. (2017). Light absorption enhancement of black carbon from urban haze in Northern China winter. *Environmental Pollution*, *221*, 418–426. https://doi.org/10.1016/j.envpol.2016.12.004

Cheng, Y. F., Berghof, M., Garland, R. M., Wiedensohler, A., Wehner, B., Müller, T., Su, H., Zhang, Y. H., Achtert, P., Nowak, A., Poschl, U., Zhu, T., Hu, M., & Zeng, L. M. (2009). Influence of soot mixing state on aerosol light absorption and single scattering albedo during air mass aging at a polluted regional site in northeastern China. *Journal of Geophysical Research Atmospheres*, *114*(11), 1–20. https://doi.org/10.1029/2008JD010883

Cheng, Y., Lee, S. C., Ho, K. F., Chow, J. C., Watson, J. G., Louie, P. K. K., Cao, J. J., & Hai, X. (2010). Chemically-speciated on-road PM2.5 motor vehicle emission factors in Hong Kong. *Science of the Total Environment*, *408*(7), 1621–1627. https://doi.org/10.1016/j.scitotenv.2009.11.061

Cheng, Yan, Chow, J. C., Watson, J. G., Zhou, J., Liu, S., & Cao, J. (2021). Decreasing concentrations of carbonaceous aerosols in China from 2003 to 2013. *Scientific Reports*, *11*(1), 1–10. https://doi.org/10.1038/s41598-021-84429-w

Chevrier, F. (2016). *Chauffage au bois et qualité de l'air en Vallée de l'Arve : définition d'un système de surveillance et impact d'une politique de rénovation du parc des appareils anciens* [Université Grenoble Alpes]. https://tel.archives-ouvertes.fr/tel-01527559/document

Cho, A. K., Sioutas, C., Miguel, A. H., Kumagai, Y., Schmitz, D. A., Singh, M., Eiguren-Fernandez, A., & Froines, J. R. (2005). Redox activity of airborne particulate matter at different sites in the Los Angeles Basin. *Environ Res*, *1*, 40–47. https://doi.org/10.1016/j.envres.2005.01.003.

Christian, T. J., Yokelson, R. J., Cárdenas, B., Molina, L. T., Engling, G., & Hsu, S. C. (2010). Trace gas and particle emissions from domestic and industrial biofuel use and garbage burning in central Mexico. *Atmospheric Chemistry and Physics*, *10*(2), 565–584. https://doi.org/10.5194/acp-10-565-2010

Chung, C. E., Lee, K., & Müller, D. (2012). Effect of internal mixture on black carbon radiative forcing. *Tellus, Series B: Chemical and Physical Meteorology*, *64*(1). https://doi.org/10.3402/tellusb.v64i0.10925

Claiborn, C. S., Larson, T., & Sheppard, L. (2002). Testing the Metals Hypothesis in Spokane , Washington. *Environmental Health Perspectives*, *110*(November 2001), 547–552.

Collaud Coen, M., Andrews, E., Lastuey, A., Petkov Arsov, T., Backman, J., Brem, B. T., Bukowiecki, N., Couret, C., Eleftheriadis, K., Flentje, H., Fiebig, M., Gysel-Beer, M., Hand, J. L., Hoffer, A., Hooda, R., Hueglin, C., Joubert, W., Keywood, M., Eun Kim, J., … Laj, P. (2020). Multidecadal trend analysis of in situ aerosol

radiative properties around the world. *Atmospheric Chemistry and Physics*, *20*(14), 8867–8908. https://doi.org/10.5194/acp-20-8867-2020

COMMISSION, E. (2022). *Proposal for a Directive of the European Parliament and of the Council on ambient air quality and cleaner air for Europe*. https://eur-lex.europa.eu/legal-content/EN/TXT/?uri=COM:2022:542:FIN

Correo del Sur. Bolivia: Importación de combustibles alcanza récord histórico. Correo del Sur, https://correodelsur.com/capitales/20220201_bolivia-importacion-de-combustibles-alcanza-record-historico.html, last access: 1 February 2022.

Crow, J. P. (1997). Dichlorodihydrofluorescein and Dihydrorhodamine 123 Are Sensitive Indicators of Peroxynitritein Vitro:Implications for Intracellular Measurement of Reactive Nitrogen and Oxygen Species. *Nitric Oxide*, *1*(2), 145–157. https://doi.org/10.1006/niox.1996.0113

Cui, X., Wang, X., Yang, L., Chen, B., Chen, J., Andersson, A., & Gustafsson, Ö. (2016). Radiative absorption enhancement from coatings on black carbon aerosols. *Science of the Total Environment*, *551–552*, 51–56. https://doi.org/10.1016/j.scitotenv.2016.02.026

Daellenbach, K. R., Uzu, G., Jiang, J., Cassagnes, L. E., Leni, Z., Vlachou, A., Stefenelli, G., Canonaco, F., Weber, S., Segers, A., Kuenen, J. J. P., Schaap, M., Favez, O., Albinet, A., Aksoyoglu, S., Dommen, J., Baltensperger, U., Geiser, M., El Haddad, I., … Prévôt, A. S. H. (2020). Sources of particulate-matter air pollution and its oxidative potential in Europe. *Nature*, *587*(7834), 414–419. https://doi.org/10.1038/s41586-020-2902-8

Dai, Q., Hopke, P. K., Bi, X., & Feng, Y. (2020). Improving apportionment of PM2.5 using multisite PMF by constraining G-values with a prioriinformation. *Science of the Total Environment*, *736*, 139657. https://doi.org/10.1016/j.scitotenv.2020.139657

DAPRO, D. G. de A. P. (2020a). *Informe Estadístico Del Municipio De El Alto* (Issue 6). https://siip.produccion.gob.bo/noticias/files/BI_060320200ac2d_INFalto.pdf

DAPRO, D. G. de A. P. (2020b). *Informe Estadístico Industrial de Bolivia*. https://siip.produccion.gob.bo/noticias/files/BI_050820209ce83_bolivia.pdf

DAPRO, D. G. de A. P. (2021). *Estado Productivo del Departamento de*.

DAPRO, D. G. de A. P. (2022). *Informe Productivo del Municipio de El Alto*. https://siip.produccion.gob.bo/noticias/files/2022-8de73-El-Alto-2022.pdf

Delfino, R. J., Staimer, N., Tjoa, T., Arhami, M., Polidori, A., Gillen, D. L., Kleinman, M. T., Schauer, J. J., & Sioutas, C. (2010). Association of biomarkers of systemic inflammation with organic components and source tracers in quasi-ultrafine particles. *Environmental Health Perspectives*, *118*(6), 756–762.

https://doi.org/10.1289/ehp.0901407

Deroubaix, A., Martiny, N., Chiapello, I., & Marticorena, B. (2013). Suitability of OMI aerosol index to reflect mineral dust surface conditions: Preliminary application for studying the link with meningitis epidemics in the Sahel. *Remote Sensing of Environment*, *133*, 116–127. https://doi.org/10.1016/j.rse.2013.02.009

Drinovec, L., Močnik, G., Zotter, P., Prévôt, A. S. H., Ruckstuhl, C., Coz, E., Rupakheti, M., Sciare, J., Müller, T., Wiedensohler, A., & Hansen, A. D. A. (2015a). The "dual-spot" Aethalometer: An improved measurement of aerosol black carbon with real-time loading compensation. *Atmospheric Measurement Techniques*, *8*(5), 1965–1979. https://doi.org/10.5194/amt-8-1965-2015

Drinovec, L., Močnik, G., Zotter, P., Prévôt, A. S. H., Ruckstuhl, C., Coz, E., Rupakheti, M., Sciare, J., Müller, T., Wiedensohler, A., & Hansen, A. D. A. (2015b). The "dual-spot" Aethalometer: An improved measurement of aerosol black carbon with real-time loading compensation. *Atmospheric Measurement Techniques*, *8*(5), 1965–1979. https://doi.org/10.5194/amt-8-1965-2015

Du, Q., Mu, Y., Zhang, C., Liu, J., Zhang, Y., & Liu, C. (2017). Photochemical production of carbonyl sulfide, carbon disulfide and dimethyl sulfide in a lake water. *Journal of Environmental Sciences (China)*, *51*, 146–156. https://doi.org/10.1016/j.jes.2016.08.006

EEA, Enviromental European Agency. (2020). *Air quality in Europe — 2020 report*. https://doi.org/10.2800/786656

EEA, Environmental European Agency. (2022). *Air quality statistics - AQ eReporting - Annual*. https://www.eea.europa.eu/data-and-maps/dashboards/air-quality-statistics

El Haddad, I., Marchand, N., Dron, J., Temime-roussel, B., Quivet, E., Wortham, H., Luc, J., Baduel, C., Voisin, D., Luc, J., & Gille, G. (2009). Comprehensive primary particulate organic characterization of vehicular exhaust emissions in France. *Atmospheric Environment*, *43*(39), 6190–6198. https://doi.org/10.1016/j.atmosenv.2009.09.001

Elbert, W., Taylor, P. E., Andreae, M. O., & Pöschl, U. (2007). Contribution of fungi to primary biogenic aerosols in the atmosphere: Wet and dry discharged spores, carbohydrates, and inorganic ions. *Atmospheric Chemistry and Physics*, *7*(17), 4569–4588. https://doi.org/10.5194/acp-7-4569-2007

Escrig Vidal, A., Monfort, E., Celades, I., Querol, X., Amato, F., Minguillón, M. C., & Hopke, P. K. (2009). Application of optimally scaled target factor analysis for assessing source contribution of ambient PM10. *Journal of the Air and Waste Management Association*, *59*(11), 1296–1307. https://doi.org/10.3155/1047-3289.59.11.1296

Evia, P. (2009). *EL SECTOR INDUSTRIAL MANUFACTURERO*. https://www.udape.gob.bo/portales_html/diagnosticos/documentos/TOMO VII - SECTOR MANUFACTURERO.pdf

Favez, O., El Haddad, I., Piot, C., Boréave, A., Abidi, E., Marchand, N., Jaffrezo, J. L., Besombes, J. L., Personnaz, M. B., Sciare, J., Wortham, H., George, C., & D'Anna, B. (2010). Inter-comparison of source apportionment models for the estimation of wood burning aerosols during wintertime in an Alpine city (Grenoble, France). *Atmospheric Chemistry and Physics*, *10*(12), 5295–5314. https://doi.org/10.5194/acp-10-5295-2010

Fernández, J. (2021). *Así nació El Alto* (F. Imaña (Ed.); 2nd Editio). FOCAPACI.

Fierce, L., Bond, T. C., Bauer, S. E., Mena, F., & Riemer, N. (2016). Black carbon absorption at the global scale is affected by particle-scale diversity in composition. *Nature Communications*, *7*, 1–8. https://doi.org/10.1038/ncomms12361

Forster, P., Storelvmo, T., Armour, K., Collins, W., Dufresne, J.-L., Frame, D., Lunt, D. J., Mauritsen, T., Palmer, M. D., Watanabe, M., Wild, M., & Zhang, H. (2021). The Earth's Energy Budget, Climate Feedbacks, and Climate Sensitivity. In V. Masson-Delmotte, P. Zhai, A. Pirani, S. L. Connors, C. Péan, S. Berger, N. Caud, Y. Chen, L. Goldfarb, M. I. Gomis, M. Huang, K. Leitzell, E. Lonnoy, J. B. R. Matthews, T. K. Maycock, T. Waterfield, O. Yelekçi, R. Yu, & B. Zhou (Eds.), *Climate Change 2021: The Physical Science Basis. Contribution of Working Group I to the Sixth Assessment Report of the Intergovernmental Panel on Climate Change* (pp. 923–1054). Cambridge University Press. https://doi.org/10.1017/9781009157896.009.923

Foster, V., & Irusta, O. (2003). *Does Infrastructure Reform Work for the Poor? A Case Study on the Cities of La Paz and El Alto in Bolivia* (Issue December). https://doi.org/https://doi.org/10.1596/1813-9450-3177

Fraser, M. P. (2000). *Using Levoglucosan as a Molecular Marker for the Long-Range Transport of Biomass Combustion Aerosols*. *34*(21), 4560–4564.

Frisancho, A. R. (1977). Developmental adaptation to high altitude hypoxia. *International Journal of Biometeorology*, *21*(2), 135–146. https://doi.org/10.1007/BF01553707

Frisancho, A. Roberto. (2013). Developmental functional adaptation to high altitude: Review. *American Journal of Human Biology*, *25*(2), 151–168. https://doi.org/10.1002/ajhb.22367

Frisancho, A. Roberto, Juliao, P. C., Barcelona, V., Kudyba, C. E., Amayo, G., Davenport, G., Knowles, A., Sanchez, D., Villena, M., Vargas, E., & Soria, R. (1999). Developmental components of resting ventilation among high- and low- altitude Andean children and adults. *American Journal of Physical Anthropology*, *109*(3), 295–301. https://doi.org/10.1002/(SICI)1096-8644(199907)109:3<295::AID-AJPA2>3.0.CO;2-U

Fukuzaki, N., Yanaka, T., & Urushiyama, Y. (1986). Effects of studded tires on roadside airborne dust pollution in Niigata, Japan. *Atmospheric Environment (1967)*, *20*(2), 377–386. https://doi.org/10.1016/0004-6981(86)90041-7

Fuller, K. A., Malm, W. C., & Kreidenweis, S. M. (1999). Effects of mixing on extinction by carbonaceous particles. *Journal of Geophysical Research: Atmospheres*, *104*(D13), 15941–15954.

https://doi.org/10.1029/1998JD100069

Fussell, J. C., & Kelly, F. J. (2021). Mechanisms underlying the health effects of desert sand dust. *Environment International*, *157*, 106790. https://doi.org/10.1016/j.envint.2021.106790

Gan, W. Q., Fitzgerald, J. M., Carlsten, C., Sadatsafavi, M., & Brauer, M. (2013). Associations of Ambient Air Pollution with Chronic Obstructive Pulmonary Disease Hospitalization and Mortality. *American Journal of Respiratory and Critical Care Medicine*, *2*. https://doi.org/10.1164/rccm.201211-2004OC

Gangl, M., Kocifaj, M., Videen, G., & Horvath, H. (2008). Light absorption by coated nano-sized carbonaceous particles. *Atmospheric Environment*, *42*(11), 2571–2581. https://doi.org/10.1016/j.atmosenv.2007.05.030

Ganor, E., Foner, H. A., Bingemer, H. G., Udisti, R., & Setter, I. (2000). Biogenic sulphate generation in the Mediterranean Sea and its contribution to the sulphate anomaly in the aerosol over Israel and the Eastern Mediterranean. *Atmospheric Environment*, *34*(20), 3453–3462. https://doi.org/10.1016/S1352-2310(00)00077-7

Garsous, G., Suárez-alemán, A., & Serebrisky, T. (2017). Cable cars in urban transport : Travel time savings from La Paz-El Alto. *Transport Policy*, *December 2016*, 0–1. https://doi.org/10.1016/j.tranpol.2017.05.005

Gianini, M. F. D., Fischer, A., Gehrig, R., Ulrich, A., Wichser, A., Piot, C., Besombes, J. L., & Hueglin, C. (2012). Comparative source apportionment of PM10 in Switzerland for 2008/2009 and 1998/1999 by Positive Matrix Factorisation. *Atmospheric Environment*, *54*(January 1998), 149–158. https://doi.org/10.1016/j.atmosenv.2012.02.036

Giraldo, M., & Huertas, J. I. (2019). Real emissions, driving patterns and fuel consumption of in-use diesel buses operating at high altitude. *Transportation Research Part D: Transport and Environment*, *77*, 21–36. https://doi.org/10.1016/j.trd.2019.10.004

Godoy, M. L. D. P., Godoy, J. M., & Artaxo, P. (2005). Aerosol source apportionment around a large coal fired plant -Thermoelectric Complex Jorge Lacerda Santa Catarina. *Atmospheric Environment*, *39*, 5307–5324. https://doi.org/10.1016/j.atmosenv.2005.05.033

Golly, B. (2014). *Etude des sources et de la dynamique atmosphérique de polluants organiques particulaires en vallées alpines : apport de nouveaux traceurs organiques aux modèles récepteurs*. 292. https://tel.archives-ouvertes.fr/tel-01089232

Goudie, A. S., & Middleton, N. J. (2001). Saharan dust storms : nature and consequences. *Earth Science Reviews*, *56*, 179–204.

Graboski, M. S., & McCormick, R. L. (1996). Effect of diesel fuel chemistry on regulated emissions at high altitude. *SAE Technical Papers*, *412*. https://doi.org/10.4271/961947

Guerreiro, C. B. B., Foltescu, V., & De Leeuw, F. (2014). *Air quality status and trends in Europe*.

https://doi.org/10.1016/j.atmosenv.2014.09.017

Gupta, T., Singh, S. P., Rajput, P., & Agarwal, A. K. (2020). *Measurement , Analysis and Remediation of Environmental Pollutants. Energy, Environment, and Sustainability* (A. K. Agarwal (Ed.)). Springer.

Gutiérrez-Castillo, M. E., Olivos-Ortiz, M., De Vizcaya-Ruiz, A., & Cebrián, M. E. (2005). Chemical characterization of extractable water soluble matter associated with PM10 from Mexico City during 2000. *Chemosphere*, *61*(5), 701–710. https://doi.org/10.1016/j.chemosphere.2005.03.063

Guttikunda, S. K., Kopakka, R. V., Dasari, P., & Gertler, A. W. (2013). Receptor model-based source apportionment of particulate pollution in Hyderabad, India. *Environmental Monitoring and Assessment*, *185*(7), 5585–5593. https://doi.org/10.1007/s10661-012-2969-2

Guttikunda, S. K., Nishadh, K. A., Gota, S., Singh, P., Chanda, A., Jawahar, P., & Asundi, J. (2019). Air quality, emissions, and source contributions analysis for the Greater Bengaluru region of India. *Atmospheric Pollution Research*, *10*(3), 941–953. https://doi.org/10.1016/j.apr.2019.01.002

Hall, D., Wu, C. Y., Hsu, Y. M., Stormer, J., Engling, G., Capeto, K., Wang, J., Brown, S., Li, H. W., & Yu, K. M. (2012). PAHs, carbonyls, VOCs and PM 2.5 emission factors for pre-harvest burning of Florida sugarcane. *Atmospheric Environment*, *55*, 164–172. https://doi.org/10.1016/j.atmosenv.2012.03.034

Hallar, A. G., Lowenthal, D. H., Chirokova, G., Borys, R. D., & Wiedinmyer, C. (2011). Persistent daily new particle formation at a mountain-top location. *Atmospheric Environment*, *45*(24), 4111–4115. https://doi.org/10.1016/j.atmosenv.2011.04.044

Harrison, R. M., Beddows, D. C. S., Hu, L., & Yin, J. (2012). Comparison of methods for evaluation of wood smoke and estimation of UK ambient concentrations. *Atmospheric Chemistry and Physics*, *12*(17), 8271–8283. https://doi.org/10.5194/acp-12-8271-2012

Hays, M. D., Geron, C. D., Linna, K. J., Smith, N. D., & Schauer, J. J. (2002). Speciation of gas-phase and fine particle emissions from burning of foliar fuels. *Environmental Science and Technology*, *36*(11), 2281–2295. https://doi.org/10.1021/es0111683

He, C., Ge, Y., Ma, C., Tan, J., Liu, Z., Wang, C., Yu, L., & Ding, Y. (2011). Emission characteristics of a heavy-duty diesel engine at simulated high altitudes. *Science of the Total Environment*, *409*(17), 3138–3143. https://doi.org/10.1016/j.scitotenv.2011.01.029

Hedayat, F., Stevanovic, S., Miljevic, B., Bottle, S., & Ristovski, Z. D. (2015). *Review-Evaluating the molecular assays for measuring the oxidative potential of particulate matter*. *21*(1), 201–210. https://doi.org/10.2298/CICEQ140228031H

Helin, A., Virkkula, A., Backman, J., Pirjola, L., Sippula, O., Aakko-Saksa, P., Väätäinen, S., Mylläri, F., Järvinen, A., Bloss, M., Aurela, M., Jakobi, G., Karjalainen, P., Zimmermann, R., Jokiniemi, J., Saarikoski, S., Tissari,

J., Rönkkö, T., Niemi, J. V., & Timonen, H. (2021). Variation of Absorption Ångström Exponent in Aerosols From Different Emission Sources. *Journal of Geophysical Research: Atmospheres*, *126*(10), 1–21. https://doi.org/10.1029/2020JD034094

Henley, R. W., & Berger, B. R. (2013). Nature's refi neries — Metals and metalloids in arc volcanoes. *Earth-Science Reviews*, *125*, 146–170. https://doi.org/10.1016/j.earscirev.2013.07.007

Herbst, N. S. (2007). *Inventario de Emisiones del Municipio de La Paz*. http://www.asocam.org/sites/default/files/publicaciones/files/b515562bd7cf36c0874c12731a36943c.pdf

Hernández-Pellón, A., & Fernández-Olmo, I. (2019). Using multi-site data to apportion PM-bound metal(loid)s: Impact of a manganese alloy plant in an urban area. *Science of the Total Environment*, *651*, 1476–1488. https://doi.org/10.1016/j.scitotenv.2018.09.261

Hopke, P. K. (2021). Approaches to reducing rotational ambiguity in receptor modeling of ambient particulate matter. *Chemometrics and Intelligent Laboratory Systems*, *210*(November 2020), 104252. https://doi.org/10.1016/j.chemolab.2021.104252

Horvath, H. (1993). Atmospheric light absorption - a review. *Atmospheric Environment Part A, General Topics*, *27*(3), 293–317. https://doi.org/10.1016/0960-1686(93)90104-7

Horvath, H. (1997). Experimental calibration for aerosol light absorption measurements using the integrating plate method - Summary of the data. *Journal of Aerosol Science*, *28*(7), 1149–1161. https://doi.org/10.1016/S0021-8502(97)00007-4

Human, D. M., Ullman, T. L., & Baines, T. M. (1990). Simulation of high altitude effects on heavy-duty diesel emissions. *SAE Technical Papers*. https://doi.org/10.4271/900883

Husaini, D. C., Reneau, K., & Balam, D. (2022). Air pollution and public health in Latin America and the Caribbean (LAC): a systematic review with meta-analysis. *Beni-Suef University Journal of Basic and Applied Sciences*, *11*(1). https://doi.org/10.1186/s43088-022-00305-0

IFP, E. N. (2021). *Light vehicle gas and particle emissions: results of the Rhapsodie project*. https://www.ifpenergiesnouvelles.com/article/light-vehicle-gas-and-particle-emissions-results-rhapsodie-project

INE, I. N. de E. (2016). *Actualidad Estadística Parque Automotor Bolivia 2016*. https://www.ine.gob.bo/index.php/estadisticas-economicas/transportes/parque-automotor-boletines/

INE, I. N. de E. (2020a). *BOLETÍN ESTADÍSTICO PARQUE AUTOMOTOR 2020*. https://www.ine.gob.bo/index.php/estadisticas-economicas/transportes/parque-automotor-

boletines/

INE, I. N. de E. (2020b). *BOLIVIA: PARQUE AUTOMOTOR, SEGÚN DEPARTAMENTO Y TIPO DE SERVICIO, 2003 – 2020*. https://www.ine.gob.bo/index.php/estadisticas-economicas/transportes/parque-automotor-cuadros-estadisticos/

INE, I. N. de E. (2020c). *BOLIVIA: PROYECCIONES DE POBLACIÓN, SEGÚN DEPARTAMENTO Y MUNICIPIO, 2012-2022*. https://www.ine.gob.bo/index.php/censos-y-proyecciones-de-poblacion-sociales/

INE, I. N. de E. (2020d). *LA PAZ EN CIFRAS*. https://www.ine.gob.bo/index.php/publicaciones/la-paz-en-cifras-2020/

Jacobson, M. Z. (2001). Strong radiative heating due to the mixing state of black carbon in atmospheric aerosols. *Nature*, *409*(6821), 695–697. https://doi.org/10.1038/35055518

Jaffrezo, J. L., Aymoz, G., & Cozic, J. (2005). Size distribution of EC and OC in the aerosol of Alpine valleys during summer and winter. *Atmospheric Chemistry and Physics*, *5*(11), 2915–2925. https://doi.org/10.5194/acp-5-2915-2005

Jaffrezo, J. L., Aymoz, G., Delaval, C., & Cozic, J. (2005). Seasonal variations of the water soluble organic carbon mass fraction of aerosol in two valleys of the French Alps. *Atmospheric Chemistry and Physics*, *5*(10), 2809–2821. https://doi.org/10.5194/acp-5-2809-2005

Jansen, G. F. A., & Basnyat, B. (2011). Brain blood flow in Andean and Himalayan high-altitude populations: Evidence of different traits for the same environmental constraint. *Journal of Cerebral Blood Flow and Metabolism*, *31*(2), 706–714. https://doi.org/10.1038/jcbfm.2010.150

Janssen, N. A., Gerlofs-Nijland, M. E., Lanki, T., Salonen, R. O., Cassee, F., Hoek, G., Fischer, P., Brunekreef, B. & Krzyzanowski, M. (2012). *Health Effects of Black Carbon*.

Janssen, N. A. H., Yang, A., Strak, M., Steenhof, M., Hellack, B., Gerlofs-Nijland, M. E., Kuhlbusch, T., Kelly, F., Harrison, R., Brunekreef, B., Hoek, G., & Cassee, F. (2014). Oxidative potential of particulate matter collected at sites with different source characteristics. *Science of the Total Environment*, *472*, 572–581. https://doi.org/10.1016/j.scitotenv.2013.11.099

Jardine, K., Yañez-Serrano, A. M., Williams, J., Kunert, N., Jardine, A., Taylor, T., Abrell, L., Artaxo, P., Guenther, A., Hewitt, C. N., House, E., Florentino, A. P., Manzi, A., Higuchi, N., Kesselmeier, J., Behrendt, T., Veres, P. R., Derstroff, B., Fuentes, J. D., … Andreae, M. O. (2015). Dymethyl sulfide in the Amazon rain forest. *Global Biogeochemical Cycles*, *29*, 19–32. https://doi.org/10.1002/2014GB004969

Ježek, I., Katrašnik, T., Westerdahl, D., & Mocnik, G. (2015). Black carbon, particle number concentration and nitrogen oxide emission factors of random in-use vehicles measured with the on-road chasing method. *Atmospheric Chemistry and Physics*, *15*(19), 11011–11026. https://doi.org/10.5194/acp-15-11011-2015

Jordan, T. B., Seen, A. J., & Jacobsen, G. E. (2006). Levoglucosan as an atmospheric tracer for woodsmoke. *Atmospheric Environment*, *40*(February), 5316–5321. https://doi.org/10.1016/j.atmosenv.2006.03.023

Julian, C. G., & Moore, L. G. (2019). *Human Genetic Adaptation to High Altitude : Evidence from the Andes*. https://doi.org/10.3390/genes10020150

Ka Wong, Y., Hilda Huang, X. H., Louie, P. K. K., Yu, A. L. C., Chan, D. H. L., & Yu, J. Z. (2020). Tracking separate contributions of diesel and gasoline vehicles to roadside PM2.5through online monitoring of volatile organic compounds and PM2.5organic and elemental carbon: A 6-year study in Hong Kong. *Atmospheric Chemistry and Physics*, *20*(16), 9871–9882. https://doi.org/10.5194/acp-20-9871-2020

Karamchandani, P., & Seigneur, C. (1999). Simulation of sulfate and nitrate chemistry in power plant plumes. *Journal of the Air and Waste Management Association*, *49*(9), 175–181. https://doi.org/10.1080/10473289.1999.10463885

Kaur, M., Chandel, J., Malik, J., & Naura, A. S. (2022). Particulate matter in COPD pathogenesis: an overview. *Inflammation Research*, *71*(7–8), 797–815. https://doi.org/10.1007/s00011-022-01594-y

Kchih, H., Perrino, C., & Cherif, S. (2015). *Investigation of Desert Dust Contribution to Source Apportionment of PM 10 and PM 2 . 5 from a Southern Mediterranean Coast*. 454–464. https://doi.org/10.4209/aaqr.2014.10.0255

Khalizov, A. F., Xue, H., Wang, L., Zheng, J., & Zhang, R. (2009). Enhanced light absorption and scattering by carbon soot aerosol internally mixed with sulfuric acid. *Journal of Physical Chemistry A*, *113*(6), 1066–1074. https://doi.org/10.1021/jp807531n

Kim, T.-Y., Kim, H., Yi, S.-M., Cheong, J.-P., & Heo, J. (2018). Short-term Effects of Ambient PM2.5 and PM2.5-10 on Mortality in Major Cities of Korea. *Aerosol and Air Quality Research*, *18*(7), 1853–1862. https://doi.org/10.4209/aaqr.2017.11.0490

Kioumourtzoglou, M. A., Zanobetti, A., Schwartz, J. D., Coull, B. A., Dominici, F., & Suh, H. H. (2013). The effect of primary organic particles on emergency hospital admissions among the elderly in 3 US cities. *Environmental Health*, *12*(1), 1–10. https://doi.org/10.1186/1476-069X-12-68

Kirchstetter, T. W., Novakov, T., & Hobbs, P. V. (2004). Evidence that the spectral dependence of light absorption by aerosols is affected by organic carbon. *Journal of Geophysical Research D: Atmospheres*, *109*(21), 1–12. https://doi.org/10.1029/2004JD004999

Kondo, Y., Sahu, L., Kuwata, M., Miyazaki, Y., Takegawa, N., Moteki, N., Imaru, J., Han, S., Nakayama, T., Oanh, N. T. K., Hu, M., Kim, Y. J., & Kita, K. (2009). Stabilization of the mass absorption cross section of black carbon for filter-based absorption photometry by the use of a heated inlet. *Aerosol Science and Technology*, *43*(8), 741–756. https://doi.org/10.1080/02786820902889879

Kong, S., Lu, B., Ji, Y., Zhao, X., Bai, Z., Xu, Y., Liud, Y., & Hua Jiangd Shaofei Kong, ab Bing Lu, ab Yaqin Ji, ab Xueyan Zhao, ab Zhipeng Bai,*abc Yonghai Xu, d Y. L. and H. J. (2012). Risk assessment of heavy metals in road and soil dusts within PM2.5, PM10 and PM100 fractions in Dongying city, Shandong Province, China. *Journal of Environmental Monitoring*, *14*, 791–803.

Korhonen, P., Kulmala, M., Laaksonen, A., Viisanen, Y., Mcgraw, R., & Seinfeld, J. H. (1999). Ternary nucleation of HSO4, NH3, and H2o in the atmosphere. *Journal of Geophysical Research*, *104*(D21), 26349–26353.

Kumagai, Y., Koide, S., Taguchi, K., Endo, A., Nakai, Y., Yoshikawa, T., & Shimojo, N. (2002). Oxidation of proximal protein sulfhydryls by phenanthraquinone, a component of diesel exhaust particles. *Chem Res Toxicol*, *4*(483–489). https://doi.org/10.1021/tx0100993

Kumar, S., Aggarwal, S. G., Sarangi, B., Malherbe, J., Barre, J. P. G., Berail, S., Séby, F., & Donard, O. F. X. (2018). Understanding the influence of open-waste burning on urban aerosols using metal tracers and lead isotopic composition. *Aerosol and Air Quality Research*, *18*(9), 2433–2446. https://doi.org/10.4209/aaqr.2017.11.0510

La Colla, N. S., Botté, S. E., & Marcovecchio, J. E. (2021). Atmospheric particulate pollution in south american megacities. *Environmental Reviews*, *29*(3), 415–429. https://doi.org/10.1139/er-2020-0105

Lack, D. A., & Cappa, C. D. (2010). Impact of brown and clear carbon on light absorption enhancement, single scatter albedo and absorption wavelength dependence of black carbon. *Atmospheric Chemistry and Physics*, *10*(9), 4207–4220. https://doi.org/10.5194/acp-10-4207-2010

Lack, D A, & Langridge, J. M. (2013). On the attribution of black and brown carbon light absorption using the Ångström exponent. *Atmospheric Chemistry and Physics*, *13*(20), 10535–10543. https://doi.org/10.5194/acp-13-10535-2013

Lack, Daniel A., Moosmüller, H., McMeeking, G. R., Chakrabarty, R. K., & Baumgardner, D. (2014). Characterizing elemental, equivalent black, and refractory black carbon aerosol particles: A review of techniques, their limitations and uncertainties. In *Analytical and Bioanalytical Chemistry* (Vol. 406, Issue 1, pp. 99–122). https://doi.org/10.1007/s00216-013-7402-3

Lanz, V. A., Weingartner, E., Baltensperger, U. R. S., Sandradewi, J., Prévôt, A. S. H., Szidat, S., Perron, N., & Alfarra, M. R. (2008). Using aerosol light absorption measurements for the quantitative determination of wood burning and traffic emission contributions to particulate matter. *Environmental Science and Technology*, *42*(9), 3316–3323. http://www.ncbi.nlm.nih.gov/pubmed/18522112

Laskin, A., Laskin, J., & Nizkorodov, S. A. (2015). Chemistry of Atmospheric Brown Carbon. *Chemical Reviews*, *115*(10), 4335–4382. https://doi.org/10.1021/cr5006167

Lavigne, É., Burnett, R. T., Stieb, D. M., Evans, G. J., Godri Pollitt, K. J., Chen, H., van Rijswijk, D., & Weichenthal, S. (2018). Fine Particulate Air Pollution and Adverse Birth Outcomes: Effect Modification by Regional

Nonvolatile Oxidative Potential. *Environmental Health Perspectives*, *126*(7), 077012. https://doi.org/10.1289/EHP2535

Leoz-garziandia, E., Tatry, V., Carlier, P., Leoz-garziandia, E., Tatry, V., & Sampling, P. C. (2014). *Sampling and analysis of PAH and oxygenated PAH in diesel exhaust and ambient air To cite this version : HAL Id : ineris-00972185*.

Lewis, E., Lewis, R., & Schwartz, S. (2004). *Sea salt aerosol production: mechanisms, methods, measurements, and models* (Vol 152). American geophysical union.

Ley 821: LEY DE MODIFICACIÓN DE LA LEY N° 165 DE 16 DE AGOSTO DE 2011, "LEY GENERAL DE TRANSPORTE." (2016). http://gacetaoficialdebolivia.gob.bo/normas/descargarPdf/153905

Li, C., Li, X., Liu, J., Fan, X., You, G., Zhao, L., & Zhou, H. (2018). *Investigation of the differences between the Tibetan and Han populations in the hemoglobin – oxygen affinity of red blood cells and in the adaptation to high-altitude environments*. *8454*. https://doi.org/10.1080/10245332.2017.1396046

Li, H., & May, A. A. (2022). Estimating mass-absorption cross-section of ambient black carbon aerosols: Theoretical, empirical, and machine learning models. *Aerosol Science and Technology*, *56*(11), 980–997. https://doi.org/10.1080/02786826.2022.2114311

Li, W., Ge, P., Chen, M., Tang, J., Cao, M., Cui, Y., Hu, K., & Nie, D. (2021). Tracers from biomass burning emissions and identification of biomass burning. *Atmosphere*, *12*(11). https://doi.org/10.3390/atmos12111401

Liu, C., Chung, C. E., Yin, Y., & Schnaiter, M. (2018). *The absorption Ångström exponent of black carbon : from numerical aspects*. *1*, 6259–6273.

Liu, P., Shao, L., Li, Y., Wang, W., Zhang, M., Yang, C.-X., & Hongya Niu 5, X. F. 1 and D. Z. (2022). Compositions , Sources , and Aging Processes of Aerosol Particles during Winter Hazes in an Inland Megacity of NW China. *Atmosphere*, *13*(521). https://doi.org/10.3390/atmos13040521

Madueño, L., Kecorius, S., Andrade, M., & Wiedensohler, A. (2020). Exposure and respiratory tract deposition dose of equivalent black carbon in high altitudes. *Atmosphere*, *11*(6), 1–14. https://doi.org/10.3390/atmos11060598

Magalhães, N. de, Evangelista, H., Condom, T., Rabatel, A., & Ginot, P. (2019). Amazonian Biomass Burning Enhances Tropical Andean Glaciers Melting. *Scientific Reports*, *9*(1), 1–12. https://doi.org/10.1038/s41598-019-53284-1

Magari, S. R., Schwartz, J., Williams, P. L., Hauser, R., Smith, T. J., & Christiani, D. C. (2002). The Association of Particulate Air Metal Concentrations with Heart Rate Variability. *Environmental Health Perspectives*, *110*(9), 875–880.

Manrique, N., Lazarte, I., Rivera, M., Cueva, K., Japura, S., & Aguilar, R. (2018). The 2016-2017 activity of the

Sabancaya volcano (Peru): petrographical and geochemical observations of the 2017 tephra deposits. *Hazard and Risk Mapping : The Arequipa - El Misti Case Study and Other Threatened Cities, 2018*, 117–122.

Mardoñez, V., Pandolfi, M., Borlaza, L. J. S., Jaffrezo, J., Alastuey, A., Besombes, J., R, I. M., Perez, N., Močnik, G., Ginot, P., Chrastny, V., Wiedensohler, A., Laj, P., Andrade, M., Uzu, G., De, G., Alpes, U. G., & Inp, G. (2022). Source apportionment study on particulate air pollution in two high- altitude Bolivian cities : La Paz and El Alto. *Atmos. Chem. Phys. Discuss. [Preprint]*, *in review*(November). https://doi.org/https://doi.org/10.5194/acp-2022-780

Marlier, M. E., Bonilla, E. X., & Mickley, L. J. (2020). How Do Brazilian Fires Affect Air Pollution and Public Health ? *GeoHealth*, *September 2019*, 1–5. https://doi.org/10.1029/2020GH000331

Marsal, A., Slama, R., Lyon-Caen, S., Borlaza, L. J. S., Jaffrezo, J.-L., Boudier, A., Darfeuil, S., Elazzouzi, R., Gioria, Y., Lepeule, J., Chartier, R., Pin, I., Quentin, J., Bayat, S., Uzu, G., & Siroux, V. (2023). Prenatal Exposure to PM2.5 Oxidative Potential and Lung Function in Infants and Preschool- Age Children: A Prospective Study. *Environmental Health Perspectives*, *131*(1). https://doi.org/10.1289/ehp11155

Martínez, J., Robles, L., Montalvo, F., Baño Morales, D., & Zambrano, I. (2022). Effects of altitude in the performance of a spark ignition internal combustion engine. *Materials Today: Proceedings*, *49*(xxxx), 72–78. https://doi.org/10.1016/j.matpr.2021.07.475

Masías, P., Lazarte, I., Apaza, F., Alvarez, M., Calderon, J., Gironda, A., Mamani, J., & Ramos, D. (2016). MONITOREO VISUAL DEL VOLCÁN UBINAS DURANTE LA ACTIVIDAD ERUPTIVA 2013-2016. *Congreso Peruano de Geología, 18, Lima, PE, 16-19 Octubre 2016, Resúmenes*, 1–4.

Mataveli, G. A. V., de Oliveira, G., Seixas, H. T., Pereira, G., Stark, S. C., Gatti, L. V., Basso, L. S., Tejada, G., Cassol, H. L. G., Anderson, L. O., & Aragão, L. E. O. C. (2021). Relationship between biomass burning emissions and deforestation in amazonia over the last two decades. *Forests*, *12*(9). https://doi.org/10.3390/f12091217

Mikhailov, E. F., Vlasenko, S. S., Podgorny, I. A., Ramanathan, V., & Corrigan, C. E. (2006). Optical properties of soot-water drop agglomerates: An experimental study. *Journal of Geophysical Research Atmospheres*, *111*(7), 1–16. https://doi.org/10.1029/2005JD006389

Moffet, R. C., & Prather, K. A. (2009). In-situ measurements of the mixing state and optical properties of soot with implications for radiative forcing estimates. *Proceedings of the National Academy of Sciences*, *106*(29), 11872–11877. https://doi.org/10.1073/pnas.0900040106

Molina, L. T., Velasco, E., Retama, A., & Zavala, M. (2019). Experience from integrated air quality management in the Mexico City Metropolitan Area and Singapore. *Atmosphere*, *10*(9). https://doi.org/10.3390/atmos10090512

Moosmüller, H., Chakrabarty, R. K., & Arnott, W. P. (2009). Aerosol light absorption and its measurement: A

review. In *Journal of Quantitative Spectroscopy and Radiative Transfer* (Vol. 110, Issue 11, pp. 844–878). https://doi.org/10.1016/j.jqsrt.2009.02.035

Moreno, L., Krishnan, J. A., Duran, P., & Ferrero, F. (2006). Development and validation of a clinical prediction rule to distinguish bacterial from viral pneumonia in children. *Pediatric Pulmonology*, *41*(4), 331–337. https://doi.org/10.1002/ppul.20364

Morton-Bermea, O., Hernández-Alvarez, E., Almorín-Avila, M. A., Ordoñez-Godínez, S. L., Bermendi-Orosco, L., & Retama, A. (2021). *Historical trends of metals concentration in PM 10 collected in the Mexico City metropolitan area between 2004 and 2014*. *0123456789*. https://doi.org/10.1007/s10653-021-00838-w

Moteki, N., Kondo, Y., Miyazaki, Y., Takegawa, N., Komazaki, Y., Kurata, G., Shirai, T., Blake, D. R., Miyakawa, T., & Koike, M. (2007). Evolution of mixing state of black carbon particles: Aircraft measurements over the western Pacific in March 2004. *Geophysical Research Letters*, *34*(11). https://doi.org/10.1029/2006GL028943

Mudway, I. S., Kelly, F. J., & Holgate, S. T. (2020). Oxidative stress in air pollution research. *Free Radical Biology and Medicine*, *151*(May), 2–6. https://doi.org/10.1016/j.freeradbiomed.2020.04.031

Mugica, V., Ortiz, E., Molina, L., De Vizcaya-Ruiz, A., Nebot, A., Quintana, R., Aguilar, J., & Alcántara, E. (2009). PM composition and source reconciliation in Mexico City. *Atmospheric Environment*, *43*(32), 5068–5074. https://doi.org/10.1016/j.atmosenv.2009.06.051

Müller, T., Henzing, J. S., De Leeuw, G., Wiedensohler, A., Alastuey, A., Angelov, H., Bizjak, M., Collaud Coen, M., Engström, J. E., Gruening, C., Hillamo, R., Hoffer, A., Imre, K., Ivanow, P., Jennings, G., Sun, J. Y., Kalivitis, N., Karlsson, H., Komppula, M., … Wang, Y. Q. (2011). Characterization and intercomparison of aerosol absorption photometers: Result of two intercomparison workshops. *Atmospheric Measurement Techniques*, *4*(2), 245–268. https://doi.org/10.5194/amt-4-245-2011

Mura, I., Franco, J. F., Bernal, L., Melo, N., & Díaz, J. J. (2020). *A Decade of Air Quality in Bogotá : A Descriptive Analysis Validation of Air Quality Data*. *8*(May), 1–12. https://doi.org/10.3389/fenvs.2020.00065

Nagpure, A. S., Gurjar, B. R., & Kumar, P. (2011). Impact of altitude on emission rates of ozone precursors from gasoline-driven light-duty commercial vehicles. *Atmospheric Environment*, *45*(7), 1413–1417. https://doi.org/10.1016/j.atmosenv.2010.12.026

Nakayama, T., Ikeda, Y., Sawada, Y., Setoguchi, Y., Ogawa, S., Kawana, K., Mochida, M., Ikemori, F., Matsumoto, K., & Matsumi, Y. (2014). Properties of light-absorbing aerosols in the Nagoya urban area, Japan, in August 2011 and January 2012: Contributions of brown carbon and lensing effect. *Journal of Geophysical Research Atmospheres*, *119*(22), 12721–12739. https://doi.org/10.1002/2014JD021744

Naota, M., Mukaiyama, T., Shimada, A., Yoshida, A., Okajima, M., Morita, T., Inoue, K., & Takano, H. (2010). Pathological Study of Acute Pulmonary Toxicity Induced by Intratracheally Instilled Asian Sand Dust

(Kosa). *Toxicologic Pathology*, *38*(7), 1099–1110. https://doi.org/10.1177/0192623310385143

Nathan, C., & Cunningham-bussel, A. (2013). Beyond oxidative stress : an immunologist ' s guide to reactive oxygen species. *Nature Publishing Group*, *13*(5), 349–361. https://doi.org/10.1038/nri3423

Nava, S., Lucarelli, F., Amato, F., Becagli, S., Calzolai, G., Chiari, M., Giannoni, M., Traversi, R., & Udisti, R. (2015). Biomass burning contributions estimated by synergistic coupling of daily and hourly aerosol composition records. *Science of the Total Environment, The*, *511*, 11–20. https://doi.org/10.1016/j.scitotenv.2014.11.034

Nawaz, M. O., & Henze, D. K. (2020). Premature Deaths in Brazil Associated With Long-Term Exposure to PM2.5 From Amazon Fires Between 2016 and 2019. *GeoHealth*, *4*(8). https://doi.org/10.1029/2020GH000268

Ni, T., Li, P., Han, B., Bai, Z., Ding, X., Wang, Q., Huo, J., & Lu, B. (2013). *Spatial and Temporal Variation of Chemical Composition and Mass Closure of Ambient PM 10 in Tianjin , China*. 1832–1846. https://doi.org/10.4209/aaqr.2012.10.0283

Nichols, J. L., Oesterling, E., Dutton, S. J., & Luben, T. J. (2013). Systematic review of the effects of black carbon on cardiovascular disease among individuals with pre-existing disease. *International Journal of Public Health*, *58*, 707–724. https://doi.org/10.1007/s00038-013-0492-z

Norris, G., & Duvall, R. (2014). *EPA Positive Matrix Factorization (PMF) 5.0 Fundamentals and User guide*. 136.

NTP, N. T. P. (2011). Polycyclic aromatic hydrocarbons: 15 Listings-benz [a] anthracene, benzo [b] fluoranthene, benzo [j] fluoranthene, benzo [k] fluoranthene, benzo [a] pyrene, dibenz [a, h] acridine, dibenz [a, j] acridine, dibenz [a, h] anthracene, 7H-dibenzo [c, g] carbaz. *Report on Carcinogens: Carcinogen Profiles*, *12*, 353–361.

Olson, E., Michalski, G., Welp, L., Larrea Valdivia, A. E., Reyes Larico, J., Salcedo Peña, J., Fang, H., Magara Gomez, K., & Li, J. (2021). Mineral dust and fossil fuel combustion dominate sources of aerosol sulfate in urban Peru identified by sulfur stable isotopes and water-soluble ions. *Atmospheric Environment*, *260*, 118482. https://doi.org/10.1016/j.atmosenv.2021.118482

Paatero, P., & Tapper, U. (1994). Positive matrix factorization: A non-negative factor model with optimal utilization of error estimates of data values. *Environmetrics*, *5*(2), 111–126. https://doi.org/10.1002/env.3170050203

Pan, X. L., Kanaya, Y., Wang, Z. F., Liu, Y., Pochanart, P., Akimoto, H., Sun, Y. L., Dong, H. B., Li, J., Irie, H., & Takigawa, M. (2011). Correlation of black carbon aerosol and carbon monoxide in the high-altitude environment of Mt. Huang in Eastern China. *Atmospheric Chemistry and Physics*, *11*(18), 9735–9747. https://doi.org/10.5194/acp-11-9735-2011

Pandolfi, M., Mooibroek, D., Hopke, P., Van Pinxteren, D., Querol, X., Herrmann, H., Alastuey, A., Favez, O.,

Hüglin, C., Perdrix, E., Riffault, V., Sauvage, S., Van Der Swaluw, E., Tarasova, O., & Colette, A. (2020). Long-range and local air pollution: What can we learn from chemical speciation of particulate matter at paired sites? *Atmospheric Chemistry and Physics*, *20*(1), 409–429. https://doi.org/10.5194/acp-20-409-2020

Paoletti, E., De Marco, A., Beddows, D. C. S., Harrison, R. M., & Manning, W. J. (2014). Ozone levels in European and USA cities are increasing more than at rural sites, while peak values are decreasing. *Environmental Pollution*, *192*, 295–299. https://doi.org/10.1016/j.envpol.2014.04.040

Pardo Martínez, C. I. (2015). Energy and sustainable development in cities: A case study of Bogotá. *Energy*, *92*, 612–621. https://doi.org/10.1016/j.energy.2015.02.003

Pareja, A., Hinojosa, M., & Marcos, L. (2011). Inventario de Emisiones Atmosféricas Contaminantes de la Ciudad de Cochabamba, Bolivia, año 2008. *Acta Nova*, *5*(3), 344–374. http://www.scielo.org.bo/pdf/ran/v5n3/v5n3a02.pdf

Park, M., Joo, H. S., Lee, K., Jang, M., Kim, S. D., Kim, I., Borlaza, L. J. S., Lim, H., Shin, H., Chung, K. H., Choi, Y.-H., Park, S. G., Bae, M.-S., Lee, J., Song, H., & Park, K. (2018). Differential toxicities of fine particulate matters from various sources. *Scientific Reports*, *8*(1), 17007. https://doi.org/10.1038/s41598-018-35398-0

Peralta, O., Ortínez-alvarez, A., Basaldud, R., Santiago, N., Alvarez-ospina, H., De, K., Barrera, V., De, M., Espinosa, L., Saavedra, I., Castro, T., Martínez-arroyo, A., Páramo, V. H., Ruíz-suárez, L. G., Vazquez-galvez, F. A., & Gavilán, A. (2019). Atmospheric black carbon concentrations in Mexico. *Atmospheric Research*, *230*(February), 104626. https://doi.org/10.1016/j.atmosres.2019.104626

Pereira, G. M., De Oliveira Alves, N., Caumo, S. E. S., Soares, S., Teinilä, K., Custódio, D., Hillamo, R., Alves, C., & Vasconcellos, P. C. (2017a). Chemical composition of aerosol in São Paulo, Brazil: influence of the transport of pollutants. *Air Quality, Atmosphere and Health*, *10*(4), 457–468. https://doi.org/10.1007/s11869-016-0437-9

Pereira, Guilherme Martins, Teinilä, K., Custódio, D., Gomes Santos, A., Xian, H., Hillamo, R., Alves, C. A., Bittencourt de Andrade, J., Olímpio da Rocha, G., Kumar, P., Balasubramanian, R., Andrade, M. de F., de Castro Vasconcellos, P., & 1Institute. (2017). Particulate pollutants in the Brazilian city of Saõ Paulo: 1-year investigation for the chemical composition and source apportionment. *Atmospheric Chemistry and Physics*, *17*(19), 11943–11969. https://doi.org/10.5194/acp-17-11943-2017

Pérez-Padilla, J. R. (2022). Adaptation to Moderate Altitude Hypoxemia: The Example of the Valley of Mexico. *Revista de Investigacion Clinica; Organo Del Hospital de Enfermedades de La Nutricion*, *74*(1), 4–15. https://doi.org/10.24875/RIC.21000159

Pérez, N., Pey, J., Querol, X., Alastuey, A., López, J. M., & Viana, M. (2008). Partitioning of major and trace components in PM10-PM2.5-PM1 at an urban site in Southern Europe. *Atmospheric Environment*, *42*(8),

1677–1691. https://doi.org/10.1016/j.atmosenv.2007.11.034

Pernigotti, D., & Belis, C. A. (2018). DeltaSA tool for source apportionment benchmarking, description and sensitivity analysis. *Atmospheric Environment*, *180*(February), 138–148. https://doi.org/10.1016/j.atmosenv.2018.02.046

Peters, J., Van den Bossche, J., Reggente, M., Van Poppel, M., De Baets, B., & Theunis, J. (2014). Cyclist exposure to UFP and BC on urban routes in Antwerp, Belgium. *Atmospheric Environment*, *92*, 31–43. https://doi.org/10.1016/j.atmosenv.2014.03.039

Petzold, A., Schloesser, H., Sheridan, P. J., Arnott, W. P., Ogren, J. A., & Virkkula, A. (2005). Evaluation of multiangle absorption photometry for measuring aerosol light absorption. *Aerosol Science and Technology*, *39*(1), 40–51. https://doi.org/10.1080/027868290901945

Pietrogrande, Russo, & Zagatti. (2019). Review of PM Oxidative Potential Measured with Acellular Assays in Urban and Rural Sites across Italy. *Atmosphere*, *10*(10), 626. https://doi.org/10.3390/atmos10100626

Pileci, R. E., Modini, R. L., Bertò, M., Yuan, J., Corbin, J. C., Marinoni, A., Henzing, B., Moerman, M. M., Putaud, J. P., Spindler, G., Wehner, B., Müller, T., Tuch, T., Trentini, A., Zanatta, M., Baltensperger, U., & Gysel-Beer, M. (2021). Comparison of co-located refractory black carbon (rBC) and elemental carbon (EC) mass concentration measurements during field campaigns at several European sites. *Atmospheric Measurement Techniques*, *14*(2), 1379–1403. https://doi.org/10.5194/amt-14-1379-2021

Pio, C., Mirante, F., Oliveira, C., Matos, M., Caseiro, A., Oliveira, C., Querol, X., Alves, C., Martins, N., Cerqueira, M., Camões, F., Silva, H., & Plana, F. (2013). Size-segregated chemical composition of aerosol emissions in an urban road tunnel in Portugal. *Atmospheric Environment*, *71*, 15–25. https://doi.org/10.1016/j.atmosenv.2013.01.037

Piot, C., Jaffrezo, J. L., Cozic, J., Pissot, N., El Haddad, I., Marchand, N., & Besombes, J. L. (2012). Quantification of levoglucosan and its isomers by High Performance Liquid Chromatography-Electrospray Ionization tandem Mass Spectrometry and its applications to atmospheric and soil samples. *Atmospheric Measurement Techniques*, *5*(1), 141–148. https://doi.org/10.5194/amt-5-141-2012

Polissar, A. V., Hopke, P. K., Paatero, P., Malm, W. C., & Sisler, J. F. (1998). Atmospheric aerosol over Alaska 2. Elemental composition and sources. *Journal of Geophysical Research Atmospheres*, *103*(D15), 19045–19057. https://doi.org/10.1029/98JD01212

Putaud, J. P., Raes, F., Van Dingenen, R., Brüggemann, E., Facchini, M. C., Decesari, S., Fuzzi, S., Gehrig, R., Hüglin, C., Laj, P., Lorbeer, G., Maenhaut, W., Mihalopoulos, N., Müller, K., Querol, X., Rodriguez, S., Schneider, J., Spindler, G., Ten Brink, H., … Wiedensohler, A. (2004). A European aerosol phenomenology - 2: Chemical characteristics of particulate matter at kerbside, urban, rural and background sites in Europe. *Atmospheric Environment*, *38*(16), 2579–2595. https://doi.org/10.1016/j.atmosenv.2004.01.041

Querol, X., Alastuey, A., Ruiz, C. R., Artiñano, B., Hansson, H. C., Harrison, R. M., Buringh, E., Ten Brink, H. M., Lutz, M., Bruckmann, P., Straehl, P., & Schneider, J. (2004). Speciation and origin of PM10 and PM2.5 in selected European cities. *Atmospheric Environment*, *38*(38), 6547–6555. https://doi.org/10.1016/j.atmosenv.2004.08.037

Querol, Xavier, Alastuey, A., Rodriguez, S., Plana, F., Mantilla, E., & Ruiz, C. R. (2001). Monitoring of PM10 and PM2.5 around primary particulate anthropogenic emission sources. *Atmospheric Environment*, *35*(5), 845–858. https://doi.org/10.1016/S1352-2310(00)00387-3

Querol, Xavier, Alastuey, A., Rosa, J. de la, Sánchez-de-la-Campa, A., Plana, F., & Ruiz, C. R. (2002). *Source apportionment analysis of atmospheric particulates in an industrialised urban site in southwestern Spain*. *36*, 3113–3125.

R Core Team. (2021). *R: A Language and Environment for Statistical Computing*. https://www.r-project.org/

Rai, P., Furger, M., El Haddad, I., Kumar, V., Wang, L., Singh, A., Dixit, K., Bhattu, D., Petit, J. E., Ganguly, D., Rastogi, N., Baltensperger, U., Tripathi, S. N., Slowik, J. G., & Prévôt, A. S. H. (2020). Real-time measurement and source apportionment of elements in Delhi's atmosphere. *Science of the Total Environment*, *742*, 140332. https://doi.org/10.1016/j.scitotenv.2020.140332

Ramírez, O., Sánchez de la Campa, A. M., Amato, F., Catacolí, R. A., Rojas, N. Y., & De la Rosa, J. (2018a). Chemical composition and source apportionment of PM10 at an urban background site in a highealtitude Latin American megacity (Bogota, Colombia). *Environmental Pollution*, *233*, 142–155. https://doi.org/10.1016/j.envpol.2017.10.045

Ramírez, O., Sánchez de la Campa, A. M., & de la Rosa, J. (2018b). Characteristics and temporal variations of organic and elemental carbon aerosols in a high–altitude, tropical Latin American megacity. *Atmospheric Research*, *210*(August 2017), 110–122. https://doi.org/10.1016/j.atmosres.2018.04.006

Rao, L., Zhang, L., Wang, X., Xie, T., Zhou, S., Lu, S., Liu, X., Lu, H., Xiao, K., Wang, W., & Wang, Q. (2020). Oxidative potential induced by ambient particulate matters with acellular assays: A review. *Processes*, *8*(11), 1–21. https://doi.org/10.3390/pr8111410

Raspet, R., Slaton, W. V., Arnott, W. P., & Moosmüller, H. (2003). Evaporation-condensation effects on resonant photoacoustics of volatile aerosols. *Journal of Atmospheric and Oceanic Technology*, *20*(5), 685–695. https://doi.org/10.1175/1520-0426(2003)20<685:ECEORP>2.0.CO;2

Raysoni, A. U., Armijos, R. X., Margaret Weigel, M., Echanique, P., Racines, M., Pingitore., N. E., & Li, W. W. (2017). Evaluation of sources and patterns of elemental composition of PM2.5 at three low-income neighborhood schools and residences in Quito, Ecuador. *International Journal of Environmental Research and Public Health*, *14*(7), 1–26. https://doi.org/10.3390/ijerph14070674

Red MoniCA, R. de M. de la C. del A. (2016). *Informe Nacional de Calidad de Aire-2015*.

http://snia.mmaya.gob.bo/web/modulos/PNGCA/#

Red MoniCA, R. de M. de la C. del A. (2017). *Informe Nacional de Calidad del Aire de Bolivia, Gestión 2016*. http://snia.mmaya.gob.bo/web/modulos/PNGCA/#

Red MoniCA, R. de M. de la C. del A. (2018). *Informe Nacional de Calidad del Aire de Bolivia, Gestión 2017*. http://snia.mmaya.gob.bo/web/modulos/PNGCA/#

Red MoniCA, R. de M. de la C. del A. (2021). *Informe Nacional de Calidad Del Aire De Bolivia, Gestión 2018*. http://snia.mmaya.gob.bo/web/modulos/PNGCA/publicaciones/items/17072022-090730-087192_209/17072022-090730-087192_209.pdf

Reff, A., Eberly, S. I., & Bhave, P. V. (2007). Receptor modeling of ambient particulate matter data using positive matrix factorization: Review of existing methods. *Journal of the Air and Waste Management Association*, *57*(2), 146–154. https://doi.org/10.1080/10473289.2007.10465319

Riemer, N., Vogel, H., & Vogel, B. (2004). Soot aging time scales in polluted regions during day and night. *Atmospheric Chemistry and Physics*, *4*(7), 1885–1893. https://doi.org/10.5194/acp-4-1885-2004

Rivellini, L. H., Chiapello, I., Tison, E., Fourmentin, M., Feron, A., Diallo, A., N'Diaye, T., Goloub, P., Canonaco, F., Prevet, A. S. H., & Riffault, V. (2017). Chemical characterization and source apportionment of submicron aerosols measured in Senegal during the 2015 SHADOW campaign. *Atmospheric Chemistry and Physics*, *17*(17), 10291–10314. https://doi.org/10.5194/acp-17-10291-2017

Rizzo, L. V, Correia, A. L., Artaxo, P., & Proc, A. S. (2011). *and Physics Spectral dependence of aerosol light absorption over the Amazon Basin*. 8899–8912. https://doi.org/10.5194/acp-11-8899-2011

Robert, M. A., Kleeman, M. J., & Jakober, C. A. (2007). Size and composition distributions of particulate matter emissions: Part 2 - Heavy-duty diesel vehicles. *Journal of the Air and Waste Management Association*, *57*(12), 1429–1438. https://doi.org/10.3155/1047-3289.57.12.1429

Robert, M. A., VanBergen, S., Kleeman, M. J., & Jakober, C. A. (2007). Size and composition distributions of particulate matter emissions: Part 1 - Light-duty gasoline vehicles. *Journal of the Air and Waste Management Association*, *57*(12), 1414–1428. https://doi.org/10.3155/1047-3289.57.12.1414

Saathoff, H., Naumann, K. H., Schnaiter, M., Schöck, W., Möhler, O., Schurath, U., Weingartner, E., Gysel, M., & Baltensperger, U. (2003). Coating of soot and (NH4)2SO4particles by ozonolysis products of α-pinene. *Journal of Aerosol Science*, *34*(10), 1297–1321. https://doi.org/10.1016/S0021-8502(03)00364-1

Saltzman, E. S., Savoie, D. L., Zika, R. G., & Prospero, J. M. (1983). Methane sulfonic acid in the marine atmosphere. *Journal of Geophysical Research*, *88*(C15), 10897–10902. https://doi.org/10.1029/JC088iC15p10897

Samaké, A., Jaffrezo, J. L., Favez, O., Weber, S., Jacob, V., Albinet, A., Riffault, V., Perdrix, E., Waked, A., Golly,

B., Salameh, D., Chevrier, F., Miguel Oliveira, D., Bonnaire, N., Besombes, J. L., Martins, J. M. F., Conil, S., Guillaud, G., Mesbah, B., … Uzu, G. (2019a). Polyols and glucose particulate species as tracers of primary biogenic organic aerosols at 28 French sites. *Atmospheric Chemistry and Physics*, *19*(5), 3357–3374. https://doi.org/10.5194/acp-19-3357-2019

Samaké, A., Jaffrezo, J. L., Favez, O., Weber, S., Jacob, V., Canete, T., Albinet, A., Charron, A., Riffault, V., Perdrix, E., Waked, A., Golly, B., Salameh, D., Chevrier, F., Miguel Oliveira, D., Besombes, J. L., Martins, J. M. F., Bonnaire, N., Conil, S., … Uzu, G. (2019b). Arabitol, mannitol, and glucose as tracers of primary biogenic organic aerosol: The influence of environmental factors on ambient air concentrations and spatial distribution over France. *Atmospheric Chemistry and Physics*, *19*(16), 11013–11030. https://doi.org/10.5194/acp-19-11013-2019

Samake, A., Uzu, G., Martins, J. M. F., Calas, A., Vince, E., Parat, S., & Jaffrezo, J. L. (2017). The unexpected role of bioaerosols in the Oxidative Potential of PM. *Scientific Reports*, *7*(1), 10978. https://doi.org/10.1038/s41598-017-11178-0

Sánchez de la Campa, A. M., de la Rosa, J. D., & Alastuey, A. (2013). An introduction to atmospheric PM and air quality. *Future Science Ltd*, 8–20.

Sandradewi, J., Prévôt, A. S. H., Weingartner, E., Schmidhauser, R., Gysel, M., & Baltensperger, U. (2008). A study of wood burning and traffic aerosols in an Alpine valley using a multi-wavelength Aethalometer. *Atmospheric Environment*, *42*(1), 101–112. https://doi.org/10.1016/j.atmosenv.2007.09.034

Sato, M., Hansen, J., Koch, D., Lacis, A., Ruedy, R., Dubovik, O., Holben, B., Chin, M., & Novakov, T. (2003). Global atmospheric black carbon inferred from AERONET. *Proceedings of the National Academy of Sciences*, *100*(11), 6319–6324. https://doi.org/10.1073/pnas.0731897100

Schnaiter, M., Linke, C., Möhler, O., Naumann, K. H., Saathoff, H., Wagner, R., Schurath, U., & Wehner, B. (2005). Absorption amplification of black carbon internally mixed with secondary organic aerosol. *Journal of Geophysical Research D: Atmospheres*, *110*(19), 1–11. https://doi.org/10.1029/2005JD006046

Scholz, W., Shen, J., Aliaga, D., Wu, C., Carbone, S., Moreno, I., Zha, Q., Huang, W., Heikkinen, L., Jaffrezo, J. L., Uzu, G., Partoll, E., Leiminger, M., Velarde, F., Laj, P., Ginot, P., Artaxo, P., Wiedensohler, A., Kulmala, M., … Hansel, A. (2022). Measurement Report: Long-range transport and fate of DMS-oxidation products in the free troposphere derived from observations at the high-altitude research station Chacaltaya (5240 m a.s.l.) in the Bolivian Andes. *EGUsphere [Preprint]*, *September*, 1–42. https://doi.org/10.5194/egusphere-2022-887

Schwarz, J. P., Gao, R. S., Fahey, D. W., Thomson, D. S., Watts, L. A., Wilson, J. C., Reeves, J. M., Darbeheshti, M., Baumgardner, D. G., Kok, G. L., Chung, S. H., Schulz, M., Hendricks, J., Lauer, A., Kärcher, B., Slowik, J. G., Rosenlof, K. H., Thompson, T. L., Langford, A. O., … Aikin, K. C. (2006). Single-particle measurements of midlatitude black carbon and light-scattering aerosols from the boundary layer to the lower

stratosphere. *Journal of Geophysical Research Atmospheres*, *111*(16), 1–15. https://doi.org/10.1029/2006JD007076

Schwarz, J. P., Spackman, J. R., Fahey, D. W., Gao, R. S., Lohmann, U., Stier, P., Watts, L. A., Thomson, D. S., Lack, D. A., Pfister, L., Mahoney, M. J., Baumgardner, D., Wilson, J. C., & Reeves, J. M. (2008). Coatings and their enhancement of black carbSchwarz, J. P., Spackman, J. R., Fahey, D. W., Gao, R. S., Lohmann, U., Stier, P., … Reeves, J. M. (2008). Coatings and their enhancement of black carbon light absorption in the tropical atmosphere. Journal of G. *Journal of Geophysical Research Atmospheres*, *113*(3), 1–10. https://doi.org/10.1029/2007JD009042

Segura, H., Espinoza, J. C., Junquas, C., Lebel, T., Vuille, M., & Garreaud, R. (2020). Recent changes in the precipitation-driving processes over the southern tropical Andes/western Amazon. *Climate Dynamics*, *54*(5–6), 2613–2631. https://doi.org/10.1007/s00382-020-05132-6

Seinfeld, J., & Pandis, S. (2016). *Atmospheric chemistry and physics: from air pollution to climate change* (3rd Editio). Wiley Interscience.

Seinfeld, J.H., & Pandis, S. . (2002). *Atmospheric Chemistry and Physics: From Air Pollution to Climate Change* (2nd Editio). Wiley Interscience.

Seinfeld, J.H., & Pandis, S. N. (2016). *Atmospheric Chemistry and Physics. From Air Pollution to Climate Change* (Second Edi). Wiley Interscience.

Seinfeld, John H, & Pandis, S. N. (1998). *From air pollution to climate change*. John Wiley & Sons New York.

Sellegri, K., Rose, C., Marinoni, A., Lupi, A., Wiedensohler, A., Andrade, M., Bonasoni, P., & Laj, P. (2019). New particle formation: A review of ground-based observations at mountain research stations. *Atmosphere*, *10*(9), 1–26. https://doi.org/10.3390/atmos10090493

SENAMHI. (n.d.). Retrieved September 29, 2021, from http://senamhi.gob.bo/index.php/sismet

Sheridan, P. J., Arnott, W. P., Ogren, J. a., Andrews, E., Atkinson, D. B., Covert, D. S., Moosmüller, H., Petzold, A., Schmid, B., Strawa, A. W., Varma, R., & Virkkula, A. (2005). The Reno Aerosol Optics Study: An Evaluation of Aerosol Absorption Measurement Methods. *Aerosol Science and Technology*, *39*(1), 1–16. https://doi.org/10.1080/027868290901891

Shiraiwa, M., Kondo, Y., Iwamoto, T., & Kita, K. (2010). Amplification of Light Absorption of Black Carbon by Organic Coating. *Aerosol Science and Technology*, *44*(1), 46–54. https://doi.org/10.1080/02786820903357686

Shiraiwa, M., Kondo, Y., Moteki, N., Takegawa, N., Miyazaki, Y., & Blake, D. R. (2007). Evolution of mixing state of black carbon in polluted air from Tokyo. *Geophysical Research Letters*, *34*(16), 2–6. https://doi.org/10.1029/2007GL029819

Shiraiwa, M., Kondo, Y., Moteki, N., Takegawa, N., Sahu, L. K., Takami, A., Hatakeyama, S., Yonemura, S., & Blake, D. R. (2008). Radiative impact of mixing state of black carbon aerosol in Asian outflow. *Journal of Geophysical Research Atmospheres*, *113*(24), 1–13. https://doi.org/10.1029/2008JD010546

Sicard, P., De Marco, A., Troussier, F., Renou, C., Vas, N., & Paoletti, E. (2013). Decrease in surface ozone concentrations at Mediterranean remote sites and increase in the cities. *Atmospheric Environment*, *79*, 705–715. https://doi.org/10.1016/j.atmosenv.2013.07.042

Sicard, P., Serra, R., & Rossello, P. (2016). Spatiotemporal trends in ground-level ozone concentrations and metrics in France over the time period 1999-2012. *Environmental Research*, *149*, 122–144. https://doi.org/10.1016/j.envres.2016.05.014

Simoneit, B. R. T. (2002). Biomass burning - A review of organic tracers for smoke from incomplete combustion. In *Applied Geochemistry* (Vol. 17, Issue 3). https://doi.org/10.1016/S0883-2927(01)00061-0

Simoneit, B. R. T., & Elias, V. O. (2000). Organic tracers from biomass burning in atmospheric particulate matter over the ocean. *Marine Chemistry*, *69*(3–4), 301–312. https://doi.org/10.1016/S0304-4203(00)00008-6

Singh, K. P., Malik, A., Kumar, R., Saxena, P., & Sinha, S. (2008). Receptor modeling for source apportionment of polycyclic aromatic hydrocarbons in urban atmosphere. *Environmental Monitoring and Assessment*, *136*(1–3), 183–196. https://doi.org/10.1007/s10661-007-9674-6

Singla, V., Mukherjee, S., Kristensson, A., Pandithurai, G., Dani, K., & Anil Kumar, V. (2018). New Particle Formation at a High Altitude Site in India: Impact of Fresh Emissions and Long Range Transport. *Atmospheric Chemistry and Physics Discussions*, *July*, 1–26. https://doi.org/https://doi.org/10.5194/acp-2018-637

Sorribas, M., Adame, J. A., Olmo, F. J., Vilaplana, J. M., Gil-Ojeda, M., & Alados-Arboledas, L. (2015). A long-term study of new particle formation in a coastal environment: Meteorology, gas phase and solar radiation implications. *Science of the Total Environment*, *511*, 723–737. https://doi.org/10.1016/j.scitotenv.2014.12.011

Squizzato, S., Masiol, M., Rich, D. Q., & Hopke, P. K. (2018). A long-term source apportionment of PM2.5 in New York State during 2005–2016. *Atmospheric Environment*, *192*(April), 35–47. https://doi.org/10.1016/j.atmosenv.2018.08.044

Strak, M., Janssen, N., Beelen, R., Schmitz, O., Vaartjes, I., Karssenberg, D., van den Brink, C., Bots, M. L., Dijst, M., Brunekreef, B., & Hoek, G. (2017). Long-term exposure to particulate matter, NO2 and the oxidative potential of particulates and diabetes prevalence in a large national health survey. *Environment International*, *108*, 228–236. https://doi.org/10.1016/j.envint.2017.08.017

Subramanian, R., Donahue, N. M., Bernardo-Bricker, A., Rogge, W. F., & Robinson, A. L. (2006). Contribution of motor vehicle emissions to organic carbon and fine particle mass in Pittsburgh, Pennsylvania: Effects of

varying source profiles and seasonal trends in ambient marker concentrations. *Atmospheric Environment*, *40*(40), 8002–8019. https://doi.org/10.1016/j.atmosenv.2006.06.055

Suglia, S. F., Gryparis, A., Schwartz, J., & Wright, R. J. (2008). *Association between Traffic-Related Black Carbon Exposure and Lung Function among Urban Women*. *10*, 1333–1337. https://doi.org/10.1289/ehp.11223

Tang, Z., Sarnat, J. A., Weber, R. J., Russell, A. G., Zhang, X., Li, Z., Yu, T., Jones, D. P., & Liang, D. (2022). The Oxidative Potential of Fine Particulate Matter and Biological Perturbations in Human Plasma and Saliva Metabolome. *Environmental Science & Technology*, *56*(11), 7350–7361. https://doi.org/10.1021/acs.est.1c04915

Tchounwou, P. B., Yedjou, C. G., Patlolla, A. K., & Sutton, D. J. (2012). Heavy metal toxicity and the environment. *Molecular, Clinical and Environmental Toxicology*, 133–164.

Terzi, E., Argyropoulos, G., Bougatioti, A., Mihalopoulos, N., Nikolaou, K., & Samara, C. (2010). *Chemical composition and mass closure of ambient PM10 at urban sites*. *44*. https://doi.org/10.1016/j.atmosenv.2010.02.019

Turpin, B. J., Lim, H., Turpin, B. J., & Lim, H. (2010). *Species Contributions to PM2 . 5 Mass Concentrations : Revisiting Common Assumptions for Estimating Organic Mass Species Contributions to PM2 . 5 Mass Concentrations : Revisiting Common Assumptions for Estimating Organic Mass*. *6826*. https://doi.org/10.1080/02786820119445

U.S. EPA, U. S. E. P. A. (2007). *Framework for Metals Risk Assessment EPA* (Issue March).

U.S. EPA, U. S. E. P. A. (2011). *Exposure Factors Handbook*. https://www.epa.gov/sites/default/files/2015-09/documents/efh-chapter06.pdf

U.S. EPA, U. S. E. P. A. (2022). *Learn About Asbestos*. https://www.epa.gov/asbestos/learn-about-asbestos

UNEP & CCAC. (2016). *Integrated assessment of short-lived climate pollutants for Latin America and the Caribbean: Improving Air Quality while mitigating climate change. Summary for decision makers.*

UNEP & CCAC. (2018). *Integrated assessment of short-lived climate pollutants for Latin America and the Caribbean: Improving Air Quality while mitigating climate change. Summary for decision makers.*

Urban, R. C., Lima-Souza, M., Caetano-Silva, L., Queiroz, M. E. C., Nogueira, R. F. P., Allen, A. G., Cardoso, A. A., Held, G., & Campos, M. L. A. M. (2012). Use of levoglucosan, potassium, and water-soluble organic carbon to characterize the origins of biomass-burning aerosols. *Atmospheric Environment*, *61*, 562–569. https://doi.org/10.1016/j.atmosenv.2012.07.082

US EPA. (2011). *Black Carbon Research and Future Strategies*. www.epa.gov/research

USEPA, U. S. E. P. A. (2007). Method 3051A: Microwave assisted acid digestion of sediments, sludges, soils, and

oils. *Cambbridge University Press*.

Valentini, S., Barnaba, F., Bernardoni, V., Calzolai, G., Costabile, F., Di Liberto, L., Forello, A. C., Gobbi, G. P., Gualtieri, M., Lucarelli, F., Nava, S., Petralia, E., Valli, G., Wiedensohler, A., & Vecchi, R. (2020). Classifying aerosol particles through the combination of optical and physical-chemical properties: Results from a wintertime campaign in Rome (Italy). *Atmospheric Research*, *235*(August 2019), 104799. https://doi.org/10.1016/j.atmosres.2019.104799

Valko, M., Morris, H., & Cronin, M. T. D. (2005). Metals, Toxicity and Oxidative Stress. *Current Medicinal Chemistry*, *12*, 1161–1208. https://doi.org/10.2174/0929867053764635

Vega, E., Eidels, S., Ruiz, H., López-Veneroni, D., Sosa, G., Gonzalez, E., Gasca, J., Mora, V., Reyes, E., Sánchez-Reyna, G., Villaseñor, R., Chow, J. C., Watson, J. G., & Edgerton, S. A. (2010). Particulate air pollution in Mexico city: A detailed view. *Aerosol and Air Quality Research*, *10*(3), 193–211. https://doi.org/10.4209/aaqr.2009.06.0042

Vega, E., Reyes, E., Ruiz, H., García, J., Sánchez, G., Martínez-villa, G., González, U., Chow, J. C., Watson, J. G., Vega, E., Reyes, E., Ruiz, H., García, J., Martínez-villa, G., González, U., Chow, J. C., Watson, J. G., Vega, E., Reyes, E., … Watson, J. G. (2012). *Analysis of PM 2 . 5 and PM 10 in the Atmosphere of Mexico City during 2000-2002 Analysis of PM 2 . 5 and PM 10 in the Atmosphere of Mexico City during 2000 – 2002*. *2247*. https://doi.org/10.1080/10473289.2004.10470952

Veld, M. in t., Alastuey, A., Pandolfi, M., Amato, F., Pérez, N., Reche, C., Via, M., Minguillón, M. C., Escudero, M., & Querol, X. (2021). Compositional changes of PM2.5 in NE Spain during 2009–2018: A trend analysis of the chemical composition and source apportionment. *Science of the Total Environment*, *795*. https://doi.org/10.1016/j.scitotenv.2021.148728

Venables, W. N., & Ripley, B. D. (2002). *Modern Applied Statistics with S* (Fourth). Springer. https://www.stats.ox.ac.uk/pub/MASS4/

Venkatachari, P., Hopke, P. K., Grover, B. D., & Eatough, D. J. (2005). Measurement of Particle-Bound Reactive Oxygen Species in Rubidoux Aerosols. *Journal of Atmospheric Chemistry*, *50*(1), 49–58. https://doi.org/10.1007/s10874-005-1662-z

Viana, M., Kuhlbusch, T. A. J., Querol, X., Alastuey, A., Harrison, R. M., Hopke, P. K., Winiwarter, W., Vallius, M., Szidat, S., Prévôt, A. S. H., Hueglin, C., Bloemen, H., Wåhlin, P., Vecchi, R., Miranda, A. I., Kasper-Giebl, A., Maenhaut, W., & Hitzenberger, R. (2008). Source apportionment of particulate matter in Europe: A review of methods and results. *Journal of Aerosol Science*, *39*(10), 827–849. https://doi.org/10.1016/j.jaerosci.2008.05.007

Virkkula, A, Chi, X., Ding, A., Shen, Y., Nie, W., Qi, X., Zheng, L., Huang, X., Xie, Y., Wang, J., Petäjä, T., & Kulmala, M. (2015). On the interpretation of the loading correction of the aethalometer. *Atmospheric Measurement*

Techniques, *8*(10), 4415–4427. https://doi.org/10.5194/amt-8-4415-2015

Virkkula, Aki, Ahlquist, N. C., Covert, D. S., Arnott, W. P., Sheridan, P. J., Quinn, P. K., & Coffman, D. J. (2005). Modification, calibration and a field test of an instrument for measuring light absorption by particles. *Aerosol Science and Technology*, *39*(1), 68–83. https://doi.org/10.1080/027868290901963

Waked, A., Favez, O., Alleman, L. Y., Piot, C., Petit, J. E., Delaunay, T., Verlinden, E., Golly, B., Besombes, J. L., Jaffrezo, J. L., & Leoz-Garziandia, E. (2014). Source apportionment of PM10 in a north-western Europe regional urban background site (Lens, France) using positive matrix factorization and including primary biogenic emissions. *Atmospheric Chemistry and Physics*, *14*(7), 3325–3346. https://doi.org/10.5194/acp-14-3325-2014

Wang, Q., Huang, R.-J., Cao, J., Han, Y., Wang, G., Li, G., Wang, Y., Dai, W., Zhang, R., & Zhou, Y. (2014). Mixing State of Black Carbon Aerosol in a Heavily Polluted Urban Area of China: Implications for Light Absorption Enhancement. *Aerosol Science and Technology*, *48*(7), 689–697. https://doi.org/10.1080/02786826.2014.917758

Wang, X., Ge, Y., Yu, L., & Feng, X. (2013a). Effects of altitude on the thermal efficiency of a heavy-duty diesel engine. *Energy*, *59*, 543–548. https://doi.org/10.1016/j.energy.2013.06.050

Wang, X., Yin, H., Ge, Y., Yu, L., Xu, Z., Yu, C., Shi, X., & Liu, H. (2013b). On-vehicle emission measurement of a light-duty diesel van at various speeds at high altitude. *Atmospheric Environment*, *81*, 263–269. https://doi.org/10.1016/j.atmosenv.2013.09.015

Wang, Y., & Boggio-Marzet, A. (2018). Evaluation of eco-driving training for fuel efficiency and emissions reduction according to road type. *Sustainability (Switzerland)*, *10*(11), 1–16. https://doi.org/10.3390/su10113891

Weber, Samuël, Salameh, D., Albinet, A., Alleman, L. Y., Waked, A., Besombes, J. L., Jacob, V., Guillaud, G., Meshbah, B., Rocq, B., Hulin, A., Dominik-Sègue, M., Chrétien, E., Jaffrezo, J. L., & Favez, O. (2019). Comparison of PM10 sources profiles at 15 french sites using a harmonized constrained positive matrix factorization approach. *Atmosphere*, *10*(6), 1–22. https://doi.org/10.3390/atmos10060310

Weber, Samuël, Uzu, G., Calas, A., Chevrier, F., Besombes, J. L., Charron, A., Salameh, D., Ježek, I., Moĉnik, G., & Jaffrezo, J. L. (2018). An apportionment method for the oxidative potential of atmospheric particulate matter sources: Application to a one-year study in Chamonix, France. *Atmospheric Chemistry and Physics*, *18*(13), 9617–9629. https://doi.org/10.5194/acp-18-9617-2018

Weber, Samuel, Uzu, G., Favez, O., Borlaza, L. J. S., Calas, A., Salameh, D., Chevrier, F., Allard, J., Besombes, J. L., Albinet, A., Pontet, S., Mesbah, B., Gille, G., Zhang, S., Pallares, C., Leoz-Garziandia, E., & Jaffrezo, J. L. (2021). Source apportionment of atmospheric PM10 oxidative potential: Synthesis of 15 year-round urban datasets in France. *Atmospheric Chemistry and Physics*, *21*(14), 11353–11378.

https://doi.org/10.5194/acp-21-11353-2021

Weichenthal, S., Crouse, D. L., Pinault, L., Godri-Pollitt, K., Lavigne, E., Evans, G., van Donkelaar, A., Martin, R. V., & Burnett, R. T. (2016). Oxidative burden of fine particulate air pollution and risk of cause-specific mortality in the Canadian Census Health and Environment Cohort (CanCHEC). *Environmental Research*, *146*, 92–99. https://doi.org/10.1016/j.envres.2015.12.013

Weichenthal, S., Lavigne, E., Traub, A., Umbrio, D., You, H., Pollitt, K., Shin, T., Kulka, R., Stieb, D. M., Korsiak, J., Jessiman, B., Brook, J. R., Hatzopoulou, M., Evans, G., & Burnett, R. T. (2021). Association of sulfur, transition metals, and the oxidative potential of outdoor pm2:5 with acute cardiovascular events: A case-crossover study of canadian adults. *Environmental Health Perspectives*, *129*(10), 1–11. https://doi.org/10.1289/EHP9449

Weingartner, E., Saathoff, H., Schnaiter, M., Streit, N., Bitnar, B., & Baltensperger, U. (2003). Absorption of light by soot particles: Determination of the absorption coefficient by means of aethalometers. *Journal of Aerosol Science*, *34*(10), 1445–1463. https://doi.org/10.1016/S0021-8502(03)00359-8

WHO. (1990). Acute respiratory infections in children: case management in small hospitals in developing countries: a manual for doctors and other senior health workers. *World Health Organization*. https://apps.who.int/iris/bitstream/handle/10665/61939/WHO_ARI_90.17.pdf?sequence=1

WHO. (2020). Severe Acute Respiratory Infections Treatment Centre. Practical manual to set up and manage a SARI treatment centre and a SARI screening facility in health care facilities. *World Health Organization*, *March*, 120. https://apps.who.int/iris/bitstream/handle/10665/331603/WHO-2019-nCoV-SARI_treatment_center-2020.1-eng.pdf

WHO Regional Europe. (2019). Noncommunicable Diseases and Air Pollution. *WHO European High-Level Conference on Noncommunicable Diseases Time to Deliver: Meeting NCD Targets to Achieve Sustainable Development Goals in Europe*, *April*, 1–7. http://www.euro.who.int/pubrequest

WHO, W. H. O. (2021a). *Ambient (outdoor) air pollution*. Fact Sheets. https://www.who.int/news-room/fact-sheets/detail/ambient-(outdoor)-air-quality-and-health

WHO, W. H. O. (2021b). *WHO global air quality guidelines: WHO global air quality guidelines: particulate matter (PM2.5 and PM10), ozone, nitrogen dioxide, sulfur dioxide and carbon monoxide*. Geneva: World Health Organization.

Wiedensohler, A., Andrade, M., Weinhold, K., Müller, T., Birmili, W., Velarde, F., Moreno, I., Forno, R., Sanchez, M. F., Laj, P., Ginot, P., Whiteman, D. N., Krejci, R., Sellegri, K., & Reichler, T. (2018). Black carbon emission and transport mechanisms to the free troposphere at the La Paz/El Alto (Bolivia) metropolitan area based on the Day of Census (2012). *Atmospheric Environment*, *194*(September), 158–169. https://doi.org/10.1016/j.atmosenv.2018.09.032

Xue, H., Khalizov, A. F., Wang, L., Zheng, J., & Zhang, R. (2009). Effects of dicarboxylic acid coating on the optical properties of soot. *Physical Chemistry Chemical Physics*, *11*(36), 7869. https://doi.org/10.1039/b904129j

Yang, H., Chen, J., Wen, J., Tian, H., & Liu, X. (2016). Composition and sources of PM2.5 around the heating periods of 2013 and 2014 in Beijing: Implications for efficient mitigation measures. *Atmospheric Environment*, *124*, 378–386. https://doi.org/10.1016/j.atmosenv.2015.05.015

Yin, H., & Xu, L. (2018). Comparative study of PM10/PM2.5-bound PAHs in downtown Beijing, China: Concentrations, sources, and health risks. *Journal of Cleaner Production*, *177*, 674–683. https://doi.org/10.1016/j.jclepro.2017.12.263

You, R., Radney, J. G., Zachariah, M. R., & Zangmeister, C. D. (2016). Measured Wavelength-Dependent Absorption Enhancement of Internally Mixed Black Carbon with Absorbing and Nonabsorbing Materials. *Environmental Science and Technology*, *50*(15), 7982–7990. https://doi.org/10.1021/acs.est.6b01473

Yu, L., Ge, Y., Tan, J., He, C., Wang, X., Liu, H., Zhao, W., Guo, J., Fu, G., Feng, X., & Wang, X. (2014). Experimental investigation of the impact of biodiesel on the combustion and emission characteristics of a heavy duty diesel engine at various altitudes. *Fuel*, *115*(X), 220–226. https://doi.org/10.1016/j.fuel.2013.06.056

Yuan, W., Huang, R.-J., Yang, L., Guo, J., Chen, Z., Duan, J., Wang, M., Wang, T., Ni, H., Han, Y., Li, Y., Chen, Q., Chen, Y., Hoffmann, T., & O'Dowd, C. (2019). Characterization of the light absorbing properties, chromophores composition and sources of brown carbon aerosol in Xi'an, Northwest China. *Atmospheric Chemistry and Physics*, *December*, 1–31. https://doi.org/10.5194/acp-2019-1100

Yus-Díez, J., Bernardoni, V., Močnik, G., Alastuey, A., Ciniglia, D., Ivančič, M., Querol, X., Perez, N., Reche, C., Rigler, M., Vecchi, R., Valentini, S., & Pandolfi, M. (2021). Determination of the multiple-scattering correction factor and its cross-sensitivity to scattering and wavelength dependence for different AE33 Aethalometer filter tapes: a multi-instrumental approach. *Atmospheric Measurement Techniques*, *14*(10), 6335–6355. https://doi.org/10.5194/amt-14-6335-2021

Zalakeviciute, R., Alexandrino, K., Rybarczyk, Y., Debut, A., Vizuete, K., & Diaz, M. (2020). Seasonal variations in PM10 inorganic composition in the Andean city. *Scientific Reports*, *10*(1), 1–13. https://doi.org/10.1038/s41598-020-72541-2

Zalakeviciute, R., López-Villada, J., & Rybarczyk, Y. (2018). Contrasted effects of relative humidity and precipitation on urban PM2.5 pollution in high elevation urban areas. *Sustainability (Switzerland)*, *10*(6). https://doi.org/10.3390/su10062064

Zalakeviciute, R., Rybarczyk, Y., Granda-Albuja, M. G., Diaz Suarez, M. V., & Alexandrino, K. (2020). Chemical characterization of urban PM10 in the Tropical Andes. *Atmospheric Pollution Research*, *11*(2), 343–356. https://doi.org/10.1016/j.apr.2019.11.007

Zhang, R., Khalizov, A. F., Pagels, J., Zhang, D., Xue, H., & McMurry, P. H. (2008). Variability in morphology,

hygroscopicity, and optical properties of soot aerosols during atmospheric processing. *Proceedings of the National Academy of Sciences*, *105*(30), 10291–10296. https://doi.org/10.1073/pnas.0804860105

Zhang, Z., Gao, J., Engling, G., Tao, J., Chai, F., Zhang, L., Zhang, R., Sang, X., Chan, C. Y., Lin, Z., & Cao, J. (2015). Characteristics and applications of size-segregated biomass burning tracers in China's Pearl River Delta region. *Atmospheric Environment*, *102*, 290–301. https://doi.org/10.1016/j.atmosenv.2014.12.009

Zielinska, B., Sagebiel, J., Arnott, W. P., Rogers, C. F., Kelly, K. E., Wagner, D. A., Lighty, J. S., Sarofim, A. F., & Palme, R. G. (2004a). *Phase and Size Distribution of Polycyclic Aromatic Hydrocarbons in Diesel and Gasoline Vehicle Emissions*. *38*(9), 2557–2567.

Zielinska, B., Sagebiel, J., Mcdonald, J. D., Whitney, K., & Lawson, D. R. (2004b). Emission Rates and Comparative Chemical Composition from Selected In-Use Diesel and Gasoline-Fueled Vehicles. *Journal of the Air & Waste Management Association*, *54*(9), 1138–1150. https://doi.org/10.1080/10473289.2004.10470973

Zíková, N., Wang, Y., Yang, F., Li, X., Tian, M., & Hopke, P. K. (2016). On the source contribution to Beijing PM2.5 concentrations. *Atmospheric Environment*, *134*, 84–95. https://doi.org/10.1016/j.atmosenv.2016.03.047

Zotter, P., Herich, H., Gysel, M., El-Haddad, I., Zhang, Y., Mocnik, G., Hüglin, C., Baltensperger, U., Szidat, S., & Prévôt, A. S. H. (2017). Evaluation of the absorption Ångström exponents for traffic and wood burning in the Aethalometer-based source apportionment using radiocarbon measurements of ambient aerosol. *Atmospheric Chemistry and Physics*, *17*(6), 4229–4249. https://doi.org/10.5194/acp-17-4229-2017